Reversible photo-induced isomerization of *cis*-[M(L-κ*S*,*O*)$_2$] (M=Pd^{II}, Pt^{II}) complexes with *N*,*N*-dialkyl-*N*'-acyl(aroyl)thiourea ligands (HL): Key to the isolation of novel geometric *trans*-[M(L-κ*S*,*O*)$_2$] and *trans*-[M(L-κ*S*,*N*)$_2$] isomers.

By

Henry Ane Nkabyo

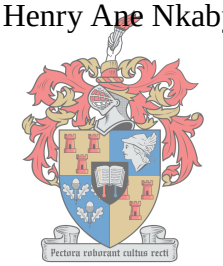

UNIVERSITEIT
iYUNIVESITHI
STELLENBOSCH
UNIVERSITY

Dissertation presented for the degree of Doctor of Chemistry in the Faculty of Science at Stellenbosch University

Supervisor: Prof. Klaus R. Koch

March 2018

Declaration

By submitting this thesis electronically, I declare that the entirety of the work contained therein is my own, original work, that I am the owner of the copyright thereof (unless to the extent explicitly otherwise stated) and that I have not previously in its entirety or in part submitted it for obtaining any qualification.

Signed: .....

Henry Ane Nkabyo

December 2017

Acknowledgements

I would sincerely like to thank:

My supervisor, Prof Klaus Koch, for his motivation, guidance and support throughout my studies.

Dr Wolf Hiller at Dortmund Technical University for giving me opportunity to do LC-NMR and NOESY experiments.

The University of Stellenbosch, The National Research Foundation(NRF) and Anglo Platinum for financial support.

Elsa Malherbe and Dr. Jaco Brand from the NMR lab for their friendship and technical assistance.

The technical staff at the Analytical Chemistry division, Shafiek Mohammed, Deidre Davids and Roger Lawrence.

All the present and past PGM group members for their friendship and creating a memorable working environment.

My wife Cordelia and my family for their support throughout the course of this work.

To God Almighty for strength and guidance throughout my studies.

Publications

Henry A. Nkabyo, and Klaus R. Koch; *Reversible photoinduced isomerisation of cis-[Pd(L-κS,O)$_2$] (L = N, N-diethyl-N'-1-naphthoylthiourea) to trans-[Pd(L-κS,O)$_2$] and its unprecedented trans-[Pd(L-κS,N)$_2$] counterpart, Dalton Transactions, Manuscript submitted.*

Henry A. Nkabyo, D. Hannekom, Jean M. Mckenzie, and Klaus R. Koch; *Light induced cis-trans isomerisation of cis-[Pd(L-κS,O)$_2$] and cis-[Pt(L-κS,O)$_2$] complexes of chelating N,N-dialkyl-N'-acylthioureas: key to the formation and isolation of trans isomers*; *Journal of Coordination Chemistry*, **2014**, 67, 4039–4060.

Conference proceedings

2016 Poster Presentation; 42nd International Conference on Coordination Chemistry (Brest, France); *Light-induced cis-[Pd(L-κS,O)$_2$] to trans-[Pd(L-κS,O)$_2$] isomerisation: Isolation of the novel trans-[Pd(L-κS,N)$_2$] complex only with N,N-diethyl-N'-naphthoylthiourea*.

2013 Poster Presentation, SACI INORG 2013 Conference, Durban South Africa; *Photoisomerisation of Pt(II) and Pd(II) acyl(aroyl)thioureas studied using reversed-phase HPLC*.

List of abbreviations

PGMs	platinum group metals
NMR	Nuclear Magnetic Resonance
Hz	Hertz
UV-Vis	Ultraviolet-Visible
DMSO	dimethyl sulphoxide
ppm	parts per million
DFT	Density Functional Theory
mins	minutes
$CDCl_3$	deuterated chloroform
CD_3CN	deuterated acetonitrile
DMF	*N*,*N*-dimethylformamide
CCDC	Cambridge Crystallographic Data Centre
RP-HPLC	reversed-phase high performance liquid chromatography
LC-MS	Liquid Chromatography-mass spectrometry
NOESY	Nuclear Overhauser effect Spectroscopy
FTIR	Fourier transform-Infra red
$^{13}C\{^{1}H\}$	proton decoupled ^{13}C spectrum
$^{195}Pt\{^{1}H\}$	proton decoupled ^{195}Pt spectrum
HSQC	heteronuclear single quantum correlation
HMBC	heteronumclear multiple quantum correlation
v/v	volume/volume
K	kelvin
ν	frequency
LED	light emitting diode
au	atomic unit
PDA	photo diode array
ESI-TOF-MS	electrospray ionization time-of-flight-mass spectrometry
m/z	mass/charge
HOMO	Highest Occupied Molecular Orbital
LUMO	Lowest Unoccupied Molecular Orbital

Abstract

The reaction of a series of selected *N*,*N*-dialkyl-*N*'-acyl(aroyl)thioureas to Pt^{II} or Pd^{II} formed exclusively *cis*-[M(L^n-κ*S*,*O*)$_2$] complexes which were fully characterized by melting point determination, ^{1}H, ^{13}C{^{1}H} NMR, FT-IR and single-crystal X-ray diffraction analyses. In acetonitrile solutions and under polychromatic light irradiation, the *cis*-[M(L^n-κ*S*,*O*)$_2$] (M = Pt(II) or Pd(II)) complexes undergo photo-induced isomerization to their respective *trans*-[M(L^n-κ*S*,*O*)$_2$] counterparts. The *cis*→*trans* isomerization was monitored by ^{1}H NMR and RP-HPLC due to differences in chemical shifts and retention times of the two geometric isomers respectively. In the photo-irradiated acetonitrile solution, the *trans*-[M(L^n-κ*S*,*O*)$_2$] complexes were less soluble than their thermodynamically stable *cis*-[M(L^n-κ*S*,*O*)$_2$] counterparts. Consequently, either controlled vapour diffusion-induced crystallization or slow evaporation of irradiated *cis*-[Pd(L^n-κ*S*,*O*)$_2$] complexes in acetonitrile led to isolation of novel *trans*-[Pd(L^n-κ*S*,*O*)$_2$] isomers in high yields > 60%. The *trans*-κ*S*,*O* configuration in the resulting complexes was confirmed by single-crystal X-ray diffraction. Also, significant differences in melting points and ^{1}H NMR chemical shifts were observed between the *cis*-*trans* isomers. For *cis*-bis(*N*,*N*-diethyl-*N*'-1-naphthoylthioureato-κ^2*S*,*O*)-palladium(II) *cis*-[Pd(L^7-κ*S*,*O*)$_2$], an unprecedented photo-induced isomerization occurred, yielding a novel four-membered *trans*-[Pd(L^7-κ*S*,*N*)$_2$] isomer in addition to *trans*-[Pd(L^7-κ*S*,*O*)$_2$]. This unusual *trans*-[Pd(L^7-κ*S*,*N*)$_2$] complex was further characterized by RP-HPLC, LC-MS and represents the first example of a *trans*-κ*S*,*N* coordination complex of Pd with the *N*,*N*-dialkyl-*N*'-acyl(aroyl)thioureas. In general, the *trans*-[Pd(L^n-κ*S*,*O*)$_2$] and *trans*-[Pd(L^n-κ*S*,*N*)$_2$] complexes were found to have significantly higher melting points compared to their *cis*-[Pd(L^n-κ*S*,*O*)$_2$] isomers, in addition to the relative upfield shift of their ^{1}H NMR resonances. Also, the Pd-S bond distances in the *trans* complexes were longer, while the Pd-O bonds experienced significant shortening compared to that of the *cis* complexes.

The addition of Pt(II) or Pd(II) solutions to asymmetrically substituted *N*,*N*-dialkyl-*N*'-acyl(aroyl)thioureas generated *cis*-[M(L^n-κ*S*,*O*)$_2$] complexes which were found to exist in chloroform as *cis*-[M(*ZZ*-L^n-κ*S*,*O*)$_2$], *cis*-[M(*EE*-L^n-κ*S*,*O*)$_2$] and *cis*-[M(*EZ*-L^n-κ*S*,*O*)$_2$] isomers. Assignment of these configurational isomers was carried out by ^{1}H, ^{13}C, HMBC and 1D NOESY NMR spectroscopy. Although significant overlap was observed between the *cis*-*EZ* and *cis*-*EE* isomers, for *cis*-[Pt(L^n-κ*S*,*O*)$_2$] complexes all the *ZZ*, *EZ* and *EE* configurational

isomers were represented by three well-resolved $^{195}Pt\{^{1}H\}$ resonances in the chemical shift range -2650 to -2750 ppm. The chemical shift and relative distribution of the *E* and *Z* isomers in chloroform were found to be dependent on the nature of ligand substituents. The presence of long chain *N*-alkyl or *N*-phenyl groups favoured a higher relative distribution of the *cis*-[Pt(*ZZ*-L-κ*S*,*O*)$_2$] isomer compared to complexes of ligands with smaller *N*-alkyl groups. In chloroform, *cis*-[Pt(*EE*-L^8-κ*S*,*O*)$_2$] complexes of Pt^{II} and Pd^{II} were isolated for HL^8 = *N*-methyl,*N*-ethyl, *N*'-benzoylthiourea, while a *cis*-[Pt(*ZZ*-L^{15}-κ*S*,*O*)$_2$] structure crystallized for HL^{15} = *N*-4-methoxy, *N*-isopropyl-*N'*-(2,2-dimethyl-pronanoyl)thiourea as revealed by single-crystal X-ray diffraction studies. Photo-induced isomerization of a mixture of *cis*-[Pt(*EE*-L^n-κS,O)$_2$], *cis*-[Pt(*EZ*-L^n-κS,O)$_2$] and *cis*-[Pt(*ZZ*-L^n-κ*S*,*O*)$_2$] isomers resulted in *trans*-[Pt(*EE*-L^n-κ*S*,*O*)$_2$], *trans*-[Pt(*EZ*-L^n-κ*S*,*O*)$_2$] and *trans*-[Pt(*ZZ*-L^n-κ*S*,*O*)$_2$] isomers in chloroform as represented by appearance of three additional $^{195}Pt\{^{1}H\}$ resonances after light irradiation. The ^{195}Pt resonances corresponding to the *trans* configurational isomers were significantly shifted downfield relative to their *cis*-counterparts by *ca* 750 ppm. By slow evaporation and under polychromatic light irradiation of an acetonitrile solution of *cis*-[Pd(L^8-κ*S*,*O*)$_2$] (HL^8 = *N*-methyl, *N*-ethyl, *N*'-benzoythiourea), a *trans*-[Pd(L^8-κ*S*,*O*)$_2$] complex was isolated as a mixture of *trans*-[Pd(*ZZ*-L^8-κ*S*,*O*)$_2$] and *trans*-[Pd(*EZ/EE*-L^8-κ*S*,*O*)$_2$] configurational isomers.

In the absence of light, all isolated *trans*-[Pd(L^n-κ*S*,*O*)$_2$] complexes were found to undergo a spontaneous *trans*→*cis* isomerization in chloroform. The presence of different ligand substituents showed no significant influence on the relative rates of *trans*→*cis* isomerization. Moreover, no consistent trend in rates of isomerization based on electronic effect of ligand substituents was observed in acetonitrile and chloroform. The relative rates of *trans*→*cis* isomerization were significantly higher in acetonitrile compared to chloroform indicating the role of coordinating acetonitrile solvent in assisting the reverse isomerization process. Addition of trace amounts of free *N*,*N*-dialkyl-*N*'-acylthioureas catalysed the *trans*→*cis* isomerization leading to a rapid dissapearance of *trans* ^{1}H NMR resonances and RP-HPLC peaks. In contrast, the presence of *N*,*N*,*N*',*N*'-tetramethyl-1,8-naphthalene diamine appeared to remove free ligands in solution leading to a decrease in the rate of *trans*→*cis* isomerization. When the concentration of added ligand in solution was increased, a first-order increase in the rate of *trans*→*cis* isomerization was observed. The ligand exchange mediated *trans*→*cis* isomerization resulted in the formation of mixed-ligand complexes of the type *cis*-[Pd(L^{a,b}-κ*S*,*O*)$_2$] evident from RP-HPLC chromatograms. Further support of an associative ligand

exchange process during *trans→cis* isomerization was provided by temperature dependence in the range 25-55°C in chloroform during which large negative activation entropy and positive activation enthalpy values were obtained.

Opsomming

Die reaksie van ’n reeks geselekteerde *N*,*N*-dialkiel-*N’*-asiel(aroïel)tioüreums met Pt^{II}, Pd^{II} vorm uitsluitlik *cis*-[M(L^n-κ*S*,*O*)$_2$] komplekse, wat ten volle gekarakteriseer is deur middel van smeltpuntmetings, ^{1}H, ^{13}C{^{1}H} KMR, FT-IR en enkel kristal X-straal diffraksie analise. In asetonitriel oplossings, onder bestraling met polichromatiese wit lig, ondergaan die *cis*-[M(L^n-κ*S*,*O*)$_2$] komplekse ’n foto-geïndusseerde isomerisasie na hul onderskeie *trans*-[M(L^n-κ*S*,*O*)$_2$] vorme. Die *cis*→*trans* isomerisasie is gemonitor deur ^{1}H KMR en RP-HPLC danksy verskille in die onderskeidelik chemiese verskuiwings en vloeitye van die twee geometriese isomere. In die bestraalde asetonitriel oplossings is die *trans*-[M(L^n-κ*S*,*O*)$_2$] komplekse minder oplosbaar as hul meer termodinamies stabiele *cis*-[M(L^n-κ*S*,*O*)$_2$] isomere. Gevolglik lei beheerde damp-diffusie of die stadige verdamping van bestraalde *cis*-[Pd(L^n-κ*S*,*O*)$_2$] komplekse in asetonitriel tot die isolasie van nuwe *trans*-[Pd(L^n-κ*S*,*O*)$_2$] isomere, met hoë opbrengs > 60%. Die *trans*-κ*S*,*O* konfigurasie in hierdie produkte is bevestig deur enkel kristal X-straal diffraksie. Verder is aansienlike verskille in die smeltpunte en ^{1}H KMR chemiese verskuiwings waargeneem tussen die *cis*-*trans* isomere. Vir *cis*-bis(*N*,*N*-diëtiel-*N’*-1-naftoïeltioüreato-κ^2*S*,*O*)-palladium(II) *cis*-[Pd(L^7-κ*S*,*O*)$_2$] het ’n ongekende foto-geïndusseerde isomerisasie plaasgevind wat gelei het tot nie net *trans*-[Pd(L^7-κ*S*,*O*)$_2$], maar ook ’n nuwe vier-lid *trans*-[Pd(L^7-κ*S*,*N*)$_2$] isomeer. Hierdie ongewone *trans*-[Pd(L^7-κ*S*,*N*)$_2$] kompleks is verder gekarakteriseer deur RP-HPLC, LC-MS en verteenwoordig die eerste voorbeeld van ’n *trans*-κ*S*,*N*-gekoördineerde kompleks van Pd met *N*,*N*-dialkiel-*N’*-asiel(aroïel)tioüreums. Oor die algemeen is daar gevind dat *trans*-[Pd(L^n-κ*S*,*O*)$_2$] en *trans*-[Pd(L^n-κ*S*,*N*)$_2$] aansienlik hoër smeltpunte as hul *cis*-[Pd(L^n-κ*S*,*O*)$_2$] isomere het, benewens hul relatiewe “upfield”, of laer frekwensie, posisies van hul ^{1}H KMR seine. Verder is gevind dat die Pd-S bindingslengtes in hierdie *trans*-komplekse langer, terwyl die Pt-O bindings aansienlik korter is as dié van die *cis*-komplekse.

Die toevoeging van Pt(II), Pd(II) oplossings tot asimmetriese-gesubstitueerde *N*,*N*-dialkiel-*N’*-asiel(aroïel)tioüreums genereer *cis*-[M(L^n-κ*S*,*O*)$_2$] komplekse en is ontdek bestaan in chloroform as *cis*-[M(*ZZ*-L^n-κ*S*,*O*)$_2$], *cis*-[M(*EE*-L^n-κ*S*,*O*)$_2$], *cis*-[M(*EZ*-L^n-κ*S*,*O*)$_2$] isomere. Toekenning van hierdie konfigurasionele isomere is uitgevoer deur ^{1}H, ^{13}C, HMBC en 1D NOESY KMR spektroskopie. Alhoewel aansienlike oorvleuling van seine waargeneem is vir die *cis*-*EZ* en *cis*-*EE* isomere, vir die *cis*-[Pt(L^n-κ*S*,*O*)$_2$] komplekse is die *ZZ*, *EZ*, *EE* konfigurasionele isomere voorgestel deur drie duidelike individuele ^{195}Pt{^{1}H} seine, met chemise verskuiwings in die gebied 2650-2750 ppm. Die chemise verskuiwing en relatiewe

verspreiding van *E,Z* isomere in chloroform is gevind om tot 'n groot mate afhanklik te wees van die aard van ligand substituente. Die teenwoordigheid van lang-ketting *N*-alkiel of *N*-fenielgroepe bevorder 'n relatiewe hoër teenwoordigheid van *cis*-[Pt(*ZZ*-L-κ*S*,*O*)$_2$], in vergelyking met komplekse waarvan die ligande oor kleiner *N*-alkiel substituente beskik. In chloroform is *cis*-[Pt(*EE*-L^8-κ*S*,*O*)$_2$] komplekse van Pt^{II}, Pd^{II} geïsoleer vir HL^8 = *N*-metiel,*N*-etiel, *N*'-bensoïeltioüreum, terwyl 'n *cis*-[Pt(*ZZ*-L^{15}-κ*S*,*O*)$_2$] struktuur gekristalliseer het vir HL^{15} = *N*-4-metoksie, *N*-isopropiel-*N'*-(2,2-dimetiel-pronanoïel)tioüreum, soos getoon deur X-straal diffraksie studies. Foto-geïndusseerde isomerisasie van 'n mengsel van *cis*-[Pt(*EE*-L^n-κS,O)$_2$], *cis*-[Pt(*EZ*-L^n-κS,O)$_2$] en *cis*-[Pt(*ZZ*-L^n-κ*S*,*O*)$_2$] isomere lei tot *trans*-[Pt(*EE*-L^n-κ*S*,*O*)$_2$], *trans*-[Pt(*EZ*-L^n-κ*S*,*O*)$_2$], *trans*-[Pt(*ZZ*-L^n-κ*S*,*O*)$_2$] isomere in chloroform, soos aangedui deur die verskyning van drie addisionele ^{195}Pt{^{1}H} seine, na bestraling met lig. Die ^{195}Pt resonansie seine wat ooreenstem met die *trans* konfigurasionele isomere kom aansienlik 'downfield' (hoër frekwensies) voor in vergelyking met hul *cis*-ekwiwalente, met *ca.* 750 ppm. Deur stadige verdamping van *cis*-[Pd(L^8-κ*S*,*O*)$_2$] (HL^8 = *N*-metiel, *N*-etielbensoïeltioüreum) in 'n asetonitrieloplossing terwyl onder bestraling met polychromatiese wit lig, is 'n *trans*-[Pd(L^8-κ*S*,*O*)$_2$] kompleks geïsoleer as 'n mengsel van *trans*-[Pd(*ZZ*-L^8-κ*S*,*O*)$_2$], *trans*-[Pd(*EZ/EE*-L^8-κ*S*,*O*)$_2$] konfigurasionele isomere.

Daar is gevind dat in die afwesigheid van lig, alle geïsoleerde *trans*-[Pd(L^n-κ*S*,*O*)$_2$] komplekse 'n spontane *trans*→*cis* isomerisasie ondergaan in chloroform. Die teenwoordigheid van verskillende ligandsubstituente toon geen beduidende invloed op die relatiewe tempo van *trans*→*cis* isomerisasie. Verder is geen konsekwent tendense in isomerisasietempo's, gebasseer op elektroniese effekte van ligandsubstituente, waargeneem in asetoon en chloroform. Die relatiewe tempo's van *trans*→*cis* isomerisasie is aansienlik hoër in asetonitriel in vergelyking met chloroform, wat dui op die rol van die koördinerende asetonitriel oplosmiddel in die terugwaardse isomerisasie proses. Toevoeging van klein hoeveelhede vry *N,N*-dialkiel-*N'*-asieltioüreums kataliseer die *trans*→*cis* isomerisasie en lei tot die vinnige verdwyning van die *trans* ^{1}H NMR resonansie seine en RP-HPLC pieke. In kontras blyk dit dat die teenwoordigheid van *N,N,N',N'*-tetrametiel-1,8-naftaleen diamine vrye ligande uit die oplossing verwyder wat lei tot 'n afname in die tempo van *trans*→*cis* isomerisasie. Wanneer die konsentrasie van vrye ligande in oplossing verhoog word, word 'n eerste-orde toename in die *trans*→*cis* isomerisasietempo waargeneem. Die ligand-uitruil-bemiddelde *trans*→*cis* isomerisasie lei tot die vorming van gemengde-ligand komplekse van die tipe *cis*-[Pd(L^{a,b}-

κ*S*,*O*)$_2$], duidelik sigbaar in die RP-HPLC chromatogramme. Verdere ondersteuning vir ’n assosiatiewe ligand-uitruil proses gedurende *trans*→*cis* isomerisasie is verkry van die temperatuur afhanklikheid, in die gebied 25-55°C in chloroform, waartydens groot negatiewe aktiverings entropie en positiewe aktiverings entalpie waardes gevind is.

Table of contents

List of Figures

Figure A6.4. Plot of natural logarithm of relative peak area *vs.* time in the dark for the *trans→cis* isomerization of *trans*-[Pd(L^7-κ*S*,*O*)$_2$] in acetonitrile at 25 °C.

Figure A6.5. Overlaid chromatograms representing *trans→cis* isomerization in acetonitrile for mixed solutions of *cis*-[Pd(L^1-κ*S*, *O*)$_2$] and *cis*-[Pd(L^6-κ*S*,*O*)$_2$]; conditions: mobile phase, 95:5% v/v acetonitrile:water; GEMINI C_{18}, 5 µm, 250 x 4.6 mm column; 20 µl injection volume; 1 $mlmin^{-1}$ flow rate; 262 nm detection; photo-irradiation with polychromatic light from a 5Watt LED lamp.

Figure A6.6. (a) An array of ^{1}H NMR spectra; and (b) comparison of plots of relative peak intensity; representing spontaneous *trans→cis* isomerization for isolated *trans*-[Pd(L^4-κ*S*,*O*)$_2$] after the addition of 1 mol % HL^3.

Figure A6.7. An array of ^{1}H NMR spectra representing spontaneous *trans→cis* isomerization for isolated *trans*-[Pd(L^4-κ*S*,*O*)$_2$] after the addition of (a) HL^3, (b) 0.12 mM HL^4, (c) 0.06 mM HL^4, and (d) 0.03 mM HL^4 in chloroform-*d* at 25 °C; Each spectrum in the array represents ^{1}H NMR data acquisition after every 20 seconds in the dark.

Figure A6.8. Overlaid UV-Vis spectra from photodiode array detection at 262 nm for ligand exchange products obtained from addition of (a) HL^2, (b) HL^5, (c) HL^7, and (d) HL^8 to a pre-irradiated solution of *trans*-[Pd(L^1-κ*S*,*O*)$_2$] in acetonitrile at 25 °C.

List of Tables

1

Introduction

1.1. General introduction

The platinum group of metals (PGMs) consist of platinum, palladium, rhodium, ruthenium, iridium, and osmium and can be used in a wide range of applications. These elements usually occur in nature together with other base metals such as nickel and copper. South Africa remains the world's leading producer of the PGMs, with the Bushveld Complex being the principal source as depicted in Figure 1.1.[1] Other deposits with PGM mines include Nroil'sk and placer deposits in Russia, Sudbury in Canada, Hartley in Zimbabwe, Stillwater in the USA and Zechstein in Poland.[2] Worldwide regions containing PGM deposits have become of great interest thanks to their uses as mineral resources. The most useful PGMs are platinum and palladium. These elements are highly useful in industrial applications including petroleum refining and nitric acid manufacture due to their high catalytic activity and strong resistance to heat and chemical attack.[3] In addition, they have the ability to function as auto-catalysts, with platinum capable of serving as an electrode for proton exchange membrane fuel cells.[4] The production of nitric acid from oxidation of ammonia has also been carried out using platinum alloy gauzes.[5] More applications of platinum are seen in the enhanced mechanical strength induced by alloying platinum and rhodium or platinum and gold, resulting in fabrications and coatings used in the manufacture of glass.[6] Platinum and its alloys are also used for designing biomedical devices such as surgical instruments, electro-medical implants and orthopaedics.[7] In addition, platinum derived complexes such as *cis*-platin have been widely used in cancer therapy.[8]

The separation of PGMs during precious metal refining is very demanding due their chemical similarities (Pt and Pd, Rh and Ir, Ru and Os). During the refining process, significantly high concentrations of the metals may also be disposed into the environment which could be harmful when consumed by humans.[9] Reliable analytical tools for the recovery and determination of the elements are therefore indispensable. Refining of the PGMs in the industry involves a number of separation or purification techniques one of which is solvent-solvent extraction. This makes use of selectivity of the extracted metal in an aqueous phase by an immiscible organic solvent. With the use of chelating ligands, the process of solvent extraction could result in complex formation.

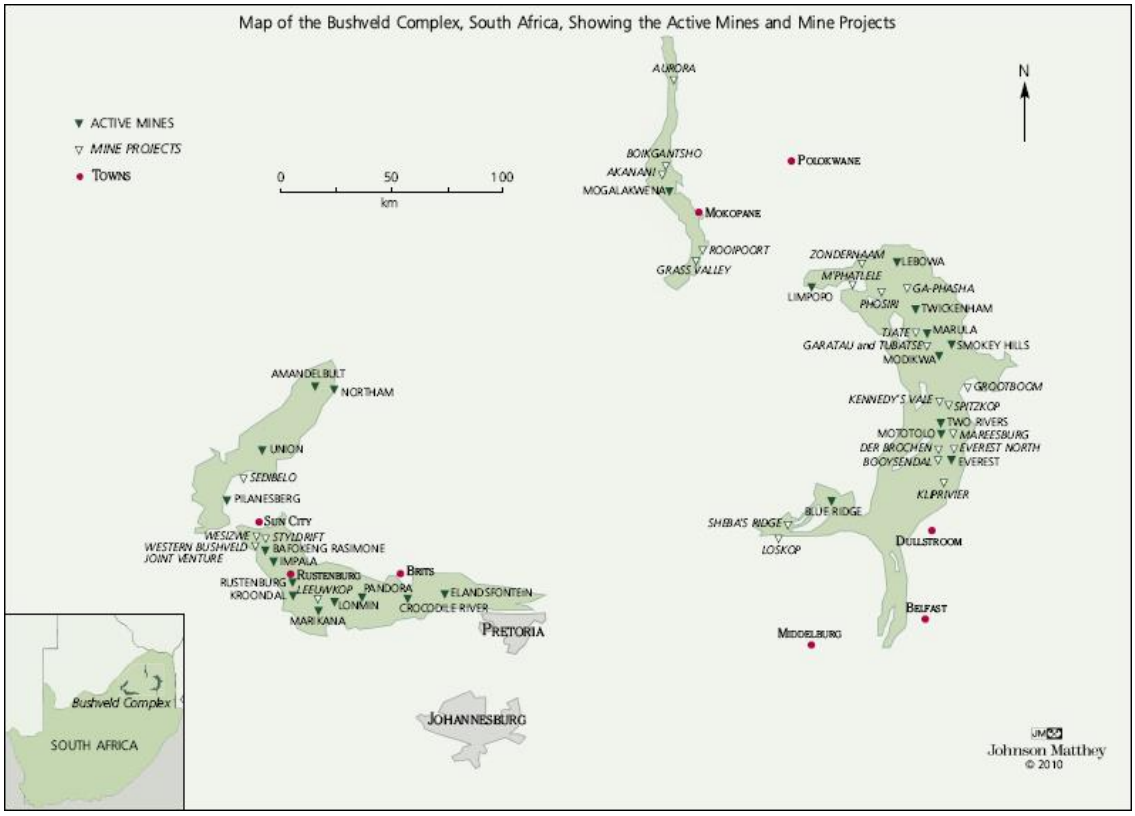

Figure 1.1. Platinum group metal distribution in South Africa showing the Bushveld complex.[1]

The *N*,*N*-dialkyl-*N*'-acyl(aroyl)thioureas are well known as useful chelating ligands for analytical determination[10] and solvent-solvent extraction of Cu(II),[11] and Pd(II).[12] Coordination of the ligands to transition metal ions could occur through sulfur, nitrogen and oxygen donor atoms, although *cis*-κ*S*,*O* coordination appears to be the most predominant. A more interesting phenomenon of the *cis*-[M(L^n-κ*S*,*O*)$_2$] complexes in particular for Pd^{II} and Pt^{II} is their ability to undergo a reversible *cis*-*trans* isomerization to their less thermodynamically stable *trans*-[M(L^n-κ*S*,*O*)$_2$] isomers.[13] The thermal *trans*→*cis* process occurs spontaneously in the dark in organic solvents. This reversible process constitutes a molecular switch. For square planar transition metal complexes, understanding the *cis*-*trans* isomerization is of upmost importance as much attention has been drawn towards their high catalytic activity especially for Pt^{II} complexes.[14] Moreover, the fact that only four *trans*-[M(L^n-κ*S*,*O*)$_2$] structures are represented in the Cambridge Structural Database (CSD) presents an interesting question as to what factors are responsible for their relative stability and possibility of isolation. A detailed study covering the preparation of the novel and light-responsive *trans*-[M(L^n-κ*S*,*O*)$_2$] (M = Pd^{II} or Pt^{II}) complexes and factors affecting the relative rates of *cis*-*trans* isomerization is therefore of great relevance.

1.2. Coordination of Pt^{II} and Pd^{II} to the *N*,*N*-dialkyl-*N*'-acyl(aroyl)thioureas

The *N*,*N*-dialkyl-*N*-acyl(aroyl)thioureas (HL) represented in Figure 1.2 (a) coordinate to divalent transition metal ions such as Pt^{II}, Pd^{II}, Cu^{II}, Ni^{II} through the oxygen and sulfur donor atoms. The origin of these ligands dates back to 1873 when they were prepared by K. Neucki.[15] The coordination chemistry of the ligands commenced several decades ago from work conducted by Hoyer and Beyer[16] on ligands such as *N*,*N*-di(2-hydroxyethyl)-*N'*-benzoylthiourea with first and second row transition metal ions. Complexes derived from the *N*,*N*-dialkyl-*N*-acyl(aroyl)thioureas are known for their use as antitumor,[17-20] anti-bacterial,[21] and anti-fungal[22] agents. A recent review on the coordination chemistry of the *N*,*N*-disubstituted acylthioureas also presents them as useful anion receptors and agents for asymmetric catalysis.[23] In addition, *N*,*N*-diethyl-*N*'-benzoylthiourea has been used for solvent extraction and selective online pre-concentration of transition metals ions such as Pd(II) in acidic media.[24,25]

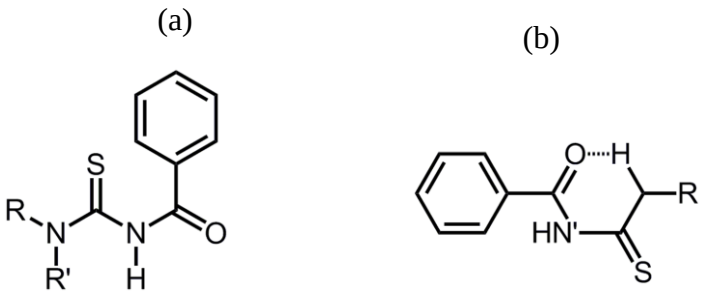

Figure 1.2. General representation of the (a) *N*,*N*-dialkyl-*N*'-aroylthioureas (HL) and (b) *N*-alkyl-*N*'-aroylthioureas (H_2L).

As a result of the versatile nature of the *N*,*N*-dialkyl-*N*'-acylthioureas, coordination with d^8 transition metal ions can occur by different modes which include monobasic bidentate (S,O), neutral monodentate (S) and neutral bidentate (N,O). These modes of coordination are common to transition metal complexes of other ligands. For example, salicylic-hydroxamate ligands, form either (N,O) or (O,O) complexes with platinum(II) and palladium(II) depending on the size of the ligand substituents.[26] The predominant mode of coordination is influenced by the nature of ligand substituents, and this could have significant effect on the properties of the resulting complexes. The effect of various *N*,*N*-disubstituted benzoylthioureas on the Cu(II)/Cu(I) electrochemical parameters of *cis*-[Cu(L-κ*S*,*O*)$_2$] complexes have previously been

reported by Mohamadou and co-workers.[27] These authors found that the tendency of Cu(II) to be electrochemically reduced to Cu(I) decreases when aliphatic *N*-alkyl groups are attached to the ligand compared to when aromatic or cyclic substituents are present. By introducing different ligand substituents, the water solubility of resulting *cis*-[Pt(L-κ*S*,*O*)$_2$] complexes could also be enhanced. This is represented by a Pt(II) complex with *N*,*N*-di-(2-hydroxyethyl)-benzoylthiourea which was found to be more water soluble than a similar complex with *N*,*N*-diethyl-*N*'-benzoylthiourea.[28] The formation and isomerization of platinum(II) complexes of the type [Pt{SC(NHR)NR}(PPh$_3$)$_2$] from a series of asymmetrically disubstituted thioureas is known to be dependent on the nature of ligand substituents.[29] In the presence of *t-butyl* substituents, a thermodynamically-favoured isomer with *distal* configuration is formed. However, for the other alkyl substituents, a *distal* isomer is initially formed which then subsequently isomerizes to a complex in which the R substituents assume a *proximal* configuration. The preference of a distal configuration when bulky *t-butyl* substituents are attached was attributed to unfavourable steric interactions which could occur in the presence of nearby PPh$_3$ groups.[29]

The monobasic bidentate mode is the most common of the three modes of coordination for *N*,*N*-disubstituted acyl(aroyl)thioureas to transition metal ions. This results in the formation of relative thermodynamically stable *cis*-[M(L^n-κ*S*,*O*)$_2$] complexes[28,30-34] which are represented in Figure 1.3 (a). Although the coordination geometry for most of these complexes is largely square planar, Arslan and co-workers[33] reported a distorted tetrahedral coordination for Ni^{II}, Cu^{II} and Co^{II} with *N*,*N*-diphenyl-*N*'-(4-chloro-benzoyl)thiourea. In the presence of trivalent transition metal ions such as Rh(III),[10] Fe(III),[31] and Co(III),[21] ligand coordination leads to the formation of *fac*-[M(L^n-κ*S*,*O*)$_3$] complexes.

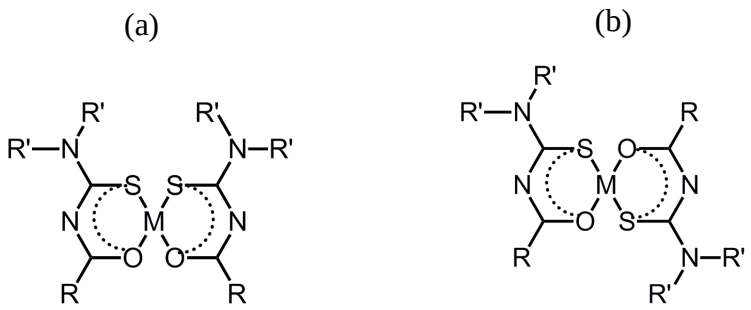

Figure 1.3. Representations of (a) *cis*-κ*S*,*O*, (b) *trans*-κ*S*,*O* modes of coordination of *N*,*N*-dialkyl-*N*'-acylthioureas to d^8 transition metal ions.

In addition to their use as antitumor,[17-20] anti-bacterial,[21] and anti-fungal[22] agents, *cis*-[M(L^n-κ*S*,*O*)$_2$] (M = Pt(II) or Pd(II)) complexes constituting the *N*,*N*-disubstituted acylthioureas as co-ligands have been prepared for their use as potential metallomesogens.[35-39] The ligands have also been incorporated for designing cyclometallated Pt^{II} complexes with some degree of luminescence properties.[40] The *cis*-[M(L^n-κ*S*,*O*)$_2$] chelates can be used for preparing other complexes with interesting chemical properties. For example, *cis*-[Pt(L^n-κ*S*,*O*)$_2$] complexes of the ligands *N*,*N*-diethyl-*N*'-benzoylthiourea and *N*,*N*-di-*n*-butyl-*N*'-benzoylthiourea undergo rapid oxidative addition in the presence of I_2 and Br_2 molecules in chloroform. This reaction leads to the formation of complexes of the type *cis*-[Pt^{IV}(L-κ*S*,*O*)$_2X_2$] (X = I, Br), in which the X_2 atoms are *trans* to each other.[41] Bipodal derivatives of the *N*,*N*-dialkyl-*N*'-acyl(aroyl)thioureas undergo molecular 'self-assembly' producing either 2:2 and 6:6 or 3:3 metallamacrocyclic complexes. This is exemplified by coordination of 3,3,3',3'-tetraalkyl-1,1'-terephthaloyl-bis(thiourea) and 3,3,3',3'-tetraalkyl-1,1'-isophthaloyl-bis(thiourea) to either Pt(II) or Pd(II).[42,43]

Another group of ligands are the *N*-monosubstituted acyl(aroyl)thioureas (Figure 1.2 (b)). They can exhibit unidentate coordination with Pd^{II} and Pt^{II} through the sulfur atom.[44] This is due to intramolecular hydrogen bonding which causes 'locking' of the -C(O)NHC(S)NHR moiety thereby preventing coordination through the oxygen atom. A consequence of this is the formation of mixtures of *cis*- and *trans*-[M(H_2L-κ*S*)X_2] (M = Pt^{II} or Pd^{II}; X = Cl, Br, I) complexes.[28,41,44] Prevention of the oxygen atom from participating in bonding could also result in coordination through both sulfur and nitrogen atoms to form *trans*-[Pt(HL-κ*N*,*S*)$_2$] type complexes. This is evinced in the unprecedented formation of *trans*-bis(*N*-propyl-*N*'-butanoylthioureato-κ^2*S*,*N*)platinum(II) after addition of a solution of Pt^{II} to *N*-propyl-*N*'-butanoylthiourea.[45] *N*-phosphorylated derivatives of acylthiourea ligands are also capable of coordinating to Ni^{II} resulting in *trans*-(1,3-κ*S*,*N*) complexes as reported by Babashkina and co-workers.[46-49]

In the presence of trace amounts of acid, protonation and subsequent ring opening of the six-membered *cis*-[Pt(L^n-κ*S*,*O*)$_2$] chelates may occur. This results in complexes with monodentate coordination of the *N*,*N*-dialkyl-*N*'-acyl(aroyl)thiourea to Pt^{II} *via* the sulfur atom.[50-52] The series of steps involved in the reversible protonation process are represented in Figure 1.4. Eventually, displacement of an oxygen atom and subsequent formation of a mixture of *trans*- or *cis*-[Pt(H_2L-κ*S*)$_2X_2$] complexes occur during the ring opening process. In the reverse reaction, the rapid ring closure occur preferentially through the oxygen atom. This was

ascribed to a higher nucleophilicity induced on the oxygen donor atom from the carbonyl group towards the Pt^{II} coordination sphere relative to that of the sulfur donor atom.[51]

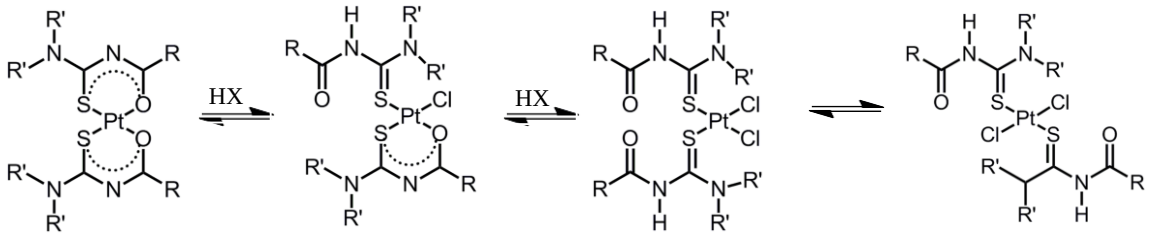

Figure 1.4. Representation of reversible ring opening of *cis*-[Pt(L^n-κ*S*,*O*)$_2$] chelates in the presence of HX (X = Cl, Br, I).[51]

Out of more than 70 *cis*-[M(L^n-κ*S*,*O*)$_2$] (M = Pt(II) or Pd(II)) structures of *N*,*N*-disubstituted acyl(aroyl)thioureas available in the literature, a search of the CSD reveals that only four *trans*-[M(L^n-κ*S*,*O*)$_2$] complexes have been reported. In these complexes (Figure 1.5), the transition metal ions coordinate to two ligand units in a *trans*-κ*S*,*O* manner as represented in Figure 1.3 (b). All the copper(II) complexes with the *trans*-κ*S*,*O* configuration (Figure 1.5 (a-c)) were isolated from a *cis*-*trans* mixture upon direct addition of methanolic solutions of *N*-pyrrolidine-*N'*-(2-chloro)-benzoylthiourea,[53] *N*,*N*-diethyl-*N'*-(*4*-nitro-benzoylthiourea,[54] and *N*,*N*-di-isopropyl-*N'*-(di-isopropoyl)thiourea[55] to solutions of copper(II) salts. The *trans*-bis(*N*,*N*-di-(*n*-butyl)-*N*'-1-naphthoylthioureato-κ^2*S*,*O*)platinum(II) complex (Figure 1.5 (d)) represents the only platinum(II) complex with *trans*-κ*S*,*O* configuration in the CSD, and was isolated more than a decade ago by Koch and co-workers[56] as a minor component from a *cis*-*trans* mixture using fractional crystallization.

Further studies carried out by Koch *et al.*[13] later revealed that the formation of the *trans*-[Pt(L-κ*S*,*O*)$_2$] (HL = *N*,*N*-di-(*n*-butyl)-*N*'-1-naphthoylthiourea) complex was due to photo-induced isomerization after exposure of a *cis*-[Pt(L-κ*S*,*O*)$_2$] solution to light. Irradiation of *cis*-Pt(II) or Pd(II) complexes of *N*,*N*-diethyl-*N*'-3,4,5-trimethoxy-benzoylthiourea in acetonitrile with visible light in the range 320-570 nm was found to generate additional RP-HPLC peaks, which were assigned to the *trans*-[M(L^n-κ*S*,*O*)$_2$] (M = Pt(II) or Pd(II)) isomers. The *cis*-*trans* isomers in the irradiated mixture were characterized by their similar UV and ESI-MS spectra. Higher relative rates of photo-induced *cis*→*trans* isomerization were observed for *cis*-[Pd(L^n-κ*S*,*O*)$_2$] complexes compared to corresponding *cis*-[Pt(L^n-κ*S*,*O*)$_2$] isomers. This was attributed to a relatively higher kinetic lability of palladium(II).[13] In the absence of light, thermal *trans*→*cis* isomerization was reported to occur spontaneously forming the more

thermodynamically stable *cis*-[M(L^n-κ*S*,*O*)$_2$] complexes. Higher thermodynamic stability of the representative *cis*-[M(L^n-κ*S*,*O*)$_2$] (M = Pt(II) or Pd(II)) isomers is not surprising as DFT calculations reveal that the gas phase minimum potential energy of *cis*-bis(*N*,*N*-dimethyl-*N*'-methylthioureato-κ^2*S*,*O*)palladium(II) is slightly lower than that of its *trans* counterpart by *ca* 2.5 kcal/mol.[57]

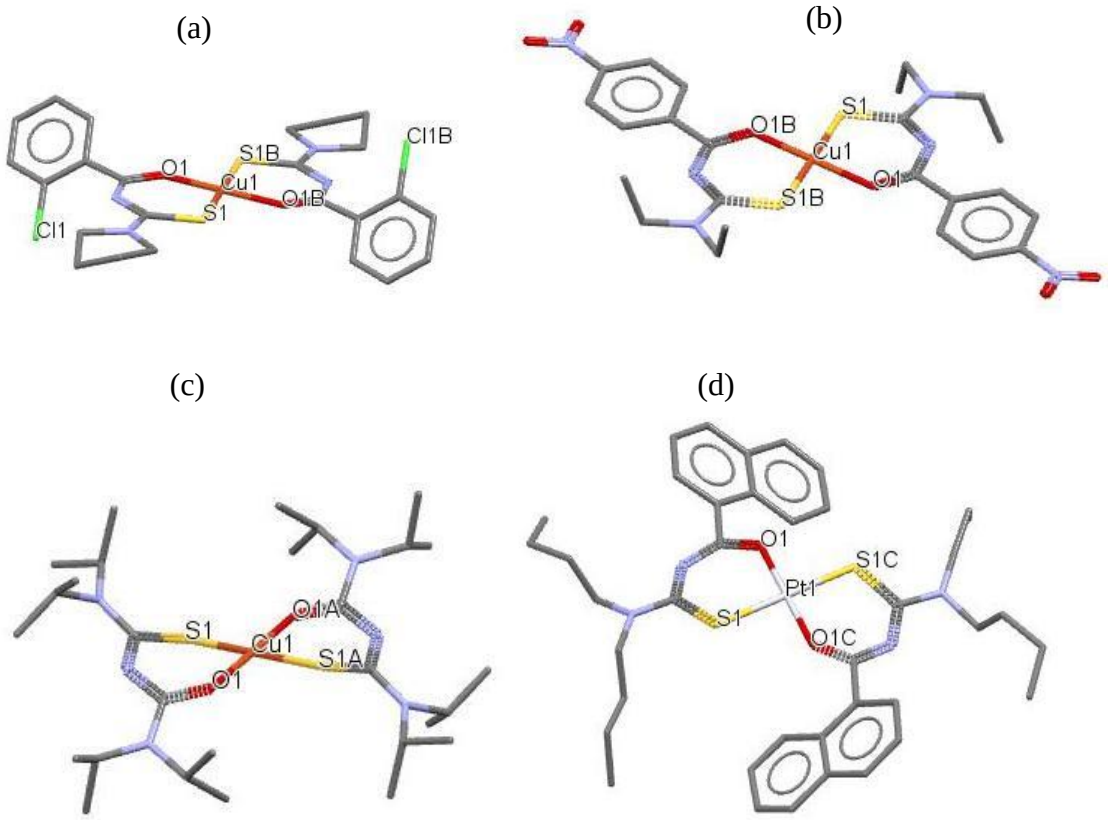

Figure 1.5. Molecular structures of (a) *trans*-bis(*N*-pyrrolidine-*N'*-(2-chlorobenzoyl)thioureato-κ^2*S*,*O*)copper(II);[53] (b) *trans*-bis(*N*,*N*-diethyl-*N'*-(*4*-nitrobenzoyl)thioureato-κ^2*S*,*O*)copper(II);[54] (c) *trans*-bis(*N*,*N*-di-isopropyl-*N'*-(di-isopropoyl)thioureato-κ^2*S*,*O*)copper(II);[55] and (d) *trans*-bis(*N*,*N*-di-(*n*-butyl)-*N'*-(1-naphthoyl)thioureato-κ^2*S*,*O*)platinum(II).[56]

Recently, the extent of photo-induced isomerization for palladium(II) and platinum(II) complexes with a series of *N*,*N*-dialkyl-*N*'-benzoylthioureas was studied using a specially designed online photochemical reactor.[58] A relatively lower extent of *cis*→*trans* conversion was observed for the Pt(II) and Pd(II) complexes when the benzoyl moiety of the ligand was substituted with three methoxy groups (HL = *N*,*N*-diethyl-*N*'-3,4,5-trimethoxy-benzoylthiourea). The *trans* isomers of complexes of this ligand showed a relatively shorter retention time on a C_{18} reversed phase column compared to their *cis* isomers. For the other

complexes studied, the *trans* isomers were more retained onto the column compared to their *cis* counterparts. Evidence of photodecomposition was observed from the RP-HPLC chromatogram of platinum(II) complexes of the *N*,*N*-dialkyl-*N*'-acylthioureas during *cis*→*trans* isomerization.[58]

1.3. Configurational isomerism in Pt(II) and Pd(II) complexes of asymmetrically substituted *N*,*N*-dialkyl-*N*'-acyl(aroyl)thioureas

The asymmetrically substituted *N*,*N*-dialkyl-*N*'-acylthioureas (HL) represented in Figure 1.6 also form exclusively *cis*-[M(L^n-κ*S*,*O*)$_2$] complexes when coordinated to Pt^{II} and Pd^{II} ions. In addition, the ligands also exhibit *E*, *Z* isomerism due to restricted C-N rotation imposed by the partial C-N double bond character. The origin of the C-N rotational barrier can be compared to closely related substituted amides.[59-63] In these compounds, the difference in conformational stability and steric or electronic effects on the C-N rotational barrier were rationalized using the resonance contributions represented in Figure 1.6. It is assumed that factors that do not favour the resonance structure II lead to a lower rotational barrier. The presence of larger *N*-alkyl substituents on the nitrogen atom could destabilize the planar ground state relative to the excited state, leading to a lower rotational barrier as observed by Isbrandt and co-workers.[62] These authors attributed their results to an increased non-planarity of the ground state relative to the transition states leading to a lower barrier of rotation. Studies performed on a series of *N*-acyl-*N*-alkyl-substituted amino acids also revealed a decrease in rotational barrier caused by the presence of larger *N*-alkyl substituents on both ends of the molecule.[63]

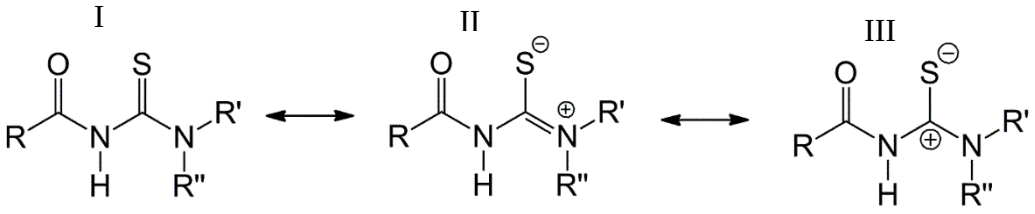

Figure 1.6. Representation of different resonance forms of the *N*,*N*-dialkyl-*N*'-acyl(aroyl)thioureas.

Electronic effects of substituents attached to either the carbonyl group or the nitrogen atom in amido-type compounds could also affect the magnitude of C-N rotational barrier. Various authors have suggested that the presence of electron-releasing substituents on a carbonyl moiety is accompanied by a decrease in rotational barrier, while a higher rotational barrier

occurs when these groups are attached to the nitrogen atom. Tafazzoli and co-workers[64] reported a decrease in C-N rotational barrier caused by electron-donating methoxy substituents on the *para* position of a phenyl ring attached to carbonyl moiety in *N*-(4-methoxybenzoyl)-pyrrolidine and *N*-(4-methoxybenzoyl)-piperidine. Also, a larger decrease in barrier of rotation occurred when phenyl groups were attached to the carbonyl moiety in comparison to alkyl groups. These observations were attributed to the fact that both a nitrogen atom and the phenyl ring are involved in electron charge transfer, consequently lowering the C-N rotational barrier. The presence of electronegative atoms attached to a carbonyl moiety in *N*,*N*-dimethylcarbamic halogenides could lead to an increase in rotational barrier as reported by Vassilev *et al*.[65] The C-N rotational barrier in ligands increase upon coordination with a metal ion.[66,67] This depends on the polarizability of the attached chalcogen atoms and follows the order Se > S[68] > O.[67]

There are relatively fewer studies in the literature related to *E*, *Z* isomerism caused by the C-N rotational barrier in the *N*,*N*-disubstituted acylthioureas. Koch and co-workers[69,70] reported that the *cis*-[Pt(L^n-κ*S*,*O*)$_2$] complexes are characterized by separate ^{1}H and ^{13}C resonances representing the *E*, *Z* isomers. Direct assignment of all *E*, *Z* isomers of *cis*-[Pt(L-κ*S*,*O*)$_2$] complexes (HL = *N*-methyl, *N*-ethyl,-*N*'-(2,2-dimethylpropanoyl)thiourea, *N*-methyl, *N*-(*n*-butyl)-*N*'-benzoylthiourea, *N*-methyl, *N*-ethyl-*N*'-(2,2-dimethylpropanoyl)thiourea) by ^{1}H NMR was not straightforward due to overlapping of the *N*-alkyl resonances. However, the set of three, well-resolved ^{195}Pt{^{1}H} resonances observed in the range -2700 to -2740 ppm led to the unambiguous assignment of *cis*-[Pt(*EE*-L-κ*S*,*O*)$_2$], *cis*-[Pt(*EZ*-L-κ*S*,*O*)$_2$] and *cis*-[Pt(*ZZ*-L-κ*S*,*O*)$_2$] isomers using a double magnetization transfer ^{1}H-(^{13}C)-^{195}Pt correlation NMR spectrum shown in Figure 1.7.[69] A scalar ^{4}J(^{195}Pt, ^{13}C) coupling of *ca* 20-40 Hz was observed for the *cis*-[Pt(L-κ*S*,*O*)$_2$] complexes in which the *N*-alkyl moiety occurs in a favourable 'W' configuration with respect to the platinum atom.[69]

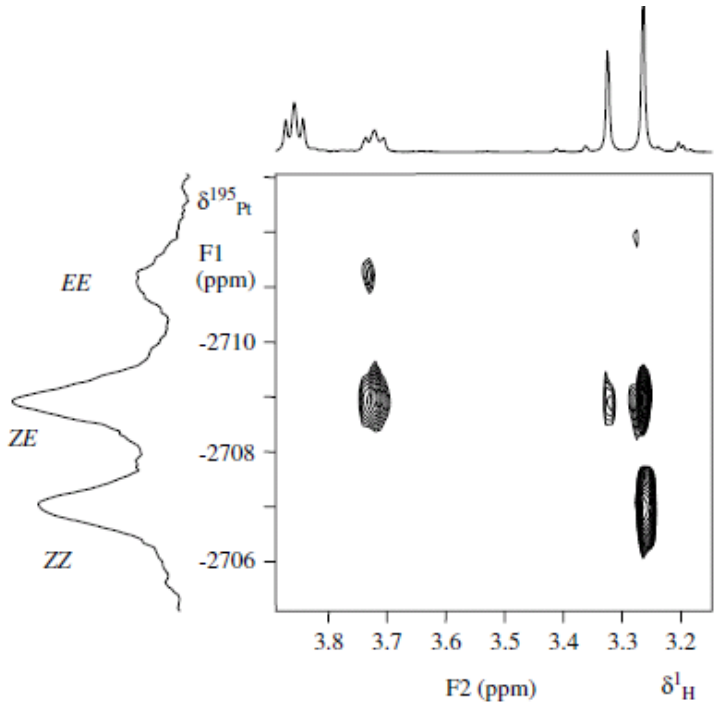

Figure 1.7. ^{1}H detected ^{1}H-(^{13}C)-^{195}Pt correlation spectra of bis(*N*-methyl-*N*-(*n*-butyl)-*N*'-benzoylthioureato-κ^{2}*S*,*O*)platinum(II).[69]

1.4. Photo-induced *cis-trans* isomerization of platinum(II) and palladium(II) complexes

There are several reports in the literature on the reversible *cis-trans* isomerization of square planar Pt(II) and Pd(II) complexes. The *cis-trans* isomerism can generally be classified as photochemical or thermal, although for most transition metal complexes the forward (*cis*→*trans*) reactions are photo-induced while the reverse processes (*trans*→*cis*) are thermally controlled. In these reactions, the *cis* complexes are generally known to be enthalpy-favoured while their *trans* counterparts are entropy-favoured.[71] Many reactions associated with *cis-trans* isomerism are monitored using UV and NMR spectroscopy. The photo-induced process is accompanied by electronic transitions between the ground and excited states of transition metal complexes. These transitions may include d-d transitions, charge transfers or intra-ligand transitions. For example, the reversible photo-induced *cis*→*trans* isomerization of bis(1,1,1-trifluoro-5,5-dimethyl-2,4-hexadionato)-platinum(II) is accompanied by localized π-π* transitions at 463 nm after light irradiation.[72] Sakamoto and co-workers[73] reported that the *trans*→*cis* photo-induced isomerization of azobenzene-conjugated dithiolato-bipyridine platinum(II) complexes is attributed to low-lying interligand charge transfer and π-π* transitions in the complexes.

Factors such as solvent polarity, temperature and electronic effect of ligand substituents could potentially affect the difference in energy between the electronic states involved in transition, thereby influencing the rates of photo-induced isomerization. Electronic effects of ligands substituents account for differences in the rates of *cis-trans* isomerization for many square planar complexes. For example, *cis*→*trans* isomerization occurs at a relatively higher rate for *cis*-[Pt(Cl)($SnCl_3$)(PPh_3)$_2$] due to the electron-withdrawing ability of the PPh_3 and $SnCl_3$ groups.[14] Studies conducted by Allen *et al.*[74] indicate that during isomerization of MX_2L_2 (M = Pd or Pt) complexes (L = organophosphorus ligands), an increase in phosphorus-metal bond strength is observed due to increase in the number of phenyl groups attached to phosphorus. A consequence of this increase in phosphorus-metal bond strength is that the *cis*-isomer was favoured in preference to *trans*. The thermodynamic equilibrium between the *cis-trans* isomers of diazido-bis(dimethyl-phenylphosphine)-palladium(II) and diazidobis-(methyl-diphenylphosphine)-palladium(II) complexes is strongly influenced by the σ-bonding ability of the phosphine ligands.[75] The metal-ligand bond strength increases with increase in the electron-donating ability of phosphine ligands. Previous photochemical studies by Al-Balushi *et al.*[76] reveal that *para* substitution of the azobenzene platinum(II) complexes of diynes and polyynes increases the rate of photo-induced *trans*→*cis* isomerization compared to that of *meta*-substituted complexes.

Steric effects of ligand substituents could also influence the stereochemistry of platinum(II) and palladium(II) complexes during photo-induced isomerization. The formation of *cis-trans* isomers of platinum(II) complexes with long-chain bis(tertiary phosphines) is influenced by the substituents on the complex precursors.[77] In the representative complexes, the thermodynamically stable *cis*-isomer has been isolated when there were no *trans*-labilizing groups in the complex precursors. Also, the formation of the *trans*-isomer did not require bulky ligand substituents as was the case with the $MLCl_2$ [M = Pt, Pd, L = (t-Bu)$_2$P(CH_2)$_n$P(t-Bu)$_2$, n=5-10] complexes which were earlier examined by Shaw *et al.*[78]

For some platinum(II) and palladium(II) complexes, the polarity of the solvent also accounts for the equilibrium thermodynamics between their *cis-trans* isomers. Nelson and co-workers[79,80] have studied the *cis*→*trans* isomerization of square planar palladium(II)-phosphine complexes. They found that the *cis*-isomers were thermodynamically favoured in polar solvents, with *cis*→*trans* conversion being entropy controlled. Both activation enthalpy and entropy during the *cis*→*trans* process were found to be predominantly controlled by

dipole-dipole interactions between the solvent and the *cis-trans* complexes. The *trans*-complexes with presumably lower dipole moments were favoured in less polar solvents.[80] The *cis*-[Pt(PEt_3)$_2$(*m*-MeC_6H_4)Cl] complex is reported to spontaneously isomerize to its *trans* counterpart as a result of a solvent-induced Pt-Cl bond cleavage.[81] Yutaka and co-workers[82] reported that the *trans→cis* isomerization of azobenzene-conjugated Pt(II) terpyridine complexes occurs in a range of solvents including acetonitrile, *N*,*N*-dimethylformamide (DMF), dimethyl sulfoxide (DMSO), and propylene carbonate. In terms of solvent polarity, their results indicated that quantum yields for the *trans→cis* reaction decrease in the order DMF > DMSO > propylene carbonate.

The rate of *cis→trans* isomerization in platinum(II) and palladium(II) complexes can also be influenced by the presence of trace amounts of additives in solution. Lewis and co-workers[83] have studied the photo-induced isomerization of *cis*- and *trans*-platinum(II) β-diketonates as well as their photodecomposition upon irradiation at 254 nm. Occurrence of this photoisomerization was found not to be favoured by the presence of hydrosilane after light irradiation. Although the photoproducts from this reaction could not be isolated, their formation was found to be dependent on the structure of the hydrosilane and β-diketonate ligand. The photo-induced *cis→trans* isomerization of phosphine and carbonyl Pt(II) complexes of the type Pt(CO)(PR_3)X_2 [X = Cl, Br, I; PR_3 = PEt_3, $PMePh_2$, PPh_3] has been reported to occur in chloro-hydrocarbon solvents such as chloroform and tetrachloromethane.[84] These photo-chemical reactions occurred at a relatively faster rate when carbon monoxide was added but were slowed down upon addition of nitrogen. The reversible *cis→trans* photo-induced isomerization of a square planar azo-conjugated benzenedithiolato complex of platinum was reported to be accelerated by the addition of trace amounts of acid.[85]

1.5. Ligand exchange and mechanism of *cis-trans* isomerization in Pt(II) and Pd(II) complexes

The *cis-trans* isomerism in some platinum(II) and palladium(II) complexes is catalysed by the presence of trace amounts of ligands in solution. These ligand-mediated reactions proceed by consecutive displacement of a ligand bound to the *cis-trans* complexes by free ligands in solution. Cooper and Powell[86] proposed a consecutive displacement mechanism for the *cis→trans* isomerization of [$PdCl_2$(Me_2RP)$_2$] (R = *o*-tolyl, *α*-naphthyl) complexes in chloroform, after these were shown to be catalysed by the addition of free PPh_3 ligands. The

stepwise ligand exchange mechanism which is generally represented in Figure 1.8 was evinced by the formation of $[PdCl(Me_2o\text{-tolylP})_3]^+Cl^-$ intermediate in a ^1H NMR spectrum of a chloroform-*d* solution of Me_2o-tolylP and $[PdCl_2(Me_2o\text{-tolylP})_2]$. In pure methanol, these authors also found that exchange of Me_2o-tolylP does not occur since chloride ligands at the axial position were essentially ripped off by methanol, resulting in the formation of $[PdCl(Me_2o\text{-tolylP})_3]^+$.

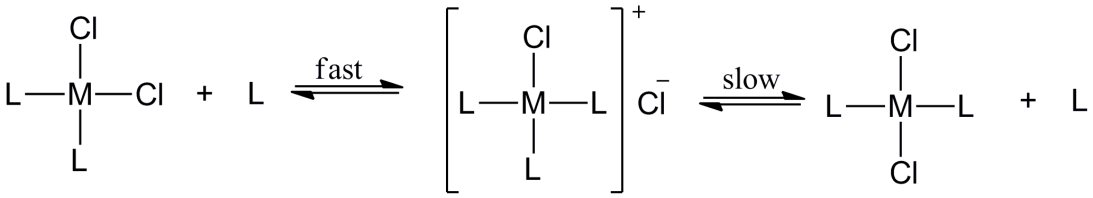

Figure 1.8. Representation of consecutive displacement by ligand (L) on square planar PtX_2L_2 complex.[86]

A few years later, Cooper and Powell[87] provided further spectroscopic evidence of a consecutive displacement for the catalysed *cis*→*trans* isomerization of $PtCl_2(PEt_3)_2$. This confirmation followed an attempt earlier made by Louw[88] to refute the proposed consecutive displacement mechanism. Instead, Louw proposed a mechanistic path involving a distorted five-coordinate intermediate with potential fluxional rotation. This was based on certain observations, one of which was the fact that addition of excess chloride to $PtCl(PEt_3)_3^+ClO_4^-$ did not result in a reaction.[88] In another report, both consecutive displacement mechanism and that involving a five-coordinate system were postulated by Louw for the catalysed *cis*→*trans* isomerization of square planar PtX_2L_2(X = Cl, Br, I; L = PMe_2Ph, PEt_3) complexes in polar and non-polar solvents respectively.[89] The results further revealed that a five coordinate PtX_2L_3 intermediate is formed after the phosphine ligand is added to *cis*- and *trans*-PtX_2L_2 in a non-polar solvent pentane, leading to a rapid isomerization. The release of phosphine from PtX_2L_2 either by dissociation, solvent substitution or dimer formation could also trigger phosphine catalysis of *cis*- or *trans*-PtX_2L_2. This could possibly occur by consecutive displacement or pseudorotation consequently leading to a spontaneous *cis*-*trans* isomerization of PtX_2L_2.[90]

Of the reports available in the literature relating to the effect of free ligands and mechanism of *cis*-*trans* isomerization of platinum(II) and palladium(II) complexes, the only study reminiscent of the *cis*-$[M(L^n\text{-}\kappa S,O)_2]$ complexes of the *N*,*N*-dialkyl-*N*'-acylthioureas is that of *cis*-$Pt(gly\text{-}\kappa N,O)_2$ (gly = glycine) complexes reported by Balzani and co-workers.[91-93] These

authors proposed different mechanisms for the thermal and photo-induced *cis*→*trans* isomerization of the platinum(II) glycinato complexes. In the absence of free glycine, heating of the *cis*-Pt(gly-κ*N*,*O*)$_2$ complex even to temperatures of *ca* 95 °C showed no isomerization.[92] An associative or intermolecular mechanism was proposed for the thermal *cis*→*trans* isomerization of *cis*-Pt(gly-κ*N*,*O*)$_2$ complexes in the presence of free labelled (*) glycine ligands (Figure 1.9). This involves a path for the substitution of a glycine ligand which occurs after a Pt-O bond cleavage to yield a *tris*-glycinato complex as intermediate, with subsequent loss of glycine molecules to give the *cis*- or *trans*-Pt(gly-κ*N*,*O*)$_2$ products.[92] An alternative path for the intermolecular isomerization requires substitution of a second glycine ligand to form a *tetra*-glycinato complex intermediate which upon release of the ligand results in the formation of the *trans*-(gly-κ*N*,*O*)$_2$ isomer.

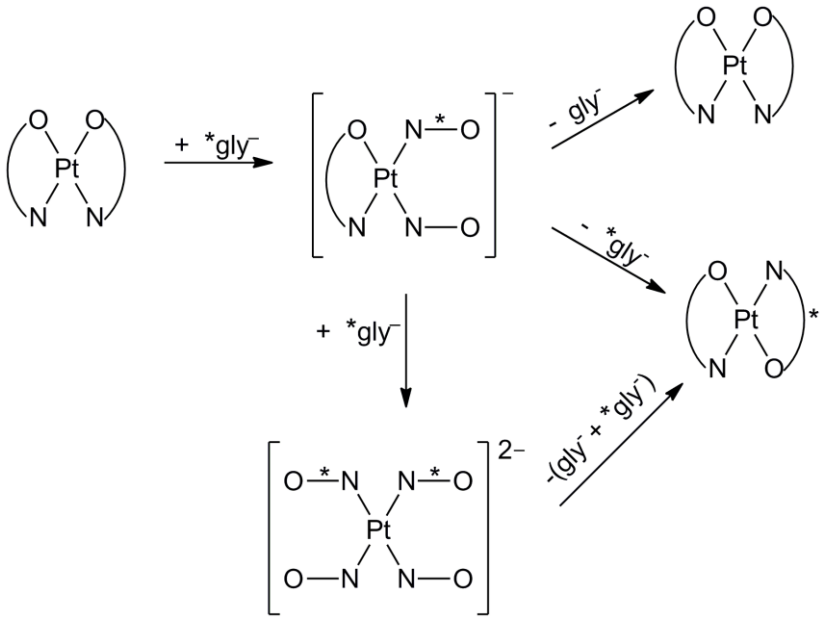

Figure 1.9. Proposed mechanistic pathways for ligand exchange and thermal *cis*-*trans* isomerization of *cis*-Pt(gly-κ*N*,*O*)$_2$.[92]

The photochemical *cis*→*trans* isomerization of *cis*-Pt(gly-κ*N*,*O*)$_2$ occurs with or without the presence of free glycine.[91,92] An intramolecular twisting mechanism was proposed for the photo-induced process as represented in Figure 1.10. A tetrahedral intermediate is presumably involved during photoisomerization of *cis*-Pt(gly-κ*N*,*O*)$_2$ and no Pt-O bond cleavage occurs as is the case of the thermal process.[91,92] Further support on this intramolecular mechanism was presented by Richardson *et al.*[94] using a semi-empirical molecular orbital calculations. These authors reported that the excited state during *cis*→*trans* isomerization of *cis*-Pt(gly-κ*N*,*O*)$_2$ has

a distorted tetrahedral equilibrium geometry and involved transitions from ($d_{xz} + d_{yz}$) → $d_{x^2-y^2}$ orbitals.

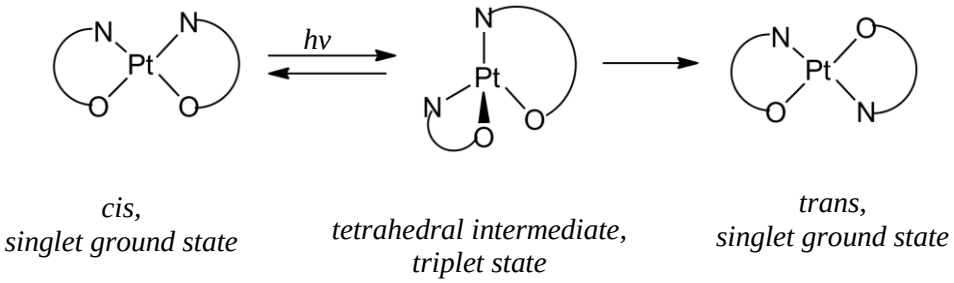

Figure 1.10. Proposed mechanism for the photo-induced isomerization of *cis*-Pt(gly-κ*N*,*O*)$_2$.[91]

1.6. Aims and objectives of research

The aim of the research presented in this thesis was to develop a method for isolating novel *trans*-[M(L^n-κ*S*,*O*)$_2$] (M = Pt(II) and Pd(II)) complexes through photo-induced *cis*→*trans* isomerization. Although irradiation of acetonitrile solutions of *cis*-[M(L^n-κ*S*,*O*)$_2$] complexes with polychromatic light readily generates the *trans*-[M(L^n-κ*S*,*O*)$_2$] isomers,[13] complete *cis*-*trans* conversion following light irradiation is never achieved as a steady state constituting both geometric isomers is always reached. The *trans*-[M(L^n-κ*S*,*O*)$_2$] complexes spontaneously isomerize to their *cis*-[M(L^n-κ*S*,*O*)$_2$] counterparts from a steady state irradiated solution.[13] The factors affecting the relative stability and possible isolation of the *trans*-[M(L^n-κ*S*,*O*)$_2$] isomers from solutions of their *cis*-[M(L^n-κ*S*,*O*)$_2$] complexes have not been investigated. Moreover, the mechanism of photo-induced (*cis*→*trans*) and thermal (*trans*→*cis*) isomerization in the representative *cis*-[M(L^n-κ*S*,*O*)$_2$] complexes is not fully understood.

The specific objectives of this study were therefore:

i. To develop vapour diffusion and slow evaporation methods for isolation of novel *trans*-[M(L^n-κ*S*,*O*)$_2$] (M = Pt(II) and Pd(II)) complexes of the *N*,*N*-disubstituted acyl(aroyl)thioureas using photo-induced *cis*→*trans* isomerization.

ii. To investigate the role of ligand substituents on the extent of photo-induced *cis*→*trans* isomerization in view of isolating other novel *trans* complexes.

iii. To investigate the photo-induced *cis*→*trans* isomerization of *cis*-[M(L^n-κ*S*,*O*)$_2$] (M = Pt(II) and Pd(II)) complexes derived from asymmetrically substituted *N*,*N*-dialkyl-*N*'-acylthioureas.

iv. To investigate factors affecting the relative rates of spontaneous *trans*→*cis* isomerization in acetonitrile and chloroform in view of gaining more insight on the mechanism of *trans*→*cis* isomerization.

In **chapter 2**, the synthesis and characterization of a series of selected *N*,*N*-dialkyl-*N*'-acylthioureas and their respective *cis*-[Pd(L^n-κ*S*,*O*)$_2$] complexes will be outlined. The use of single-crystal X-ray diffraction confirmed the *cis*-κ*S*,*O* coordination of the ligands to Pd^{II} in these complexes.

Chapter 3 consists of photo-induced isomerization studies performed on six *cis*-[Pd(L^n-κ*S*,*O*)$_2$] complexes derived from a series of symmetrically substituted *N*,*N*-dialkyl-*N*'-benzoylthioureas. The major challenge relating to isolation of *trans*-[Pd(L^n-κ*S*,*O*)$_2$] complexes is the fact that irradiated solutions of the *cis*-[Pd(L^n-κ*S*,*O*)$_2$] complexes always consist of a mixture of *cis*-*trans* isomers in equilibrium, hence no direct means of isolating the *trans*-[M(L^n-κ*S*,*O*)$_2$] (M = Pt(II), Pd(II) complexes have been reported. Vapour-diffusion and slow evaporation were successfully used to prepare six novel *trans*-[Pd(L^n-κ*S*,*O*)$_2$] complexes from photo-induced isomerization of their *cis*-[Pd(L^n-κ*S*,*O*)$_2$] counterparts as described in **chapter 3**. The characterization of the isolated *trans*-[Pd(L^n-κ*S*,*O*)$_2$] complexes will also be discussed.

In **chapter 4**, the effects of varying ligand substituents on photo-induced isomerization will serve as a probe for preparing and isolating a novel square planar *trans*-[Pd(L-κ*S*,*N*)$_2$] complex for *N*,*N*-diethyl-*N*'-1-naphthoylthiourea. Unambiguous characterization of the isolated *trans*-[Pd(L-κ*S*,*N*)$_2$] isomer in addition to *trans*-[Pd(L-κ*S*,*O*)$_2$] was performed by LC-MS and single-crystal X-ray diffraction.

There have so-far been no photo-induced isomerization studies on representative *cis*-[M(*ZZ*-L-κ*S*,*O*)$_2$], *cis*-[M(*EZ*-L-κ*S*,*O*)$_2$] and *cis*-[M(*EE*-L-κ*S*,*O*)$_2$] (M = Pt(II), Pd(II)) complexes derived from asymmetrically substituted *N*,*N*-dialkyl-*N*'-acyl(aroyl)thioureas. This study will be presented in **chapter 5**, commencing with confirmation of assignment of ligands and the *cis*-[M(*ZZ*-L-κ*S*,*O*)$_2$], *cis*-[M(*EZ*-L-κS,O)$_2$] and *cis*-[M(*EE*-L-κ*S*,*O*)$_2$] complexes. Evidence of the formation of *trans*-[M(*ZZ*-L-κ*S*,*O*)$_2$], *trans*-[M(*EZ*-L-κ*S*,*O*)$_2$], *trans*-[M(*EE*-L-κ*S*,*O*)$_2$] isomers was provided using $^{195}Pt\{^1H\}$ spectroscopy after irradiation with polychromatic light. Studies on the isolation and characterization of a *trans*-[Pd(L-κ*S*,*O*)$_2$] complex (HL =*N*-methyl, *N*-ethyl-*N*'-benzoylthiourea) will conclude **chapter 5**.

All the *trans*-[Pd(L^n-κ*S*,*O*)$_2$] complexes isolated in this study were eventually used to study ligand exchange accompanying the spontaneous *trans*→*cis* isomerization in the dark as

presented in **chapter 6**. This study commenced with investigation of the effect of ligand substituents on the relative rates of thermal *trans→cis* isomerization in both acetonitrile and chloroform. The effect of ligand concentration and temperature on the rates of *trans→cis* isomerization was also studied. **Chapter 6** ends with results confirming the formation of mixed-ligand complexes using RP-HPLC after ligand exchange involving the *cis*-*trans* isomers in solution.

2

Synthesis, characterization of ligands and cis-[M(L^n-S,O)$_2$](M = Pt(II) or Pd(II)) complexes; Experimental methods

This chapter describes the synthesis of all N,N-dialkyl-N'-aroylthioureas (HL$^{1-15}$) and their corresponding cis-[M(L^n-κS,O)$_2$](M = Pt(II), Pd(II)) complexes. Relatively high yields of ligands and complexes were obtained. Spectroscopic evidence of the ligands coordinating to Pd^{II} and Pt^{II} via sulfur and oxygen donor atoms is provided through characterization by FT-IR and ^{1}H NMR spectroscopy. Furthermore, presentation of X-ray crystallographic bond distances and angles of the cis-[Pd(L^n-κS,O)$_2$] complexes confirms cis-κS,O mode of coordination consistent with the ^{1}H NMR and FT-IR characterization. All the experimental procedures used during investigations presented in this chapter as well as the other chapters (3-6) will also be discussed in this chapter

2.1. Synthesis and characterization of ligands and complexes

2.1.1. Synthesis of *N*,*N*-dialkyl-*N*'-acyl(aroyl)thioureas (HL)

A series of *N*,*N*-dialkyl-*N*'-acyl(aroyl)thiourea ligands HL[1-15] were synthesized using the Douglass and Dains[95] method. The two-step synthesis involves initial addition of mixtures of an acyl chloride and potassium thiocyanate in anhydrous acetone, followed by addition of appropriate amounts of solution of a secondary amine as shown in Figure 2.1. The reaction between the acyl chloride and potassium thiocyanate has been proposed to initially involve a nucleophilic thiocyanate anion undergoing a thermal isomerization to produce an 'active' isothiocyanate anion, followed by the formation of an acylisothiocyanate intermediate in the presence of an acyl chloride.[96] This could then possibly react with the secondary amine in acetone to yield the *N*,*N*-dialkyl-*N*'-acyl(aroyl)thioureas.[97] In some cases, ammonium thiocyanate is used for substitution of Cℓ in the acyl chlorides during synthesis of acylthioureas. Other methods have also been proposed for preparing 3,3-diethyl-1'-(4-methoxy)-benzoylthiourea from condensation of the corresponding 1,1-diethylthiourea and 4-methylbenzoic acid on a solid support and under microwave irradiation.[98] Saeed and co-workers[99] have utilized tetrabutyl ammonium bromide as phase-transfer catalysts to prepare aroyl thiourea derivatives from isothiocyanates.

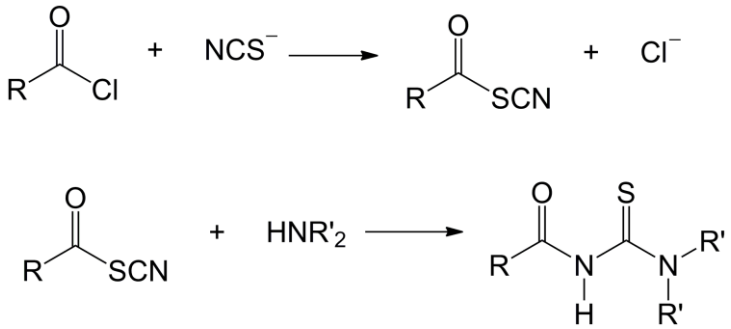

Figure 2.1. Steps involved for synthesis of *N*,*N*-dialkyl-*N*'-acyl(aroyl)thioureas.

The series of *N*,*N*-dialkyl-*N*'-acyl(aroyl)thiourea ligands HL[1-15] used in this study are presented in Figure 2.2 with their names and abbreviations given. Of the selected ligands, HL[1-9] were synthesized, while HL[10-15] were donated by Dr S. Mtongana, a former student from Prof Koch's research group. The ligands HL[1-7] are symmetrically substituted and will be presented in **chapters 3, 4 and 6**, whereas HL[8-15] belong to the group of asymmetrically substituted *N*,*N*-dialkyl-*N*'-acylthioureas and will be examined in **chapters 5 and 6**.

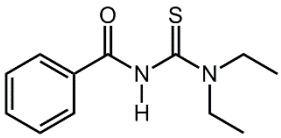

HL[1]
N,N-diethyl-N'-benzoylthiourea

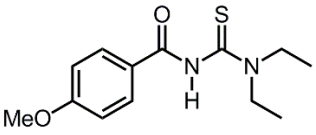

HL[2]
N,N-diethyl-N'-4-methoxy-benzoylthiourea

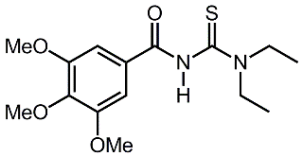

HL[3]
N,N-diethyl-N'-3,4,5-trimethoxy-benzoylthiourea

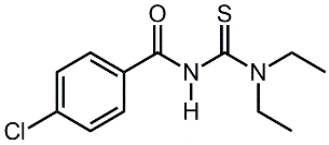

HL[4]
N,N-diethyl-N'-4-chloro-benzoylthiourea

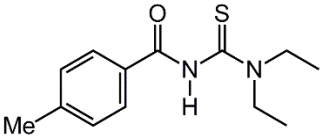

HL[5]
N,N-diethyl-N'-4-methyl-benzoylthiourea

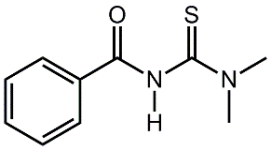

HL[6]
N,N-dimethyl-N'-benzoylthiourea

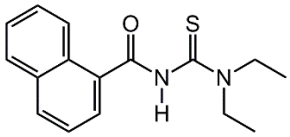

HL[7]
N,N-diethyl-N'-1-naphthoylthiourea

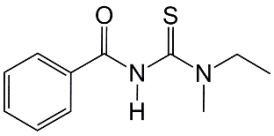

HL[8]
N-methyl,N-ethyl-N'-benzoylthiourea

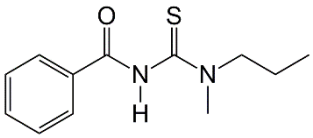

HL[9]
N-methyl,N-propyl-N'-benzoylthiourea

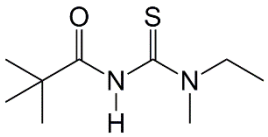

HL[10]
N-methyl,N-ethyl-N'-(2,2-dimethylpropanoyl)thiourea

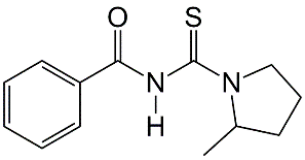

HL[11]
N-methylpirrolidyl-N'-benzoyllthiourea

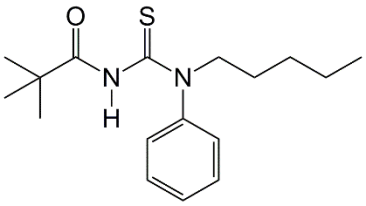

HL[12]
N-pentyl,N-phenyl-N'-(2,2-dimethylpropanoyl)thiourea

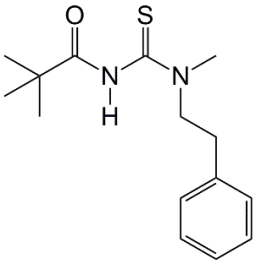

HL[13]
N-Phenethyl,N-methyl-N'-(2,2-dimethylpropanoyl)thiourea

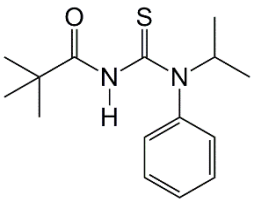

HL[14]
N-Isopropyl,N-phenyl-N'-(2,2-dimethylpropanoyl)thiourea

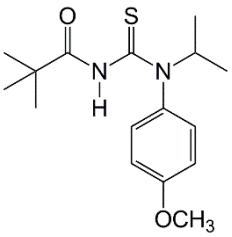

HL[15]
N-Isopropyl,N-(4-methoxy-phenyl)-N'-(2,2-dimethylpropanoyl)thiourea

Figure 2.2. A list of selected *N,N*-dialkyl-*N'*-acyl(aroyl)thioureas used for this study.

2.1.2. Synthesis of *cis*-[M(L^n-κ*S*,*O*)$_2$] (M = Pt(II), Pd(II)) complexes

Treatment of a solution of the *N*,*N*-dialkyl-*N*'-acyl(aroyl)thioureas (HL$^{1\text{-}15}$) with appropriate amounts of K_2PtCl_4 or K_2PdCl_4 in an acetonitrile:water mixture (50:50 % v/v) forms exclusively the *cis*-[M(L^n-κ*S*,*O*)$_2$] (M = Pt(II) or Pd(II)) complexes. The reaction was aided by the presence of stoichiometric amounts of sodium acetate base which assists ligand deprotonation. This occurs presumably *via* the loss of a proton from the neutral ligands to yield anionic intermediates, which then coordinates to the metal ion to generate the neutral *cis*-[M(L^n-κ*S*,*O*)$_2$] (M = Pt(II) or Pd(II)) complex as illustrated in Figure 2.3. The Pd^{II} ion coordinates strongly to two *N*,*N*-dialkyl-*N*'-aroylthioureas through the carbonyl oxygen and thiocarbonyl sulfur. The process is accompanied by the release of potassium chloride which is removed by dissolution upon addition of water, while the insoluble *cis*-[M(L^n-κ*S*,*O*)$_2$] (M = Pt(II) or Pd(II)) complex precipitates out.

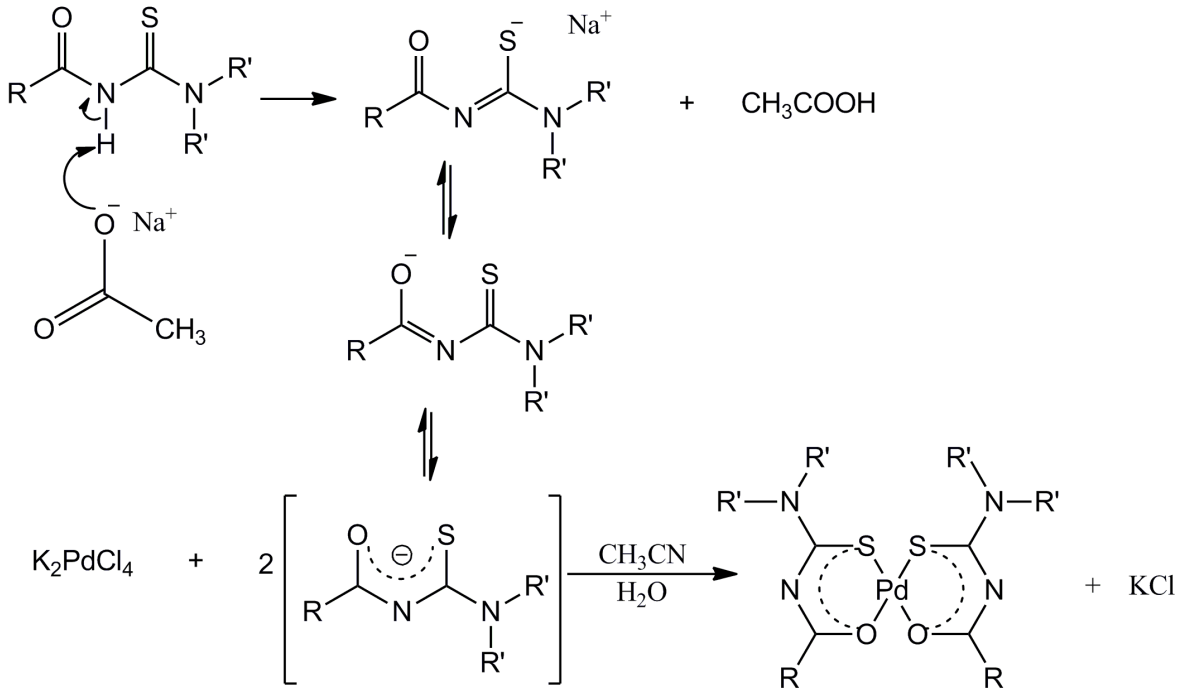

Figure 2.3. Synthesis of palladium(II) complexes of *N*,*N*-dialkyl-*N*'-acyl(aroyl)thioureas.

2.1.3. Characterization of *N*,*N*-dialkyl-*N'*-acylthioureas and *cis*-[M(L-κ*S*,*O*)$_2$] (M = Pt(II) or Pd(II)) complexes

The ligands HL[1-15] were characterized by elemental analysis, melting point determination, as well as ^{1}H and ^{13}C NMR spectroscopy. Figure 2.4 gives the representative ^{1}H NMR spectrum of *N*,*N*-diethyl-*N'*-1-napthoylthiourea (HL[7]) from which two salient features are observed.

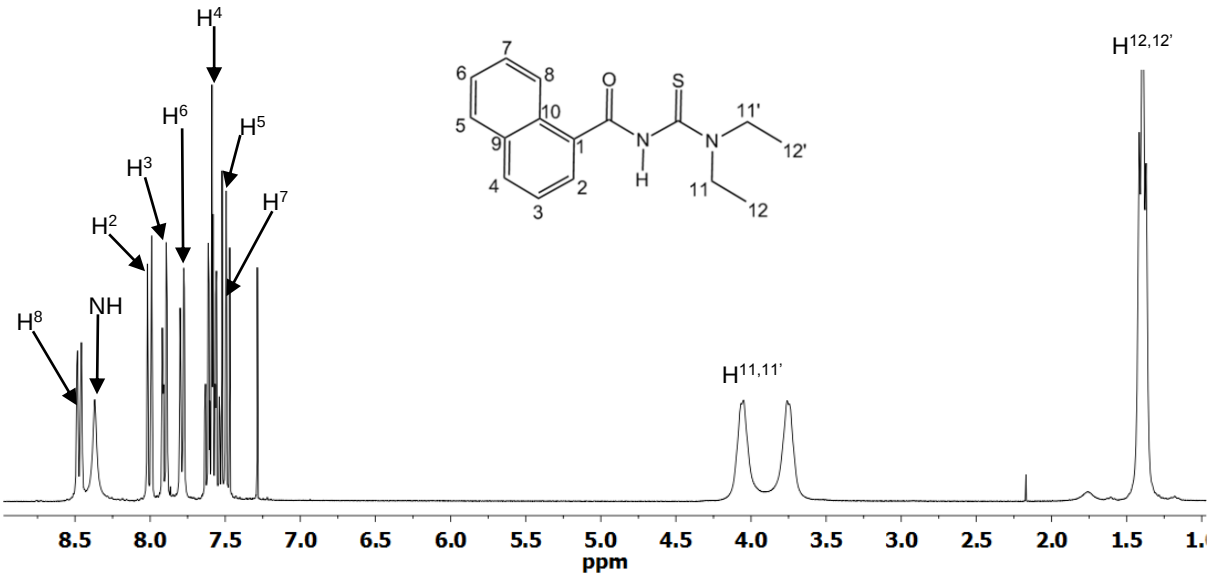

Figure 2.4. ^{1}H NMR spectrum and assignments of *N*,*N*-diethyl-*N'*-1-naphthoylthiourea (HL[7]) in chloroform-*d* at 25°C.

A broad N-H singlet is observed downfield at chemical shift (δ) of 8.34 ppm. This N-H singlet is also observed for the other ligands and occurs at similar chemical shift positions for *N*,*N*-diethyl-*N'*-benzoylthiourea and *N*,*N*-diethyl-*N'*-4-chloro-benzoylthiourea at chemical shifts of 8.34 ppm and 8.35 ppm respectively. A slight upfield shift occurs for the N-H singlets of *N*,*N*-diethyl-*N*'-4-methoxy-benzoylthiourea (δ = 8.21 ppm) and *N*,*N*-diethyl-*N*'-4-methyl-benzoylthiourea (δ = 8.27 ppm) presumably induced by the presence of electron-releasing methoxy and methyl groups respectively at the *para* position of the phenyl ring. Significant downfield shifts relative to that of *N*,*N*-diethyl-*N'*-benzoylthiourea are observed for *N*,*N*-diethyl-*N'*-3,4,5-trimethoxy-benzoylthiourea (δ = 8.55 ppm). A downfield N-H shift is also observed for *N*,*N*-dimethyl-*N'*-benzoylthiourea (δ = 8.69 ppm). Substitutions of the phenyl ring show a slight upfield shift for the *ortho* H$^{2,2'}$ phenyl protons of *N*,*N*-diethyl-*N'*-4-methoxy-benzoylthiourea (δ = 7.79 ppm), *N*,*N*-diethyl-*N*'-4-chloro-benzoylthiourea (δ = 7.77 ppm), *N*,*N*-diethyl-*N'*-4-methyl-benzoylthiourea (δ = 7.72 ppm), *N*,*N*-dimethyl-*N'*-benzoylthiourea (δ = 7.81 ppm), relative to *N*,*N*-diethyl-*N'*-benzoylthiourea (δ = 8.11 ppm). In *N*,*N*-diethyl-*N'*-

3,4,5-trimethoxy-benzoylthiourea, the three electron-releasing methoxy substituents induce a marked upfield shift of the $H^{2,2'}$ protons (δ = 7.05 ppm) relative to *N*,*N*-diethyl-*N'*-benzoylthiourea. Figure 2.4 also shows two separate multiplets centred at δ = 3.86 ppm for *N*,*N*-diethyl-*N'*-1-napthoylthiourea (HL^7). These represent the two magnetically inequivalent N-CH_2 groups. This is caused by partial double bond character in the C-N bond as shown in the different resonance structures in Figure 2.5. The other *N*,*N*-dialkyl-*N*'-acylthioureas also show two separate sets of *N*-CH_2 and *N*-CH_3 multiplets.

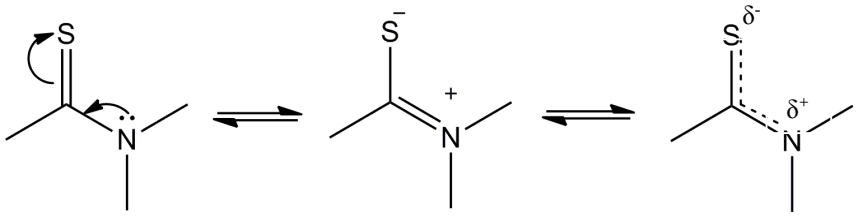

Figure 2.5. Representation of restricted rotation across C-N bond in *N*,*N*-dialkyl-*N*'-acyl(aroyl)thioureas.

The *cis*-[$M(L^n$-κ*S*,*O*$)_2$] (M = Pt(II) or Pd(II)) complexes derived from the *N*,*N*-dialkyl-*N'*-acyl(aroyl)thioureas were characterized by ^{1}H-, and $^{13}C\{^1H\}$ NMR spectroscopy, melting point determination as well as elemental composition analyses. For complexes in which suitable crystals could be obtained, X-ray crystallography was used to ascertain their c*is*-κ*S*,*O* mode of coordination. In general, two pertinent features can be addressed in the ^{1}H NMR of the *cis*-[$M(L^n$-κ*S*,*O*$)_2$] complexes relative to their corresponding HL ligands. Firstly, complete disappearance occurs for the broad amido N-H singlet which was evident in the ^{1}H NMR spectra of the ligands. The disappearance of the N-H resonances indicates ligand deprotonation. Also, smaller chemical shift differences occur between the two N-CH_2 resonances in all the *cis*-[$M(L^n$-κ*S*,*O*$)_2$] complexes relative to the corresponding ligands. This suggests that restricted C-N rotation in the *cis*-[$M(L^n$-κ*S*,*O*$)_2$] complexes occurs to a relatively lower extent compared to the ligands. The disappearance of N-H resonances in the *cis*-[$M(L^{1-15}$-κ*S*,*O*$)_2$] (M = Pt(II) or Pd(II)) complexes are fully consistent with changes in ^{1}H NMR resonances reported for similar complexes.[27,31,32,99]

The ^{1}H NMR spectra of the *cis*-[$Pd(L^{1-6}$-κ*S*,*O*$)_2$] complexes are provided in Figures A2.1 to A2.6, with the numbering scheme used for atoms also given. Figure A2.1 shows the ^{1}H NMR spectrum of the *cis*-[$Pd(L^1$-κ*S*,*O*$)_2$] complex (HL^1 = *N*,*N*-diethyl-*N'*-benzoylthiourea). This serves as a starting point for assigning the other complexes and to investigate any possible

effect of ligand substituents on chemical shift positions. From Figure A2.1, partially resolved doublet of doublets are evident downfield at δ = 8.25 ppm representing the aromatic $H^{2,2'}$ protons ($^3J_{H2\text{-}H3}$ = 8.1 Hz, $^4J_{H1\text{-}H3}$ = 1.4 Hz) as well as two partially resolved multiplets shifted upfield for $H^{2',2'}$ protons at δ = 7.49 ppm ($^3J_{H2\text{-}H1,H2\text{-}H3}$ = 7.2 Hz) and $H^{3,3}$ protons at δ = 7.41 ppm ($^3J_{H3\text{-}H2}$ = 7.9 Hz, $^4J_{H3\text{-}H1}$ =1.6 Hz). The low field region of the spectrum reveals a set of overlapping quartets (δ = 3.85 ppm) and two well-resolved triplets centred at δ = 1.31 ppm, representing the sets of magnetically inequivalent methylene and methyl protons respectively.

In general, the introduction of ligand substituents at different phenyl positions does not markedly affect the relative chemical shift positions for the *cis*-[Pd($L^{1\text{-}6}$-κ*S*,*O*)$_2$] complexes. Inspection of the ^{1}H NMR spectrum of the *cis*-[Pd(L^2-κ*S*,*O*)$_2$] complex (HL^2 = *N*,*N*-diethyl-*N'*-4-methoxy-benzoylthiourea) shows no significant shielding of the $H^{2,2'}$ protons and aliphatic protons by introduction of an electron-releasing methoxy substituent at the *para* position of the phenyl ring (Figure A2.2). However, the nearby $H^{3,3'}$ protons are significantly shielded by *ca* 0.58 ppm. This is associated with a greater $^3J_{H1\text{-}H2}$ coupling of 8.91 Hz compared to that of the *cis*-[Pd(L^1-κ*S*,*O*)$_2$] complex ($^3J_{H1\text{-}H2}$ = 8.1 Hz). Similar chemical shift trends are observed between the *cis*-[Pd(L^5-κ*S*,*O*)$_2$] (HL^5 = *N*,*N*-diethyl-*N'*-4-methyl-benzoylthiourea) in Figure A2.5 and *cis*-[Pd(L^1-κ*S*,*O*)$_2$] complexes. However, for the *cis*-[Pd(L^5-κ*S*,*O*)$_2$] complex a relatively lower upfield shift of *ca* δ 0.28 ppm occurs for the $H^{2,2}$ proton (^3J = 8.2 Hz) compared to that of *cis*-[Pd(L^1-κ*S*,*O*)$_2$]. A relatively smaller upfield shift of *ca* 0.11 ppm occurs for the $H^{2,2'}$ doublets in the *cis*-[Pd(L^4-κ*S*,*O*)$_2$] complex (HL^4 = *N*,*N*-diethyl-*N'*-4-chloro-benzoylthiourea) provided in Figure A2.4. The presence of three methoxy groups at the *ortho*, *meta* and *para* positions of the phenyl ring produces a marked upfield shift for $H^{2,2'}$ protons (δ = 0.70 ppm) in *cis*-[Pd(L^3-κ*S*,*O*)$_2$] (HL^3 = *N*,*N*-diethyl-*N'*-3,4,5-trimethoxy-benzoylthiourea; see Figure A2.3). Variation of the thioamido alkyl chain length does not significantly affect the shielding of the aromatic protons of the *cis*-[Pd(L^6-κ*S*,*O*)$_2$] complex (HL^6 = *N*,*N*-dimethyl-*N'*-benzoylthiourea; see Figure A2.6) relative to *cis*-[Pd(L^1-κ*S*,*O*)$_2$]. However, the two magnetically inequivalent methyl protons in *cis*-[Pd(L^6-κ*S*,*O*)$_2$] directly attached to the thioamido nitrogen atom experience increased deshielding.

The assignment of the ^{1}H and ^{13}C{^{1}H} resonances of the *cis*-[Pd($L^{1\text{-}6}$-κ*S*,*O*)$_2$] complexes was relatively straightforward except for *cis*-[Pd(L^7-κ*S*,*O*)$_2$] (HL^7 = *N*,*N*-diethyl-*N'*-1-

naphthoylthiourea) in which the naphthyl moiety produces interesting resonance features as depicted in Figure 2.6.

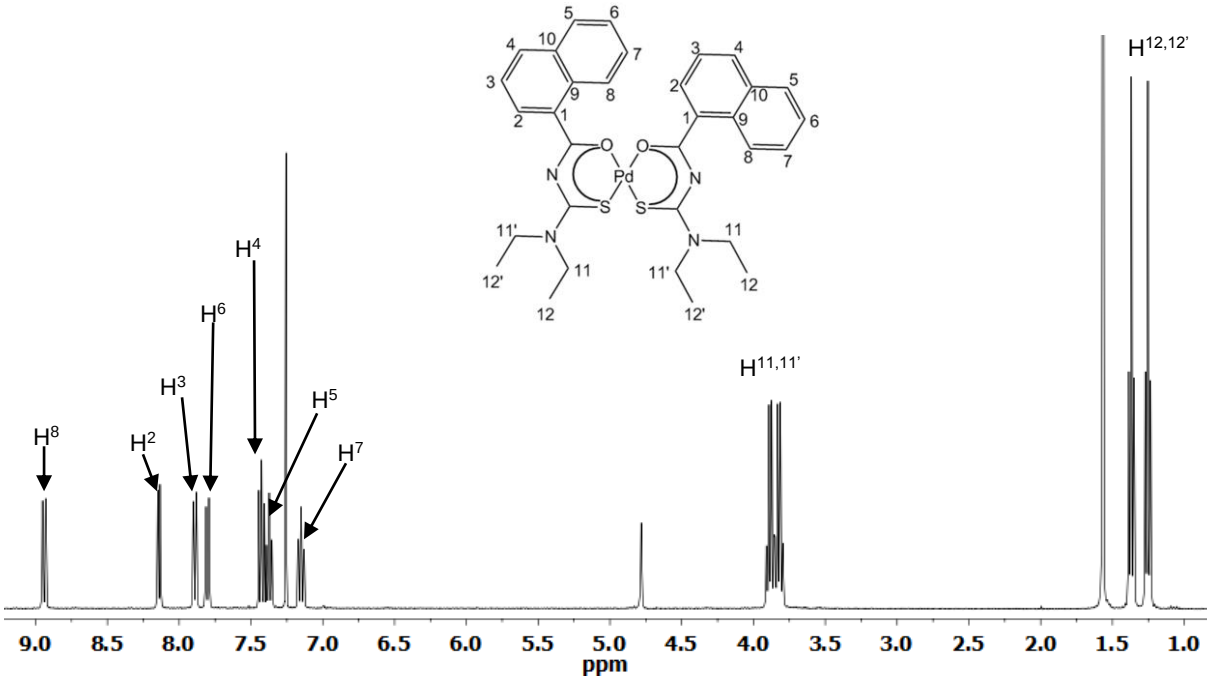

Figure 2.6. ^{1}H NMR spectrum of *cis*-bis(*N*,*N*-diethyl-*N'*-1-naphthoylthioureato-κ^{2}*S*,*O*)palladium(II) *cis*-[Pd(L^{7}-κ*S*,*O*)$_{2}$] in chloroform-*d* at 25°C.

The downfield resonances of the *cis*-[Pd(L^{7}-κ*S*,*O*)$_{2}$] complex, HL^{7} = *N*,*N*-diethyl-*N*'-1-napthoylthiourea (Figure 2.6) clearly show the N-H disappearance as well as seven sets of resonances accounting for the naphthyl protons H^{2} to H^{8}. In this complex, the H^{8} and H^{2} protons are coplanar with and pointing towards the six-membered chelate ring and are expected to be more deshielded compared to the other naphthyl protons. A marked deshielding of the H^{8} proton is observed (δ = 8.94 ppm) resulting in a partially resolved doublet of doublets with a strong $^{3}J_{H8\text{-}H7}$ coupling of 8.69 Hz and a relatively smaller $^{4}J_{H8\text{-}H6}$ coupling of 0.9 Hz. This significant downfield shift is most likely as a consequence of the electronic or steric influence of the presumably bulky naphthyl moiety. A similar but relatively lower $^{3}J_{H2\text{-}H3}$ coupling of 7.3 Hz occurs for the H^{2} proton. As in the case of the H^{8} proton, substitution of the naphthyl moiety and associated chemical shift anisotropy of the H^{2} proton coplanar with the six-membered chelate ring induces a downfield shift relative to the other protons. Also, the signals representing the H^{3} and H^{6} protons appear as well resolved sets of triplets with $^{3}J_{H4\text{-}H3}$ coupling of 8.2 Hz and $^{3}J_{H5\text{-}H6}$ coupling of 8.2 Hz respectively, while the set of H^{3} triplets do overlap. A relatively higher shielding is experienced for the H^{4} and H^{5} protons, both resulting to two sets

of overlapping triplets. For the more shielded H^7 proton, similar coupling patterns are observed as that of the H^4 and H^6 protons resulting to overlapping multiplets with $^3J_{H7\text{-}H8,H7\text{-}H6}$ coupling of 7.8 Hz and $^4J_{H7\text{-}H5}$=1.4 Hz.

With all assigned protons of the *cis*-[Pd(L^7-κ*S*,*O*)$_2$] complex, assignment of the naphthyl carbons was achieved by means of ^{13}C-, ^{1}H, gradient HSQC and HMBC correlation experiments. The ^{1}H region of the HSQC and HMBC (Figures 2.7 and 2.8) shows traces of additional resonances which could have been due to impurities obtained after dissolving the *cis*-[Pd(L^7-κ*S*,*O*)$_2$] complex in chloroform. The gradient HSQC plot (see Figure A2.7) for *cis*-[Pd(L^7-κ*S*,*O*)$_2$] in chloroform-*d* is based on direct ^{13}C chemical shift correlation with all the nearby protons. It shows correlation across the molecule and is particularly useful for distinguishing the naphthyl carbons C^2-C^8 from the quaternary carbons C^1, C^9 and C^{10} at δ = 131.5, 133.9 and 135.2 ppm respectively. Full assignment of the other carbons C^1, C^9, C^{10}, C(S) and C(O) was achieved using the ^{1}H-^{13}C HMBC correlation plot (Figure 2.7) over longer ranges of between 2-4 bonds. This shows two C-H bond correlation between the methyl and methylene carbon atoms and protons as well as those of the naphthyl carbons C^2-C^8. Inspection of the aromatic region of the HMBC plot (Figure 2.8) leads to the full assignment of the carbons based on the following C-H correlations: H^8 to C^5 at δ = 125.6 ppm (4 bonds), C^9 (2 bonds) and C^{10} (3 bonds); H^2 to C^1 (2 bonds) and C^8 (4 bonds); H^3 to C^3 at δ = 128.1 ppm (2 bonds) and C^1 (2 bonds); H^6 to C^4 (4 bonds) and C^8 at δ = 131.3 ppm (3 bonds); H^4 to C^2 at δ = 121.9 ppm (3 bonds), C^9 (3 bonds) and C^{10} (2 bonds); H^5 to C^4 at δ = 126.7 ppm (3 bonds) and C^{10} (2 bonds); H^7 to C^6 at δ = 127.1 ppm (2 bonds) and C^1 (4 bonds).

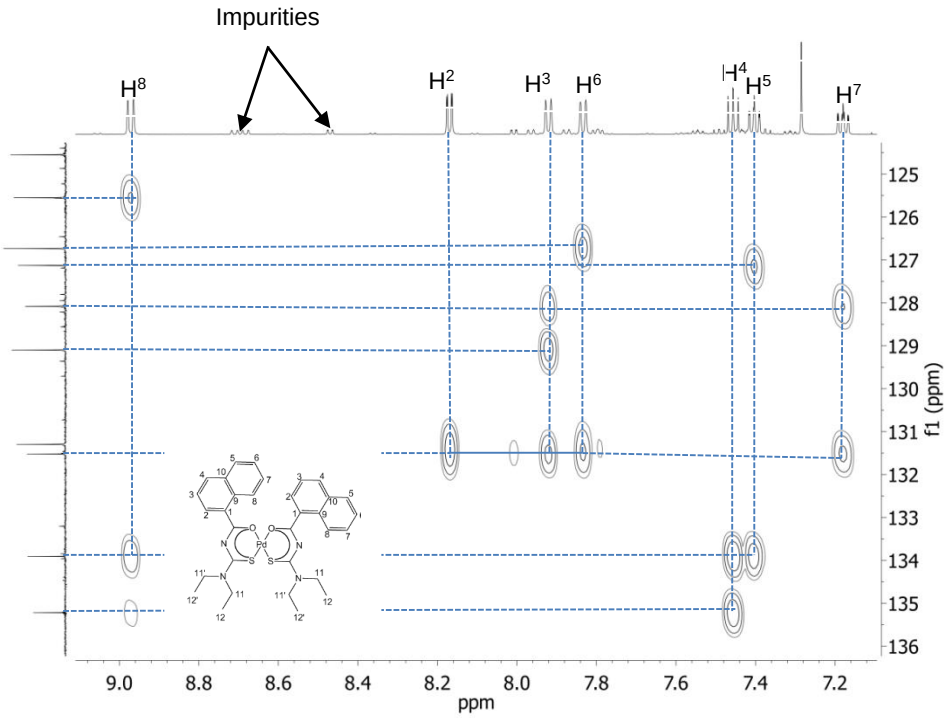

Figure 2.7. Assignment of the HMBC spectrum for the naphthyl region of *cis*-[Pd(L^7-κ*S*,*O*)$_2$] in chloroform-*d* at 25°C showing correlations between ^{13}C and ^{1}H.

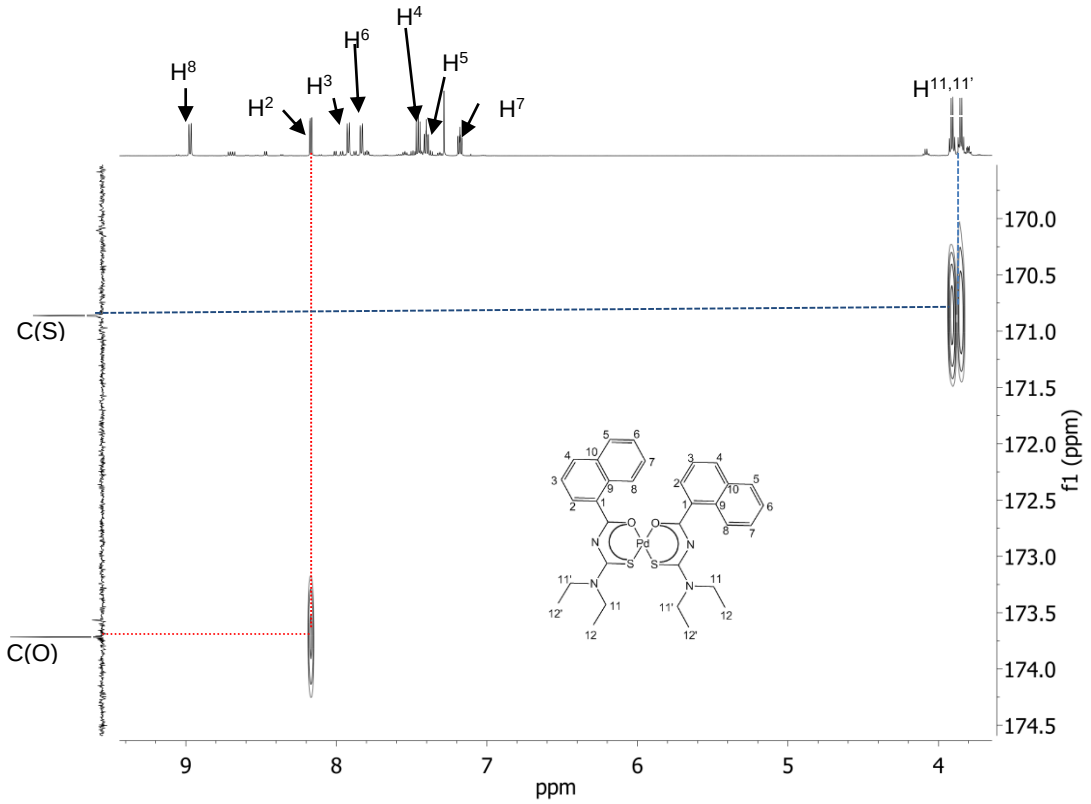

Figure 2.8. Assignment of the carbonyl and thiocarbonyl carbons of the naphthyl group from the HMBC spectrum of *cis*-[Pd(L^7-κ*S*,*O*)$_2$] in chloroform-*d* at 25°C.

The HMBC spectrum was particularly useful for distinguishing the C(O) and C(S) carbons in *cis*-[Pd(L^7-κ*S*,*O*)$_2$] as is depicted in Figure 2.8. The carbonyl carbon experiences a greater chemical shift anisotropy and consequently is more deshielded than the thiocarbonyl carbon. Figure 2.8 shows that the thiocarbonyl carbon at δ = 170.9 ppm experiences a three bond correlation through the C-N bond to the methylene hydrogens and does not correlate to any of the naphthyl carbons by long range coupling. The assignment of the carbonyl carbon at δ = 173.7 ppm is based on its three bond correlation to the H^2 proton *via* the *ipso* carbon C^1 which is not possible with C(S).

Characterization of the ligands and *cis*-[Pd(L^n-κ*S*,*O*)$_2$] complexes was also performed by FT-IR. The ligands reveal characteristic broad ν(N-H) stretching frequencies in the region 3450-3100 cm^{-1} and ν(C=O) stretching mode around the region 1700-1650 cm^{-1} as shown in Table 2.1. The ligands HL^{1-5} show very similar ν(N-H) and ν(C=O) stretching frequencies consistent with their changes in the ^{1}H NMR resonances.

Table 2.1. Selected N-H and C=O stretching frequencies for HL ligands and *cis*-[Pd(L-κ*S*,*O*)$_2$] complexes.

	ν(N-H) /cm^{-1}	**ν(CO) /cm^{-1}**
HL^1	3260.92	1649.97
***cis*-[Pd(L^1-κ*S*,*O*)$_2$]**	-	1485.55
HL^2	3297.04	1631.81
***cis*-[Pd(L^2-κ*S*,*O*)$_2$]**	-	1516.39
HL^4	3272.77	1642.18
***cis*-[Pd(L^4-κ*S*,*O*)$_2$]**	-	1513.24
HL^5	3291.06	1637.90
***cis*-[Pd(L^5-κ*S*,*O*)$_2$]**	-	1483.84
HL^6	3133.87	1681.62
***cis*-[Pd(L^6-κ*S*,*O*)$_2$]**	-	1499.99
HL^7	3171.41	1676.31
***cis*-[Pd(L^7-κ*S*,*O*)$_2$]**	-	1488.82

The FT-IR spectra of *cis*-[Pd($L^{1,4,5,6}$-κ*S*,*O*)$_2$] complexes are provided in Figures A2.8 to A2.11, while that of the *cis*-[Pd(L^7-κ*S*,*O*)$_2$] complex relative to the uncoordinated *N*,*N*-diethyl-*N*'-1-napthoylthiourea (HL^7) is given in Figure 2.9. The stretching frequencies of all *cis*-[Pd(L^n-κ*S*,*O*)$_2$] complexes are provided in Table 2.1. It is evident that the ν(N-H) stretching bands which are observed in the free ligands (ν(N-H) = 3171.41 cm^{-1} for *N*,*N*-diethyl-*N'*-1-naphthoylthiourea) are absent in the FT-IR spectra of *cis*-[Pd(L^{1-7}-κ*S*,*O*)$_2$] complexes indicative of ligand deprotonation. In addition, shifts to lower frequencies for ν(C=O) 1488.82 cm^{-1}) stretching bands are observed compared to that of the unbound ligand (ν(C=O) = 1676.31 cm^{-1}) further confirming coordination of ligands to Pd^{II} through the carbonyl group. The disappearance of the broad ν(N-H) bands as well as shift to lower vibration frequencies of the ν(C=O) bands observed for the *cis*-[Pd(L^{1-7}-κ*S*,*O*)$_2$] complexes is consistent with the changes in ^{1}H NMR chemical shifts and has been observed for closely related complexes.[27,30,31]

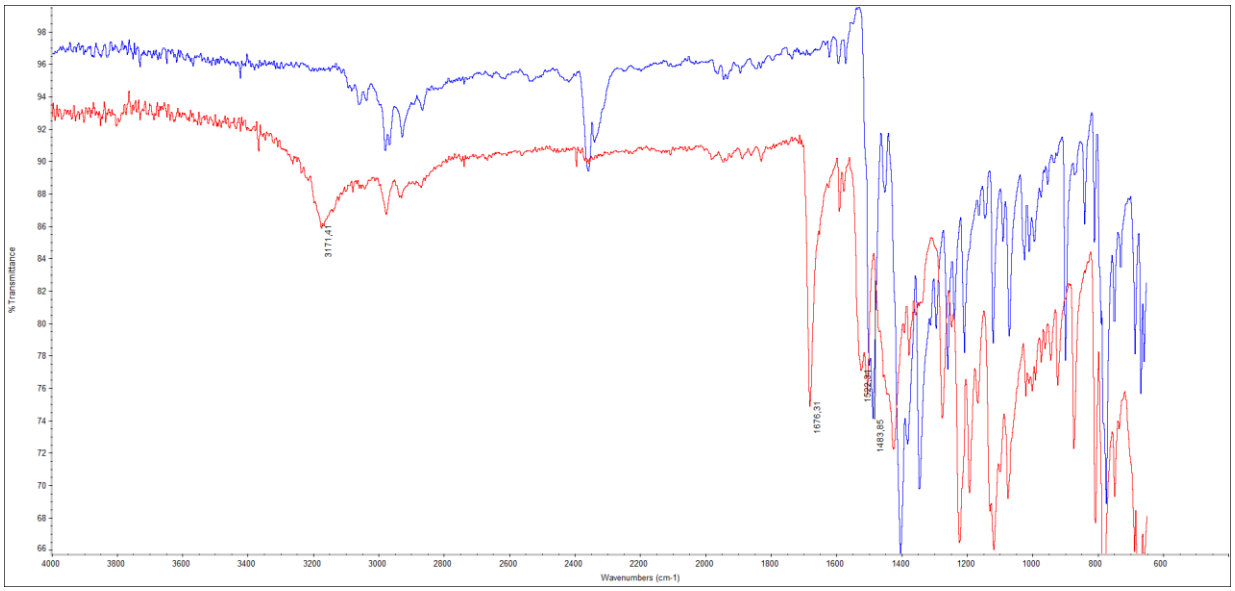

Figure 2.9. Overlaid FT-IR spectra of *N*,*N*-diethyl-*N*'-1-napthoylthiourea, HL^7 (red) and *cis*-[Pd(L^7-κ*S*,*O*)$_2$] (blue).

2.2. Crystal structures of *cis*-[Pd(L^n-κ*S*,*O*)$_2$] complexes

Crystals of the *cis*-[Pd(L^n-κ*S*,*O*)$_2$] complexes suitable for single-crystal X-ray diffraction were carefully grown by slow evaporation in acetonitrile solutions in the absence of light, as these readily isomerize to their *trans* counterpart upon exposure to daylight. The refinement data for all complexes and their important bond lengths and angles are given in Tables A2.1 and A2.2. Significant changes in C-O, C-S and C-N bond distances are observed for the series of complexes relative to their unbound ligands as shown in Table 2.2. These are well within the range of values reported for related complexes.[10,27,30-33] In general, a decrease in C-O and C-S bond distances is observed for the complexes relative to their free ligands. This signifies electron delocalization and chelate ring formation upon coordination of Pd(II) to the ligands. A slight shortening of the average C-N bonds is also observed for the complexes relative to their respective ligands, confirming ligand deprotonation upon coordination. This is consistent with the ^{1}H NMR and FT-IR results discussed in section 2.1.3. All the *cis*-[Pd(L$^{2,4-7}$-κ*S*,*O*)$_2$] structures show that Pd is coordinated to two ligands in a *cis*-κ*S*,*O* manner. The Pd-O and Pd-S bond distances presented in Table 2.3, show that for the *cis*-[Pd(L$^{2.4-7}$-κ*S*,*O*)$_2$] complexes, the presence of different ligand substituents has no significant effect on the bond distances. This suggests that different ligand substituents do not significantly affect the extent of delocalization of electrons across the six-membered chelate rings.

Table 2.2. Selected C=O, C=S and C-N bond lengths (Å) in the ligands (HL^2),[100] (HL^4),[101] (HL^5),[102] (HL^6),[103] and their respective *cis*-[Pd(L-κ*S*,*O*)$_2$] complexes.

	C=O	**C=S**	**C-N**
HL^2	1.237(2)	1.666(2)	1.391(2)
***cis*-[Pd(L^2-κ*S*,*O*)$_2$]**	1.264(2)	1.744(2)	1.336(2)
HL^4	1.228(3)	1.663(2)	1.395(3)
***cis*-[Pd(L^4-κ*S*,*O*)$_2$]**	1.268(6)	1.744(5)	1.344(7)
HL^5	1.223(4)	1.656(3)	1.391(4)
***cis*-[Pd(L^5-κ*S*,*O*)$_2$]**	1.265(8)	1.738(7)	1.36(1)
HL^6	1.213(2)	1.676(2)	1.393(2)
***cis*-[Pd(L^6-κ*S*,*O*)$_2$]**	1.269(4)	1.741(4)	1.334(4)

Table 2.3. Selected Pd-O, Pd-S and C-N bond lengths (Å) of *cis*-[Pd(L-κ*S*,*O*)$_2$] complexes.

	Pd-O	**Pd-S**
***cis*-[Pd(L^2-κ*S*,*O*)$_2$]**	2.012(1)	2.2351(4)
***cis*-[Pd(L^4-κ*S*,*O*)$_2$]**	2.016(5)	2.246(1)
***cis*-[Pd(L^5-κ*S*,*O*)$_2$]**	2.020(6)	2.242(2)
***cis*-[Pd(L^6-κ*S*,*O*)$_2$]**	2.025(4)	2.233(9)
***cis*-[Pd(L^7-κ*S*,*O*)$_2$]**	2.032(2)	2.224(1)

Figure 2.10 depicts the crystal structure of *cis*-[Pd(L^2-κ*S*,*O*)$_2$] (HL^2 = *N*,*N*-diethyl-*N*'-4-methoxy-benzoylthiourea). The compound crystallizes in the monoclinic space group P2$_1$/n, with Pd coordinated to sulfur and oxygen atoms of the ligand in a *cis* configuration. There are no marked differences in the average Pd-S (2.235(4) Å) and Pd-O (2.012(4) Å bond lengths compared to the *cis*-[Pd(L^1-κ*S*,*O*)$_2$] complex,[17] indicating that the presence of the *para* substituted electron-donating methoxy group on the phenyl ring does not affect the delocalization of electron density across the chelate ring. A closer look at the S(1A)-Pd1-O(1B) 178.94° and S(1B)-Pd1-O(1A) 177.52° bond angles in the six-membered metallocycle also indicates slight deviation from a perfect square planarity of 180°. A deviation from the coordination plane for the two phenyl rings is observed represented by the C(1A)-C(8A)-N(1A)-C(9A) -179.3(1) and C(1B)-C(8B)-N(1B)-C(9B) -178.6(1) torsion angles.

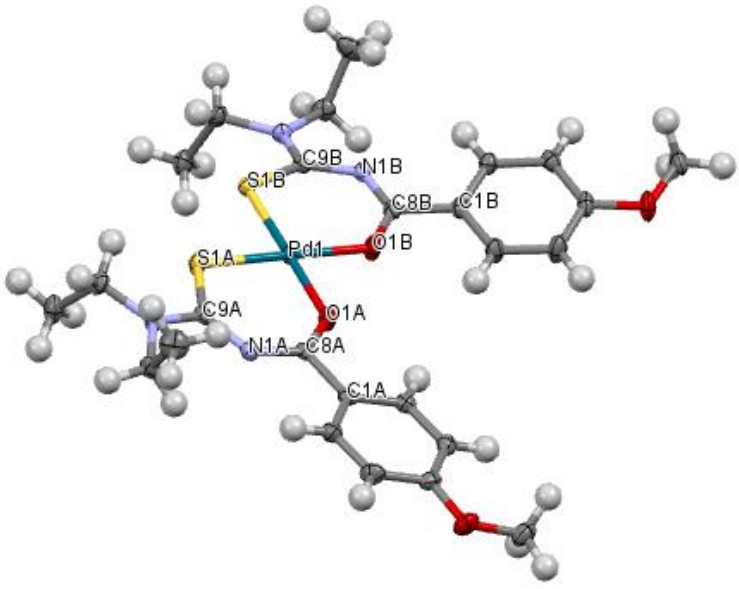

Figure 2.10. Molecular structure from single-crystal X-ray difraction of *cis-bis(N,N-diethyl-N'-4-methoxy-benzoylthioureato-κ^{2}S,O)palladium(II) cis*-[Pd(L^2-κ*S*,*O*)$_2$] isolated from acetonitrile by slow evaporation.

Figure 2.11 shows the molecular structure of *cis*-[Pd(L^4-*S*,*O*)$_2$] (HL^4 = *N*,*N*-diethyl-*N'*-4-chloro-benzoylthiourea). The *cis*-[Pd(L^4-κ*S*,*O*)$_2$] complex crystallizes in the triclinic space group P-1. The Pd-O bond distance of 2.016(5) Å is essentially the same as that reported in the literature for the Pd(II) complex with *N*,*N*-diethyl-*N*'-benzoylthiourea.[17] This suggests that the presence of chloro substituents at the *para* position of the phenyl ring has no significant effect on the extent of electron delocalization across the six-membered Pd-O-C-N-C-S chelate. The two chelate rings in *cis*-[Pd(L^4-κ*S*,*O*)$_2$] are slightly distorted from ideal square planarity as illustrated by the S-Pd-O bond angles of 176.8(1)° and 178.2(1)°. The two phenyl rings are slightly out of the coordination plane represented by C-N-C-C torsion angles of 172.4(4)° and 178.1(4)°.

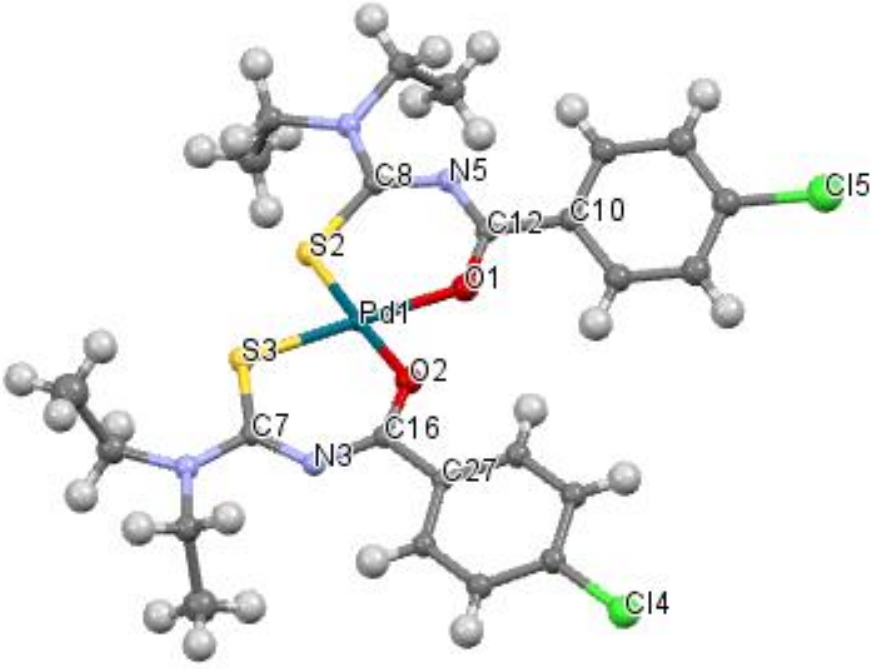

Figure 2.11. Molecular structure from single-crystal X-ray difraction of *cis-bis(N,N-diethyl-N'-4-chloro-benzoylthioureato-κ²S,O)palladium(II)cis*-[Pd(L^4-κ*S*,*O*)$_2$] isolated from acetonitrile by slow evaporation.

In the *cis*-[Pd(L^5-κ*S*,*O*)$_2$] complex, *cis*-κ*S*,*O* coordination of Pd(II) to two *N*,*N*-diethyl-*N*'-4-methyl-benzoylthiourea ligands is also evident as shown in Figure 2.12. The compound crystallizes in the triclinic space group P-1. The Pd-O bond and Pd-O distances of 2.020(6) Å are essentially the same as that of *cis*-[Pd($L^{2,4,7}$-κ*S*,*O*)$_2$]. A slight distortion from square planarity is also observed from the S-Pd-O bond angles of 176.8(1)° and 178.2(1) 175.7(2)° and 176.8(2)°.

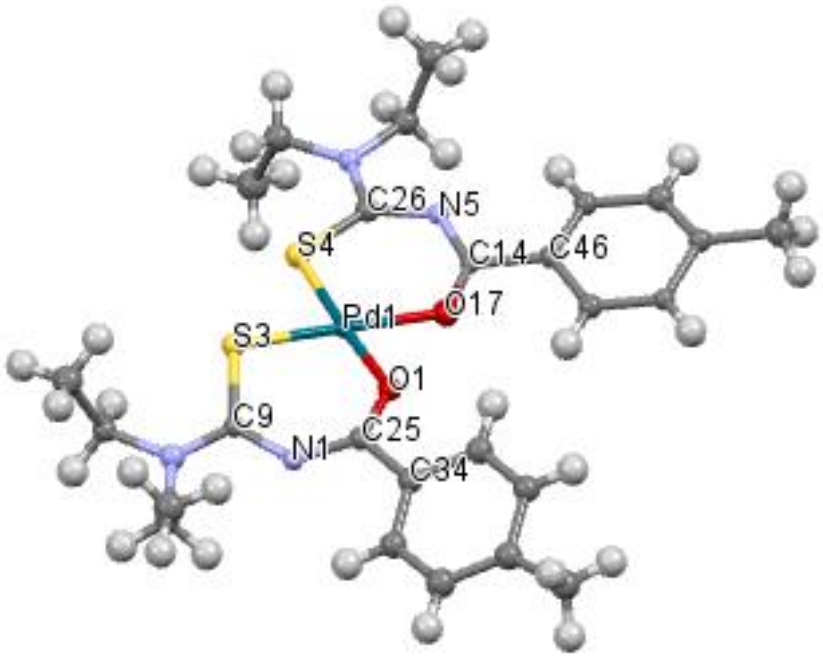

Figure 2.12. Molecular structure from single-crystal X-ray diifraction of *cis-bis(N,N-diethyl-N'-4-methyl-benzoylthioureato-κ^2S,O)palladium(II)* *cis*-[Pd(L^5-κ*S*,*O*)$_2$] isolated from acetonitrile solutions by slow evaporation.

The *cis*-[Pd(L^6-κ*S*,*O*)$_2$] structure (Figure 2.13) crystallizes in the monoclinic space group $P2_1/c$. No significant difference Pd-O bond length is observed (2.025(4) Å) compared to the *cis*-[Pd(L^1-κ*S*,*O*)$_2$] complex (2.023(1) Å).[17] However, a slight shortening of the Pd-S bond distance (2.233(9) Å) is observed compared to *cis*-[Pd(L^1-κ*S*,*O*)$_2$] probably due to electronic effects of the smaller thioamido substituents on the chelate ring. Deviations from square planarity are represented by the S1(A)-Pd(1)-O(1B) 176.07(7)° and S(1B)-Pd(1)-O(1A) 176.97(7)° bond angles, while the two phenyl rings deviate from the coordination plane as evident from the C(8A)-N(2A)-C(1A)-C(2A) -172.37(3)° and C(8B)-N(2B)-C(1B)-C(2B) 172.15(3)°.

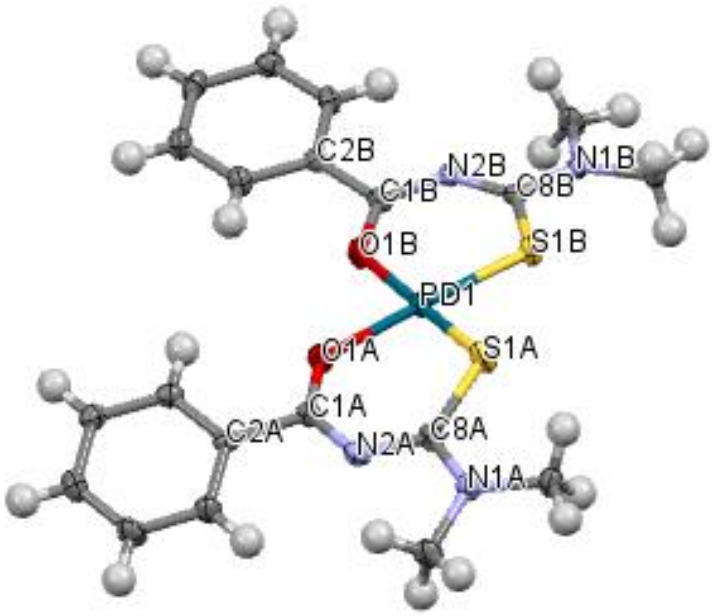

Figure 2.13. Molecular structure from single-crystal X-ray diifraction of *cis-bis(N,N-dimethyl-N'-benzoylthioureato-κ^2S,O)palladium(II)* *cis*-[Pd(L^6-κ*S*,*O*)$_2$] isolated from acetonitrile by slow evaporation.

The *cis*-[Pd(L^7-κ*S*,*O*)$_2$] complex crystallizes in the orthorhombic space group Pbcn, with the Pd atom coordinating to the sulfur and oxygen atoms in a *cis*-κ*S*,*O* manner. Its molecular structure and crystal packing are given in Figure 2.14 (a) and (b) respectively. There are no significant differences in the average Pd-S (2.234 Å) and Pd-O (2.023 Å) bond lengths of this isomer compared to those of the *cis*-[Pd(L^1-κ*S*,*O*)$_2$] complex,[17] suggesting that the presence of the bulky naphthyl moiety does not significantly affect distribution of delocalized electrons density across the six-membered chelate ring in the *cis*-[Pd(L^7-κ*S*,*O*)$_2$] complex. A closer inspection of the crystal structure also shows a deviation from square planarity, with S(1A)-Pd1-O(1B) and S(1B)-Pd1-O(1A) of 177.99 (7)° and 179.09 (8)° respectively. Moreover, the two naphthyl groups are not coplanar with the six-membered chelate rings as reflected by differences in the torsion angles C(12B)-N(1B)-C(11B)-C(1B) -172.5(2)° compared to C(12A)-N(1A)-C(11A)-C(1A) -167.3 (3)°. The crystal packing for *cis*-[Pd(L^7-κ*S*,*O*)$_2$] (Figure 2.14 (b)) shows intermolecular π-π interactions of the naphthyl rings. Also observed are weak intermolecular C-H interactions between the naphthyl moieties and the methyl hydrogen atoms at the thioamido end.

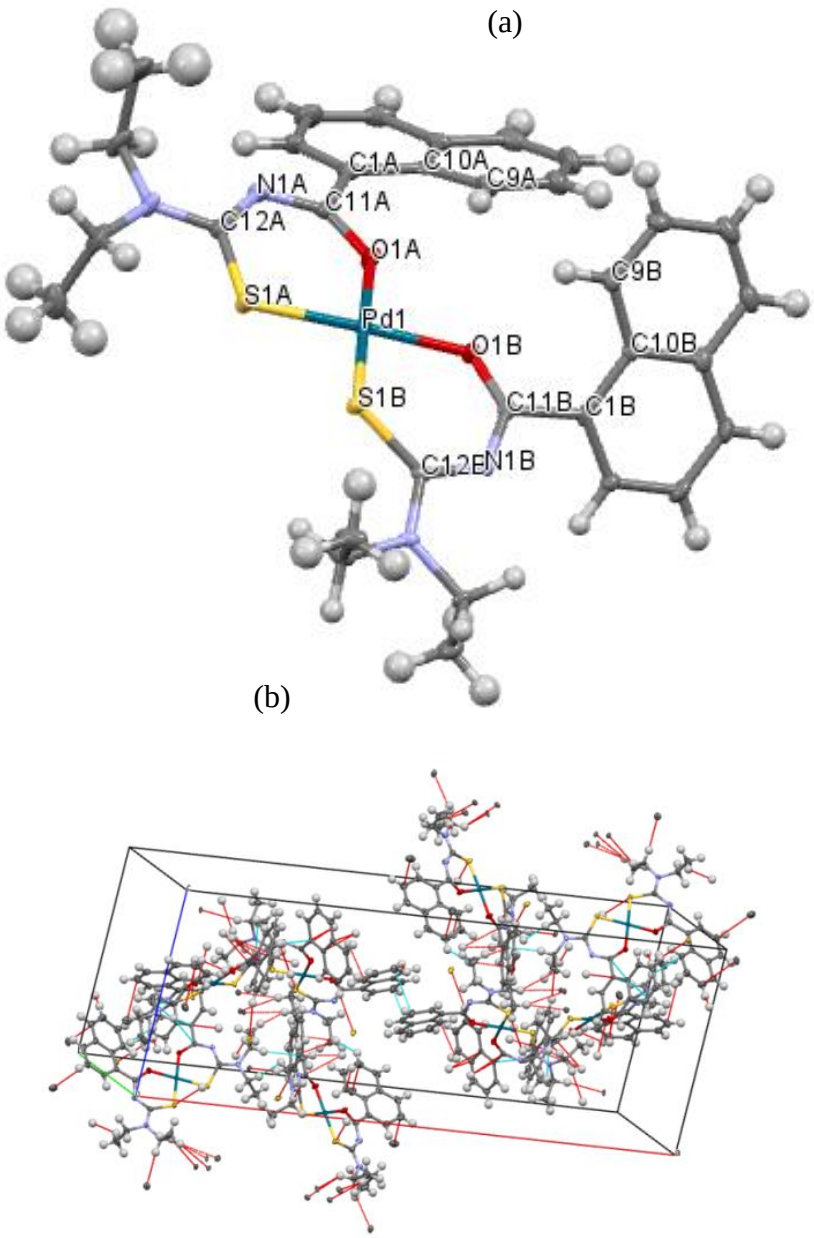

Figure 2.14. (a) Molecular structure from single-crystal X-ray diifraction and (b) crystal packing of *cis-bis(N,N-diethyl-N'-1-naphthoylthioureato-κ^2S,O)palladium(II)* *cis*-[Pd(L^7-κ*S*,*O*)$_2$] isolated from acetonitrile by slow evaporation.

2.3. Conclusion

In conclusion, a series of fifteen *N*,*N*-dialkyl-*N*'-aroylthioureas were found to react with Pd(II) or Pd(II) to form exclusively *cis*-[Pd(L^n-κ*S*,*O*)$_2$] complexes in relatively high yields of > 80 %. All ligands and complexes were successfully characterized by elemental analysis, FT-IR, ^{1}H, ^{13}C NMR while assignment of the *cis*-[Pd(L^7-κ*S*,*O*)$_2$] resonances was aided by the use of ^{1}H/^{13}C HSQC and HMBC correlations. The ^{1}H NMR resonances of the phenyl ring protons in the *cis*-[Pd(L^n-κ*S*,*O*)$_2$] complexes were not significantly affected by the presence of different

ligand substituents on the aroyl moiety, except for *cis*-[Pd(L^5-κ*S*,*O*)$_2$] where a significant upfield shift of *ca* 0.3 ppm was observed for the proton $H^{2,2'}$. The presence of the sterically hindered naphthyl groups in the *cis*-[Pd(L^7-κ*S*,*O*)$_2$] complex was manifested by a significant deshielding of the naphthyl H^7 protons leading to a marked downfield shift compared to $H^{2,2'}$ protons in the other *cis*-[Pd(L^{1-6}-*S*,*O*)$_2$] complexes. ^{1}H NMR characterization of the *cis*-[Pd(L^{1-7}-κ*S*,*O*)$_2$] complexes was complemented by the FT-IR analysis, whereby the spectra of all *cis*-[Pd(L^{1-7}-κ*S*,*O*)$_2$] complexes exhibited disappearances of the N-H bands at *ca* 3200 cm^{-1} as well as shifts of *ca* 120 cm^{-1} for the C=O band indicating ligand deprotonation.

Confirmation of the *cis*-κ*S*,*O* configuration in the *cis*-[Pd(L^n-κ*S*,*O*)$_2$] complexes was derived from their single-crystal X-ray structures. The C-O and C-S bond lengths for all complexes were significantly longer than that reported for their respective unbound ligands, which indicates significant delocalization of electrons across the six-membered *cis*-[Pd(L^n-κ*S*,*O*)$_2$] chelates. The presence of different aroyl and thioamido substituents showed no significant changes in crystallographic bond angles and distances for all the *cis*-[Pd(L^n-κ*S*,*O*)$_2$] complexes. The single-crystal X-ray structures clearly revealed that the Pd atoms adopt a nearly square planar geometry, the with sulfur and oxygen atoms located *trans* to each other. A greater distortion from square planarity was experienced by the *cis*-[Pd(L^7-κ*S*,*O*)$_2$] complex presumably due to steric effects of the bulky naphthyl groups. The most notable intermolecular interaction observed was π-π interaction between two naphthyl rings in the *cis*-[Pd(L^7-κ*S*,*O*)$_2$] complex.

2.4. Experimental

2.4.1. Materials and general methods

All chemicals used for synthesis of ligands and complexes were commercially available from Sigma Aldrich SA and were used without further purification, while K_2PdCl_4 and K_2PtCl_4 salts of > 99 % purity were obtained from Johnson Matthey PLC. ^{1}H and ^{13}C NMR spectra of ligands and complexes were recorded at 25 °C in chloroform-*d* using Varian UNITY INOVA 300 MHz, 400 MHz and 600 MHz NMR spectrometers. All ^{195}Pt{^{1}H} NMR spectra were recorded at 25 °C in chloroform-*d* using a Varian INOVA 600 MHz spectrometer.

Melting points were obtained using Electrothermal IA 9000 series digital melting point apparatus. Elemental analyses were performed using a Carlo Erba EA 1108 elemental analyzer

from University of Cape Town. FT-IR analyses were performed on a Thermo Nicolet Avatar 330 Smart Performer ATR instrument using a ZnSe crystal. Thin Layer Chromatography (TLC) was carried out using silica plates (Merck) with dichloromethane/hexane mixtures of varying compositions as eluents, with visualization using either molecular iodine vapor or UV light.

2.4.2. General procedure for synthesis of ligands and complexes

All ligands were prepared by the simple "one-pot" Douglass and Dains[95] method and characterized by standard procedures, including melting points, elemental analysis, FT-IR, ^{1}H and $^{13}C\{^{1}H\}$ NMR in chloroform-*d*.

A typical procedure for the platinum(II) and palladium(II) complexes was as follows: Solutions containing 40 mg of K_2PdCl_4 or K_2PtCl_4 (*ca* 0.12 mmol Pd^{II}) in 15 ml water and 10 ml acetonitrile were added drop-wise to a stirred solution of 0.25 mmol ligand HL^n, in a mixture of 15 ml acetonitrile and 10 ml water containing ~ 0.25 mmol of sodium acetate. The resulting mixture was stirred for 1 hour at room temperature, during which time a yellow precipitate was formed. Addition of *ca* 100 ml distilled water completed the precipitation, while dissolving excess soluble salts such as K/NaCl and sodium acetate. The precipitates were collected by centrifugation, rinsed with water followed by drying at *ca* 60-70 ^{o}C in vacuum. Recrystallization of complexes from mixtures of chloroform and ethanol afforded yellow/orange crystals in good yields typically > 80 % of the expected, apart from mechanical losses.

N,N-diethyl-N'-benzoylthiourea (HL^1).

Yield of 86 %; m.p. 98-100 °C; (Found: C, 61.15; H, 6.93; N, 12.00; S, 13.61%; calculated for $C_{12}H_{16}N_2OS$: C, 60.98; H, 6.82; N, 11.85; S, 13.57%); ^{1}H NMR (400 MHz, $CDCl_3$)/ppm δ 8.34 (s, 1H, N-H), 7.82 (d, 2H, Ar-H^2), 7.56 (t, 1H, Ar-H^4), 7.46 (t, 2H, Ar-H^3), 3.81 (d, 4H, N-CH_2), 1.32 (t, 6H, CH_3); ^{13}C NMR (100 MHz, $CDCl_3$)/ppm δ 11.3, 13.1, 47.5, 50.6, 129.2, 131.7, 134.1, 137.9, 164.2, 180.0.

N,N-diethyl-N'-(4-methoxybenzoyl)thiourea (HL^2).

Yield of 78 %; m.p. 134 – 135 ^{o}C; (Found: C, 59.12; H, 7.45; N, 10.74; S, 11.74%; calculated for $C_{13}H_{18}N_2O_2S$: C, 56.73; H, 6.80%; N, 9.45; S, 10.82); ^{1}H NMR (400 MHz, $CDCl_3$)/ppm δ 1.27 (m, 6H, CH_3), 3.57 (m, 2H, CH_2), 3.84 (s, 3H, Ar-H), 6.93 (d, 2H, Ar-H), 8.21 (s, 1H, N-

H); $^{13}C\{^{1}H\}$ NMR (100 MHz, $CDCl_3$)/ppm δ 11.3, 12.9, 47.7, 51.4, 114.2, 125.0, 130.0, 163.6, 179.9.

N,N-diethyl-N'-(3,4,5-trimethoxybenzoy)thiourea (HL^3).

Yield of 80 %; m.p. 143 –145 ºC, (Found: C, 55.30; H, 7.16; N, 8.62; S, 9.37%; calculated for $C_{15}H_{22}N_2O_4S$: C, 55.19; H, 6.79; N, 8.58; S, 9.82%); ^{1}H NMR (400 MHz, $CDCl_3$)/ppm δ 1.31 (m, 6H, CH_3), 3.55 (m, 2H, CH_2), 3.85 (s, 3H, CH_3), 3.87 (s, 6H, CH_3), 7.05 (s, 2H, Ar-H^2), 8.82 (s, 1H, N-H); $^{13}C\{^{1}H\}$ NMR (100 MHz, $CDCl_3$)/ppm δ 11.4, 13.3, 47.7, 56.4, 60.9, 105.2, 127.4, 142.1, 153.1, 163.3, 179.6.

N,N-diethyl-N'-(4-chlorobenzoyl)thiourea (HL^4).

Yield of 83 %, m.p. 163 – 165 °C; (Found: C, 48.00; H, 4.89; N, 9.42; S, 10.7%; calculated for $C_{12}H_{15}N_2OSCl$: C, 47.78; H, 48.68; N, 9.29; S, 10.63; Cl, 11.76%; ^{1}H NMR (400 MHz, $CDCl_3$)/ppm δ 1.33 (t, 6H, CH_3), 3.80 (q, 4H, CH_2), 7.44 (d, 2H, Ar-H^3), 7.77 (d, 2H, Ar-H^2), 8.35 (s, 1H, N-H); $^{13}C\{^{1}H\}$ NMR (100 MHz, $CDCl_3$)/ppm δ 11.7, 13.5, 48.0, 48.3, 112.8, 129.3, 131.3, 139.6, 163.1, 179.3.

N,N-diethyl-N'-4-methyl-benzoylthiourea (HL^5).

Yield of 89 %; m.p. 116-118 °C; (Found: C, 62.12; H, 7.95; N, 10.93; S, 12.10%; calculated for $C_{13}H_{18}N_2SO$: C, 62.37; H, 7.25; N, 11.19; S, 12.81%); ^{1}H NMR (400 MHz, $CDCl_3$)/ppm δ 8.27 (s, 1H, N-H), 7.72 (d, 2H, Ar-H^2), 7.26 (d, 2H, Ar-H^3), 3.81 (m, 4H, N-CH_2), 2.41 (s, 3H, CH_3), 1.32 (m, 6H, CH_3) ; $^{13}C\{^{1}H\}$ NMR (100 MHz, $CDCl_3$)/ppm δ 9.4, 21.7, 35.7, 128.0, 129.6, , 130.0, 143.8, 163.8, 179.5.

N,N-dimethyl-N'-(benzoyl)thiourea (HL^6).

Yield of 90 %, m.p. 122 – 124 °C; (Found: C, 57.02; H, 5.87; N, 13.44; S, 15.21%; calculated for $C_{10}H_{12}N_2OS$: C, 57.69; H, 5.77; N, 13.46; S, 15.39%; ^{1}H NMR (400 MHz, $CDCl_3$)/ppm δ 3.22 (s, 3H, CH_3), 3.46 (s, 3H, CH_3), 7.44 (m, 2H, Ar-H^3), 7.55 (m, 1H, Ar-H^4), 7.81 (d, 2H, Ar-H^2), 8.69 (s, 1H, N-H); $^{13}C\{^{1}H\}$ NMR (100 MHz, $CDCl_3$)/ppm δ 43.2, 44.3, 128.0, 128.9, 132.4, 133.0, 163.5, 180.2.

N,N-diethyl-N'-1-naphthoylthiourea (HL^7).

Yield of 86 %; m.p. 138-140 °C; (Found: C, 66.21; H, 6.45; N, 9.78; S, 10.80%; calculated for $C_{16}H_{18}N_2OS$: C, 67.13; H, 6.29; N, 9.79; S, 11.20%); ^{1}H NMR (400 MHz, $CDCl_3$)/ppm δ 8.44 (dd, 1H, Ar-H^8), 8.34 (s, 1H, N-H), 7.98 (d, 1H, Ar-H^2), 7.88 (m, 1H, Ar-H^4), 7.76 (m, 1H, Ar-

H^5), 7.58 (m, 1H, Ar-H^3), 7.53 (m, 1H, Ar-H^6), 7.47 (m, 1H, Ar-H^7), 3.86 (d, 4H, N-CH_2), 1.37 (t, 6H, CH_3); ^{13}C NMR (100 MHz, $CDCl_3$)/ppm δ 178.9, 165.4, 133.8, 132.4, 131.5, 130.3, 128.5, 127.8, 126.7, 126.5, 125.2, 124.5, 47.9, 13.4, 11.6.

N-methyl-N-ethyl-N'-benzoylthiourea (HL^8).

Yield of 83 % (Found: C, 59.13; H, 6.83; N, 12.49; S, 12.59%; calculated for $C_{11}H_{14}N_2SO$: C, 59.43; H, 6.35; N, 12.60; S, 14.42%); ^1H NMR (400 MHz, $CDCl_3$)/ppm δ 8.61 (s, 1H, N-H), 7.82 (d, 2H, Ar-H^2), 7.55 (dt, 1H, Ar-H^4), 7.44 (m, 2H, Ar-H^3), 3.97 (q, 2H, N-CH_2(ZZ)), 3.60 (q, 2H, N-CH_2(EZ, EE)), 3.41 (s, 3H, N-CH_3(EZ, EE)), 3.18 (s, 3H, N-CH_3(ZZ)), 1.33 (t, 3H, CH_3(ZZ)), 1.26 (t, 3H, CH_3(EZ, EE)); $^{13}C\{^1H\}$ NMR (100 MHz, $CDCl_3$)/ppm δ 10.7, 12.8, 39.9, 40.9, 50.2, 51.1, 127.6, 128.7, 132.4, 132.8, 163.1, 179.2.

N-methyl-N-propyl-N'-benzoylthiourea (HL^9).

Yield of 78 % (Found: C, 60.83; H, 7.23; N, 11.45; S, 11.33%; calculated for $C_{12}H_{16}N_2SO$: C, 60.99; H, 6.82; N, 11.85; S, 13.57%); ^1H NMR (400 MHz, $CDCl_3$)/ppm δ 0.88 (t, 3H, CH_3(EZ/ZZ)), 1.02 (t, 3H, CH_3(ZZ)), 1.71 (m, 2H, CH_2(EZ/EE)), 1.84 (m, 2H, CH_2(ZZ)), 3.22 (s, 3H, CH_3(ZZ), 3.43 (s, 3H, CH_3(EZ/EE)), 3.53 (t, 2H, CH_2(EZ/EE)), 3.93 (t, 2H, CH_2(ZZ)), 7.47 (t, 2H, Ar-H), 7.57 (t, 1H, Ar-H-H), 7.83 (d, 2H, Ar-H), 8.46 (s, 1H, N-H); $^{13}C\{^1H\}$ NMR (100 MHz, $CDCl_3$)/ppm δ 11.2, 19.5, 21.3, 41.0, 41.7, 57.4, 58.1, 128.0, 128.9, 132.6, 133.0, 163.4, 179.9.

N-methyl-N-ethyl-N'-(2,2-dimethylpropanoyl)thiourea (HL^{10}).

(Found: C, 53.98; H, 8.71; N, 13.69%; calculated for $C_9H_{18}N_2OS$: C, 53.43; H, 8.97; N, 13.84%); %); ^1H NMR (400 MHz, $CDCl_3$)/ppm δ 1.25 (s, 9H, CH_3), 1.30 (t, 3H, CH_3), 3.08 (s, 3H, CH_3(ZZ)), 3.37 (s, 3H, CH_3(EZ/EE)), 3.48 (q, 2H, CH_2(EZ/EE)), 3.93 (q, 2H, CH_2(ZZ)), 7.77 (s, 1H, N-H); $^{13}C\{^1H\}$ NMR (100 MHz, $CDCl_3$)/ppm δ 10.9, 12.9, 27.1, 39.7, 39.8, 51.1, 174.5, 174.6, 179.7, 180.1.

N-methylpyrrolidyl-N'-benzoyllthiourea (HL^{11}).

(Found: C, 62.28; H, 6.95; N, 10.97; S, 10.62%; calculated for $C_{13}H_{16}N_2SO$: C, 62.87; H, 6.49; N, 11.28; S, 12.91%); ^1H NMR (400 MHz, $CDCl_3$)/ppm δ 1.24 (d, 3H, CH_3(EZ,ZZ)), 1.47 (d, 3H, CH_3(ZZ)), 1.75 (m, 2H, CH_2(ZZ)), 1.84 (m, 2H, CH_2(EZ/EE)), 2.00 (m, 2H, CH_2(EZ/EE)), 2.26 (m, 2H, CH_2(ZZ)), 3.66 (m, 2H, CH_2(ZZ)), 3.73 (m, 2H, CH_2(EZ,EE)), 3.95 (m, 2H, CH_2), 4.37 (m, 2H, CH_2(EZ,ZZ)), 4.67 (m, 2H, CH_2(ZZ)), 7.46 (m, 2H, Ar-H), 7.57 (m, 1H, Ar-H),

7.82 (d, 2H, Ar-H), 8.47 (s, 1H, N-H); $^{13}C\{^{1}H\}$ NMR (100 MHz, $CDCl_3$)/ppm δ 18.4, 19.6, 22.4, 24.6, 32.6, 34.2, 53.1, 55.2, 59.3, 60.5, 128.0, 129.0, 132.8, 133.0, 163.4, 176.3.

N-pentyl-N-phenyl-N'-(2,2-dimethylpropanoyl)thiourea (HL^{12}).

(Found: C, 66.37; H, 8.53; N, 9.14; S, 10.42%; calculated for $C_{17}H_{26}N_2OS$: C, 66.62; H, 8.53; N, 9.14; S, 10.42%); ^{1}H NMR (400 MHz, $CDCl_3$)/ppm δ 7.83 (s, 1H, N-H), 7.39 (t, 2H, Ar-H(E)), 7.31 (tt, 1H, Ar-H(E)), 7.19 (d, 2H, Ar-H(E)), 4.14 (m, 2H, N-CH_2(E)), 1.67 (m, 2H, CH_2(E)), 1.25 (m, 4H, $(CH_2)_2$(E)), 0.83 (s, 9H, $C(CH_3)_3$), 0.81 (t, 3H, CH_3(E)); $^{13}C\{^{1}H\}$ NMR (100 MHz, $CDCl_3$)/ppm δ 14.1, 22.3, 25.6, 26.5, 28.57, 39.5, 56.8, 126.2, 142.6, 173.1, 179.0.

N-Phenethyl-N-methyl-N'-(2,2-dimethylpropanoyl)thiourea (HL^{13}).

(Found: C, 64.23; H, 7.65; N, 10.74; S, 11.75%; calculated for $C_{15}H_{22}N_2OS$: C, 64.71; H, 7.96; N, 10.06; S, 11.52%); ^{1}H NMR (400 MHz, $CDCl_3$)/ppm δ 7.85 (s, 1H, N-H(Z)), 7.52 (s, 1H, N-H(E)), 7.29 (m, 5H, Ar-H(E and Z)), 4.06 (t, 3H, N-CH_2(E)), 3.65 (t, 2H, N-CH_2(Z)), 3.43 (s, 3H, N-CH_2(Z)), 3.09 (t, 2H, N-CH_2(E)), 3.08 (s, 3H, N-CH_3(E)), 2.93 (t, 2H, N-CH_2(E)), 1.26 (s, 9H, $C(CH_3)_3$(E)), 1.19 (s, 9H, $C(CH_3)_3$(Z)) ; $^{13}C\{^{1}H\}$ NMR (100 MHz, $CDCl_3$)/ppm δ 26.9, 27.0, 31.9, 34.1, 39.5, 39.6, 41.1, 42.1, 57.0, 58.0, 126.5, 138.2, 174.4, 180.2, 180.5.

N-Isopropyl-N-phenyl-N'-(2,2-dimethylpropanoyl)thiourea (HL^{14}).

(Found: C, 64.74; H, 8.57; N, 10.17; S, 11.10%; calculated for $C_{15}H_{22}N_2OS$: C, 64.71; H, 7.96; N, 10.06; S, 11.52%); ^{1}H NMR (400 MHz, $CDCl_3$)/ppm δ 0.82 (s, 9H, CH_3(Z)), 1.12 (d, 6H, CH_3(E)), 5.74 (m, 1H, N-CH), 7.12 (d, 2H, Ar-H(E)), 7.45 (m, 3H, Ar-H(E/Z)), 7.89 (s, 1H, N-H); $^{13}C\{^{1}H\}$ NMR (100 MHz, $CDCl_3$)/ppm δ 20.3, 26.4, 39.7, 52.4, 137.2, 174.1, 178.0.

N-Isopropyl,N-(4-methoxy-phenyl)-N'-(2,2-dimethylpropanoyl)thiourea (HL^{15}).

(Found: C, 62.02; H, 7.47; N, 9.14; S, 10.83%; calculated for $C_{16}H_{24}N_2O_2S$: C, 62.30; H, 7.84; N, 9.08; S, 10.40%); ^{1}H NMR (400 MHz, $CDCl_3$)/ppm δ 0.82 (s, 9H, CH_3(E)), 1.10 (d, 6H, CH_3(E)), 3.83 (s, 3H, O-CH_3(E)), 5.74 (m, 1H, -CH), 6.95 (d, 2H, Ar-H(E)), 7.10 (d, 2H, Ar-H(Z)), 8.88 (s, 1H, N-H); $^{13}C\{^{1}H\}$ NMR (100 MHz, $CDCl_3$)/ppm δ 20.3, 26.5, 39.9, 52.0, 55.5, 129.8, 174.2, 178.0.

***cis-bis(N,N-diethyl-N'-(benzoylthioureato-κ^2S,O)palladium(II), cis-*[Pd(L^1-κS,O)$_2$].**

Yield of 88 %; m.p. 159-163 °C; (Found: C, 50.09; H, 5.22; N, 9.12; S, 10.93%; calculated for $C_{24}H_{30}N_4S_2O_2Pd$: C, 49.95; H, 5.24; N, 9.71; S, 11.11%); ^{1}H NMR (400 MHz, $CDCl_3$)/ppm δ 8.26 (d, 2H, Ar-H^2), 7.50 (m, 1H, Ar-H^4), 7.44 (m, 2H, Ar-H^3), 3.85 (q, 4H, N-CH_2), 3.50 (q,

4H, CH_2), 1.33 (m, 4H, CH_2), 1.23 (t, 6H, CH_3); $^{13}C\{^1H\}$ NMR (100 MHz, $CDCl_3$)/ppm δ 12.6, 13.1, 15.3, 46.1, 47.2, 65.9, 127.9, 129.7, 131.4, 137.1, 170.6, 171.1.

***cis*-bis(*N*,*N*-diethyl-*N'*-(4-methoxy-benzoylthioureato-κ^2*S*,*O*)palladium(II), *cis*-[Pd(L^2-κ*S*,*O*)$_2$].**

Yield 86 %; m.p. 138-140 °C; (Found: C, 48.63; H, 5.59; N, 8.38; S, 9.71%; calculated for $C_{26}H_{34}N_4S_2O_4Pd$: C, 49.05; H, 5.38; N, 8.79; S, 10.07%); ^1H NMR (400 MHz, $CDCl_3$)/ppm δ 1.33 (dt, 6H, CH_3), 3.84 (m, 4H, CH_2), 3.87 (s, 3H, O-CH_3), 7.29 (m, 2H, Ar-H^2), 7.03 (m, 2H, Ar-H^3); $^{13}C\{^1H\}$ NMR (100 MHz, $CDCl_3$)/ppm δ 12.6, 13.1, 46.1, 47.2, 55.2, 114.3, 117.8, 122.1, 128.8, 138.6.

***cis*-bis(*N*,*N*-diethyl-*N'*-(3,4,5-trimethoxybenzoylthioureato-κ^2*S*,*O*)palladium(II) *cis*-[Pd(L^3-κ*S*,*O*)$_2$].**

Yield 85 %; m.p. 198 – 202 °C; (Found: C, 47.40; H, 5.63; N, 6.61; S, 7.92%; calculated for $C_{30}H_{42}N_4S_2O_8Pd$: C, 47.59; H, 5.59; N, 7.40; S, 8.47%); ^1H NMR (400 MHz, $CDCl_3$)/ppm, δ 1.28 (t, 6H, CH_3), 1.32 (t, 6H, CH_3), 3.82 (q, 4H, CH_2), 3.83 (s, 12H, CH_3), 6.85 (t, 2H, Ar-H), 7.44 (d, 4H, Ar-H^2); $^{13}C\{^1H\}$ NMR (100 MHz, $CDCl_3$)/ppm δ 12.3, 13.1, 46.2, 47.23, 55.3, 103.9, 107.4, 139.2, 160.2, 170.0, 171.2.

***cis*-bis(*N*,*N*-diethyl-*N'*-(3,4,5-trimethoxybenzoylthioureato-κ^2*S*,*O*)platinum(II) *cis*-[Pt(L^3-κ*S*,*O*)$_2$].**

Yield 79 %; m.p. 218 – 221 °C; (Found: C, 42.43; H, 4.88; N, 6.55; S, 7.00%; calculated for $C_{30}H_{42}N_4S_2O_8Pd$: C, 42.39; H, 5.46; N, 6.59; S, 7.55%); ^1H NMR (400 MHz, $CDCl_3$)/ppm, δ 1.29 (t, 6H, CH_3), 1.32 (t, 6H, CH_3), 3.75 (q, 4H, CH_2), 3.80 (s, 12H, CH_3), 6.85 (t, 2H, Ar-H), 7.55 (d, 4H, Ar-H^2); $^{13}C\{^1H\}$ NMR (100 MHz, $CDCl_3$)/ppm δ 12.4, 13.1, 30.8, 47.1, 107.4, 132.9, 141.6, 152.6, 166.9, 167.9; $^{195}Pt\{^1H\}$ NMR (128 MHz, $CDCl_3$)/ppm, δ -2723 (*cis*), -1982 (*trans*, post-irradiation with 5Watt LED lamp).

***cis*-bis(*N*,*N*-diethyl-*N'*-(4-chlorobenzoylthioureato-κ^2*S*,*O*)palladium(II) *cis*-[Pd(L^4-κ*S*,*O*)$_2$].**

Yield 88 %; m.p. 179-181 °C; (Found: C, 44.35; H, 4.46; N, 8.27; S, 9.58%; calculated for $C_{24}H_{28}N_4S_2O_2PdCl$: C, 44.63; H, 4.37; N, 8.67; S, 9.23%); ^1H NMR (400 MHz, $CDCl_3$)/ppm δ 1.30 (dt, 6H, CH_3), 3.83 (q, 4H, CH_2), 7.38 (m, 2H, Ar-H^3), 8.14 (m, 2H, Ar-H^2); $^{13}C\{^1H\}$ NMR (100 MHz, $CDCl_3$)/ppm δ 12.6, 13.1, 46.1, 47.3, 128.2, 131.0, 135.6, 137.7, 169.6, 171.2.

cis-bis(N,N-diethyl-N'-4-methyl-benzoylthioureato-κ²S,O)palladium(II) ***cis*-[Pd(L⁵-κS,O)₂].**

Yield of 89 %; m.p. 218-220 °C; (Found: C, 51.43; H, 5.87; N, 9.04; S, 9.82%; calculated for $C_{26}H_{34}N_4S_2O_2Pd$: C, 51.61; H, 5.66; N, 9.26; S, 10.60%); ^{1}H NMR (400 MHz, $CDCl_3$)/ppm δ 1.27 (t, 3H, CH_3), 1.33 (t, 3H, CH_3), 3.84 (m, 4H, $N(CH_2)$, 7.21 (d, 2H, Ar-H^2), 8.13 (d, 2H, Ar-H^3); ^{13}C{^{1}H} (100 MHz, $CDCl_3$)/ppm δ 12.9, 13.4, 21.8, 46.2, 47.4, 128.9, 130.0, 134.6, 142.1, 170.9, 171.1.

cis-bis(N,N-dimethyl-N'-(benzoylthioureato-κ²S,O)palladium(II) cis-[Pd(L⁶-κS,O)₂].

Yield of 63 %; m.p. Decomposes at 245 °C; (Found: C, 47.03; H, 4.37; N, 10.53; S, 12.47%; calculated for $C_{20}H_{22}N_4O_2S_2Pd$: C, 46.12; H, 4.23; N, 10.76; S, 12.3%; ^{1}H NMR (400 MHz, $CDCl_3$)/ppm δ 1.28 (t, 6H, CH_3), 1.34 (t, 6H, CH_3), 3.77 (q, 4H, CH_2), 3.83 (q, 4H, CH_2), 7.42 (t, 2H, Ar-H^4), 7.51 (t, 1H, Ar-H^3), 8.26 (d, 2H, Ar-H^2); ^{13}C{^{1}H} (100 MHz, $CDCl_3$)/ppm δ 12.3, 13.1, 46.0, 128.1, 129.3, 131.3, 137.6, 167.0, 168.4.

cis-bis(N,N-diethyl-N'-(1-naphthoylthioureato-κ²S,O)palladium(II) cis-[Pd(L⁷-κS,O)₂].

Yield of 86 %; m.p. 157-159 °C; (Found: C, 56.08; H, 5.11; N, 7.67; S, 9.15%; calculated for $C_{32}H_{34}N_4O_2S_2Pd$: C, 56.77; H, 5.03; N, 8.28; S, 9.46%); ^{1}H NMR (400 MHz, $CDCl_3$)/ppm δ 8.94 (d, 1H, Ar-H^8), 8.14 (d, 1H, Ar-H^2), 7.89 (d, 1H, Ar-H^4), 7.80 (d, 1H, Ar-H^5), 7.43 (t, 1H, Ar-H^3), 7.37 (m, 1H, Ar-H^6), 7.15 (m, 1H, Ar-H^7), 3.88 (q, 4H, N-CH_2), 3.82 (q, 4H, N-CH_2) 1.37 (t, 3H, CH_3), 1.25 (t, 3H, CH_3); ^{13}C{^{1}H} NMR (100 MHz, $CDCl_3$)/ppm δ 12.6, 13.1, 15.3, 46.1, 47.2, 65.9, 127.9, 129.7, 131.4, 137.1, 170.6, 171.1.

cis-bis(N-methyl,N-ethyl-N'-(benzoylthioureato-κ²S,O)palladium(II), cis-[Pd(L⁸-κS,O)₂].

Yield of 75 %; (Found: C, 47.93; H, 4.87; N, 9.74; S, 10.90%; calculated for $C_{22}H_{26}N_4S_2O_2Pd$: C, 48.13; H, 4.77; N, 10.20; S, 12.68%); ^{1}H NMR (400 MHz, $CDCl_3$)/ppm δ 8.26 (m, 2H, Ar-H^2); 7.49 (m, 1H, Ar-H^4); 7.42 (m, 2H, Ar-H^3); 3.96 (q, 2H, N-CH_2(ZZ)); 3.90 (q, 2H, N-CH_2(EE, EZ)); 3.39 (s, 3H, N-CH_3(EZ, EE)); 3.37 (s, 3H, N-CH_3(ZZ)); 1.31 (t, 3H, CH_3(ZZ)); 1.27 (t, 3H, CH_3(EZ, EE); ^{13}C{^{1}H} NMR (100 MHz, $CDCl_3$)/ppm δ 12.1, 12.6, 38.5, 40.0, 48.5, 49.3, 128.0, 129.7, 129.8, 131.5, 131.6, 137.0, 137.1, 170.7, 170.9, 171.5, 171.8.

cis-bis(N-methyl,N-propyl-N'-(benzoylthioureato-κ²S,O)palladium(II), cis-[Pd(L⁹-κS,O)₂].

Yield of 82.3 %(Found: C, 49.39; H, 5.47; N, 9.62; S, 10.72%; calculated for $C_{24}H_{30}N_4S_2O_2Pd$: C, 49.95; H, 5.24; N, 9.71; S, 11.11%); ^{1}H NMR (400 MHz, $CDCl_3$)/ppm δ 8.26 (m, 2H, Ar-H2); 7.50 (m, 1H, Ar-H^4); 7.42 (m, 2H, Ar-H^3); 3.88 (q, 2H, N-CH_2(ZZ)); 3.80 (q, 2H, N-

CH_2(EZ, EE)); 3.39 (s, 3H, N-CH_3(EZ, EE)); 3.38 (s, 3H, N-CH_3(ZZ)); 1.76 (m, 2H, CH_2); 0.96 (t, 3H, CH_3); $^{13}C\{^1H\}$ NMR (100 MHz, $CDCl_3$)/ppm δ 11.3, 11.4, 20.5, 21.1, 39.3, 40.8, 55.2, 56.2, 127.9, 128.0, 129.7, 129.8, 131.5, 131.6, 137.0, 137.2, 170.6, 170.9, 171.9, 172.2.

cis-bis(N-methyl,N-ethyl-N'-(2,2-dimethylpropanoylthioureato-κ²S,O)palladium(II), cis-[Pd(L¹⁰-κS,O)₂].

Yield of 80 %; (Found: C, 41.96; H, 7.07; N, 11.07; S, 11.17%; calculated for $C_{18}H_{34}N_4S_2O_2Pd$: C, 42.27; H, 6.73; N, 11.01; S, 12.60%); ^1H NMR (400 MHz, $CDCl_3$)/ppm δ 1.33 (dt, 6H, CH_3); 3.40 (s, 3H, CH_3(ZZ)); 3.45 (s, 3H, CH_3(EZ/EE)); 3.98 (m, 2H, CH_2); 7.44 (m, 2H, Ar-H); 7.35 (m, 1H, Ar-H); 8.07 (m, 2H, Ar-H); $^{13}C\{^1H\}$ NMR (100 MHz, $CDCl_3$)/ppm δ 12.6, 13.1, 46.1, 47.2, 55.2, 114.3, 117.8, 122.1, 128.8, 138.6.

cis-bis(N-methylpyrrolidyl-N'-(benzoylthioureato-κ²S,O)palladium(II), cis-[Pd(L¹¹-κS,O)₂].

Yield of 87 %; (Found: C, 51.34; H, 5.11; N, 9.14; S, 9.80%; calculated for $C_{26}H_{30}N_4S_2O_2Pd$: C, 51.95; H, 5.03; N, 9.32; S, 10.67%); ^1H NMR (400 MHz, $CDCl_3$)/ppm δ 8.28 (d, 2H, Ar-H^2); 7.49 (m, 1H, Ar-H^4); 7.42 (m, 2H, Ar-H^3); 4.82 (m, 1H, N-CH(ZZ)); 4.56 (m, 1H, N-CH(EZ, EE)); 3.99 (m, 2H, CH_2(EE, EZ)); 3.84 (m, 2H, CH_2(ZZ))); 3.68 (m, 2H, CH_2(EE, ZZ, EZ)); 2.11 (m, 2H, CH_2(ZZ)); 1.77 (m, 2H, CH_2(EZ,EE)); 1.38 (d, 3H, CH_3(EE)); 1.36 (d, 3H, CH_3(EZ)); 1.34 (d, 3H, CH_3(ZZ)); $^{13}C\{^1H\}$ NMR (100 MHz, $CDCl_3$)/ppm δ 18.8, 19.6, 19.7, 22.4, 23.2, 32.1, 32.6, 50.7, 50.9, 57.4, 57.7, 128.0, 128.1, 129.8, 129.9, 131.6, 137.2, 137.4, 170.0, 170.3.

cis-bis(N-methyl,N-ethyl-N'-(benzoylthioureato-κ²S,O)platinum(II), cis-[Pt(L⁸-κS,O)₂].

Yield of 88 %; (Found: C, 41.21; H, 4.13; N, 8.59; S, 8.81%); calculated for $C_{22}H_{26}N_4S_2O_2Pt$: C, 41.44; H, 4.11; N, 8.79; S, 10.06%); ^1H NMR (400 MHz, $CDCl_3$)/ppm δ 8.28 (m, 2H, Ar-H2); 7.52 (m, 1H, Ar-H4); 7.42 (m, 2H, Ar-H3); 3.93 (q, 2H, N-CH_2(ZZ)); 3.83 (q, 2H, N-CH_2(EZ, EE)); 3.35 (s, 3H, N-CH_3(ZZ)); 3.29 (s, 3H, N-CH_3(EZ, EE)); 1.34 (t, 3H, CH_3(ZZ)); 1.30 (t, 3H, CH_3 (EZ, EE)); $^{13}C\{^1H\}$ NMR (100 MHz, $CDCl_3$)/ppm δ 11.9, 12.6, 38.4, 39.8, 48.3, 49.0, 128.1, 129.4, 131.4, 131.5, 137.5, 137.6, 167.4, 167.7, 168.4, 168.5, 168.7, 168.8.

cis-bis(N-methyl,N-propyl-N'-(benzoylthioureato-κ²S,O)platinum(II), cis-[Pt(L⁹-κS,O)₂].

Yield of 82 %; (Found: C, 43.35; H, 4.67; N, 8.20; S, 9.06%; calculated for $C_{24}H_{30}N_4S_2O_2Pt$: C, 43.30; H, 4.54; N, 8.41; S, 9.63%); ^1H NMR (400 MHz, $CDCl_3$)/ppm δ 0.96 (t, 3H, CH_3(ZZ); 0.99 (t, 3H, CH_3(EZ,EE)); 1.74 (m, 2H, CH_2(ZZ)); 1.78 (m, 2H, CH_2(EZ, EE)); 3.30 (s, 3H,

N-CH_3(ZZ)); 3.36 (s, 3H, N-CH_3(EZ, EE)); 3.72 (t, 2H, N-CH_2(EZ, EE)); 3.85 (t, 2H, N-CH_2(ZZ)); 7.42 (m, 2H, Ar-H3); 7.52 (m, 1H, Ar-H4); 8.28 (m, 2H, Ar-H1); $^{13}C\{^1H\}$ NMR (100 MHz, $CDCl_3$)/ppm δ 11.5, 20.4, 21.2, 21.3, 39.3, 40.7, 40.9, 55.1, 56.0, 128.1, 128.2, 129.5, 129.6, 131.5, 131.6, 137.6, 137.7, 137.8, 167.9, 168.2, 168.4, 168.5, 168.8, 168.9.

cis-bis(N-methyl,N-ethyl-N'-(2,2-dimethylpropanoylthioureato-κ²S,O)platinum(II), cis-[Pt(L^{10}-κS,O)₂]. Yield of 80 %; (Found: C, 36.45; H, 6.08; N, 9.42%; calculated for $C_{18}H_{34}N_4O_2S_2Pt$: C, 36.17; H, 5.73; N, 9.37%); ^1H NMR (400 MHz, $CDCl_3$)/ppm δ 1.13 (m, 3H, CH_3(ZZ); 1.14 (m, 3H, CH_3(EZ, EE)); 1.20 (s, 9H, CH_3); 3.15 (s, 3H, N-CH_3(EZ, EE)); 3.19 (s, 3H, N-CH_3(ZZ)); 3.71 (m, 2H, N-CH_2(EZ,EE)); 3.75 (m, 2H, N-CH_2(ZZ)); $^{13}C\{^1H\}$ NMR (100 MHz, $CDCl_3$)/ppm δ 11.9, 11.97, 12.4, 12.5, 28.4, 28.5, 38.1, 39.6, 39.8, 42.3, 42.4, 47.5, 48.0, 48.8, 167.1, 167.4, 183.1, 183.2.

cis-bis(N-methylpyrrolidyl-N'-(benzoylthioureato-κ²S,O)platinum(II), cis-[Pt(L^{11}-κS,O)₂].

Yield of 78 %; (Found: C, 44.91; H, 4.43; N, 7.80; S, 9.02%; calculated for $C_{26}H_{30}N_4S_2O_2Pt$: C, 45.28; H, 4.38; N, 8.12; S, 9.30%); ^1H NMR (400 MHz, $CDCl_3$)/ppm δ 1.36 (m, 3H, CH_3); 1.76 (m, 2H, CH_2(EZ, EE)), 2.09 (m, 32H, CH_2(ZZ)), 3.56 (m, 2H, CH_2(EZ, EE)), 3.76 (m, 2H, CH_2(ZZ)), 3.96 (m, 2H, CH_2), 4.50 (m, 2H, CH_2(EZ,EE)), 4.79 (m, 2H, CH_2(ZZ)), 7.42 (m, 2H, Ar-H), 7.52 (m, 1H, Ar-H), 8.30 (d, 2H, Ar-H); $^{13}C\{^1H\}$ NMR (100 MHz, $CDCl_3$)/ppm δ 12.6, 13.1, 46.1, 47.2, 55.2, 114.3, 117.8, 122.1, 128.8, 138.6.

cis-bis(N-n-pentyl,N-phenyl-N'-(2,2-dimethylpropanoylthioureato-κ²S,O)platinum(II), cis-[Pt(L^{12}-κS,O)₂].

Yield of 91 %; (Found: C, 49.76; H, 6.90; N, 6.86; S, 8.79%; calculated for $C_{34}H_{50}N_4O_2S_2Pt$: C, 50.67; H, 6.25; N, 6.95; S, 7.96%); ^1H NMR (400 MHz, $CDCl_3$)/ppm δ 7.47 (t, 2H, Ar-H(EE, EZ)); 7.34 (m, 2H, Ar-H(ZZ, EZ)); 7.14 (d, 1H, Ar-H(ZZ, EZ)); 6.98 (d, 1H, Ar-H(EE, EZ)); 3.89 (m, 2H, CH_2(EZ)); 3.82 (m, 2H, CH_2(ZZ)); 3.76 (m, 2H, CH_2(EE)); 1.56 (m, 4H, $(CH_2)_2$(ZZ, EZ, EE)); 1.24 (s, 9H, $C(CH_3)_3$(EZ)); 1.22 (s, 9H, $C(CH_3)_3$(ZZ)); 0.78 (s, 9H, $C(CH_3)_3$(EE)); 1.18 (m, 2H, CH_2(EZ, EE, ZZ); 0.81 (t, 3H, CH_3(EE, EZ, ZZ)); $^{13}C\{^1H\}$ NMR (100 MHz, $CDCl_3$)/ppm δ 14.1, 22.4, 27.0, 27.4, 28.1, 28.8, 41.7, 42.2, 42.3, 55.7, 126.7, 127.0, 127.9, 128.1, 128.6, 129.5, 129.6, 143.9, 144.0, 144.7, 167.9, 182.8, 183.6, 183.7.

cis-bis(N-Phenethyl,N-methyl-N'-(2,2-dimethylpropanoylthioureato-κ²S,O)platinum(II), cis-[Pt(L^{13}-κS,O)₂].

Yield of 83 %; (Found: C, 48.17; H, 5.51; N, 7.23; S, 8.11%; calculated for $C_{38}H_{42}N_4O_2S_2Pt$: C, 48.05; H, 5.65; N, 7.47; S, 8.55%); ^{1}H NMR (400 MHz, $CDCl_3$)/ppm δ 7.38-7.16 (m, 5H, Ar-H(ZZ, EE, EE)); 3.92 (t, 2H, N-CH_2(ZZ, EZ)); 3.88 (t, 3H, N-CH_2(EZ, EE)); 3.11 (s, 3H, CH_3(EZ)); 3.10 (s, 3H, CH_2(EE)); 3.08 (s, 3H, CH_3(ZZ)); 3.04 (t, 2H, CH_2(EE, EZ)); 2.90 (t, 2H, CH_2(ZZ, EZ)); 1.26 (s, 9H, $(CH_3)_3$(ZZ, EZ)); 1.23 (s, 9H, $(CH_3)_3$(EE, EZ); ^{13}C{^{1}H} NMR (100 MHz, $CDCl_3$)/ppm δ 28.3, 33.1, 34.0, 39.4, 40.8, 42.3, 54.9, 55.7, 126.5, 138.6, 167.3, 167.4, 167.6, 183.12, 183.19, 183.57.

cis-bis(N-Isopropyl,N-phenyl-N'-(2,2-dimethylpropanoylthioureato-κS,O)platinum(II), cis-[Pt(L^{14}-κ^2S,O)$_2$].

Yield of 91 %; (Found: C, 47.61; H, 5.61; N, 7.42; S, 8.40%; calculated for $C_{30}H_{42}N_4O_2S_2Pt$: C, 48.05; H, 5.65; N, 7.47; S, 8.55%); ^{1}H NMR (400 MHz, $CDCl_3$)/ppm δ 7.43 (dd, 2H, Ar-H(EE, EZ)); 7.34 (dd, 2H, Ar-H(ZZ, EZ)); 7.16 (dd, 2H, Ar-H(EZ, EE)); 7.03 (dd, 2H, Ar-H(ZZ, EZ)); 6.94 (dd, 1H, Ar-H(EE, EZ)); 6.87 (dd, 1H, Ar-H(ZZ, EZ)); ^{13}C{^{1}H} NMR (100 MHz, $CDCl_3$)/ppm δ 20.8, 20.9, 21.1, 27.3, 28.1, 41.6, 42.3, 50.3, 128.2, 128.3, 128.8, 129.0, 129.1, 129.7, 129.9, 139.4, 140.1, 168.1, 182.6, 183.4, 183.6, .

cis-bis(N-Isopropyl,N-4-methoxy-phenyl-N'-(2,2-dimethyl-propanoyl)thioureato-κS,O)platinum(II), cis-[Pt(L^{15}-κ^2S,O)$_2$].

Yield of 93 %; (Found: C, 47.42; H, 5.66; N, 6.90; S, 7.60%; calculated for $C_{32}H_{46}N_4O_4S_2Pt$: C, 47.45; H, 5.72; N, 6.92; S, 7.92%); ^{1}H NMR (400 MHz, $CDCl_3$)/ppm δ 7.05 (d, 2H, Ar-H(EZ)); 6.93 (d, 2H, CH_3(ZZ)); 6.79 (d, 2H, Ar-H(ZZ)); 5.45 (m, 1H, CH_2(EZ)); 5.40 (m, 1H, CH_2(ZZ)); 5.18 (m, 1H, CH_2(EE)), 3.81 (s, 3H, O-CH_3(EZ)), 3.79 (s, 3H, O-CH_3(EE)), 3.72 (s, 3H, O-CH_3(ZZ)), 1.23 (s, 9H, $C(CH_3)_3$(EZ)), 1.22 (s, 9H, $C(CH_3)_3$(ZZ)), 0.76 (s, 9H, $C(CH_3)_3$(EE)); ^{13}C{^{1}H} NMR (100 MHz, $CDCl_3$)/ppm δ 20.8, 21.0, 27.5, 28.1, 42.3, 50.3, 55.3, 114.0, 113.9, 129.6, 130.6, 130.7, 132.2, 132.3, 133.0, 157.8, 158.6, 158.8, 168.5, 182.7, 183.3, 183.5.

2.4.3. Preparation of *trans*-[Pd(L^n-κ*S*,*O*)$_2$] and *trans*-[Pd(L^7-κ*S*,*N*)$_2$] complexes

The *trans*-[Pd(L^{1-8}-κ*S*,*O*)$_2$] and *trans*-[Pd(L^7-κ*S*,*N*)$_2$] complexes were prepared by dissolving 20 mg of their respective *cis*-[Pd(L^{1-8}-κS,*O*)$_2$] complexes in 25 ml acetonitrile followed by continuous irradiation with a 5 Watt LED lamp. The *trans*-[Pd(L^{1-8}-κ*S*,*O*)$_2$] complexes were isolated in the solid state from their respective *cis*-[Pd(L^{1-8}-κ*S*,*O*)$_2$] geome by

vapor diffusion-induced crystallization in acetonitrile with irradiation using a 5 Watt LED lamp. The vapour diffusion setup specially designed for this purpose is shown in Figure 2.15. An acetonitrile solution of the *cis*-[Pd(L^{1-8}-κ*S*,*O*)$_2$] complexes is irradiated in a sealed glass vessel directly connected to another vessel containing diethyl ether. Under controlled conditions, diethyl ether vapor diffuses into the acetonitrile solution of the irradiated *cis*-[Pd(L^{1-8}-κ*S*,*O*)$_2$] complexes to selectively crystallize out their *trans* isomers. Alternatively, the *trans*-[Pd(L^{1-8}-κ*S*,*O*)$_2$] complexes were isolated by slow evaporation of an acetonitrile solution following continuous irradiation with a 5 Watt LED lamp.

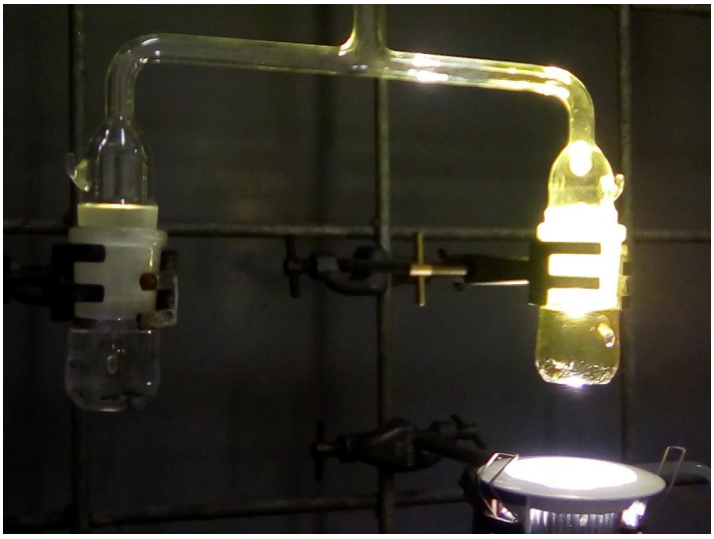

Figure 2.15. Vapour-diffusion induced crystallization apparatus for isolation of *trans*-[Pd(L^{1-8}-κ*S*,*O*)$_2$] complexes in acetonitrile solutions of their *cis*-[Pd(L^{1-8}-κ*S*,*O*)$_2$] isomers by photo-induced isomerization.

trans-bis(N,N-diethyl-N'-(benzoylthioureato-κ^{2}S,O)palladium(II), trans-[Pd(L^1-κS,O)$_2$].

Yield of 63 %; m.p. 194-196 °C; ^{1}H NMR (400 MHz, $CDCl_3$)/ppm δ 8.05 (d, 2H, Ar-H^2), 7.42 (m, 1H, Ar-H^4), 7.35 (m, 2H, Ar-H^3), 3.90 (q, 4H, N-CH_2), 1.40 (m, 4H, CH_2), 1.29 (t, 6H, CH_3).

trans-bis(N,N-diethyl-N-(4-methoxybenzoylthioureato-κ^{2}S,O)palladium(II) trans-[Pd(L^2-κS,O)$_2$].

Yield 60 %; m.p. 180-182 °C; ^{1}H NMR (400 MHz, $CDCl_3$)/ppm δ 8.01 (m, 2H, Ar-H^2), 6.42 (m, 2H, Ar-H^3), 3.85 (m, 4H, CH_2), 1.39 (t, 3H, CH_3), 1.27 (t, 3H, CH_3).

trans-bis(N,N-diethyl-N'-(3,4,5-trimethoxybenzoylthioureato-κ^{2}S,O)palladium(II) trans-[Pd(L^3-κS,O)$_2$].

Yield 84 %; m.p. 213 – 215 °C; ^{1}H NMR (400 MHz, $CDCl_3$)/ppm, δ 7.34 (s, 2H, Ar-H^2), 3.85 (q, 4H, CH_2), 1.38 (t, 3H, CH_3), 1.31 (t, 3H, CH_3).

trans-bis(N,N-diethyl-N'-(4-chlorobenzoylthioureato-κ^{2}S,O)palladium(II) trans-[Pd(L^4-κS,O)$_2$].

Yield 72 %; m.p. 196-198 °C; ^{1}H NMR (400 MHz, $CDCl_3$)/ppm δ 7.97 (m, 2H, Ar-H^2), 7.31 (m, 2H, Ar-H^3), 3.88 (dq, 4H, CH_2), 1.33 (t, 3H, CH_3), 1.27 (t, 3H, CH_3).

trans-bis(N,N-diethyl-N'-4-methyl-benzoylthioureato-κ^{2}S,O)palladium(II) trans-[Pd(L^5-κS,O)$_2$].

Yield of 62 %; m.p. 138-140 °C; ^{1}H NMR (400 MHz, $CDCl_3$)/ppm δ 7.94 (d, 2H, Ar-H^2), 7.15 (d, 2H, Ar-H^3), 3.89 (m, 4H, N(CH_2), 2.37 (s, 2H, Ar-CH_3), 1.40 (t, 3H, CH_3), 1.27 (t, 3H, CH_3).

trans-bis(N,N-dimethyl-N'-(benzoylthioureato-κ^{2}S,O)palladium(II) trans-[Pd(L^6-κS,O)$_2$].

Yield of 64 %; m.p. Decomposes at 245 °C; ^{1}H NMR (400 MHz, $CDCl_3$)/ppm δ 3.41 (s, 3H, CH_3), 3.49 (s, 3H, CH_3), 7.34 (m, 2H, Ar-H4), 7.49 (m, 1H, Ar-H^3), 8.08 (d, 2H, Ar-H^2).

trans-bis(N,N-diethyl-N'-(1-naphthoyl)thioureato-κ^{2}S,O)palladium(II) trans-[Pd(L^7-κS,O)$_2$].

Yield of 62 %; m.p. 174-176 °C (*trans-S,O*), 187-189°C(*trans-S,N*); ^{1}H NMR (400 MHz, $CDCl_3$)/ppm δ 8.63 (d, 1H, Ar-H8((*trans-S,O*)), 8.48 (d, 1H, Ar-H8((*trans-S,N*)), 7.96 (d, 1H, Ar-H^2), 7.89 (d, 1H, Ar-H^4), 7.84 (d, 1H, Ar-H^5), 7.56 (m, 1H, Ar-H^3), 7.48 (m, 1H, Ar-H^6), 7.43 (m, 1H, Ar-H^7), 3.88 (q, 4H, N-CH_2), 3.82 (q, 4H, N-CH_2), 1.36 (t, 3H, CH_3), 1.26 (t, 3H, CH_3).

2.4.4. Light irradiation, reversed phase HPLC and ESI-TOF-MS

Sample irradiation for photoisomerization was performed with either a low-heat (5 Watt OSRAM, Germany) white light-emitting diode (LED) lamp or a hand held blue-violet laser diode (100 mW, λ = 405 nm).

HPLC-UV-Vis experiments were performed using an Agilent 1260 Infinity system fitted with a photodiode array (PDA) detector and an autosampler (Agilent Technologies, Waldronn, Germany). Separation was achieved at room temperature on a GEMINI C_{18} column (4.6 x 150 mm) of particle size 5 μm and with a flow rate of 1 ml min^{-1}. A mobile phase composition of

95:5 (% v/v) acetonitrile:water was used under isocratic elution and detection of chromatographic traces was carried out at 262 nm, with 20 µl sample injection volume. In all cases, the mobile phase was composed only of de-ionized water filtered through a 0.45 µm filter and HPLC grade acetonitrile. All LC-MS experiments were performed using a Waters Synapt G2 mass spectrometer equipped with an ESI source (Waters, Milford, MA, USA). All UHPLC-ESI-MS experiments were carried out in the positive mode using a Waters BEH C_{18} (2.1 X 100 mm) column with the mobile phase composed of acetonitrile and 0.1 % formic acid under isocratic conditions.

2.4.5. Rates of isomerization

5 mg of each *trans*-[Pd(L^n-κ*S*,*O*)$_2$] complex was rapidly dissolved in *ca* 1 ml chloroform-*d* in a NMR tube and then quickly inserted into the NMR spectrometer for analysis. For each analysis, *ca* 2 minutes time lapse was allowed for shimming the spectrometer at 25 °C (± 0.1 °C). Alternatively, 2 mg of each *cis*-[Pd(L^n-κ*S*,*O*)$_2$] complex was dissolved in 10 ml acetonitrile and the resulting solution irradiated for 30 minutes with a 5 Watt LED lamp to generate *cis*-*trans* isomers in solution to a steady state. The irradiated sample was then rapidly injected onto a C_{18} column for RP-HPLC analysis at room temperature and at intervals of *ca* 10-16 minutes in the absence of light, with the chromatographic traces detected on a photodiode-array detector at 262 nm. The reactions were then monitored from changes in relative peak areas of *cis*-*trans* isomers as a function of time in dark.

The relative concentrations of the *trans*-[Pd(L^n-κ*S*,*O*)$_2$] complexes were estimated from ^{1}H NMR and RP-HPLC relative peak areas. The first-order rate constants were estimated from slopes of plots of natural logarithm of relative peak intensity *vs*. time in dark, with least-square regression analysis carried out using Microsoft Excel or Sigma Plot software. All rate constants for the *trans*→*cis* isomerization represent the average of at least three kinetic runs.

2.4.6. Single crystal X-ray diffraction

Crystals suitable for single-crystal X-ray diffraction for the *cis* complexes were grown from acetonitrile solutions in a glass vial sealed with a perforated wax-film under slow evaporation of the solvent at room temperature and in the dark. Crystals of the *trans*-[Pd(L^n-κ*S*,*O*)$_2$] complexes suitable for X-ray diffraction were obtained either by slow evaporation or

vapour diffusion of diethyl ether into acetonitrile solutions of their respective *cis*-[Pd(L^n-κ*S*,*O*)$_2$] complexes irradiated with a 5 Watt LED lamp using the setup in Figure 2.15.

X-ray diffraction intensity data was collected on a Bruker SMART APEX single-crystal X-ray diffractometer equipped with a molybdenum fine-focus sealed tube, monocap collimator and an APEXII detector with Incoatec IμS molybdenum and copper micro-focus X-ray sources. The temperature of the crystals was regulated to 100 K using an Oxford Cryostream Cooler. The crystal structures were all solved and refined using the SHELXS-97.[104] X-seed software[105] was used as a graphic interface for SHELX. All non-hydrogen atoms were refined anisotropically by means of full-matrix least-squares calculations for F_2 using SHELXL-97. Hydrogen atoms were placed using riding model and isotropic thermal parameters were assigned values of 1.2 – 1.5 times the *U*eq of their parent atoms. Molecular graphics were generated using POV-Ray.[106] The crystallographic refinement data for the *cis* and *trans* complexes is presented in Tables 2.4 and 2.5. The checkcif reports are provided in Appendix C.

Table 2.4. Crystallographic refinement data for *cis*-[Pd($L^{2,4-7}$-κ*S*,*O*)$_2$], *trans*-[Pd($L^{1,5}$-κ*S*,*O*)$_2$] complexes.

Compound	***cis*-[Pd(L^2-κ*S*,*O*)$_2$]**	***cis*-[Pd(L^4-κ*S*,*O*)$_2$]**	***cis*-[Pd(L^5-κ*S*,*O*)$_2$]**	***cis*-[Pd(L^6-κ*S*,*O*)$_2$]**	***cis*-[Pd(L^7-κ*S*,*O*)$_2$]**	***trans*-[Pd(L^1-κ*S*,*O*)$_2$]**	***trans*-[Pd(L^5-κ*S*,*O*)$_2$]**
Empirical formula	$C_{26}H_{34}N_4O_4PdS_2$	$C_{24}H_{28}N_4O_2PdS_2Cl_2$	$C_{26}H_{34}N_4O_2PdS_2$	$C_{20}H_{22}N_4O_2PdS_2$	$C_{32}H_{34}N_4O_2PdS_2$	$C_{24}H_{30}N_4O_2PdS_2$	$C_{26}H_{34}N_4O_2PdS_2$
Formula weight	637.11	645.96	605.12	520.42	677.11	577.07	605.12
Crystal system	monoclinic	triclinic	triclinic	monoclinic	orthorhombic	monoclinic	monoclinic
Space group	*P*2$_1$/*c*	*P*-1	*P*-1	*P*2$_1$/*c*	*Pcbn*	*P*2$_1$/*n*	*P*2$_1$/*n*
a (Å)	10.8538(4)	7.7353(7)	7.7879(4)	11.5686(17)	43.068(8)	12.302(3)	10.712(11)
b (Å)	9.7700(4)	13.73209(13)	13.6956(7)	11.8051(18)	9.323(18)	8.456(18)	10.683(11)
c (Å)	27.0136(11)	13.8536(13)	13.8798(7)	15.199(2)	15.204(3)	8.456(18)	11.996(12)
α/°	90.000	112.8130(10)	112.3770(10)	90.000	90.000	90.00	90.00
β/°	93.3989(1)	92.3590(10)	96.1610(10)	94.540(2)	110.198	110.198	99.436
γ/°	90.000	95.9360(10)	91.7590(10)	90.000	90.000	90.000	90.000
Z	4	8	12	4	2	2	2
T/K	100	100	100	100	100	100	100
μ/mm^{-1}	0.840	3.354	4.383	1.123	0.781	0.917	0.864
Independent reflections	6501	6104	11854	4779	7077	2933	3121

R_{int}	0.018	0.0193	0.0114	0.0191	0.080	0.042	0.0337
Final R1, wR2[I > 2σ(I)]	0.0210, 0.0500, 1.03	0.0651, 0.1475, 1.028	0.0371, 0.0976, 1.045	0.0417, 0.1064, 1.006	0.0490, 0.1043	0.0408, 0.0981, 1.06	0.0526, 0.2102, 0.752

Table 2.5. Crystallographic refinement data for *trans*-[Pd($L^{6,7}$-κ*S*,*O*)$_2$], *trans*-[Pd(L^{7}-κ*S*,*N*)$_2$], *cis*-[Pd(*EE*-L^{8}-κ*S*,*O*)$_2$], *cis*-[Pt(*EE*-L^{8}-κ*S*,*O*)$_2$] and *cis*-[Pt(*ZZ*-L^{15}-κ*S*,*O*)$_2$] complexes.

Compound	***trans*-[Pd(L^{6}-κ*S*,*O*)$_2$]**	***trans*-[Pd(L^{7}-κ*S*,*O*)$_2$]**	***trans*-[Pd(L^{7}-κ*S*,*N*)$_2$]**	***cis*-[Pd(*EE*-L^{8}-κ*S*,*O*)$_2$]**	***cis*-[Pt(*EE*-L^{8}-κ*S*,*O*)$_2$]**	***cis*-[Pt(*ZZ*-L^{15}-κ*S*,*O*)$_2$]**
Empirical formula	$C_{20}H_{22}N_4O_2PdS_2$	$C_{32}H_{34}N_4O_2PdS_2$	$C_{32}H_{34}N_4O_2PdS_2$	$C_{22}H_{26}N_4O_2PdS_2$	$C_{22}H_{26}N_4O_2PtS_2$	$C_{32}H_{42}N_4O_4PtS_2$
Formula weight	520.42	677.11	677.11	549.02	637.68	809.93
Crystal system	monoclinic	monoclinic	monoclinic	monoclinic	monoclinic	triclinic
Space group	$P2_1/n$	$P2_1/c$	$P2_1/n$	$P2_1/c$	$P2_1/c$	P-1
a (Å)	5.680(2)	11.640(15)	12.471(3)	12.684(5)	12.7293(14)	10.134(3)
b (Å)	21.231(9)	8.444(11)	7.387(2)	11.806(5)	11.7920(12)	12.361(4)
c (Å)	8.498(4)	14.795(19)	15.924(5)	15.285(6)	15.2466(16)	14.603(5)
α/°	90.000	90.000	90.000	90.000	90.000	74.457(4)
β/°	93.332	96.132(2)	92.975(4)	93.008(6)	93.2590(10)	87.018(4)
γ/°	90.000	90.000	90.000	90.000	90.000	77.579(4)
Z	2	2	2	4	4	2
T/K	100	100	100	100	100	100
μ/mm^{-1}	1.136	0.824	0.812	1.020	6.351	4.238

Independent reflections	2183	3344	3387	5308	5253	11143
R_{int}	0.0259	0.017	0.045	0.0414	0.0240	0.0323
Final R1, wR2[I > 2σ(I)]	0.0317, 0.0682, 1.037	0.0245, 0.0668, 1.07	0.0245, 0.0668, 1.07	0.0432, 0.0973, 1.042	0.0340, 0.0765, 1.047	0.0555, 0.1481, 1.055

3

Photo-induced isomerization leading to isolation of novel trans-[Pd(L^n-κS,O)$_2$] complexes with N,N-dialkyl-N'-benzoylthioureas

The results discussed in this chapter have been published in the Journal of Coordination Chemistry (Appendix B)

Synopsis

This chapter describes the photo-induced isomerization of cis-[Pd(L^n-κS,O)$_2$] complexes derived from the N,N-dialkyl-N'-benzoylthioureas (HL$^{1-6}$). Isolation of a series of novel trans-[Pd(L-κS,O)$_2$] isomers has been carried out using vapour diffusion-induced crystallization and slow evaporation following light irradiation in acetonitrile. The trans-[Pd(L^n-κS,O)$_2$] complexes were produced in reasonable yields and represent the first example of trans-[Pd(L^n-κS,O)$_2$] complexes deliberately prepared by conventional procedures. A full characterization of the ^{1}H NMR spectra of the isolated trans-[Pd(L^n-κS,O)$_2$] complexes as well as X-ray crystallographic description of some of the complexes is also presented.

3.1. Introduction

Several reports in the literature indicate the formation of relatively stable and neutral six-membered *cis*-[M(L^n-κ*S*,*O*)$_2$] (M = Pt(II) or Pd(II)) chelates[10,27,30-34] from reaction of platinum(II) or palladium(II) with the *N*,*N*-dialkyl-*N*'-acylthioureas. The formation of the *cis*-[M(L^n-κ*S*,O)$_2$] complexes in preference to their *trans*-[M(L^n-κ*S*,*O*)$_2$] counterparts has been ascribed to a higher *trans*-effect of the sulfur donor atoms relative to oxygen.[58] As a result of the relatively high thermodynamic stability of the *cis*-[M(L^n-κ*S*,O)$_2$] isomers of d^8 transition metal ions, only four *N*,*N*-dialkyl-*N*'-acylthiourea complexes of Cu(II)[53-55] and Pt(II)[56] are reported in the Cambridge Structural Database. The *trans*-[Cu(L-κ*S*,O)$_2$] complexes were prepared in a mixture consisting of their *cis*-[Cu(L-κ*S*,O)$_2$] isomers after solutions of Cu(II) salts were directly added to the ligand solutions.[53-55] Recently, two *trans*-[Cu(L-κ*S*,O)$_2$] (HL = *N*-Isopropyl, *N*-phenyl-*N*'-2,4,6-trimethyl-benzoylthiourea, *N*, *N*-diethyl, *N*'-2,4,6-trimethyl-benzoylthiourea) complexes were isolated by Roesky and co-workers[107] after addition of their respective ligands to solutions of CuI and $CuCl_2$. The other three complexes prepared by these authors were found to have a *cis*-[Cu(L-κ*S*,O)$_2$] configuration. The unexpected formation of the two *trans*-[Cu(L-κ*S*,O)$_2$] complexes was attributed to less steric bulk exhibited by the ligand substituents.

The only *trans*-[Pt(L-κ*S*,*O*)$_2$] (HL = *N*,*N*-di-(*n*-butyl)-*N*'-naphthoylthiourea) complex reported in the literature was fortuitously isolated more than two decades ago after crystallization in a chloroform/ethanol mixture with *ca* 15 % yield.[56] Later on, it was revealed by Koch and co-workers that *trans*-[M(L^n-κ*S*,*O*)$_2$] (M = Pt(II) or Pd(II)) complexes of the *N*,*N*-dialkyl-*N*'-acylthioureas are readily generated in acetonitrile solutions by photo-induced isomerization of their *cis*-[M(L^n-κ*S*,*O*)$_2$] counterparts upon irradiation with polychromatic light of wavelength < 480 nm.[13] The photo-induced *cis*-[M(L^n-κ*S*,*O*)$_2$]→*trans*-[M(L^n-κ*S*,*O*)$_2$] reaction is influenced by the wavelength of light used for irradiation.[13] Hence isomerization occurs when acetonitrile solutions of the *cis*-[M(L^n-κ*S*,*O*)$_2$] complexes were irradiated with blue and yellow light, but not with red light. The geometric isomers from photo-induced isomerization exhibit differences in RP-HPLC retention times and $^1H/^{195}Pt\{^1H\}$ NMR chemical shifts.[13]

In chapter 2, it was shown that the *N*,*N*-dialkyl-*N*'-acylthioureas (HL^{1-15}) react with solutions of platinum(II) and palladium(II) salts forming exclusively *cis*-[M(L^n-κ*S*,*O*)$_2$] complexes. In this chapter, photo-induced isomerization studies conducted on the *cis*-[M(L^{1-6}-

κ*S*,*O*)$_2$] (M = Pd(II) or Pt(II)) complexes with the *N*,*N*-dialkyl-*N*'-benzoylthioureas (HL$^{1-6}$) will be presented. The names and structures of the HL$^{1-6}$ ligands were presented in chapter 2, Figure 2.2, page 20.

Isolation of the *trans*-[Pd(L^n-κ*S*,*O*)$_2$] complexes was carried out after irradiation of their *cis*-[Pd(L^n-κ*S*,*O*)$_2$] counterparts using the steps represented in Figure 3.1. Characterization of the isolated *trans*-[Pd(L$^{1-6}$-κ*S*,*O*)$_2$] complexes was performed by melting point, ^{1}H NMR and single-crystal X-ray diffraction. Isolation of the *trans*-[Pt(L^3-κ*S*,*O*)$_2$] complex was not attempted since photo-induced isomerization of platinum(II) complexes with the *N*,*N*-dialkyl-*N*'-acylthioureas under intense light irradiation is known to be accompanied by formation of considerable amounts of photodecomposition products.[58]

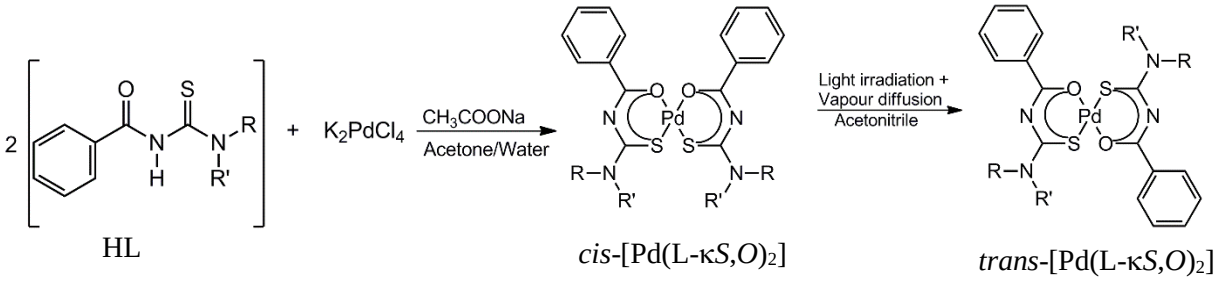

Figure 3.1. General method for preparation of *trans*-[Pd(L^n-κ*S*,*O*)$_2$] complexes from *cis*-[Pd(L^n-κ*S*,*O*)$_2$] isomers following photo-induced isomerization in acetonitrile.

3.2. Results and discussion

3.2.1. Photo-induced isomerization of *cis*-[M(L-κ*S*,*O*)$_2$] (M = Pt(II) or Pd(II)) complexes: ^{1}H, ^{195}Pt{^{1}H} NMR and RP-HPLC studies

The photo-induced *cis*→*trans* isomerization in the *cis*-[M(L$^{1-6}$-κ*S*,*O*)$_2$] (M = Pd(II) or Pt(II)) complexes of the *N*,*N*-diethyl-*N'*-benzoylthioureas (HL$^{1-6}$) was examined using ^{1}H, ^{195}Pt{^{1}H} NMR spectroscopy and RP-HPLC. In order to monitor the *cis*-*trans* isomerism in *cis*-[Pd(L^1-κ*S*,*O*)$_2$] (HL^1 = *N*,*N*-diethyl-*N*'-benzoylthiourea) by ^{1}H NMR spectroscopy, *ca* 5 mg/mL solution of the complex was prepared in acetonitrile-d_3. This was followed by rapid NMR data acquisition before and after irradiation in an NMR tube with a 5 Watt LED lamp. Figure 3.2 shows a representative ^{1}H NMR spectrum of the *cis*-[Pd(L^1-κ*S*,*O*)$_2$] complex after irradiation for 20 minutes with a 5 Watt LED lamp. The formation of a new set of doublets for the proton H$^{2,2'}$ is evident at δ = 8.05 ppm assigned to the *trans*-[Pd(L^1-κ*S*,*O*)$_2$] isomer. The new *trans*-H$^{2,2'}$ resonance is formed at the expense of *cis*-resonance at δ = 8.26 ppm due to

photo-induced isomerization of the *cis*-[Pd(L^1-κ*S*,*O*)$_2$] complex. As the time of irradiation increases, the intensity of *trans*-$H^{2,2'}$ increases while that of *cis* decreases steadily until a steady state is achieved. In the absence of light, a slow *trans*→*cis* reversion occurs and within an hour only *cis*-resonances were observed.

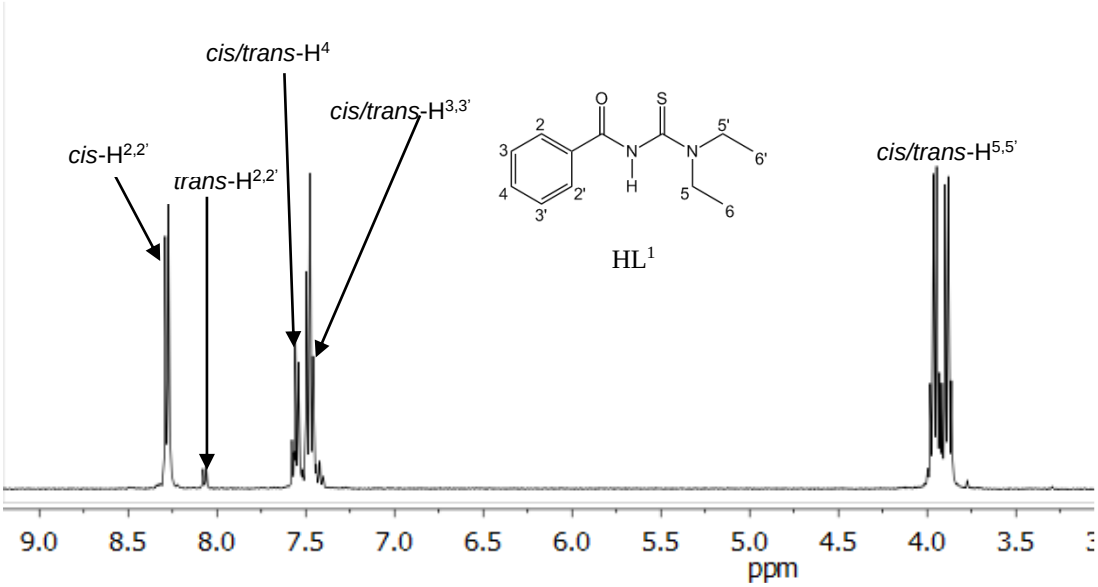

Figure 3.2. Partial ^{1}H NMR spectrum of an acetonitrile-d_3 solution *cis*-bis(*N*,*N*-diethyl-*N*'-benzoylthioureato-κ^2*S*,*O*)palladium(II) after irradiation with polychromatic light from a 5 Watt LED lamp for 15 minutes at 25 °C.

For the more soluble *cis*-[Pt(L^3-κ*S*,*O*)$_2$] complex, the use of ^{195}Pt{^{1}H} NMR spectroscopy also enabled monitoring of *cis*→*trans* isomerism. Figure 3.3 shows the ^{195}Pt{^{1}H} NMR spectra of *ca* 50 mg/mL *cis*-[Pt(L^3-κ*S*,*O*)$_2$] (HL^3 = *N*,*N*-diethyl-*N'*-3,4,5-trimethoxy-benzoylthiorea) in chloroform-*d* before and after irradiation for *ca* 20-30 minutes with a 5 Watt LED lamp, followed by ^{195}Pt{^{1}H} NMR data acquisition. In the absence of light, the *cis*-[Pt(L^3-κ*S*,*O*)$_2$] complex generates a single ^{195}Pt{^{1}H} resonance at -2700 ppm as shown by Figure 3.3 (a). After irradiation, an additional ^{195}Pt{^{1}H} resonance is clearly evident at *ca* -1980 ppm. This is assigned to the photo-isomerized *trans*-[Pt(L^3-κ*S*,*O*)$_2$] isomer (Figure 3.3 (b)). The new *trans*-^{195}Pt{^{1}H} resonance is significantly less shielded than its *cis* counterpart by *ca* 748 ppm. This is consistent with the difference in ^{195}Pt chemical shift reported for *cis*-*trans* isomers of similar *cis*-[Pt(L-κ*S*,*O*)$_2$] complexes.[50] When the irradiated solution of the *cis*-[Pt(L^3-κ*S*,*O*)$_2$] complex was allowed to stand in the dark for several hours, slow *trans*→*cis* reversion occurred resulting almost completely to the *cis*-[Pt(L-κ*S*,*O*)$_2$] resonance.

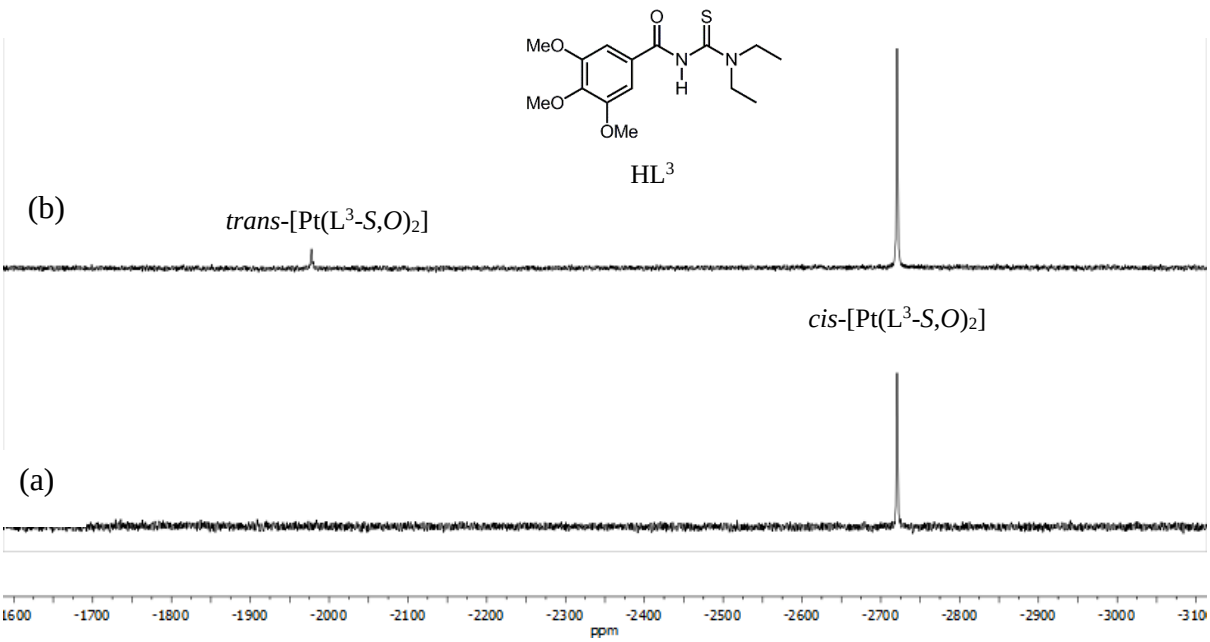

Figure 3.3. $^{195}Pt\{^{1}H\}$ NMR spectra of a chloroform-*d* solution *cis*-bis(*N*,*N*-diethyl-*N*'-3,4,5-trimethoxy-benzoylthioureato-κ^2*S*,*O*)platinum(II) (a) before and (b) after irradiation with polychromatic light from a 5 Watt LED lamp for 20 minutes at 25 °C.

Photo-induced isomerization of the *cis*-[Pd(L^{1-6}-κ*S*,*O*)$_2$] complexes was also studied using RP-HPLC since both *cis* and *trans* isomers are known to be relatively stable on a C_{18} column and have different retention times.[13] The separation of all *cis*-*trans* isomers was achieved using 95:5 (% v/v acetonitrile:water) mixture as mobile phase. New chromatographic peaks appear after irradiation of the *cis*-[Pd(L^{1-6}-κ*S*,*O*)$_2$] complexes (Figure 3.4) and these are unambiguously assigned to the photo-isomerised *trans*-[Pd(L^{1-6}-κ*S*,*O*)$_2$] products. The retention times of the *cis*-*trans* isomers for the six complexes are presented in Table 3.1 and follow the order:

[Pd(L^6-κ*S*,*O*)$_2$] < [Pd(L^3-κ*S*,*O*)$_2$] < [Pd(L^2-κ*S*,*O*)$_2$] < [Pd(L^1-κ*S*,*O*)$_2$] < [Pd(L^5-κ*S*,*O*)$_2$] < [Pd(L^4-κ*S*,*O*)$_2$]

The above trend is consistent with the expected electronic effect of ligand substituents on retention of the *cis*-[Pd(L^n-κ*S*,*O*)$_2$] complexes on a relatively apolar C_{18} column as reported in the literature.[58] The presence of smaller methyl substituents attached to the thiaomido nitrogen appears to remarkably decrease the polarity of the *cis*-[Pd(L^6-κ*S*,*O*)$_2$] (HL^6 = *N*,*N*-dimethyl-*N*'-benzoylthiourea) complex thereby leading to the shortest retention time of 8.4 minutes. Introduction of three electron-releasing methoxy groups at the 3,4,5 phenyl positions in the *cis*-[Pd(L^3-κ*S*,*O*)$_2$] complex (HL^3 = *N*,*N*-diethyl-*N'*-3,4,5-trimethoxy-benzoylthiourea) also leads to decrease in peak retention time (12.1 minutes) compared to *cis*-[Pd(L^2-κ*S*,*O*)$_2$] (HL^2 = *N*,*N*-

diethyl-*N'-4*-methoxy-benzoylthiourea) which elutes after 13.1 minutes. The presence of electron-releasing methyl substituents at the *para* position of the phenyl ring in the *cis*-[Pd(L^5-κ*S*,*O*)$_2$] (HL^5 = *N*,*N*-diethyl-*N'-4*-methyl-benzoylthiourea) complex increases retention time (23.0 minutes) relative to the unsubstituted *cis*-[Pd(L^1-κ*S*,*O*)$_2$] complex (15.6 minutes). Finally, the presence of electron-withdrawing chloro substituents at the *para* position of the phenyl ring in the *cis*-[Pd(L^4-κ*S*,*O*)$_2$] (HL^4 = *N*,*N*-diethyl-*N'-4*-chloro-benzoylthiourea) complex significantly increases its retention onto the C_{18} column (retention time of 35.0 minutes) relative to *cis*-[Pd(L^1-κ*S*,*O*)$_2$].

The extent of photo-induced *cis*→*trans* isomerization was found to be dependent on the nature of the ligand substituents. Similar extent of *cis*→*trans* conversion was obtained for the *cis*-[Pd(L^1-κ*S*,*O*)$_2$] (27.1 %), *cis*-[Pd(L^2-κ*S*,*O*)$_2$] (28.2 %) and *cis*-[Pd(L^5-κ*S*,*O*)$_2$] (24.2 %) complexes after 10 minutes of exposure to light . A decrease in extent of isomerization was observed for the *cis*-[Pd(L^3-κ*S*,*O*)$_2$] (15.2 %) complex. This indicates that the presence of three electron-releasing methoxy groups at the 3,4,5-poistions of the phenyl ring stabilizes the *cis*-[Pd(L^3-κ*S*,*O*)$_2$] complex relative to its *trans*-[Pd(L^3-κ*S*,*O*)$_2$] isomer. A lower extent of isomerization was also obtained for the *cis*-[Pd(L^6-κ*S*,*O*)$_2$] (12.1%) complex relative to *cis*-[Pd(L^1-κ*S*,*O*)$_2$]. The RP-HPLC chromatograms of the *cis*-[Pd(L^3-κ*S*,*O*)$_2$], *cis*-[Pd(L^5-κ*S*,*O*)$_2$] and *cis*-[Pd(L^6-κ*S*,*O*)$_2$] complexes (Figures 3.4 (c), (d) and (e) respectively) show evidence some degree of photodecomposition with the formation of free ligands. This could possibly also account for the differences in the extents of photo-induced isomerization observed for the *cis*-[Pd(L^n-κ*S*,*O*)$_2$] complexes. It is evident from the RP-HPLC chromatograms (Figure 3.4) that the *cis*-[Pd(L^n-κ*S*,*O*)$_2$] isomers are less retained onto a C_{18} column than their corresponding *trans*-[Pd(L^n-κ*S*,*O*)$_2$] counterparts. A notable exception is the *cis*-[Pd(L^3-κ*S*,*O*)$_2$] complex in which the *trans* isomer elutes much earlier than the *cis* isomer.

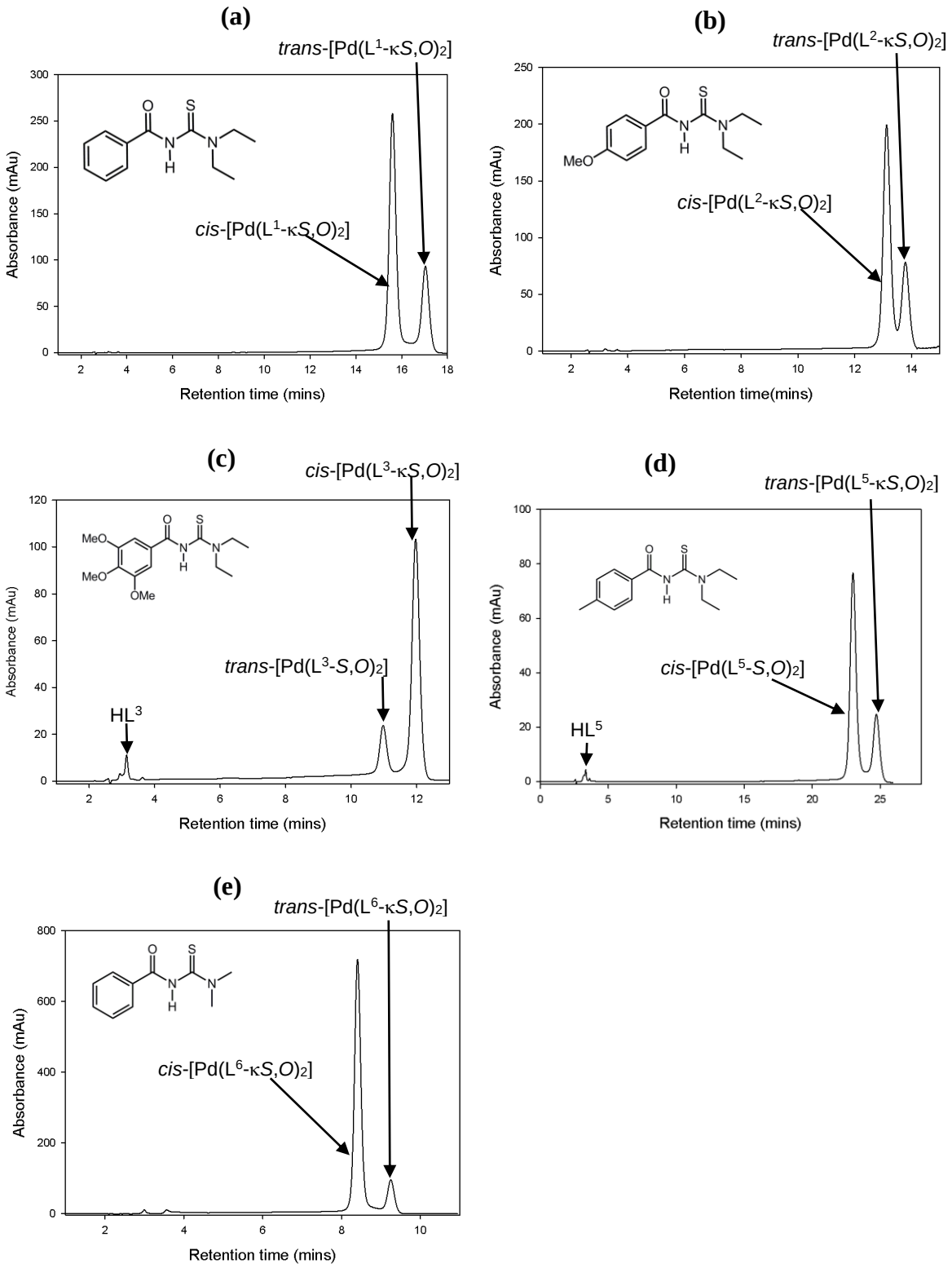

Figure 3.4. Chromatograms showing RP-HPLC separation of an acetonitrile solution of *cis*-[Pd($L^{1\text{-}3,5\text{-}6}$-κ*S*,*O*)$_2$] complexes after irradiation for 10 minutes with polychromatic light from a 5Watt LED lamp; conditions: mobile phase, 90:10 (% v/v) acetonitrile:water; GEMINI C_{18}, 5 µm, 250 x 4.6 mm column; 20 µl injection volume; 1 ml min^{-1} flow rate; 262 nm detection.

Table 3.1. Retention times and % *trans* conversion representing RP-HPLC separation of *cis-trans* isomers of *cis*-[Pd($L^{1\text{-}6}$-κ*S*,*O*)$_2$] chelates in 90:10 (% v/v) acetonitrile:water mixture, after 10 mins irradiation with polychromatic light from a 5 Watt LED lamp.

	Retention time (min)		**% *trans*-κ*S*,*O***
	cis-S,O	*trans-S,O*	
[Pd(L^1-κ*S*,*O*)$_2$]	15.6	17.0	27.1
[Pd(L^2-κ*S*,*O*)$_2$]	13.1	13.8	28.2
[Pd(L^3-κ*S*,*O*)$_2$]	12.0	11.0	15.2
[Pd(L^4-κ*S*,*O*)$_2$]	35.0	-	-
[Pd(L^5-κ*S*,*O*)$_2$]	23.0	24.7	24.2
[Pd(L^6-κ*S*,*O*)$_2$]	8.4	9.2	12.1

The geometric isomers of *cis*-[Pd(L^1-κ*S*,*O*)$_2$] were also monitored using RP-HPLC separation with online NMR detection. This involved direct flow of *ca* 5 mg/mL of a pre-irradiated acetonitrile solution of *cis*-[Pd(L^1-κ*S*,*O*)$_2$] into an NMR flow cell. The continuous spectra acquisition and detection of the *cis-trans* resonances was aided by solvent suppression. Figure 3.5 shows the representative HPLC-^{1}H NMR spectra of irradiated acetonitrile solution of *cis*-[Pd(L^1-κ*S*,*O*)$_2$]. Consistent with the HPLC-UV detection results, new sets of *trans*-$H^{2,2'}$ resonances are seen to emerge attributed to *trans*-[Pd(L^1-κ*S*,*O*)$_2$], eluting after 17.1 minutes.

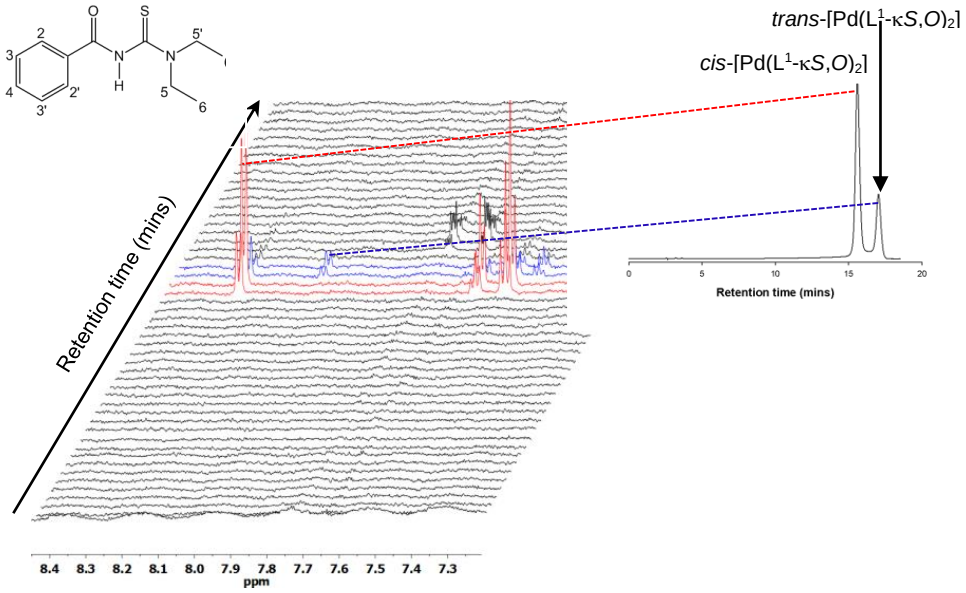

Figure 3.5. Downfield region of HPLC-^{1}H NMR spectra of acetonitrile solutions of *cis*-[Pd(L^1-κ*S*,*O*)$_2$] irradiated with polychromatic light from a 5 Watt LED lamp; conditions: mobile phase, acetonitrile:water (90:10 % v/v) mixture; GEMINI C_{18}, 5 µm, 250 x 4.6 mm column; 20 µl injection volume; 1 ml min^{-1} flow rate; 262 nm detection.

3.2.2. Characterization of isolated *trans*-[Pd(L^n-κ*S*,*O*)$_2$] (HL = *N*,*N*-diethyl-*N'*-benzoylthiourea) complexes

The *trans*-[Pd(L^n-κ*S*,*O*)$_2$] complexes were isolated in high yields (> 60 %) by either vapour diffusion or slow evaporation as discussed in section 2.2.3, page 44. All isolated *trans*-[Pd(L$^{1-6}$-κ*S*,*O*)$_2$] complexes were characterized by melting point determination and ^{1}H NMR spectroscopy. Single-crystal X-ray crystallography was also used to confirm their *trans*-κ*S*,*O* configuration when suitable crystals were grown. Table 3.2 summarises the melting points as well as ^{1}H NMR chemical shift of the isolated *trans*-[Pd(L$^{1-6}$-κ*S*,*O*)$_2$] complexes relative to those observed for the *cis*-[Pd(L$^{1-6}$-κ*S*,*O*)$_2$] complexes. In general, higher melting points were obtained for the *trans*-[Pd(L$^{1-6}$-κ*S*,*O*)$_2$] isomers relative to their *cis*-[Pd(L$^{1-6}$-κ*S*,*O*)$_2$] counterparts, although *trans*-[Pd(L^5-κ*S*,*O*)$_2$] (HL^5 = *N*,*N*-diethyl-*N'*-*4*-methyl-benzoylthiourea) melts at 138-140 °C compared to *cis*-[Pd(L^5-κ*S*,*O*)$_2$] with melting point of 218-220 °C. The differences in melting points between the *cis*-*trans* isomers could be ascribed to their different packing modes and interactions involved in the solid states. The melting points of both *cis*-[Pd(L^6-κ*S*,*O*)$_2$] and *trans*-[Pd(L^6-κ*S*,*O*)$_2$] (HL^6 = *N*,*N*-dimethyl-*N'*-benzoylthiourea) could not be determined as both unfortunately decomposed above 247 °C.

Table 3.2. Melting points and ^{1}H NMR chemical shift differences between isolated *trans*-[Pd(L$^{1-6}$-κ*S*,*O*)$_2$] complexes relative to the *cis*-[Pd(L$^{1-6}$-κ*S*,*O*)$_2$] isomers.

Complex	δ/ppm (H$^{2,2'}$)		m.p/°C		% Yield of *trans* complexes
	cis	***trans***	***cis***	***trans***	
[Pd(L^1-κ*S*,*O*)$_2$]	8.25	8.06	159-163	194-196	63.4
[Pd(L^2-κ*S*,*O*)$_2$]	8.20	8.02	138-140	180-182	60.0
[Pd(L^3-κ*S*,*O*)$_2$]	7.55	7.36	198-202	213-215	84.0
[Pd(L^4-κ*S*,*O*)$_2$]	8.15	7.97	179-189	196-198	72.5
[Pd(L^5-κ*S*,*O*)$_2$]	8.13	7.94	218-220	138-140	62.5
[Pd(L^6-κ*S*,*O*)$_2$]	8.95	8.63	> 247	> 247	62.0

Figures 3.6 to 3.11 show the ^{1}H NMR spectra of the isolated *trans*-[Pd($L^{1\text{-}6}$-κ*S*,*O*)$_2$] complexes relative to their *cis*-[Pd($L^{1\text{-}6}$-κ*S*,*O*)$_2$] isomers in chloroform-*d*. The *cis*-*trans* isomers have similar resonances but at different chemical shift positions. A relatively small proportion of *cis*-[Pd(L^1-κ*S*,*O*)$_2$] (Figure 3.6) for the phenyl protons $H^{2,2'}$ is barely evident at = δ 8.25 ppm in the *trans*-[Pd(L^1-κ*S*,*O*)$_2$] spectrum. This is ascribed to the slow *trans*→*cis* reversion resulting from time lapses of *ca* 3 minutes during sample preparation and data acquisition. The *trans*-$H^{2,2'}$ resonances experience a considerable shift upfield relative to that of *cis* by *ca* 0.19 ppm. This chemical shift difference is suggestive of a higher anisotropic shielding effect of the $H^{2,2'}$ protons in the *trans* position. A much smaller downfield shift is experienced by the other two phenyl protons $H^{3,3'}$ and H^4 at the *cis* and *trans* orientations. For the methyl ($H^{6,6'}$) and methylene ($H^{5,5'}$) protons, slight downfield shifts are evident for the *trans*-[Pd(L^1-κ*S*,*O*)$_2$] isomer relative to the *cis*-[Pd(L^1-κ*S*,*O*)$_2$] complex. Furthermore, greater chemical shifts differences are evident between the magnetically inequivalent methyl ($H^{5,5'}$) and methylene ($H^{4,4'}$) protons. Figure 3.7 (b) shows the ^{1}H NMR spectrum of the isolated *trans*-[Pd(L^2-κ*S*,*O*)$_2$] (HL^2 = *N*,*N*-diethyl-*N*'-4-methoxy-benzoylthiourea) complex compared to that of *cis*-[Pd(L^2-κ*S*,*O*)$_2$] represented in Figure 3.7(a). Both *cis*-*trans* isomers of the [Pd(L^2-κ*S*,*O*)$_2$] complex are characterized by two sets of doublets representing the aromatic protons $H^{2,2'}$ and $H^{3,3'}$. An upfield shift of *ca* 0.18 ppm is observed for the proton $H^{2,2'}$ in the *trans*-[Pd(L^2-κ*S*,*O*)$_2$] complex relative to $H^{2,2'}$ resonances of the *cis*-[Pd(L^2-κ*S*,*O*)$_2$] isomer. Figures 3.8 (a) and (b) show the ^{1}H NMR spectra of *cis*-[Pd(L^3-κ*S*,*O*)$_2$] and isolated *trans*-[Pd(L^3-κ*S*,*O*)$_2$] respectively (HL^3 = *N*,*N*-diethyl-*N'*-3,4,5-timethoxy-benzoylthiourea). A greater upfield shift of *ca* δ 0.69 ppm is obvious for the $H^{2,2'}$ singlet of *cis*-[Pd(L^3-κ*S*,*O*)$_2$] complex relative to *cis*-[Pd(L^1-κ*S*,*O*)$_2$] and *cis*-[Pd(L^2-κ*S*,*O*)$_2$]. An upfield shift of *ca* 0.19 ppm exists for the $H^{2,2'}$ resonances of the *cis*-[Pd(L^3-κ*S*,*O*)$_2$] complex relative to that of the *trans*-[Pd(L^3-κ*S*,*O*)$_2$] isomer. The ^{1}H NMR spectrum of the isolated *trans*-[Pd(L^4-κ*S*,*O*)$_2$] (HL^4 = *N*, *N*-diethyl-*N*'-4-chloro-benzoylthiourea) complex is represented in Figure 3.9 (b). It shows that an upfield shift of *ca* 0.17 ppm exists between the $H^{2,2'}$ resonances relative to that of the *cis*-[Pd(L^4-κ*S*,*O*)$_2$] isomer. The resonances in the ^{1}H NMR spectra of the isolated *trans*-[Pd(L^5-κ*S*,*O*)$_2$] and *cis*-[Pd(L^5-κ*S*,*O*)$_2$] complexes (Figure 3.10) are similar to those of *trans*-[Pd(L^4-κ*S*,*O*)$_2$] and *cis*-[Pd(L^4-κ*S*,*O*)$_2$] complexes (Figure 3.9). Irradiation of an acetonitrile solution of *cis*-[Pd(L^6-κ*S*,*O*)$_2$] (HL^6 = *N*,*N*-dimethyl-*N'*-benzoylthiourea) complex led to isolation of a mixture of *cis*-*trans* complexes as seen in the ^{1}H NMR spectrum in Figure 3.11 (b).

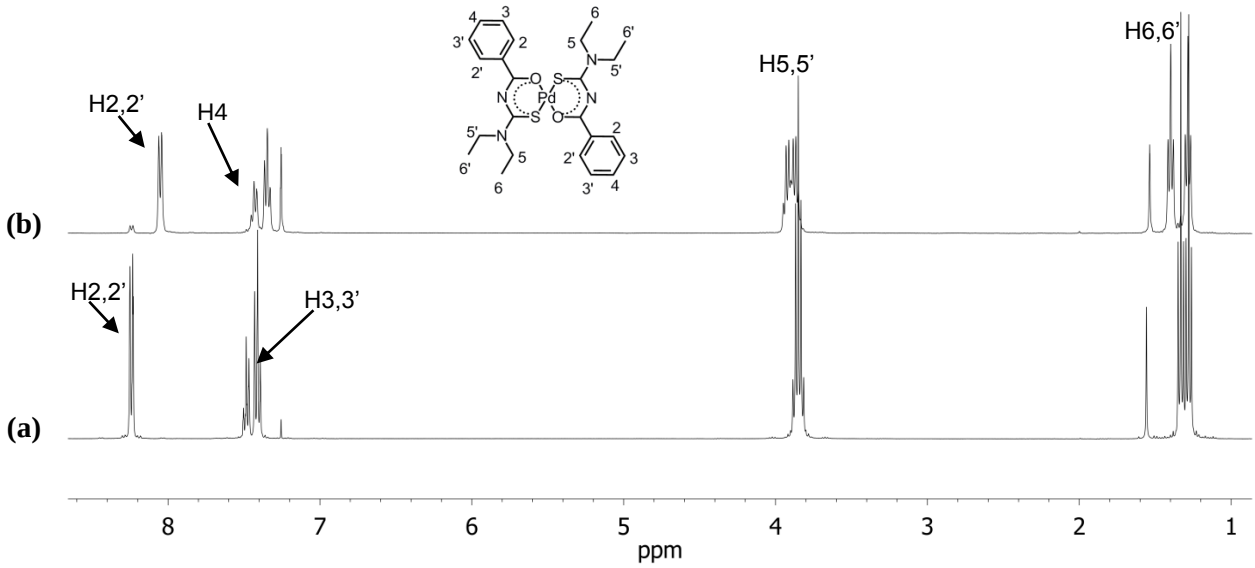

Figure 3.6. ^{1}H NMR spectra of (a) pure *cis* and (b) isolated *trans* complexes of bis(*N*,*N*-diethyl-*N*'-benzoylthioureato-κ*S*,*O*)palladium(II) in chloroform-*d* at 25 °C.

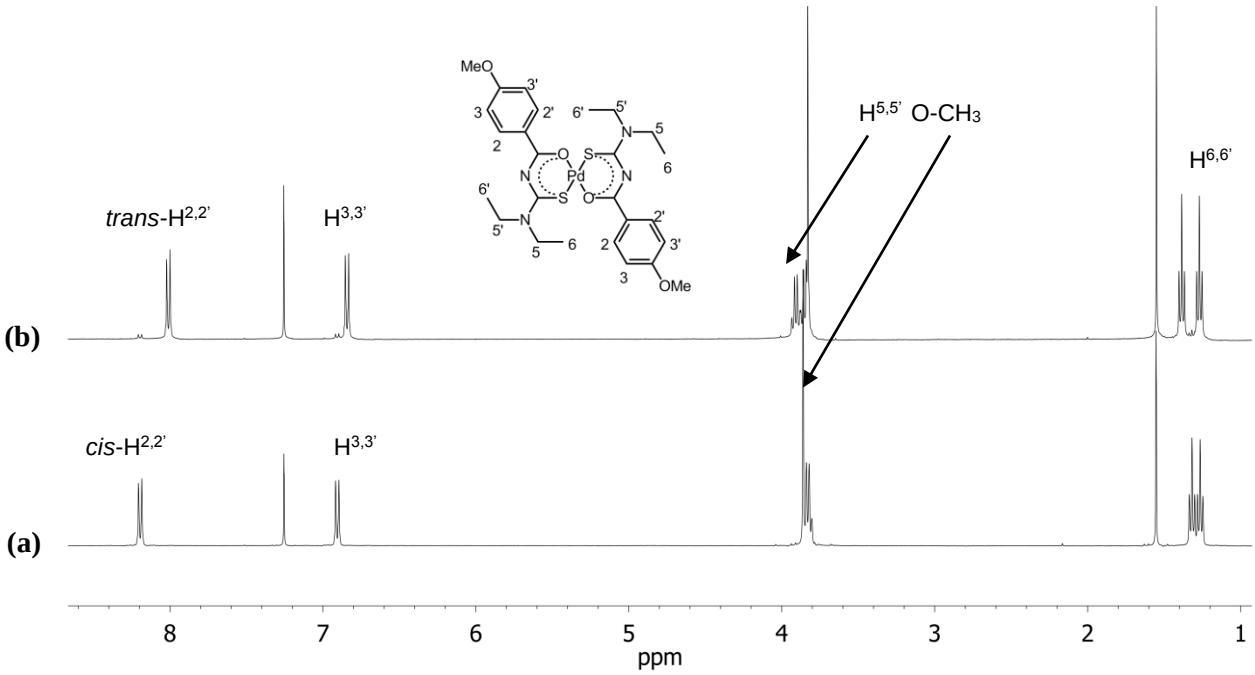

Figure 3.7. ^{1}H NMR spectra of (a) pure *cis* and (b) isolated *trans* complexes of bis(*N*,*N*-diethyl-*N*'-4-methoxy-benzoylthioureato-κ^{2}*S*,*O*)palladium(II), in chloroform-*d* at 25 °C.

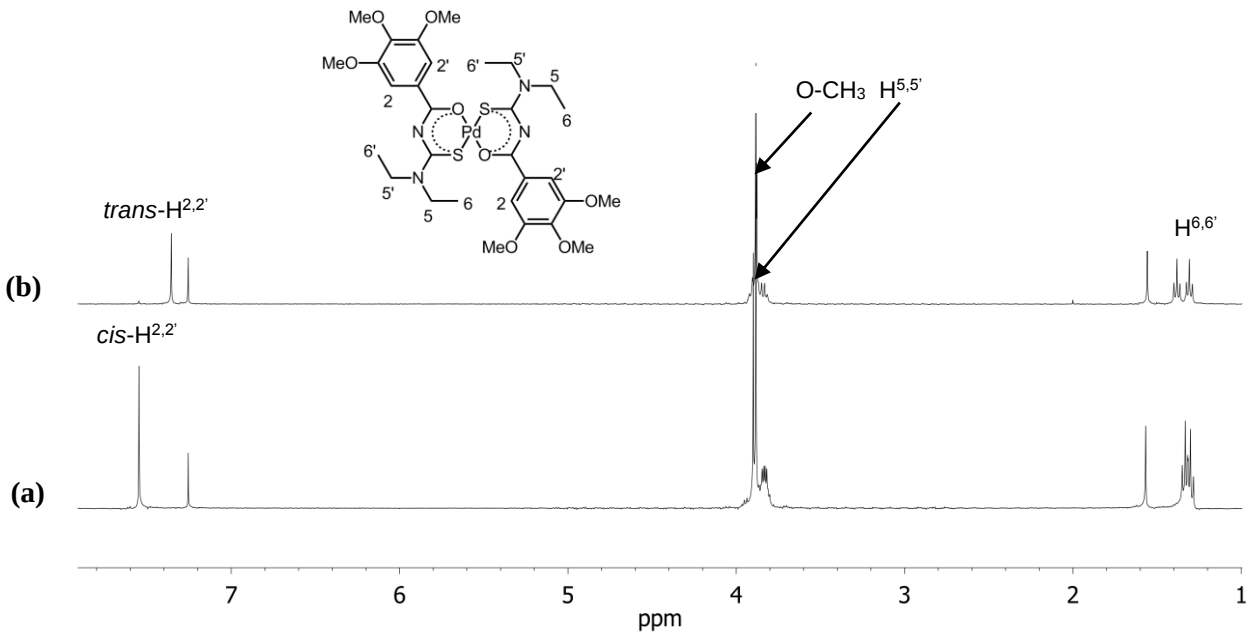

Figure 3.8. ^{1}H NMR spectra of (a) pure *cis* and (b) isolated *trans* complexes of bis(*N*,*N*-diethyl-*N*'-3,4,5-trimethoxy-benzoylthioureato-κ^{2}*S*,*O*)palladium(II) in chloroform-*d* at 25 °C.

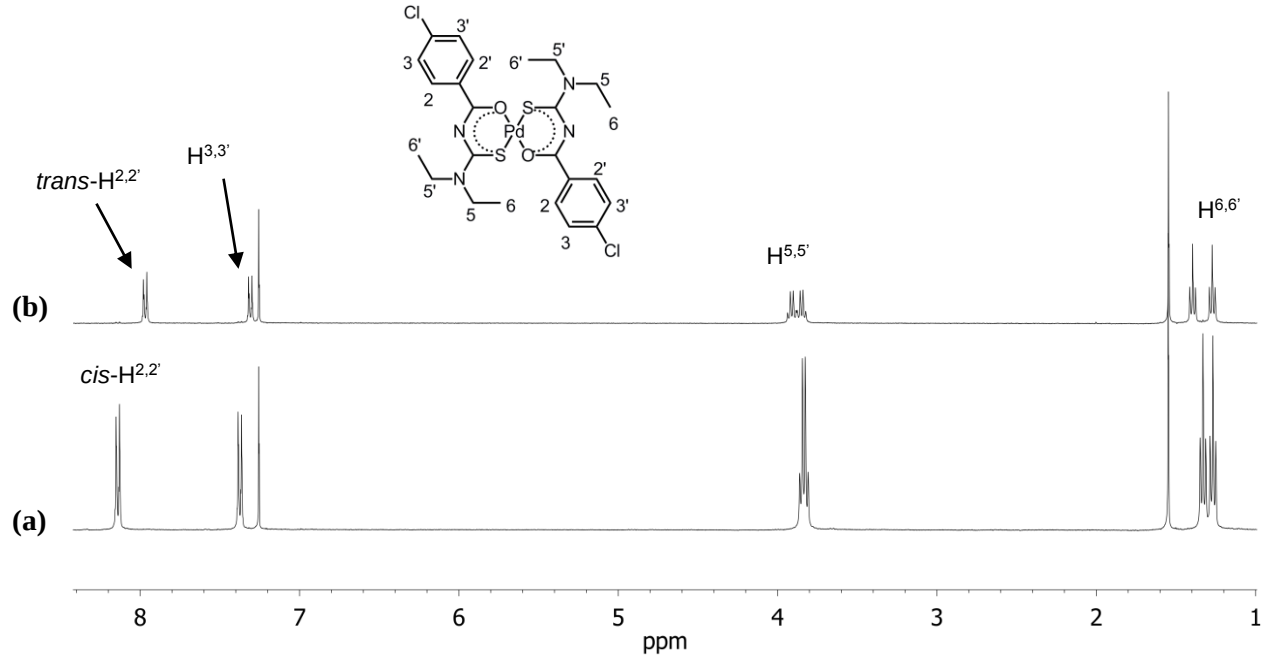

Figure 3.9. ^{1}H NMR spectra of (a) pure *cis* and (b) isolated *trans* complexes of bis(*N*,*N*-diethyl-*N*'-4-chloro-benzoylthioureato-κ^{2}*S*,*O*)palladium(II) in chloroform-*d* at 25 °C.

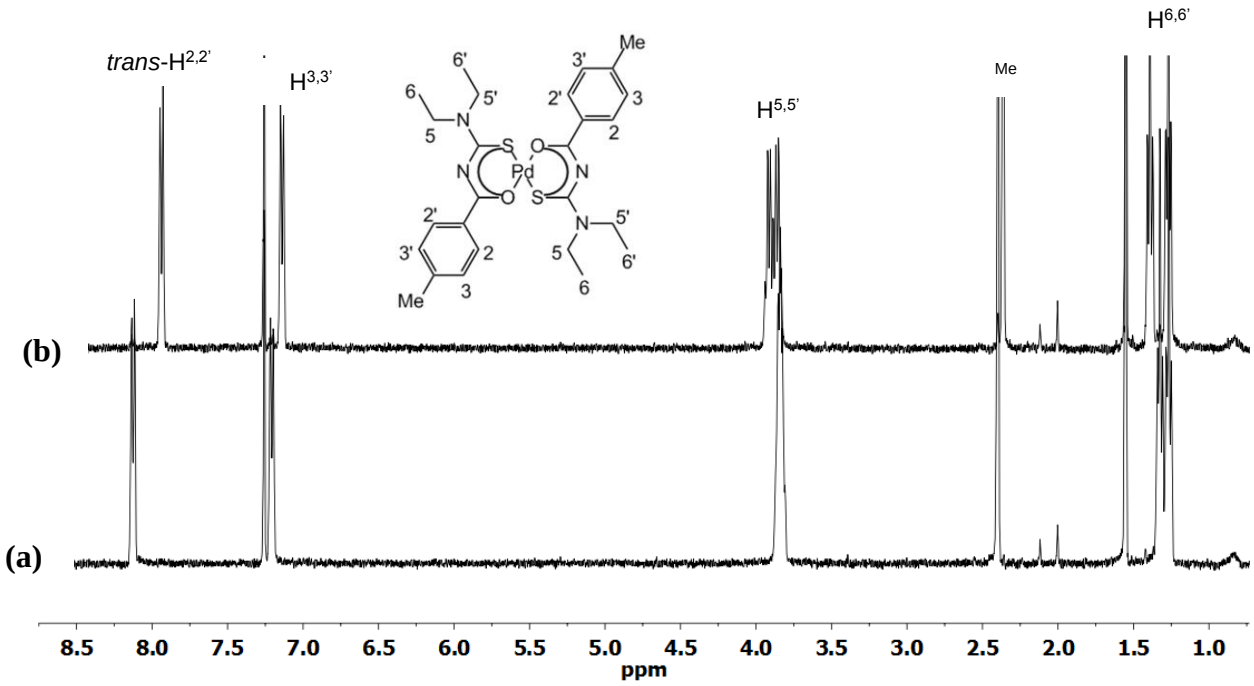

Figure 3.10. ^{1}H NMR spectra of (a) pure *cis* and (b) isolated *trans* complexes of bis(*N*,*N*-diethyl-*N*'-4-methyl-benzoylthioureato-κ^2*S*,*O*)palladium(II) in chloroform-*d* at 25 °C.

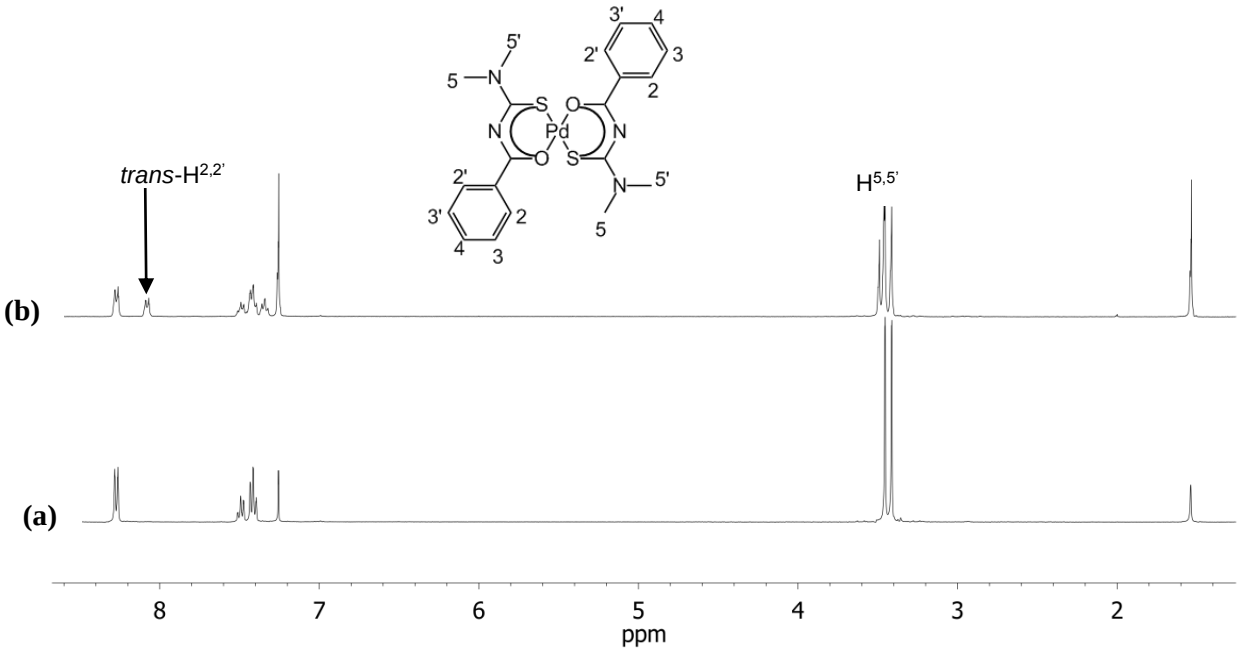

Figure 3.11. ^{1}H NMR spectra of (a) pure *cis* and (b) mixture of isolated *trans* and *cis* complexes of bis(*N*,*N*-dimethyl-*N*'-benzoylthioureato-κ^2*S*,*O*)palladium(II) in chloroform-*d* at 25 °C.

When all the isolated *trans*-[Pd(L^{1-6}-κ*S*,*O*)$_2$] complexes dissolved in chloroform-*d* are left in the dark, a spontaneous *trans*→*cis* reversion occurs and after several hours in the dark, the *cis*-[Pd(L-κ*S*,*O*)$_2$] isomers are completely restored. Figure 3.12 (a) and (b) shows the changes in $H^{2,2'}$ resonance intensity when a chloroform-*d* solution of the *trans*-[Pd(L^1-κ*S*,*O*)$_2$] (HL^1 = *N*,*N*-diethyl-*N'*-benzoylthiourea) complex is left in the dark. It is evident that the intensity of the *trans*-$H^{2,2'}$ resonance slowly diminishes with time at the expense of the *cis* resonance and after *ca* 6 hours in the dark, the *cis*-[Pd(L^1-κ*S*,*O*)$_2$] isomer is completely restored. The relative rates of spontaneous *trans*→*cis* reversion of all isolated *trans*-[Pd(L^{1-6}-κ*S*,*O*)$_2$] complexes will be discussed further in chapter 6.

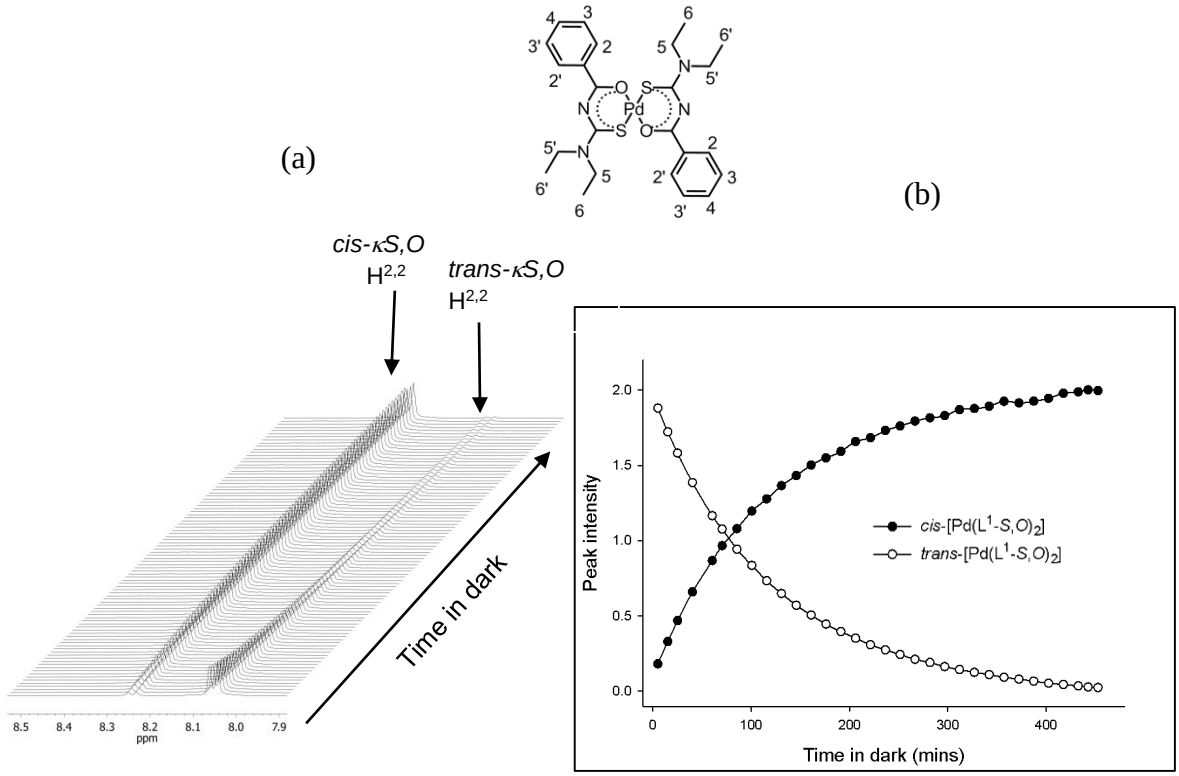

Figure 3.12. Representations of slow thermal *trans*→*cis* reversion of *trans*-[Pd(L^1-κ*S*,*O*)$_2$] in chloroform-*d* at 25 °C in the dark.

3.2.3. Crystal structures of isolated *trans*-[Pd(L^n-κ*S*,*O*)$_2$] complexes

In order to confirm their *trans*-κ*S,O* configuration, single-crystal X-ray structure elucidation was performed on the isolated *trans*-[Pd($L^{1,5,6}$-κ*S*,*O*)$_2$] complexes. Crystals of the *trans*-[Pd($L^{1,5,6}$-κ*S*,*O*)$_2$] complexes were obtained as described in chapter 2, section 2.3.6 (page 44). Since isolation of these complexes is reported for the first time, the crystal structures reported here represent the first example of a Pd complex coordinated to the *N*,*N*-disubstituted

acylthioureas in a *trans*-κ*S,O* configuration and which were deliberately prepared following *cis*→*trans* isomerization. The other *trans*-[Pd($L^{2,3}$-κ*S,O*)$_2$] complexes could not be crystallized despite several attempts. The crystallographic refinement data for the isolated *trans* structures were given in Tables 2.4 and 2.5 (page 48), and their selected Pd-O and Pd-S bond distances are presented in Table 3.3. The other bond distances are given in Table A3.1. In general, the Pd-S bond distances in the *trans*-[Pd($L^{1,5,6}$-κ*S,O*)$_2$] structures are longer than that of their *cis*-[Pd($L^{1,5,6}$-κ*S,O*)$_2$] isomers. Consequently, shortening of the Pd-O bonds are observed in the *trans*-[Pd($L^{1,5,6}$-κ*S,O*)$_2$] complexes. The two chelates rings in the *trans*-[Pd($L^{1,5,6}$-κ*S,O*)$_2$] structures are essentially the same and are square planar in comparison to their *cis*-[Pd($L^{1,5,6}$-κ*S,O*)$_2$] counterparts which were shown in chapter 2 to deviate slightly from ideal square planarity.

Table 3.3. Selected Pd-O and Pd-S bond distances of isolated *trans* complexes relative to their *cis* counterparts.

	Pd-O	**Pd-S**
***cis*-[Pd(L^1-κ*S,O*)$_2$]**	2.203(1)	2.243(1)
***trans*-[Pd(L^1-κ*S,O*)$_2$]**	1.992(2)	2.283(11)
***cis*-[Pd(L^5-κ*S,O*)$_2$]**	2.202(6)	2.242(2)
***trans*-[Pd(L^5-κ*S,O*)$_2$]**	1.975(3)	2.282(2)
***cis*-[Pd(L^6-κ*S,O*)$_2$]**	2.205(4)	2.233(4)
***trans*-[Pd(L^6-κ*S,O*)$_2$]**	1.989(2)	2.297(1)

trans-bis(N,N-diethyl-N'-benzoylthioureato-κ^{2}S,O)palladium(II) trans-[Pd(L^1-κS,O)$_2$]

The isolated *trans*-[Pd(L^1-κ*S,O*)$_2$] (HL^1 = *N,N*-diethyl-*N'*-benzoylthiourea) complex crystallizes in the monoclinic space group $P2_1/n$. The Pd(II) ion is coordinated in a square-planar manner and the ligands are oriented to give a *trans*-configuration (Figure 3.13). Inspection of the structure reveals that the six-membered Pd1-S1-C8-N1-C7-O1 metallocycles show differences in bond angles and lengths in the *trans* complex relative to that of the *cis*. By comparison with the *cis*-[Pd(L^1-κ*S,O*)$_2$] isomer,[17] the Pd-S bond length (2.2830 Å) in the *trans* complex is slightly longer than in the *cis* (2.231 Å) whereas the Pd-O bond length (1.992 Å) is slightly shorter than in the corresponding *cis* complex (2.017 Å). This can be ascribed to the higher *trans*-influence of the sulfur donor atom leading to longer Pd-S and shorter Pd-O bond

distances in the *trans*-[Pd(L^1-κ*S*,*O*)$_2$] isomer.[58] The other bond distances across the chelate rings remain essentially unchanged. Also, the *trans* structure shows ideal square planarity indicated by the S(1)-Pd(1)-S1_a) bond angle of 180°, whereas the *cis* structure shows deviations from 180° with bond angles S(1)-Pd(1)-O(2) 178.34(4)°.[17] Also, the *trans*-[Pd(L^1-κ*S*,*O*)$_2$] complex shows interactions between CH of the phenyl rings and both sulfur and oxygen atoms of the six-membered chelate ring (Figure 3.13 (b)).

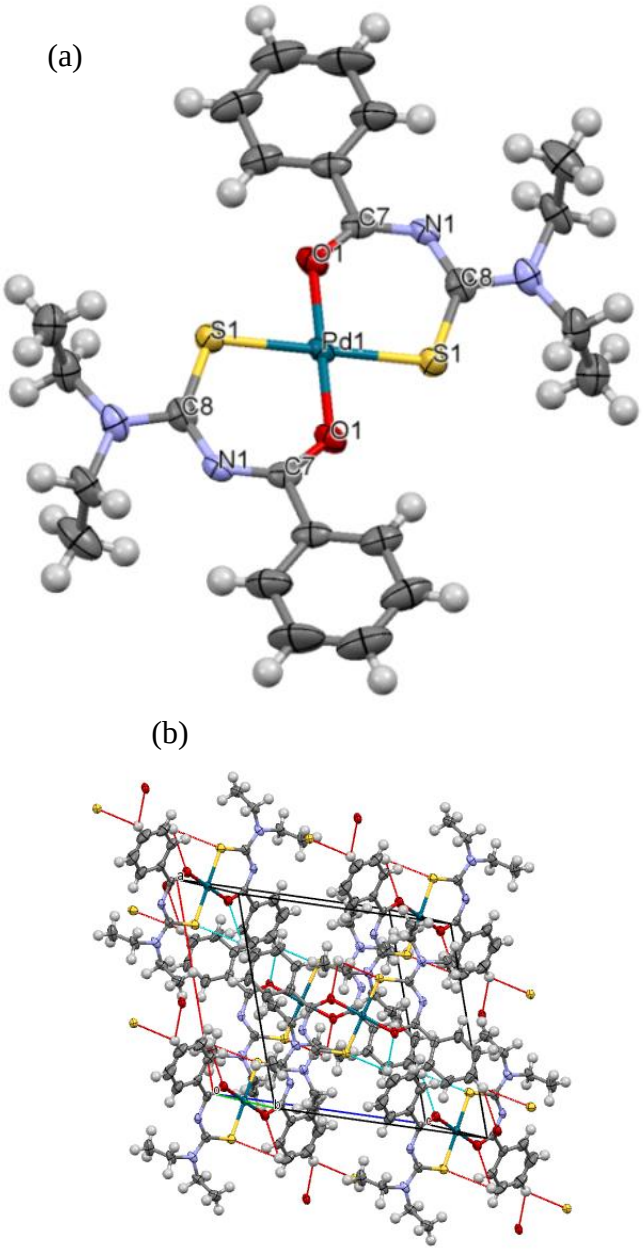

Figure 3.13. (a) Molecular structure from single-crystal X-ray difraction and (b) crystal packing of the first example of a *trans*-bis(*N*,*N*-diethyl-*N'*-(benzoyl-thioureato-κ^2*S*,*O*)palladium(II) *trans*-[Pd(L^1-κ*S*,*O*)$_2$] isolated by irradiation of *cis*-[Pd(L^1-κ*S*,*O*)$_2$] in acetonitrile with polychromatic light and vapor diffusion.

trans-bis(N,N-diethyl-N'-4-methyl-benzoylthioureato-κ²S,O)-palladium(II) trans-[Pd(L⁵-κS,O)₂]

Figures 3.14 (a) and (b) show the molecular structure and crystal packing of the *trans*-[Pd(L^5-κ*S*,*O*)$_2$] (HL^5 = *N*,*N*-diethyl-*N'*-4-methyl-benzoylthiourea) complex. The structure crystallizes in the monoclinic space group $P2_1/n$. The Pd(1)-S(2) bond distance (2.282(2) Å) is significantly longer than the average Pd-O bond length in *cis*-[Pd(L^5-κ*S*,*O*)$_2$] (2.245(2) Å). This is associated with shortening of the Pd(1)-O(1) bond distance (1.975(3) Å) relative to *cis*-[Pd(L^5-κ*S*,*O*)$_2$] (2.021(5) Å). These changes are attributed to the higher *trans*-influence of sulfur relative to oxygen.[58] The two chelate rings in this isomer are square planar as represented by S(2)-Pd(1)-S(2) and O(1)-Pd(1)-O(1) angles of 180.0°. The bond distances and angles in the *trans*-[Pd(L^5-κ*S*,*O*)$_2$] complex are very similar to that of the *trans*-[Pd(L^1-κ*S*,*O*)$_2$] structure, indicating that the presence of methyl substituents at the *para* position of the phenyl rings have no significant effect on electron delocalization of the six-membered chelate. No intermolecular interactions exist between the molecules of the *trans*-[Pd(L^5-κ*S*,*O*)$_2$] complex as revealed by the crystal packing in Figure 3.14(b).

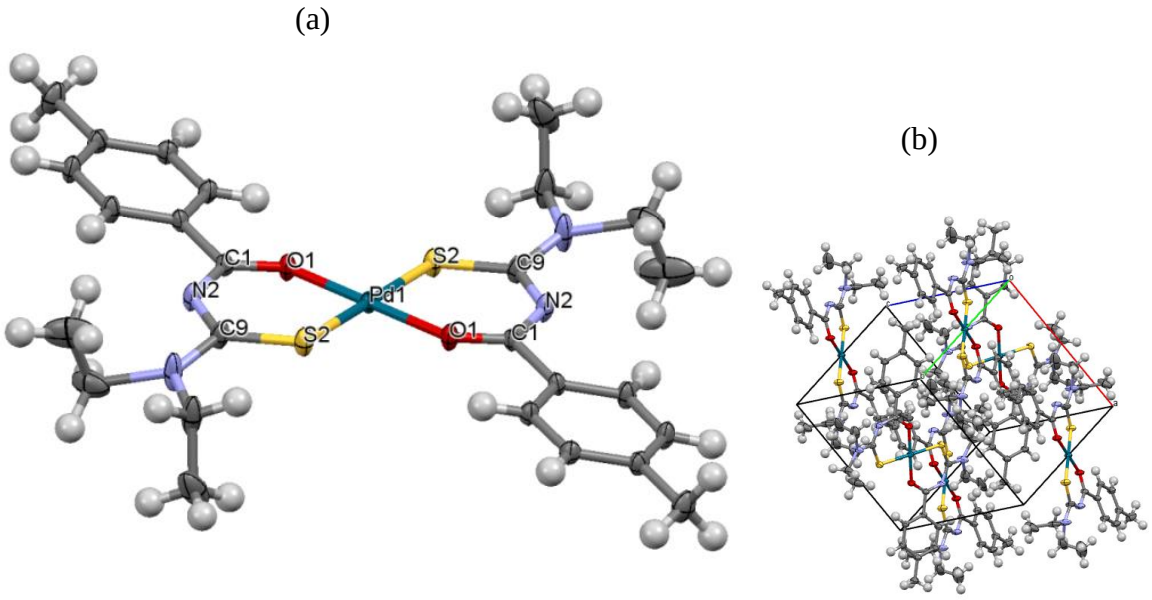

Figure 3.14. (a) Molecular structure from single-crystal X-ray difraction and (b) crystal packing of *trans*-bis(*N*,*N*-diethyl-*N*'-4-methyl-benzoylthioureato-κ²*S*,*O*)palladium(II) *trans*-[Pd(L^5-κ*S*,*O*)$_2$] isolated by slow evaporation upon irradiation of *cis*-[Pd(L^5-κ*S*,*O*)$_2$] in acetonitrile with polychromatic light from a 5 Watt LED lamp.

***trans*-bis(*N*,*N*-dimethyl-*N'*-benzoylthioureato-κ^2*S*,*O*)palladium(II) *trans*-[Pd(L^6-κ*S*,*O*)$_2$]**

The molecular structure of the isolated *trans*-bis(*N*,*N*-dimethyl-*N'*-benzoylthioureato-κ*S*,*O*)palladium(II) complex (Figure 3.15 (a)) clearly shows *trans*-κ*S*,*O* coordination, the complex crystallizing in a monoclinic space group $P2_1/n$. The structure also shows strictly square planar coordination, S(1)-Pd(1)-S(1)/O(1)-Pd(1)-O(1) bond angle of 180°(3). Similar to *trans*-[Pd(L^1-κ*S*,*O*)$_2$], no significant effect of the thioamido methyl substituents on the six-membered chelate system is observed in the *trans*-[Pd(L^6-κ*S*,*O*)$_2$] complex as reflected in the similar Pd(1)-S(1) (2.297(1) Å) and Pd(1)-O(1) (1.989(2) Å) bond lengths. Intermolecular C—H interactions are observed between carbon atoms of the phenyl ring and hydrogen atoms from alkyl groups (Figure 3.15 (b)).

(a)

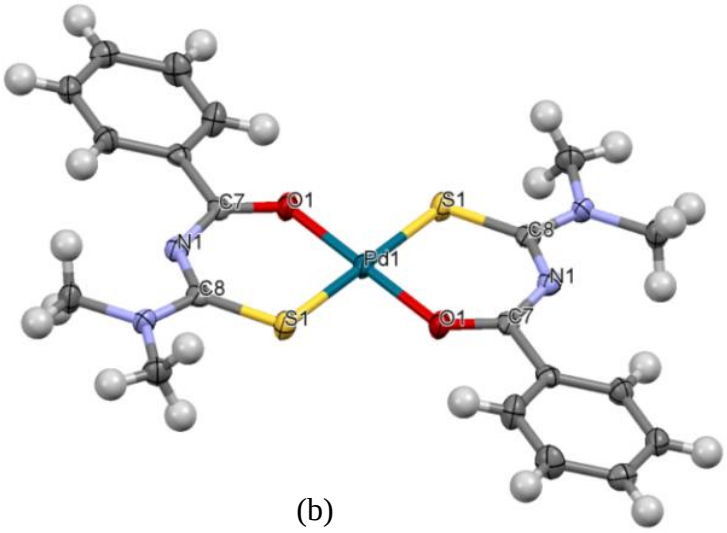

(b)

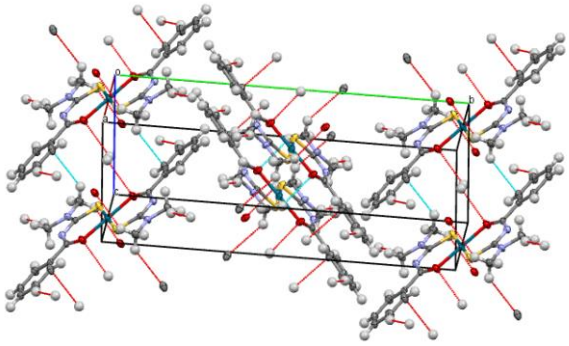

Figure 3.15. (a) Molecular structure from single-crystal X-ray difraction and (b) crystal packing of *trans*-bis(*N*,*N*-dimethyl-*N*'-benzoylthioureato-κ^2*S*,*O*)palladium(II) *trans*-[Pd(L^6-κ*S*,*O*)$_2$] isolated by slow evaporation upon irradiation of *cis*-[Pd(L^6-κ*S*,*O*)$_2$] in acetonitrile with polychromatic light from a 5 Watt LED lamp.

3.3. Conclusions

In conclusion, all *cis*-[Pd(L^{1-6}-κ*S*,*O*)$_2$] complexes of the *N*,*N*-dialkyl-*N*'-benzoylthioureas (HL^{1-6}) were found to photo-isomerize to their *trans*-[Pd(L^{1-6}-κ*S*,*O*)$_2$] isomers when irradiated with polychromatic light in acetonitrile. The *cis*-*trans* isomers were characterized by different ^{1}H and ^{195}Pt{^{1}H} resonances after irradiation. The ^{1}H NMR resonances of the phenyl ortho protons in all *trans*-complexes were shifted upfield by *ca* 0.4 ppm relative to their *cis*-resonances, while a significant downfield shift of *ca* 745 ppm occurred for the ^{195}Pt{^{1}H} *trans* resonances. In addition, all *trans*-isomers generally showed higher elution times on a reversed-phase C_{18} column relative to their *cis*-counterparts. Two techniques namely vapour diffusion and slow evaporation with photo-irradiation led to the isolation of > 60% of the *trans*-[Pd(L^{1-6}-κ*S*,*O*)$_2$] complexes. The isolated *trans*-[Pd(L^{1-6}-κ*S*,*O*)$_2$] complexes were successfully distinguished from their *cis*-[Pd(L^{n}-κ*S*,*O*)$_2$] counterparts by differences in melting points. In general, the *trans*-[Pd(L^{n}-κ*S*,*O*)$_2$] isomers showed significantly higher melting points than their *cis*-[Pd(L^{n}-κ*S*,*O*)$_2$] counterparts. The isolated *trans*-[Pd(L^{1-6}-κ*S*,*O*)$_2$] complexes were found to be insoluble in acetonitrile in contrast to their *cis*-[Pd(L^{1-6}-κ*S*,*O*)$_2$] counterparts which readily dissolved in acetonitrile. Hence it is more likely that the selective isolation of the *trans*-[Pd(L^{1-6}-κ*S*,*O*)$_2$] complexes from an irradiated *cis*-*trans* mixture was based on their relatively lower solubility in acetonitrile compared to the *cis*-[Pd(L^{1-6}-κ*S*,*O*)$_2$] isomers.

Structure elucidation of the novel six-membered *trans*-[Pd($L^{1,5,6}$-κ*S*,*O*)$_2$] complexes was provided by their single-crystal X-ray structures. In comparison to their respective *cis*-[Pd(L^{n}-κ*S*,*O*)$_2$] complexes, the *trans*-[Pd(L^{n}-κ*S*,*O*)$_2$] isomers were found to have longer Pd-S and shorter Pd-O bond distances. This could be attributed to the higher *trans*-influence of the sulfur donor atom relative to the oxygen atom.[58] The molecular structures of the complexes also revealed that each six-membered *trans*-[Pd(L^{n}-κ*S*,*O*)$_2$] complex is essentially planar in contrast to their *cis*-[Pd(L^{n}-κ*S*,*O*)$_2$] counterparts which show slight deviations from square planarity. No significant changes in bond distances and angles were observed for the isolated *trans*-[Pd($L^{1,5,6}$-κ*S*,*O*)$_2$] complexes (HL^{1} = *N*,*N*-diethyl-*N*'-benzoylthiourea, HL^{5} = *N*,*N*-diethyl-*N*'-4-methylbenzoylthiourea, HL^{6} = *N*,*N*-dimethyl-*N*'-benzoylthiourea) strongly suggesting that ligand substituents do not affect electron delocalization across the six-membered chelate ring.

4

Photo-induced isomerization and isolation of a novel trans-[Pd(L-κS,N)$_2$] complex for HL=N, N-diethyl-N'-1-naphthoylthiourea

Synopsis

This chapter describes the unprecedented formation and isolation of a novel trans-[Pd(L^7-κS,N)$_2$] isomer from photo-induced isomerization of the cis-[Pd(L^7-κS,O)$_2$] complex only for N,N-diethyl-N'-1-naphthoylthiourea (HL^7) using vapour diffusion crystallization and slow evaporation after light irradiation in acetonitrile. The new trans-[Pd(L^7-κS,N)$_2$] complex was isolated in addition to the trans-[Pd(L^7-κS,O)$_2$] complex, with both trans isomers showing significant differences in melting points relative to the cis-[Pd(L-κS,O)$_2$] isomer. Characterization of both trans-[Pd(L^7-κS,O)$_2$] and trans-[Pd(L-κS,N)$_2$] complexes was further achieved by ^{1}H NMR and LC-MS. The trans-[Pd(L-κS,N)$_2$] mode of coordination in the four-membered chelate was confirmed by single-crystal X-ray diffraction analysis.

4.1. Introduction

The *N*,*N*-disubstituted acylthioureas are highly versatile due to the presence of the carbonyl and thiocarbonyl groups. Consequently, coordination of the ligands to d^8 transition metal ions may occur through nitrogen, oxygen or sulfur donor atoms. The preferential mode of coordination could be influenced by electronic or steric effects of ligand substituents. For example, the bis-sulfur-bridged-copper(II) dimer complexes of the type [{CuL(HL)Cl}] are formed from reaction of *N*-ferrocenecarbonyl-*N*',*N*'-dimethylthioureas with copper(II) chloride solutions.[108] This was attributed to the overall structural and steric effects of the *N*,*N*-dimethyl substituents in the ligand. The bridged complexes were not formed if diethyl-substituted analogues of the ligand were used, but instead the usual mononuclear c*is*-κ*S*,*O* type of complexes were formed. Intramolecular hydrogen bonding in the *N*,*N*-dialkyl-*N*'-acyl(aroyl)thioureas and their derivatives could influence their coordination to transition metal ions. This is more pronounced between a carbonyl oxygen and a thioamido N-H in the *N*-alkyl-*N*'-acyl(aroyl)thioureas (**H_2L**) and leads to monodentate coordination of the ligand only through the sulfur atom.[45] Consequently, mixtures of *cis*- and *trans*-[Pt(H_2L-*S*)$_2$$Cl_2$] type complexes are formed after coordination of the *N*-alkyl-*N*'-acyl(aroyl)thioureas with Pt(II). In the case of derivatives of *N*-phosphorylated thioureas, the presence of intramolecular hydrogen bond leads to the formation of complexes with rare *trans*-κ*S*,*N* mode of coordination to Ni(II),[46] Pd(II)[47] and Co(II).[48] This was ascribed to the higher thermodynamic stability of the square planar *trans*-1,3 (*S*,*N*) complexes relative to their *trans*-1,5 (*S*,*S*) or *trans*-1,5 (*S*,*O*) analogues. There are three complexes of copper(II)[53,54,55] with *trans*-κ*S*,*O* mode of coordination which are reported in the literature. Also, one *trans*-[Pt(L-κ*S*,*O*)$_2$] complex of *N*,*N*-(di-*n*)-butyl-*N*'-napthoylthiourea was fortuitously isolated more than two decades ago.[56] However, a search into the Cambridge Structural Database shows no *trans*-[M(L-κ*S*,*N*)$_2$] complex of the *N*,*N*-dialkyl-*N*'-acyl(aroyl)thioureas with d^8 transition metal ions.

In the previous chapter, it was shown that the *cis*-[Pd($L^{1\text{-}6}$-κ*S*,*O*)$_2$] complexes of the *N*,*N*-dialkyl-*N'*-benzoylthioureas produce the *trans*-[Pd($L^{1\text{-}6}$-κ*S*,*O*)$_2$] isomers by photo-induced isomerization. In addition, isolation of the *trans*-[Pd($L^{1\text{-}6}$-κ*S*,*O*)$_2$] complexes was carried out by irradiation of acetonitrile solutions of the *trans*-[Pd($L^{1\text{-}6}$-κ*S*,*O*)$_2$] complexes with polychromatic light using vapour-diffusion crystallization or slow evaporation. In this chapter, the unusual photo-induced *cis*→*trans* isomerization of the complex *cis*-bis-(*N*,*N*-diethyl-*N*'-naphthoylthioureato)palladium(II) *cis*-[Pd(L^7-κ*S*,*O*)$_2$] will be examined, leading to the unprecedented isolation of a novel *trans*-[Pd(L^7-κ*S*,*N*)$_2$] isomer in addition to the *trans*-[Pd(L^7-

κ*S*,*O*)$_2$] isomer. The formation of the two *trans* isomers of the *cis*-[Pd(L^7-κ*S*,*O*)$_2$] complex is represented in Figure 4.1.

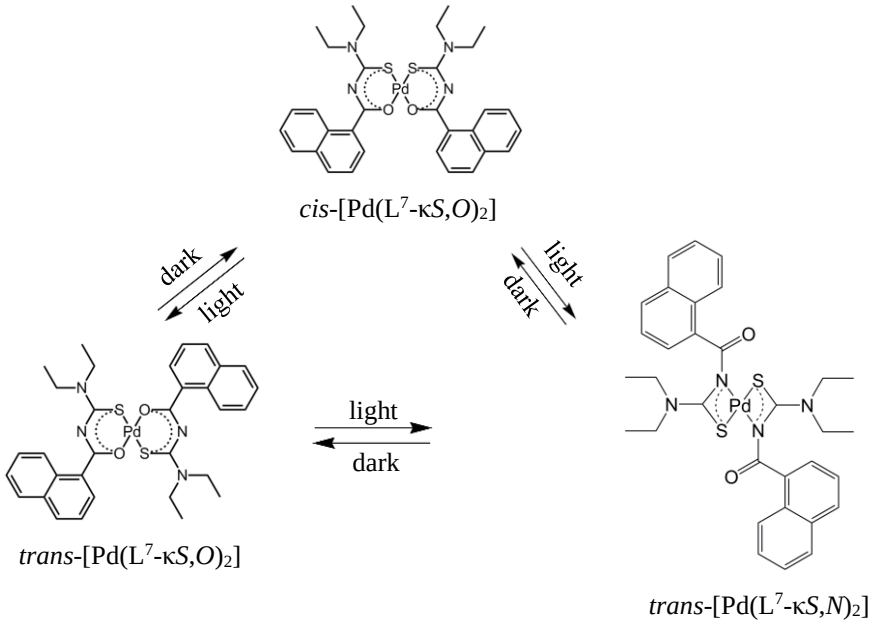

Figure 4.1. Representation of the photo-induced isomerization of the *cis*-[Pd(L^7-κ*S*,*O*)$_2$] isomer to *trans*-[Pd(L^7-κ*S*,*O*)$_2$] and *trans*-[Pd(L^7-κ*S*,*N*)$_2$] isomers in acetonitrile after irradiation with polychromatic light from a 5Watt LED lamp.

4.2. Results and discussion

4.2.1 Photo-induced isomerization of *cis*-bis(*N*,*N*-diethyl-*N*'-1-naphthoylthioureato)palladium(II) *cis*-[Pd(L^7-κ*S*,*O*)$_2$]

Irradiation of solutions of the *cis*-[Pd(L^7-κ*S*,*O*)$_2$] complex (HL^7 = *N*,*N*-diethyl-*N'*-1-naphthoylthiourea) in acetonitrile with polychromatic light generates the *trans*-[Pd(L^7-κ*S*,*O*)$_2$] isomer in solution due to *cis*→*trans* isomerization. Figure 4.2 shows a representative ^{1}H NMR spectra of an acetonitrile-d_3 solution of the *cis*-[Pd(L^7-κ*S*,*O*)$_2$] complex before and after irradiation of the solution in a NMR tube with a 5 Watt LED lamp. Additional ^{1}H NMR resonances are evident upon irradiation in particular for the naphthyl H^8 proton, and this is attributed to the *trans*-[Pd(L^7-κ*S*,*O*)$_2$] isomer formation. The methyl and methylene protons appear relatively unaffected by light exposure. The differences in chemical shifts observed for the *cis*-*trans* geometric isomers are consistent with the chemical shift changes reported in the literature.[56] The intensity of the new *trans*-resonances appear to increase slowly as time of irradiation increases at the expense of their *cis* counterparts, attaining a steady state after 30

minutes of irradiation. The new *trans*-H^8 doublets are shifted upfield by *ca* 0.36 ppm relative to the *cis*-H^8 resonance. This could be ascribed to differences in orientation of the *cis-trans* H^8 proton in the naphthyl moiety relative to the plane of coordination resulting in differences in magnetic anisotropy.[56] Additional resonances are also evident for the other naphthyl protons H^{2-7} during photo-induced isomerization, although their upfield shifts relative to *cis* are significantly lower compared to that of proton H^8.

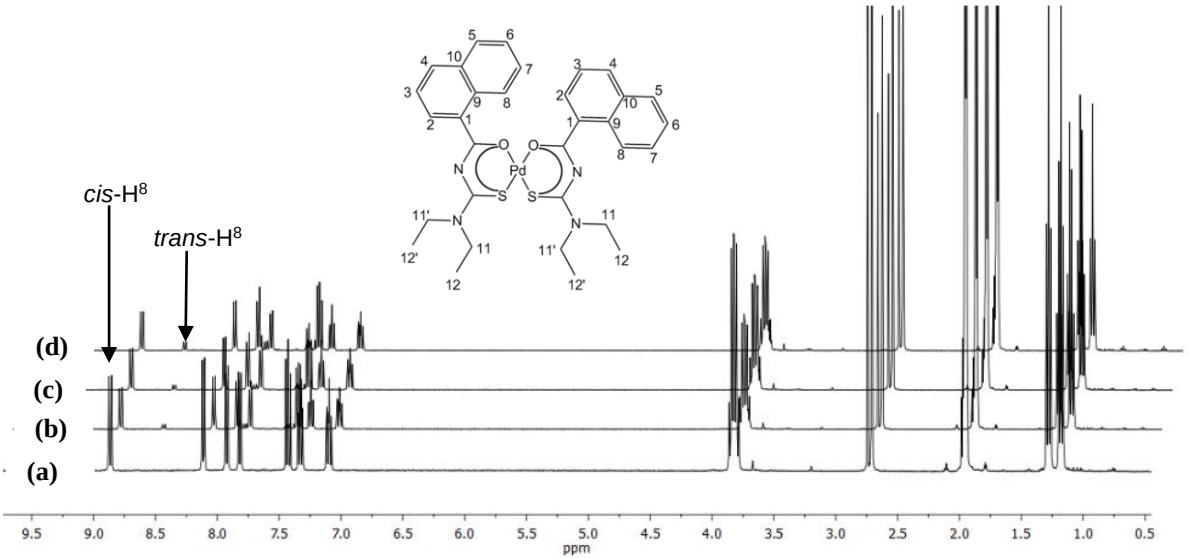

Figure 4.2. ^{1}H NMR spectra of an acetonitrile-d_3 solution *cis*-bis-(*N*,*N*-diethyl-*N*'-1-naphthoylthioureato-κ^2*S*,*O*)palladium(II) (a) before and after irradiation with polychromatic light from a 5 Watt LED lamp for (b) 3 minutes, (c) 10 minutes, (d) 15 minutes at 25 °C.

Photo-induced *cis*→*trans* isomerism of the *cis*-bis(*N*,*N*-diethyl-*N'*-1-naphthoyl-thioureato)palladium(II) complex was also studied using RP-HPLC after irradiation of its acetonitrile solution with polychromatic light. A solution containing *ca* 0.2 mg/mL of the *cis*-[Pd(L^7-κ*S*,*O*)$_2$] complex was prepared in acetonitrile in the absence of light and rapidly injected onto a C_{18} column for RP-HPLC analysis before and after irradiation with a 5 Watt LED lamp. Figure 4.3 shows the representative RP-HPLC chromatogram after irradiation of an acetonitrile solution of the *cis*-[Pd(L^7-κ*S*,*O*)$_2$] complex. In the absence of light, only a single peak is observed with a retention time of 8.6 minutes. After irradiation of a solution of *cis*-[Pd(L^7-κ*S*,*O*)$_2$], two peaks emerge in the chromatogram assigned to the *trans*-[Pd(L^7-κ*S*,*O*)$_2$] (after 5.8 minutes) isomer and a new *trans*-[Pd(L^7-κ*S*,*N*)$_2$] isomer which elutes earlier after 4.1 minutes. The peaks assigned to the *trans*-[Pd(L^7-κ*S*,*O*)$_2$] and *trans*-[Pd(L^7-κ*S*,*N*)$_2$] geometric isomers of *cis*-[Pd(L^7-κ*S*,*O*)$_2$] show marked differences in retention times of *ca* 3 minutes with the use of 97:3 (% v:v acetonitrile:water) as mobile phase. This is significantly higher than that recorded

for *cis-trans* isomers of complexes with *N*,*N*-diethyl-*N*'-benzoylthioureas studied in the previous chapter (Table 3.1, page 59). These differences could be ascribed to electronic effects of the naphthyl groups which presumably influence the polarity of the *cis-trans* isomers of the *cis*-[Pd(L^7-κ*S*,*O*)$_2$] complex. Also, a much lower extent of *cis-trans* isomerization was obtained for the *cis*-[Pd(L^7-κ*S*,*O*)$_2$] complex as determined from the relative peak areas of the *cis-trans* isomer (2.6 % for *trans*-[Pd(L^7-κ*S*,*O*)$_2$] and 1.8 % for *trans*-[Pd(L^7-κ*S*,*N*)$_2$]) after 10 minutes of irradiation. This is significantly lower compared to the extent of *cis*→*trans* conversion obtained for the *cis*-[Pd(L^{1-6}-κ*S*,*O*)$_2$] complexes of the *N*,*N*-diethyl-*N*'-benzoylthioureas studied in chapter 3 (Table 3.1, page 59).

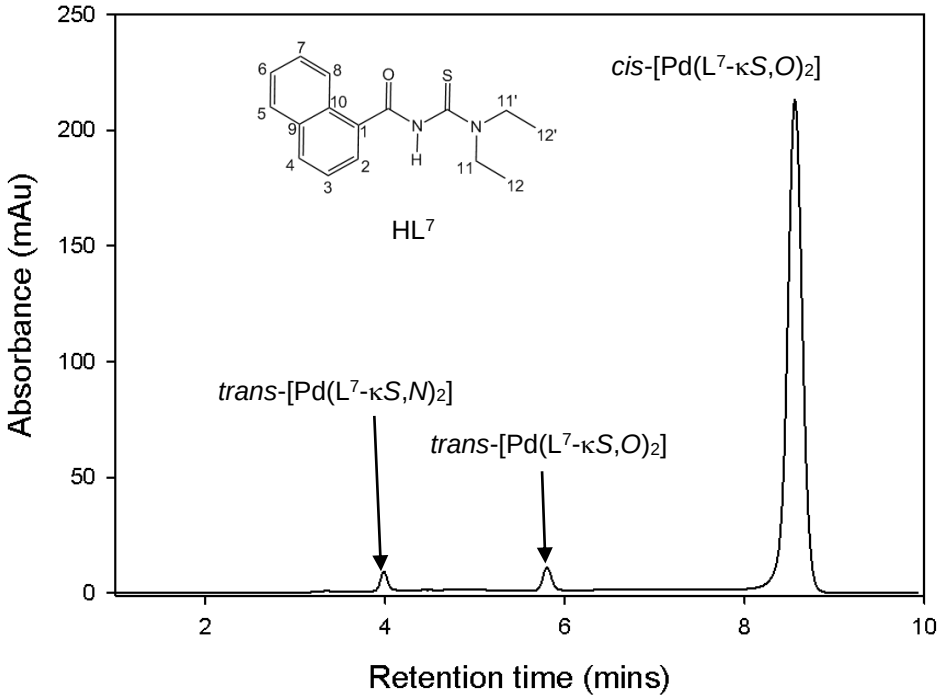

Figure 4.3. Chromatogram showing RP-HPLC separation of an acetonitrile solution of *cis*-[Pd(L^7-κ*S*,*O*)$_2$] after irradiation with polychromatic light from 5 Watt LED lamp for 10 minutes; conditions: mobile phase, acetonitrile:water (97:3 %v/v); GEMINI C_{18}, 5 µm, 250 x 4.6 mm column; 20 µl injection volume; 1 mlmin^{-1} flow rate; 262 nm detection.

The relative changes in UV spectra of the *cis-trans* isomers of the *cis*-[Pd(L^7-κ*S*,*O*)$_2$] complex were also investigated before and after irradiation with polychromatic light. UV spectra analysis was performed by continuous *in-situ* 5 Watt LED lamp irradiation of an acetonitrile solution of the *cis*-[Pd(L^7-κ*S*,*O*)$_2$] complex at room temperature and at intervals of 3 minutes. Each *cis*→*trans* cycle consisted of irradiating the *cis*-[Pd(L^7-κ*S*,*O*)$_2$] solution for 15 minutes to enable steady state between *cis-trans* isomers to be attained. After this, the LED

lamp was switched off and the changes in absorbance of the complex was followed with time. Figure 4.4 shows the UV absorption spectra of the *cis*-[Pd(L^7-κ*S*,*O*)$_2$] complex before and after irradiation. The absorbance spectra of the irradiated complex is as a result of contributions from all three geometric isomers of [Pd(L^7-κ*S*,*O*)$_2$] that is *cis*-[Pd(L^7-κ*S*,*O*)$_2$], *trans*-[Pd(L^7-κ*S*,*O*)$_2$] and *trans*-[Pd(L^7-κ*S*,*N*)$_2$]. A maximum decrease in absorbance is observed in the range 220–278 nm with corresponding increase between 278–320 nm. Also, multiple isosbestic points are observed at 220 nm, 278 nm, and 320 nm. The existence of these isosbestic points is indicative of either involvement of multiple absorbing species or formation of a substantial amount of an intermediate in solution. This further suggests the presence of at least two *trans* components in the irradiated solution of the *cis*-[Pd(L^7-κ*S*,*O*)$_2$] complex, consistent with the RP-HPLC chromatogram shown in Figure 4.3.

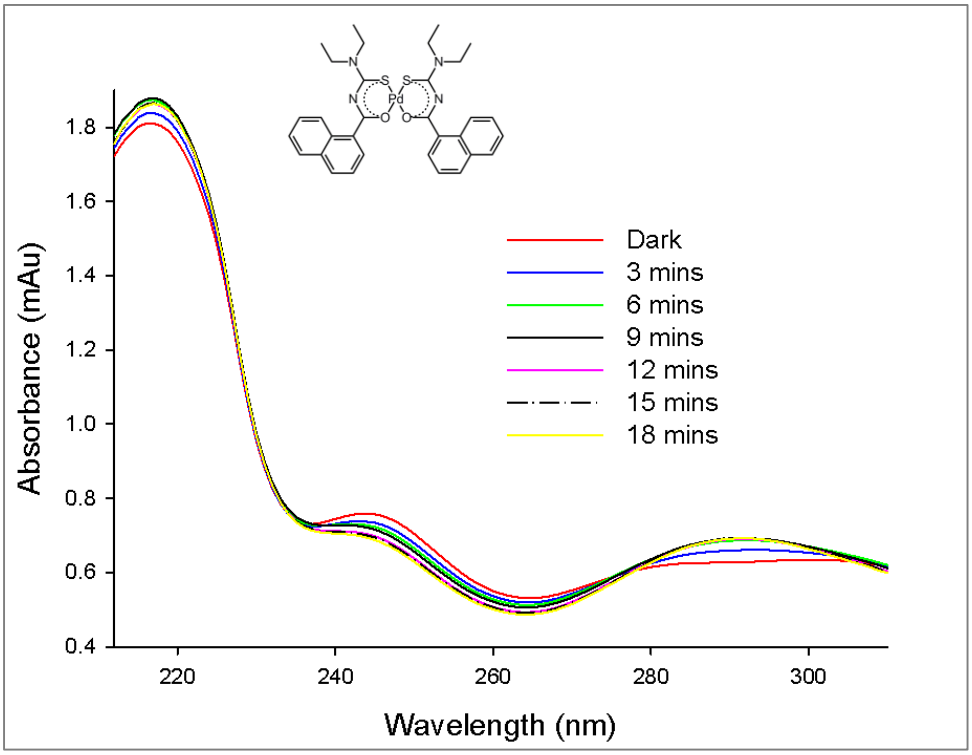

Figure 4.4. Overlaid UV-Vis spectra of *cis*-[Pd(L^7-κ*S*,*O*)$_2$] in the dark and after irradiation in acetonitrile with polychromatic light from 5 Watt LED lamp.

The changes in absorbance with time of irradiation were selectively followed at 270 nm and 290 nm (where maximum changes in absorbance occurred). At 290 nm, irradiation of the solution of the *cis*-[Pd(L^7-κ*S*,*O*)$_2$] complex led to a steady increase in absorbance represented by a small change of *ca* 0.06 au. This was continued until a steady state was achieved after 15 minutes, followed by *ca* 2 hours period in the dark. During this time, the absorbance decreases

significantly to its initial value. The irradiation/dark procedure was repeated for several cycles and the spectra changes observed were found to be reproducible. This suggests that no significant degradation occurred during the photo-induced isomerization of the *cis*-[Pd(L^7-κ*S*,*O*)$_2$] complex. At 270 nm, an initial steady decrease in absorbance represented by *ca* 0.035 au is observed after 47 minutes. This is however interrupted by an unexpected increase in absorbance for a further 70 minutes, again suggesting the presence of more than one *trans* isomers in solution. Although changes in UV spectra were observed after irradiation of the *cis*-[Pd(L^7-κ*S*,*O*)$_2$] complex, these changes are relatively small and hence UV-Vis spectroscopy cannot be used to conveniently monitor the *cis-trans* isomerism. Hence for most parts of this chapter, RP-HPLC and NMR spectroscopy were preferably employed for monitoring the formation of the *trans*-[Pd(L^7-κ*S*,*O*)$_2$] and *trans*-[Pd(L^7-κ*S*,*N*)$_2$] isomers.

4.2.2. Further evidence of unprecedented formation of *trans*-[Pd(L^7-κ*S*,*N*)$_2$] (*HL^7 = N,N-diethyl-N'-1-naphthoylthiourea*) during photo-induced isomerization

The results presented in the previous section suggest the unprecedented photo-induced formation of a new *trans*-[Pd(L^7-κ*S*,*N*)$_2$] isomer of the *cis*-[Pd(L^7-κ*S*,*O*)$_2$] complex in addition to the formation of a *trans*-[Pd(L^7-κ*S*,*O*)$_2$] isomer. This unusual *trans*-[Pd(L^7-*S*,*N*)$_2$] isomer was not observed for the *cis*-[Pd($L^{1\text{-}6}$-κ*S*,*O*)$_2$] complexes of *N*,*N*-dialkyl-*N*'-benzoylthioureas studied in chapter 3, and could presumably be ascribed to either steric or electronic effects of the naphthyl substituents. Further evidence of the photo-induced formation of the *trans*-[Pd(L^7-κ*S*,*N*)$_2$] isomer was provided by HPLC-UV and HPLC-MS analyses.

4.2.2.1. RP-HPLC separation with UV detection

For HPLC-UV analysis, *ca* 0.1 mg/mL of the *cis*-[Pd(L^7-κ*S*,*O*)$_2$] complex in acetonitrile was prepared and injected onto a C_{18} column before and after irradiation with a 5 Watt LED lamp. Each chromatographic run consisted of a 20 µl injection of an aliquot of the irradiated solutions under isocratic conditions, with a flow rate of 1 ml min^{-1} and photodiode-array detection at 262 nm. Figure 4.5 (a) shows overlaid RP-HPLC chromatograms obtained before and after irradiation of acetonitrile solutions of the *cis*-[Pd(L^7-κ*S*,*O*)$_2$] complex. Without light irradiation, only a single chromatographic peak was observed after 10.1 minutes and assigned to the *cis* isomer (Figure 4.5 (a_i)). When the *cis*-[Pd(L^7-κ*S*,*O*)$_2$] solution was exposed to

daylight for *ca.* 5 minutes before RP-HPLC injection, a peak corresponding to the *trans*-[Pd(L^7-κ*S*,*O*)$_2$] isomer was seen to elute after 6.4 minutes (Figure 4.5 (a_ii)). Irradiation of a freshly prepared solution of the *cis*-[Pd(L^7-κ*S*,*O*)$_2$] complex generates an additional peak at retention time of 4.2 minutes (Figure 4.5 (a_iii)). This new peak is assigned to the *trans*-[Pd(L^7-*S*,*N*)$_2$] isomer, while the other peak represents the *trans*-[Pd(L^7-κ*S*,*O*)$_2$] (retention time of 6.4 minutes) isomer. The intensities of the two *trans* peaks increase as time of irradiation increases. Upon continuous light exposure, a steady state constituting a mixture of *ca* 8% *trans*-[Pd(L^7-κ*S*,*O*)$_2$] and *ca* 5.6% *trans*-[Pd(L^7-κ*S*,*N*)$_2$] (estimated from [*trans*]/[*cis*] peak area ratios) is attained. In order to unambiguously assign the RP-HPLC peaks from the irradiated mixture to the *trans*-[Pd(L^7-κ*S*,*O*)$_2$] and *trans*-[Pd(L^7-κ*S*,*N*)$_2$] isomers, solutions of their pure *trans*-[Pd(L^7-κ*S*,*O*)$_2$] and *trans*-[Pd(L^7-κ*S*,*N*)$_2$] complexes had to be injected for RP-HPLC analysis. However, the *trans* complexes isolated (isolation to be discussed in section 4.2.3) were found to be insoluble in acetonitrile, hence RP-HPLC analysis of the pure samples could not be carried out.

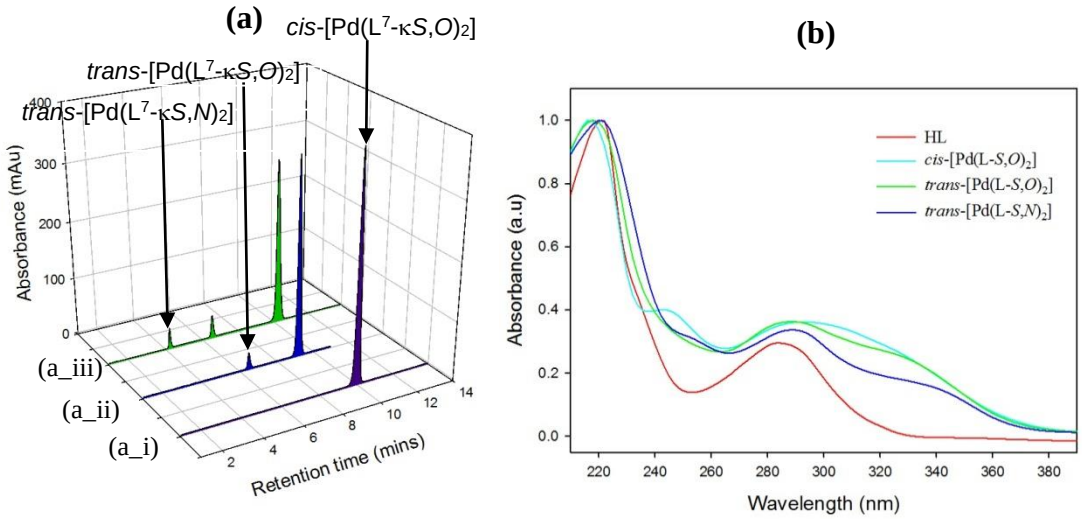

Figure 4.5. (a) Chromatogram showing RP-HPLC separation of an acetonitrile solution of *cis*-[Pd(L^7-κ*S*,*O*)$_2$] in the dark (purple), upon exposure under ambient light for 10 minutes (blue), and after irradiation with polychromatic light from 5 Watt LED lamp for 30 mins (green); conditions: mobile phase, acetonitrile:water (97:3 %v/v); GEMINI C_{18}, 5 µm, 250 x 4.6 mm column; 20 µl injection volume; 1 $mlmin^{-1}$ flow rate; 262 nm detection; (b) Overlaid photo-diode UV Spectra of HL^7, *cis*-[Pd(L^7-κ*S*,*O*)$_2$], *trans*-[Pd(L^7-κ*S*,*O*)$_2$] and *trans*-[Pd(L^7-κ*S*,*N*)$_2$] at 262 nm.

Figure 4.5 (b) shows the normalised UV-Vis absorption spectra of the isomers obtained from the photodiode array detection of the RP-HPLC peaks of the *cis*-[Pd(L^7-κ*S*,*O*)$_2$] (magenta line), *trans*-[Pd(L^7-κ*S*,*O*)$_2$](green line) and *trans*-[Pd(L^7-κ*S*,*N*)$_2$](blue line) geometric isomers relative to that of the free HL^7 ligand (red line). The similarity in the spectral features for the three compounds suggests that they are isomers of each other, with strong absorption bands observed at 217 nm and 290 nm. Also pronounced in the absorption spectrum of the *cis*-[Pd(L^7-κ*S*,*O*)$_2$] isomer is a slight shoulder at 246 nm which could be due to d-d transitions. This band is absent from that of the free ligand HL^7 and could signify coordination of the ligand in the *cis*-[Pd(L^7-κ*S*,*O*)$_2$] complex. Slight shoulders are also evident in the two *trans* complexes around the region 330–360 nm. A marked difference in absorbance is observed for all three isomers between the region 260–360 nm, which is significantly higher than that reported for *cis*-*trans* isomers of Pt(II), Pd(II) complexes with *N*,*N*-dialkyl-*N*'-benzoylthioureas.[13]

In order to gain more insight into changes leading to the formation of the *trans*-[Pd(L^7-κ*S*,*N*)$_2$] isomer, the reverse and spontaneous *trans*→*cis* isomerization of the *trans*-[Pd(L^7-κ*S*,*N*)$_2$] isomer was also studied in acetonitrile using RP-HPLC. A solution of the *cis*-[Pd(L^7-κ*S*,*O*)$_2$] complex was irradiated for 30 minutes so that a steady state between the isomers was be achieved. This solution was then allowed to stand in the dark and subsequently injected onto the C_{18} column after every 13 minutes in the dark. Figures 4.6 (a) and (b) show the overlaid chromatograms and changes in relative peak intensity respectively as a function of time in the dark. The chromatographic traces clearly indicate that the intensity of peak assigned to the *trans*-[Pd(L^7-κ*S*,*O*)$_2$] isomer decreases steadily with time. The *trans*-[Pd(L^7-κ*S*,*N*)$_2$] peak initially rises and reaches a maximum within 50 minutes after which it drops steadily. The relative rates of reversion of the *trans*-[Pd(L^7-κ*S*,*O*)$_2$] and *trans*-[Pd(L^7-κ*S*,*N*)$_2$] isomers back to the *cis*-[Pd(L^7-κ*S*,*O*)$_2$] isomer are similar in acetonitrile as depicted from Figure 4.6 (b). After *ca* 6 hours in the dark, the *cis*-[Pd(L^7-κ*S*,*O*)$_2$] isomer is fully restored.

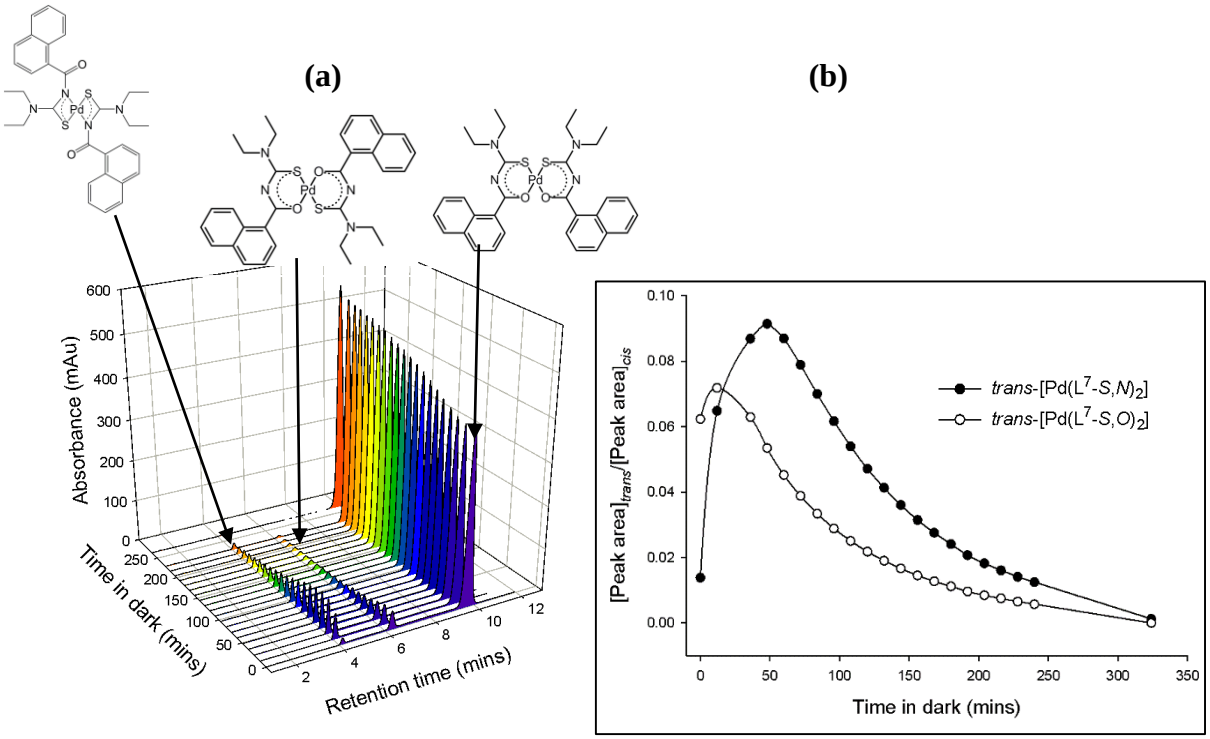

Figure 4.6. (a) Overlaid chromatograms showing *trans*→*cis* isomerization in acetonitrile for solutions of *cis*-[Pd(L^7-κ*S*,*O*)$_2$] pre-irradiated with polychromatic light from a 5 Watt LED lamp and allowed in the dark between 13 minutes time intervals; conditions: mobile phase, 90:10(%v/v acetonitrile:water); GEMINI C_{18}, 5 µm, 250 x 4.6 mm column; 20 µl injection volume; 1 $mlmin^{-1}$ flow rate; 262 nm detection; **(b)** change in *trans*/*cis* peak area ratios as a function of time in dark for *trans*-*cis* isomerization of *trans*-[Pd(L^7-*S*,*O*)$_2$] and *trans*-[Pd(L^7-κ*S*,*N*)$_2$] in acetonitrile and at room temperature.

The effect of wavelength of light on the unprecedented photo-induced formation of *trans*-[Pd(L^7-κ*S*,*N*)$_2$] was also investigated. The *cis*-[Pd(L^7-κ*S*,*O*)$_2$] complex was dissolved in acetonitrile (*ca* 0.1 mg/mL), irradiated for 15 minutes with a 5 Watt LED lamp and passed through yellow, blue and red optical filters. Figure 4.7 shows the representative overlaid chromatograms obtained from irradiation of the *cis*-[Pd(L^7-κ*S*,*O*)$_2$] complex. The use of blue (470 nm) and yellow (*ca* 600 nm) filters produces the *trans*-[Pd(L^7-κ*S*,*O*)$_2$] and *trans*-[Pd(L^7-κ*S*,*N*)$_2$] peaks (Figure 4.7 (i) and (ii)) from photo-induced isomerization of the *cis*-[Pd(L^7-κ*S*,*O*)$_2$] isomer. However, irradiation with red light (*ca* 620–750 nm) does not lead to photoisomerization of the *cis*-[Pd(L^7-κ*S*,*O*)$_2$] complex as it is obvious that neither the *trans*-[Pd(L^7-κ*S*,*O*)$_2$] nor *trans*-[Pd(L^7-κ*S*,*N*)$_2$] peaks are observed (Figure 4.7 (iii)). This is consistent with the fact that photo-induced isomerization of Pt(II) and Pd(II) *N*,*N*-dialkyl-*N*'-acyl(aroyl)thioureas occur only at wavelengths < 480 nm .[13]

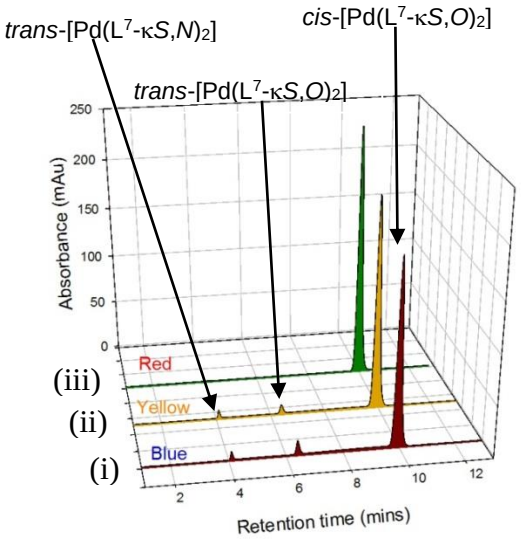

Figure 4.7. Chromatogram showing RP-HPLC separation of an acetonitrile solution of *cis*-[Pd(L^7-κ*S*,*O*)$_2$] after irradiation with polychromatic light from a 5 Watt LED lamp for 30 mins using red, blue and yellow optical filters; conditions: mobile phase, acetonitrile:water (90:10 %v/v); GEMINI C_{18}, 5 µm, 250 x 4.6 mm column; 20 µl injection volume; 1 mlmin^{-1} flow rate; 262 nm detection.

4.2.2.2. RP-HPLC separation with ESI-MS detection

The geometric *cis-trans* isomers resulting from photo-induced isomerization of Pt(II) and Pd(II) complexes of *N*,*N*-dialkyl-*N'*-acylthioureas are characterized by similar mass spectra following RP-HPLC separation.[13] Further confirmation of formation of the *trans*-[Pd(L^7-κ*S*,*N*)$_2$] isomer in addition to the *trans*-[Pd(L^7-κ*S*,*O*)$_2$] isomer was obtained by RP-HPLC separation with ESI-TOF-MS detection. A sample of the [Pd(L^7-κ*S*,*O*)$_2$] complex in acetonitrile was irradiated for 30 minutes with a 5 Watt LED lamp and then injected for LC-ESI-TOF-MS analysis. The total ion chromatographic traces are depicted in Figure 4.8 (a). It shows main eluted peaks at retention times of 1.4 minutes, 1.8 minutes, and 2.8 minutes. These are assigned to *trans*-[Pd(L^7-κ*S*,*N*)$_2$], *trans*-[Pd(L^7-κ*S*,*O*)$_2$] and *cis*-[Pd(L^7-κ*S*,*O*)$_2$] isomers respectively since they show same *m/z* values of 677.12.

Figure 4.8 (b) shows the high resolution ESI mass spectrum of the *cis*-[Pd(L^7-κ*S*,*O*)$_2$] complex. The most intense set of peaks observed are in the *m/z* range 673.123-683.125 and corresponds to the parent molecular ion $[C_{32}H_{34}N_4O_2PdS_2 + H]^+$. The other isotopic peaks of the *cis*-[Pd(L^7-κ*S*,*O*)$_2$] complex are centred at *m/z* = 432.036, 525.081 and 963.239 and 389.015. The compound which accounts for the relatively low abundance fragmentation peaks at *m/z* = 963.239 is likely the $[M+L]^+$ (L = ligand) ion in which the metal centre is coordinated to three HL^7 ligands as opposed to the more stable ML_2 form. Also evident are fragmentation

peak patterns centred at *m/z* = 1355.242 amu representing addition of a fragment of *m/z* = 678.118 to the parent molecular ion. This peak is most likely to due to a $[2M+H]^+$ fragment formed from two similar fragments of the parent molecular ion. The peak at *m/z* = 525.081 represents a mass difference of 154.043 amu relative to the molecular ion. The most likely candidate resulting to this peak is the loss of a $[NaphCO]^+$ fragment with *m/z* = 154.485. The remaining peak at *m/z* = 434.036 represents a *m/z* difference of 243.089 amu relative to the molecular ion and this difference could possibly represent an initial loss of a ligand HL^7 (*m/z* = 286) followed by a further loss of a $[CS]^+$ fragment (*m/z* = 44.077).

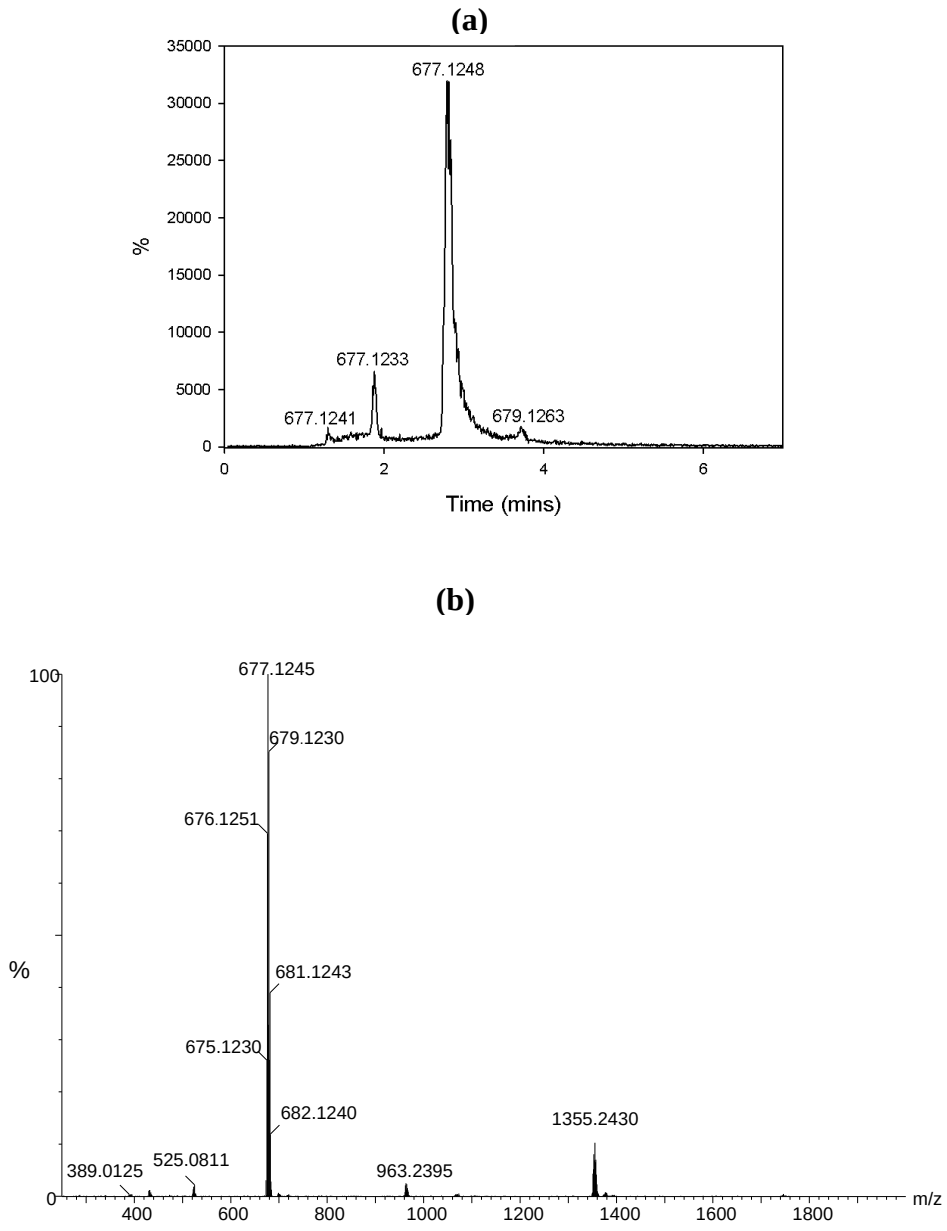

Figure 4.8. (a) Total ion chromatogram of a solution of *cis*-[Pd(L^7-κ*S*,*O*)$_2$] after 30 mins irradiation with a 5 Watt LED lamp; (b) Mass spectrum of *cis*-[Pd(L^7-κ*S*,*O*)$_2$].

Inspection of the high resolution mass spectra of the *trans*-[Pd(L^7-κ*S*,*O*)$_2$] (Figure 4.9 (a)) and *trans*-[Pd(L^7-κ*S*,*N*)$_2$] isomers (Figure 4.9(b)) reveal similar isotopic peak patterns as that of the *cis*-[Pd(L^7-κ*S*,*O*)$_2$] complex, in particular for the peaks at *m/z* = 963.239, 677.124 and 432.036. Also present in both the *trans*-[Pd(L^7-κ*S*,*O*)$_2$] and *trans*-[Pd(L^7-κ*S*,*N*)$_2$] spectra is the peak pattern with *m/z* = 390.009. This represents a difference of 287.112 amu and could be attributed to the loss of a HL^7 ligand.

(a)

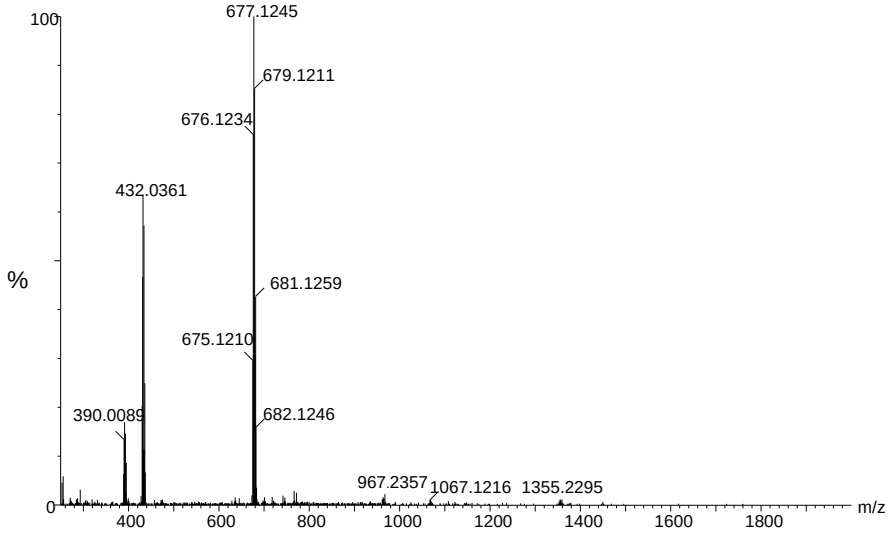

(b)

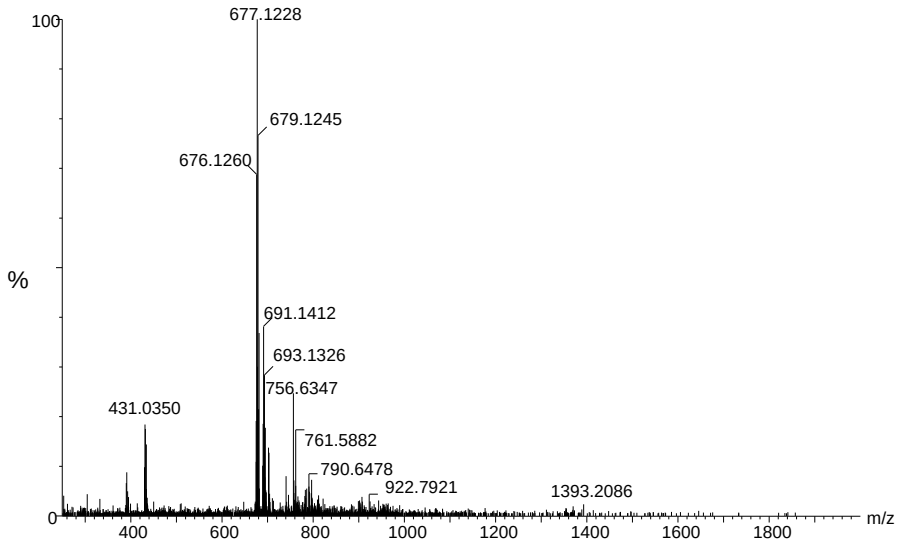

Figure 4.9. Mass spectra of *trans*-bis(*N*,*N*-diethyl-*N*'-1-naphthoylthioureato-κ^2*S*,*O*)palladium(II) complexes, (a) *trans*-[Pd(L^7-κ*S*,*O*)$_2$] and (b) *trans*-[Pd(L^7-κ*S*,*N*)$_2$].

4.2.3. Isolation and characterization of *trans*-[Pd(L^7-κ*S*,*O*)$_2$] and *trans*-[Pd(L^7-κ*S*,*N*)$_2$] (HL^7 = *N*,*N*-diethyl-*N*'-1-naphthoylthiourea) isomers

Continuous irradiation of a solution of the *cis*-[Pd(L^7-κ*S*,*O*)$_2$] complex in acetonitrile with a 5 Watt LED lamp for several hours accompanied by vapour diffusion or slow evaporation led to the isolation of a mixture of *trans*-[Pd(L^7-κ*S*,*O*)$_2$] and *trans*-[Pd(L^7-κ*S*,*N*)$_2$] complexes. When the vapour diffusion setup was placed in an ice bath with irradiation for *ca* 8 hours, crystals of the *trans*-[Pd(L^7-κ*S*,*O*)$_2$] complex were isolated. When the irradiation was extended for several days with cooling, the *trans*-[Pd(L^7-κ*S*,*N*)$_2$] complex was obtained. The pure *cis*-[Pd(L^7-κ*S*,*O*)$_2$] complex has a significantly lower melting point (157 – 159 °C) compared to both isolated *trans*-[Pd(L^7-κ*S*,*O*)$_2$] (174 – 176 °C) and *trans*-[Pd(L^7-κ*S*,*N*)$_2$] (187 -189 °C) isomers. This is consistent with the higher melting point observed in chapter 3 for *trans*-[Pd(L^{1-6}-κ*S*,*O*)$_2$] complexes of the *N*,*N*-dialkyl-*N*'-benzoylthioureas relative to their *cis*-[Pd(L^{1-6}-*S*,*O*)$_2$] counterparts (Table 3.2, page 60). The isolated *trans*-[Pd(L^7-κ*S*,*O*)$_2$] and *trans*-[Pd(L^7-κ*S*,*N*)$_2$] complexes were found to be less soluble in acetonitrile compared to their *cis*-[Pd(L^7-κ*S*,*O*)$_2$] counterpart. This could be due to higher solvation energies for the *trans*-[Pd(L^7-κ*S*,*O*)$_2$] and *trans*-[Pd(L^7-κ*S*,*N*)$_2$] complexes compared to *cis*-[Pd(L^7-κ*S*,*O*)$_2$] and is consistent with the higher melting points of the two *trans* complexes.

The isolated *trans*-[Pd(L^7-κ*S*,*O*)$_2$] complex was soluble in chloroform-*d* and hence its ^{1}H NMR characterization could be carried out. A solution of the *trans*-[Pd(L^7-κ*S*,*O*)$_2$] complex (5 mg/mL) in chloroform-*d* was prepared, followed by ^{1}H NMR data acquisition. Figure 4.10 (b) shows the ^{1}H NMR spectrum of a freshly prepared solution of the isolated *trans*-[Pd(L^7-κ*S*,*O*)$_2$] complex in chloroform-*d* in comparison to that of *cis*-[Pd(L^7-κ*S*,*O*)$_2$] (Figure 4.10 (a)). The ^{1}H NMR assignment of the *cis*-[Pd(L^7-κ*S*,*O*)$_2$] complex was discussed in chapter 2 (Figure 2.6, page 25). It is evident that the ^{1}H NMR resonances of the isolated *trans*-[Pd(L^7-κ*S*,*O*)$_2$] complex are at different positions from that of its *cis*-[Pd(L^7-κ*S*,*O*)$_2$] isomer in particular for the naphthyl protons H^8 and H^2. These resonances experience relative upfield shifts by *ca* 0.32 ppm and 0.19 ppm respectively. Also, the set of multiplets representing the proton H^7 are significantly more deshielded at the *trans* position by *ca* 0.403 ppm compared to its *cis* isomer. The other protons H^3, H^4, H^5 and H^6 appear at similar chemical shift positions in the *cis*-*trans* complexes.

The new *trans*-[Pd(L^7-κ*S*,*N*)$_2$] complex unfortunately did not dissolve in chloroform hence ^{1}H NMR studies could not be directly conducted on *trans*-[Pd(L^7-κ*S*,*N*)$_2$]. However, ^{1}H NMR evidence of formation of the *trans*-[Pd(L^7-κ*S*,*N*)$_2$] isomer was provided by results from the spontaneous *trans*→*cis* isomerization of the isolated *trans*-[Pd(L^7-κ*S*,*O*)$_2$] complex in the dark in chloroform-*d*. Figure 4.10 (c) shows the ^{1}H NMR spectra after a solution of the *trans*-[Pd(L^7-κ*S*,*O*)$_2$] complex was left in the dark for 25 minutes. For the aromatic proton H^8, a trace of the *cis*-[Pd(L^7-κ*S*,*O*)$_2$] resonance at δ = 8.95 ppm is present in the spectrum due to reversion from *trans*-[Pd(L^7-κ*S*,*O*)$_2$] to *cis*-[Pd(L^7-κ*S*,*O*)$_2$]. Also evident is the presence of an additional doublet situated upfield at δ = 8.48 ppm relative to the *trans*-[Pd(L^7-κ*S*,*O*)$_2$] resonances for the proton H^8. This new resonance is ascribed to the formation of the *trans*-[Pd(L^7-κ*S*,*N*)$_2$] isomer. Additional resonances assigned to the -N(CH_2) and CH_3 protons of the *trans*-[Pd(L^7-κ*S*,*N*)$_2$] isomer are also observed at δ = 3.45 ppm and δ = 1.05 ppm respectively (Figure 4.10) .

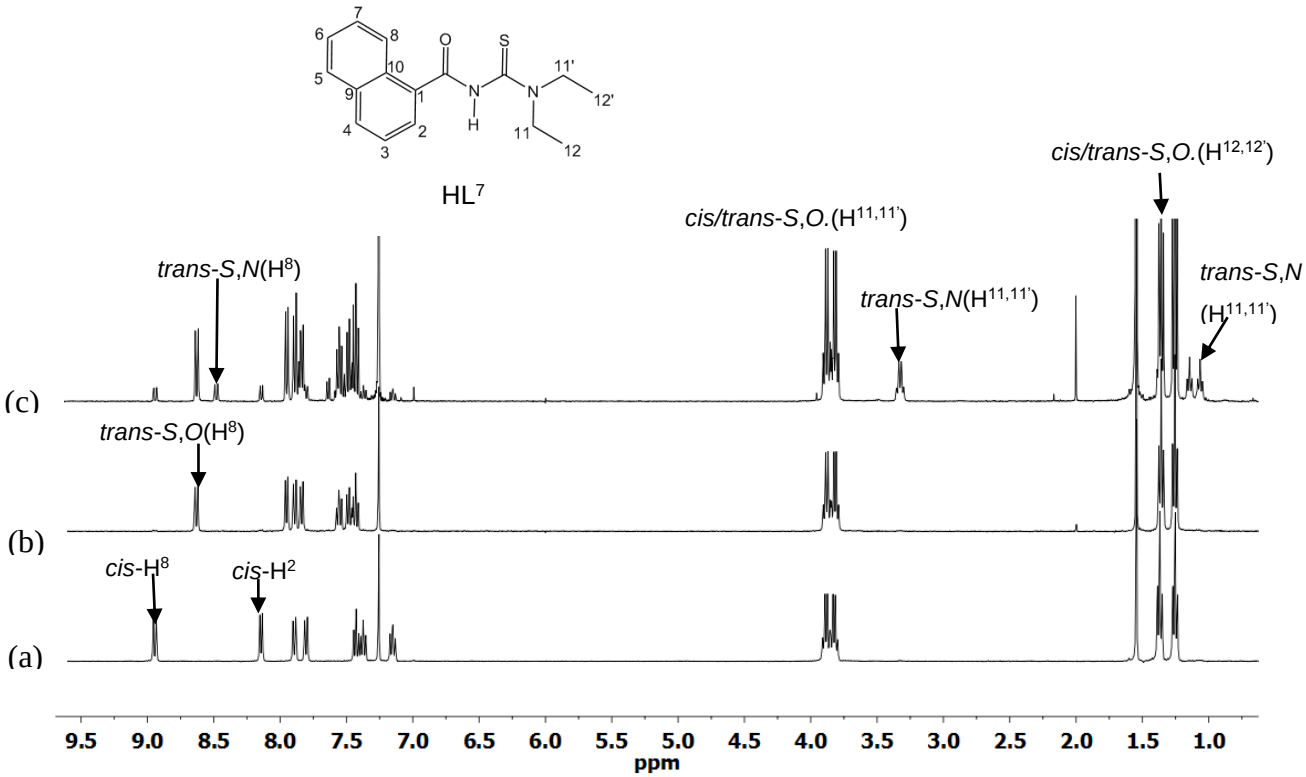

Figure 4.10. ^{1}H NMR spectra of (a) pure *cis*-[P(L^7-κ*S*,*O*)$_2$]; (b) isolated pure *trans*-[Pd(L^7-κ*S*,*O*)$_2$] and (c) solution of *trans*-[Pd(L^7-κ*S*,*O*)$_2$] after 25 minutes in dark in chloroform-*d* at 25 °C.

When a solution containing the *trans*-[Pd(L^7-κ*S*,*O*)$_2$] and *trans*-[Pd(L^7-κ*S*,*N*)$_2$] isomers is left in the dark, spontaneous *trans*→*cis* isomerization occurs to form the *cis*-[Pd(L^7-κ*S*,*O*)$_2$] isomer. Figure 4.11 (a) shows the arrayed ^{1}H NMR spectra of a mixture of the *trans*-[Pd(L^7-

κ*S*,*O*)$_2$] and *trans*-[Pd(L^7-κ*S*,*N*)$_2$] complexes dissolved in chloroform-*d* with NMR data acquisition at 15 minutes time interval in the dark. Only the naphthyl protons H^8 are represented for clarity. The changes in relative peak intensities of the three geometric isomers are also given in Figure 4.11(b). It is evident that as the sample time in the dark increases, the intensity of the *cis*-[Pd(L^7-κ*S*,*O*)$_2$] H^8 proton increases at the expense of the *trans*-[Pd(L^7-κ*S*,*O*)$_2$] resonance which decreases steadily. Also, the *trans*-[Pd(L^7-κ*S*,*N*)$_2$] H^8 resonance initially increases to a steady state after *ca* 3 hours and then decreases slowly with time. After *ca* 3 hours in the dark, the *trans*-[Pd(L^7-κ*S*,*O*)$_2$] H^8 resonance completely vanishes. However for the *trans*-[Pd(L^7-κ*S*,*N*)$_2$] isomer, a much longer residence time of 84 hours in the dark was required for complete reversion to the *cis*-[Pd(L^7-κ*S*,*O*)$_2$] isomer to be achieved as illustrated by the overlaid ^{1}H NMR spectra in Figure A4.1.

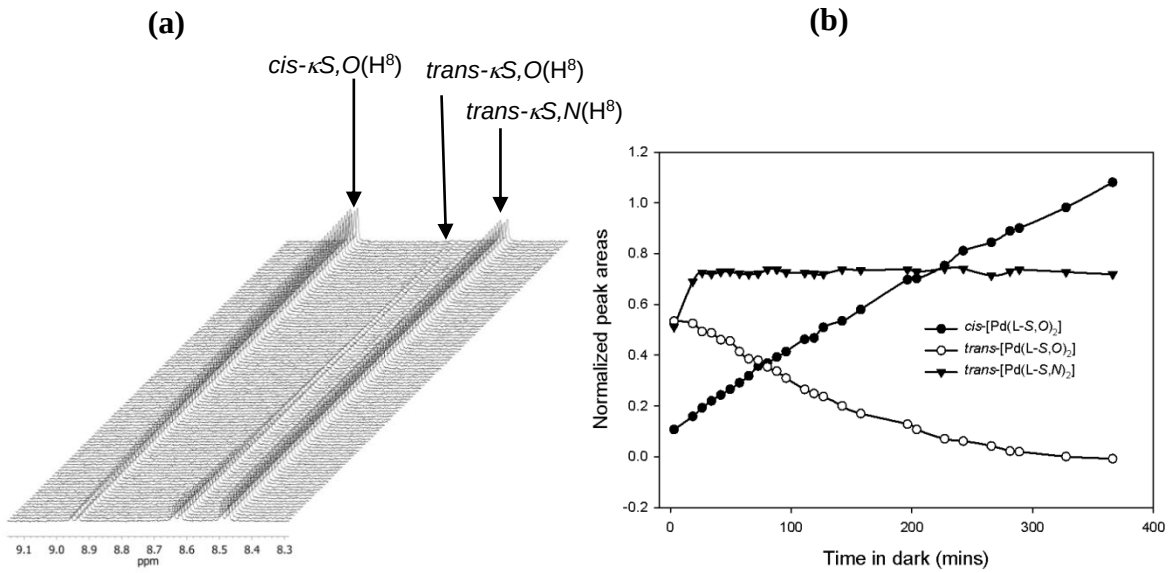

Figure 4.11. Changes in H^8 resonance intensity with time for *cis*-, *trans*-isomers of *trans*-[Pd(L^7-κ*S*,*O*)$_2$] and at 25 °C with time in the dark.

The isolated *trans*-[Pd(L^7-κ*S*,*O*)$_2$] and *trans*-[Pd(L^7-κ*S*,*N*)$_2$] complexes were also characterized by FT-IR. Figure 4.12 shows overlaid FT-IR spectra for the *cis*-[Pd(L^7-κ*S*,*O*)$_2$], *trans*-[Pd(L^7-κ*S*,*O*)$_2$] and *trans*-[Pd(L^7-κ*S*,*N*)$_2$] complexes. The changes in FT-IR bands for the three geometric isomers were compared to that of the unbound HL^7 ligand discussed in chapter 2, section 2.1.3, page 28 (ν (N-H) = 3171.41 cm^{-1}), ν(C=O) = 1676.31 cm^{-1}). The *cis*-[Pd(L^7-κ*S*,*O*)$_2$], *trans*-[Pd(L^7-κ*S*,*O*)$_2$] and *trans*-[Pd(L^7-κ*S*,*N*)$_2$] isomers show disappearance of the N-H stretching frequency confirming ligand deprotonation in these complexes. In addition, shifts to lower ν(C=O) frequencies are observed for the *cis*-[Pd(L^7-κ*S*,*O*)$_2$] (1488.82 cm^{-1}) and *trans*-

[Pd(L^7-κ*S*,*O*)$_2$] (1489.47 cm^{-1}) isomers compared to the unbound HL^7 ligand. This signifies a decrease in double bond character for the two complexes after coordination of the Pd(II) through the carbonyl group. For the *trans*-[Pd(L^7-κ*S*,*N*)$_2$] complex, the ν(C=O) stretching band decreases only slightly (1628.57 cm^{-1}). This indicates that in this *trans*-κ*S*,*N* isomer, the carbonyl oxygen is uncoordinated to the Pd^{II} ion.

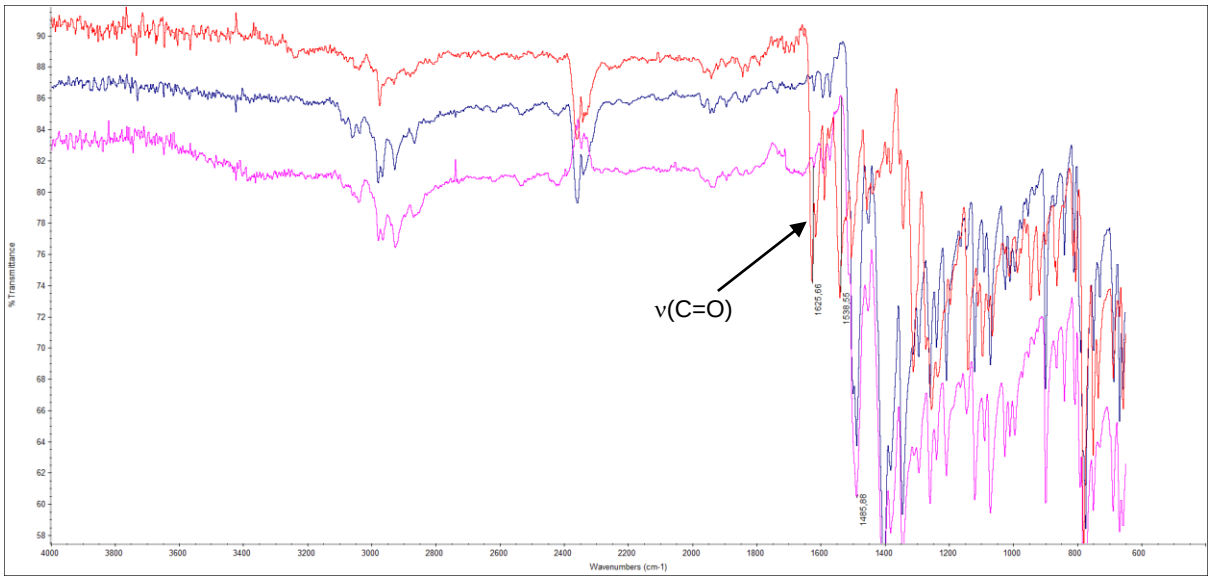

Figure 4.12. Overlaid FT-IR spectra of *cis*-[Pd(L^7-κ*S*,*O*)$_2$] (blue), *trans*-[Pd(L^7-κ*S*,*O*)$_2$] (pink) and *trans*-[Pd(L^7-κ*S*,*N*)$_2$] (red) isolated through photo-induced isomerization.

4.2.4. Single-crystal X-ray structures of *trans*-[Pd(L^7-κ*S*,*O*)$_2$] and *trans*-[Pd(L^7-κ*S*,*N*)$_2$] (HL^7 = *N*,*N*-diethyl-*N*'-1-naphthoylthiourea)

Single crystals suitable for X-ray diffraction of the isolated *trans*-[Pd(L^7-*S*,*O*)$_2$] and *trans*-[Pd(L^7-*S*,*N*)$_2$] complexes were grown as described in chapter 2, section 2.3.3 (page 44).

trans-bis(N,N-diethyl-N'-1-napthoylthioureato-κ^{2}S,O)palladium(II) trans-[Pd(L^7-κS,O)$_2$]

The molecular structure of the *trans*-[Pd(L^7-κ*S*,*O*)$_2$] complex (Figure 4.13) evidently shows bidentate *trans*-κ*S*,*O* coordination of the ligand to Pd(II) in the six-membered Pd1-S1-C12-N1-C11-O1 chelate ring. The *trans*-[Pd(L^7-κ*S*,*O*)$_2$] complex crystallizes in the monoclinic space group $P2_1/c$. The structure displays crystallographic disorders at two positions corresponding to one of the ethyl moieties linked to section C12-N1B of the chelate ring. There are no significant differences in the average Pd-S [2.281(12) Å] and Pd-O [1.978(13) Å] bond lengths compared to similar bond lengths in *trans*-[Pd(L^1-κ*S*,*O*)$_2$] (Pd-S = 2.283 Å, Pd-O = 1.992 Å).[17] This suggests that the bulky nature of the naphthyl groups in the *trans*-[Pd(L^7-

κ*S*,*O*)$_2$] complex has no significant effect on the delocalization of electrons across the six-membered chelate ring. Moreover, no significant changes are observed for the Pd-S and Pd-O bond distances in this *trans*-κ*S*,*O* isomer compared to that of the reported *trans*-[Pt(L-κ*S*,*O*)$_2$] (L = *N*,*N*-(di-*n*)-butyl-*N*'-naphthoylthiourea) complex [Pt-S = 2.250(4), Pt-O = 1.980(1) Å].[56] This suggests that the introduction of longer *n*-butyl substituents do not influence the distribution of electron delocalization across the chelate ring.

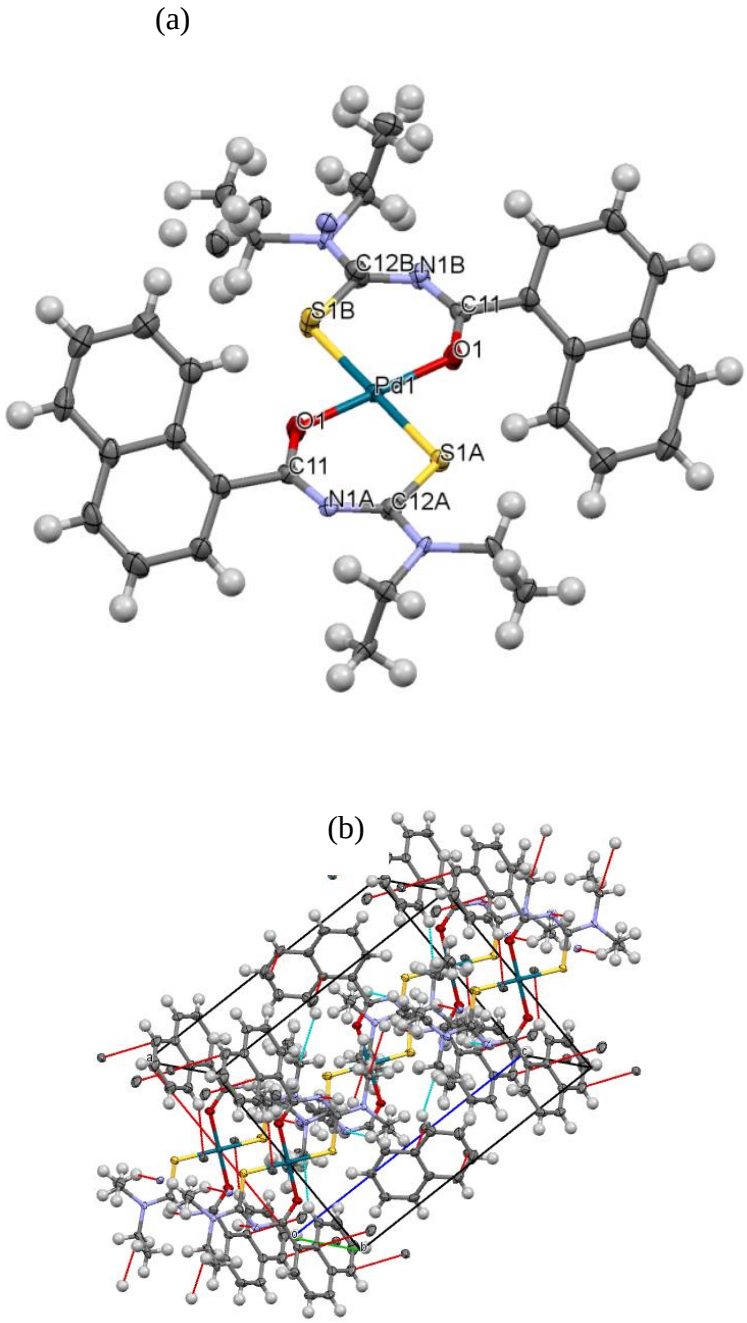

Figure 4.13. (a) Molecular structure from single-crystal X-ray difraction and (b) crystal packing of a novel *trans*-bis(*N*,*N*-diethyl-*N*'-1-naphthoylthioureato-κ^2*S*,*O*)palladium(II) *trans*-[Pd(L^7-κ*S*,*O*)$_2$] isolated by slow vapour diffusion using photo-induced isomerization of *cis*-[Pd(L^7-κ*S*,*O*)$_2$] in acetonitrile after irradiation with polychromatic light from a 5 Watt LED lamp.

Furthermore, the crystal structure of the *trans*-[Pd(L^7-κ*S*,*O*)$_2$] complex shows that the average Pd-S [2.281(12) Å] and Pd-O [1.9789(13) Å] bond lengths are slightly longer and shorter than those of *cis*-[Pd(L^7-κ*S*,*O*)$_2$] [Pd-S = 2.234 Å, Pd-O = 2.023 Å] respectively. This is ascribed to the higher *trans*-influence of the sulfur donor[58] atom leading to longer Pd-S and shorter Pd-O bond distances in the *trans*-[Pd(L^7-κ*S*,*O*)$_2$] isomer. The *trans*-[Pd(L^7-κ*S*,*O*)$_2$] structure is square planar as represented by S1-Pd1-S1 and O1-Pd1-O1 bond angles of 180°. However the two naphthyl rings are not coplanar with the six-membered chelate system as evident by the torsion angles C12A-N1A-C11-C1=171.19°, C12B-C-11B-C11-C1=-175.00°. Crystal packing of the *trans*-[Pd(L^7-κ*S*,*O*)$_2$] isomer is presented in Figure 4.13 (b) and reveals the presence of intermolecular C-H interactions between the naphthyl and methyl groups.

trans-bis(N,N-diethyl-N'-1-napthoylthioureato-κ²S,N)palladium(II) trans-[Pd(L^7-κS,N)$_2$]

The isolated *trans*-[Pd(L^7-κ*S*,*N*)$_2$] complex crystallizes in the monoclinic space group $P2_1/n$. The structure (Figure 4.14) has an unusual four-membered *trans-S,N* chelate ring different from the six-membered chelates formed by the *cis*-[Pd(L^7-κ*S*,*O*)$_2$] and *trans*-[Pd(L^7-κ*S*,*O*)$_2$] isomers. Inspection of the S1-Pd1-S(1_a) bond angle of 180° within the four-membered Pd-S1-C11-C1 ring reveals that the two chelate rings are similar and assume a perfect square planar coordination relative to the plane of coordination. The bulky naphthyl groups are not coplanar with the four-membered chelate ring as seen from the torsion angle S1-C12-N2-C11= 138.93°. Intermolecular π-π interactions exist between the two naphthyl rings as well as interactions between a naphthyl hydrogen and the sulfur atoms in the chelate ring (Figure 4.14 (b)). Also obvious is the fact that the Pd-S bonds are slightly longer (2.325 Å) in the *trans*-[Pd(L^7-κ*S*,*N*)$_2$] complex compared to both *trans*-[Pd(L^7-κ*S*,*O*)$_2$] (2.281 Å) and *cis*-[Pd(L^7-κ*S*,*O*)$_2$] (2.234 Å) complexes. This lengthening is consistent with a higher *trans* influence of the sulfur donor atom relative to either oxygen or nitrogen which consequently weakens the Pd-S bonds.[58] Moreover, a slight shortening of the C-O bond distance (1.2250 Å) in this *trans*-[Pd(L^7-*S*,*N*)$_2$] isomer is observed compared to the average bond distances of the coordinated C-O bond in either *cis*-[Pd(L^7-κ*S*,*O*)$_2$] (1.2720 Å) or *trans*-[Pd(L^7-κ*S*,*O*)$_2$] [1.282(2)Å] complexes. This is accounted for by extensive delocalization of electrons across the six-membered chelate rings in the *cis*-[Pd(L^7-κ*S*,*O*)$_2$] and *trans*-[Pd(L^7-κ*S*,*O*)$_2$] isomers involving coordination of the carbonyl moiety. However, in the *trans*-[Pd(L^7-κ*S*,*N*)$_2$] isomer

there is a substantial amount of double bond character in the C=O bond which is not bonded to the Pd^{II} metal ion. The changes in C=O bond distances for the *cis*-[Pd(L^7-κ*S*,*O*)$_2$], *trans*-[Pd(L^7-κ*S*,*O*)$_2$] and *trans*-[Pd(L^7-κ*S*,*N*)$_2$] complexes are consistent with the differences in FT-IR ν(C=O) stretching frequencies (section 4.2.3, Figure 4.12, page 87).

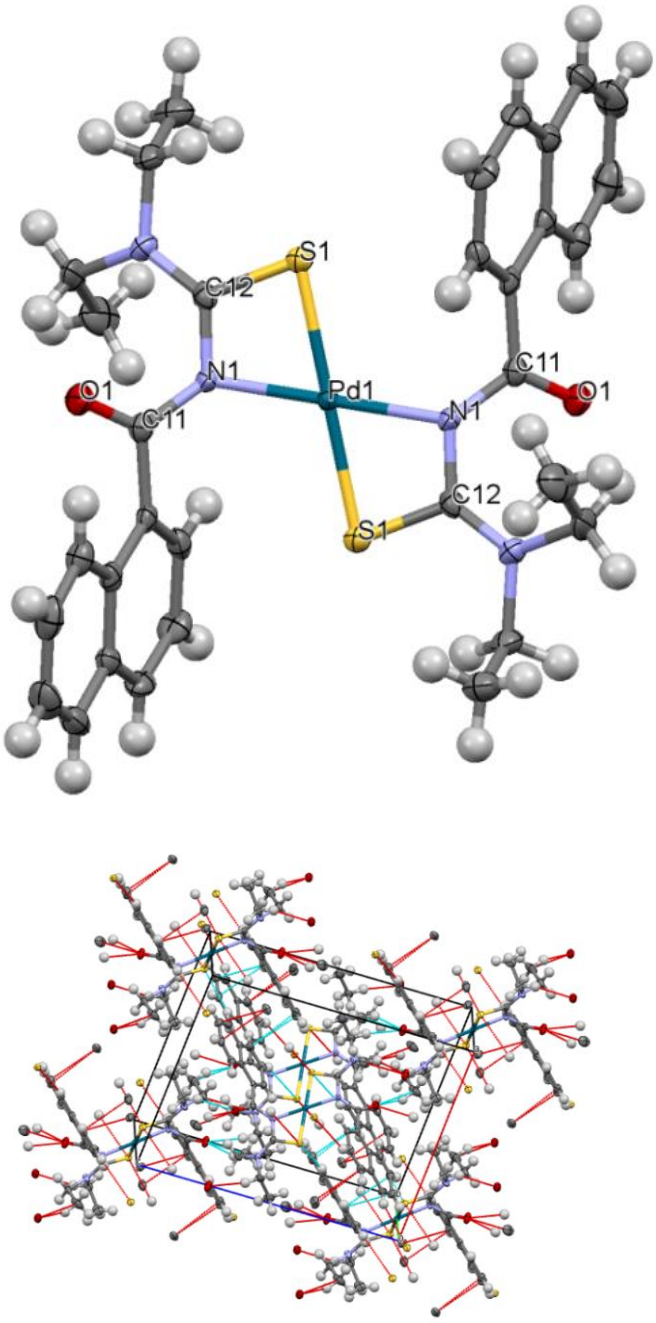

Figure 4.14. (a) Molecular structure from single-crystal X-ray difraction and (b) crystal packing of a first example of a *trans-bis(N,N-diethyl-N'-1-naphthoylthioureato-κ^{2}S,O)palladium(II) trans*-[Pd(L^7-κ*S*,*N*)$_2$] complex isolated by vapour diffusion following photo-induced isomerization of *cis*-[Pd(L^7-κ*S*,*O*)$_2$] in acetonitrile when irradiated with polychromatic light from a 5 Watt LED lamp.

4.3. Conclusions

In conclusion, photo-induced *cis*→*trans* isomerization of the *cis*-[Pd(L^7-κ*S*,*O*)$_2$] complex (HL^7 = *N*,*N*-diethyl-*N*'-1-naphthoylthiourea) in acetonitrile produced an unprecedented square planar *trans*-[Pd(L^7-κ*S*,*N*)$_2$] isomer in addition to the *trans*-[Pd(L^7-κ*S*,*O*)$_2$] isomer. The new *trans*-[Pd(L^7-κ*S*,*N*)$_2$] isomer showed significant differences in retention time and ^{1}H NMR chemical shifts from the *trans*-[Pd(L^7-κ*S*,*O*)$_2$] and *cis*-[Pd(L^7-κ*S*,*O*)$_2$] isomers. Further confirmation of formation of the *trans*-[Pd(L^7-κ*S*,*N*)$_2$] isomer was provided by LC-ESI-MS with all three isomers giving a molecular ion with *m/z* 677.12. The formation of the unique four-membered *trans*-[Pd(L^7-κ*S*,*N*)$_2$] chelate is attributed to the potential steric or electronic effects of the bulky naphthyl substituents in the *cis*-[Pd(L^7-κ*S*,*O*)$_2$] complex. This is presumably capable of enhancing the nucleophilicity of nitrogen atom relative to the oxygen atom after a Pd-O or Pd-S bond cleavage during photo-induced isomerization. When an irradiated mixture of the *cis*-[Pd(L^7-κ*S*,*O*)$_2$], *trans*-[Pd(L^7-κ*S*,*O*)$_2$] and *trans*-[Pd(L^7-κ*S*,*N*)$_2$] isomers in acetonitrile was allowed to stand in the dark, the RP-HPLC peaks assigned to the *trans*-[Pd(L^7-κ*S*,*O*)$_2$] isomer slowly diminished in intensity as a result of a thermal *trans*→*cis* isomerization. The intensity of the *trans*-[Pd(L^7-κ*S*,*N*)$_2$] peaks initially increased in the dark and then gradually decreased at the expense of the peaks representing either the *cis*-[Pd(L^7-κ*S*,*O*)$_2$] or *trans*-[Pd(L^7-κ*S*,*O*)$_2$] isomer.

Prolonged irradiation of acetonitrile solution of the *cis*-[Pd(L^7-κ*S*,*O*)$_2$] complex with vapour diffusion or slow evaporation led to the isolation of a mixture of the *trans*-[Pd(L^7-κ*S*,*O*)$_2$] and *trans*-[Pd(L^7-κ*S*,*N*)$_2$] complexes. All three geometric isomers showed significant differences in melting points in the order *cis*-[Pd(L^7-κ*S*,*O*)$_2$] < *trans*-[Pd(L^7-κ*S*,*O*)$_2$] < *trans*-[Pd(L^7-κ*S*,*N*)$_2$]. Further characterization of the *trans*-[Pd(L^7-κ*S*,*N*)$_2$] complex by FT-IR revealed a lower shift in the ν (C=O) stretching band relative to its *trans*-[Pd(L^7-κ*S*,*O*)$_2$] and *cis*-[Pd(L^7-κ*S*,*O*)$_2$] isomers. This confirmed that the oxygen atom of the *trans*-[Pd(L^7-κ*S*,*N*)$_2$] complex does not participate in bonding. Dissolution of an isolated *trans*-[Pd(L^7-κ*S*,*O*)$_2$] complex in chloroform-*d* in the dark resulted in a slow *trans*→*cis* reversion to completely generate the *cis*-[Pd(L^7-κ*S*,*O*)$_2$] isomer after *ca* 6 hours. The reversion of the *trans*-[Pd(L^7-κ*S*,*N*)$_2$] isomer was much slower and required *ca* 84 hours in the dark for the *trans*-[Pd(L^7-κ*S*,*N*)$_2$] resonances to completely vanish.

Unambiguous confirmation of the *trans*-[Pd(L^7-κ*S*,*O*)$_2$] and *trans*-[Pd(L^7-κ*S*,*N*)$_2$] modes of coordination was provided by single-crystal X-ray diffraction analysis. In comparison to the *cis*-[Pd(L^7-κ*S*,*O*)$_2$] isomer, the *trans*-[Pd(L^7-κ*S*,*O*)$_2$] and *trans*-[Pd(L^7-κ*S*,*N*)$_2$] structures showed longer Pd-S and shorter Pd-O bond distances. In addition, the six-membered *trans*-[Pd(L^7-κ*S*,*O*)$_2$] and four-membered *trans*-[Pd(L^7-κ*S*,*N*)$_2$] structures showed ideal square planar geometries.

5

Photo-induced isomerization of cis-[M(L-κS,O)$_2$] (M=Pt^{II} or Pd^{II})complexes with asymmetrically substituted N,N-dialkyl-N'-acyl(aroyl)thioureas

Synopsis

The asymmetrically substituted N,N-dialkyl-N'-acylthioureas (HL) exist as E or Z isomers due to restricted rotation across the C-N thioamido bonds. This is reflected in their corresponding cis-[M(L-κS,O)$_2$] (M = Pt(II)/Pd(II)) complexes which exist in solution as cis-EE, cis-EZ and cis-ZZ isomers. Unambiguous assignment of the sets of configurational isomers is achieved by ^{1}H, ^{13}C{^{1}H} correlated HMBC and 1D NOESY experiments. The distribution of configurational isomers in solution is dependent on the nature of ligand substituents. This leads to the isolation of cis-[Pt(EE-L-κS,O)$_2$] isomers for complexes with smaller N-ethyl substituents, and a cis-[Pt(ZZ-L-κS,O)$_2$] isomer when relatively larger N-alkyl groups are involved. The sets of cis-ZZ, EZ and EE complexes undergo photo-induced isomerization in chloroform-d leading to corresponding trans-ZZ, EE and EZ isomers as determined by formation of three additional ^{195}Pt{^{1}H} resonances.

5.1. Introduction

The asymmetrically substituted *N*,*N*-dialkyl-*N*'-acyl(aroyl)thioureas exhibit configurational *E*, *Z* isomerism resulting from restricted rotation across the C-N bond of the thioamido moiety.[69,70] The *E* (entgegen) conformation is considered as that in which the larger *N*-alkyl group points away from the sulfur atom, while in the *Z* (zusammen) conformation the sulfur atom and the larger *N*-alkyl group are on the same side of the molecule. The ligands show separate ^{1}H and ^{13}C{^{1}H} NMR signals of the different alkyl substituents attached to the thioamido nitrogen. The restricted C-N bond rotation is also reflected in the respective *cis*-[M(L^{n}-κ*S*,*O*)$_2$] (M = Pt^{II} or Pd^{II}) complexes with an increase in C-N rotational barrier observed after complex formation.[66] Consequently, the *cis*-[M(L^{n}-κ*S*,*O*)$_2$] complexes exist as *cis*-*ZZ*, *cis*-*EZ* and *cis*-*EE* isomers in solution. The conformations of the *cis*-[M(*EE*-L^{n}-κ*S*,*O*)$_2$], *cis*-[M(*ZZ*-L^{n}-κ*S*,*O*)$_2$] and *cis*-[M(*EZ*-L^{n}-κ*S*,*O*)$_2$] isomers are determined by the orientation of the sulfur atom and the larger *N*-alkyl groups relative to the coordination plane. By ^{1}H detected ^{1}H-(^{13}C)-^{195}Pt correlation experiments, the well resolved ^{195}Pt{^{1}H} resonances have been assigned by Koch and co-workers.[69] The restricted rotation and hence distribution of configurational isomers of related complexes is dependent on several factors, some of which include steric effects of bulky substituents,[60,63,109] and the presence of electron-donating groups.[64,110] Also, the energy of the C-N rotational barrier is reported to increase significantly with increase in polarity of solvent,[64,111,112] and ring strain.[64,113]

In chapter 2, the preparation of *cis*-[M(L^{n}-κ*S*,*O*)$_2$] (M = Pt(II) or Pd(II)) complexes of both symmetrically (HL$^{1-7}$) and asymmetrically (HL$^{8-15}$) substituted *N*,*N*-dialkyl-*N*'-acyl(aroyl)thioureas was discussed. The *cis*-[M(L$^{1-7}$-κ*S*,*O*)$_2$] (M = Pt(II) or Pd(II)) complexes of ligands HL$^{1-7}$ were shown in chapters 3 and 4 to undergo reversible photo-induced *cis*→*trans* isomerization in acetonitrile to yield *trans*-[M(L$^{1-7}$-κ*S*,*O*)$_2$] isomers. In this chapter, photo-induced *cis*→*trans* isomerization studies conducted on the *cis*-[M(L$^{8-15}$-κ*S*,*O*)$_2$] complexes derived from the asymmetrically substituted ligands HL$^{8-15}$ (Figure 2.2) will be disccused. The use of ^{195}Pt{^{1}H} enabled the determination of configurational isomers of *trans*-[M(L$^{8-15}$-κ*S*,*O*)$_2$] complexes, while characterization of the *cis*-[M(L^{8}-κ*S*,*O*)$_2$] complex was achieved by HSQC, HMBC and 1D NOESY. The distribution of configurational *E*, *Z* isomers in the *cis*-[M(L$^{8-15}$-κ*S*,*O*)$_2$] and *trans*-[M(L$^{8-15}$-κ*S*,*O*)$_2$] geometric isomers was found to be dependent on the nature of ligand substituents.

5.2. Results and discussion

5.2.1. Evidence of configurational *E*, *Z* isomerism in asymmetrically substituted *N*,*N*-dialkyl-*N*'-acyl(aroyl)thioureas

The asymmetrically substituted *N*,*N*-dialkyl-*N*'-acylthioureas (HL^{8-15}) presented in chapter 2 (Figure 2.2, page 20) were characterized using ^{1}H and $^{13}C\{^{1}H\}$ NMR spectroscopy. Figure 5.1 shows the partial ^{1}H NMR spectra for ligands HL^{8-11} with emphasis on the N-CH_3 and N-(CH_2) resonances for simplicity. The ligands exhibit configurational *E*, *Z* isomerism in a chloroform-*d* solution at 25 °C due to hindered rotation across the C-N bond. This gives rise to two sets of resonances at different chemical shifts positions in particular for the *N*-alkyl protons. The relative distribution of the *E*, *Z* isomers was obtained by integration of the ^{1}H NMR peaks. The values indicate that in all the ligands, the larger *N*-alkyl groups prefer to assume the *Z* conformation. For the larger *N*-alkyl groups, the *Z* resonances are shifted upfield relative to the *E* resonances. This suggests that the *N*-alkyl groups are coplanar to the sulfur atom of the thiocarbonyl moiety leading to a significant deshielding. A downfield shift of *ca.* 0.22 ppm is experienced by the *E* N-CH_3 protons relative to their *E* isomers for the ligands HL^{9-11}. A significant upfield shift of *ca*. 0.37 ppm exists for the N-(CH_2) multiplets in relation to the resonances of their *Z* isomers. This is associated with two sets of quartets (methylene) and singlets (methyl) representing the *Z* and *E* isomers with relative distribution of 75:25 % (obtained from peak integration).

Confirmation of the assignment of the *E*, *Z* isomers of *N*-methyl,*N*-ethyl, *N*'-benzoylthiourea (HL^{8}) was achieved by benzene titration. Different volumes of benzene-d_6 were added stepwise to chloroform-*d* solutions of the HL^{8} ligand as shown in Table 5.1, followed by ^{1}H NMR data acquisition. Figure 5.2 represents the changes in ^{1}H NMR chemical shift observed with only the N(CH_3) and N(CH_2) resonances shown for clarity. It is evident that as the concentration of benzene increases, an upfield shift occurs for all N(CH_2) and N(CH_3) resonances. The N-CH_3 groups in the *Z* configuration presumably experience a greater diamagnetic shielding by the benzene ring leading to a corresponding upfield shift relative to resonances of N(CH_3) for the *E* isomer. This is consistent with the upfield shifts reported for resonances in *N*,*N*-dimethylformamides.[114]

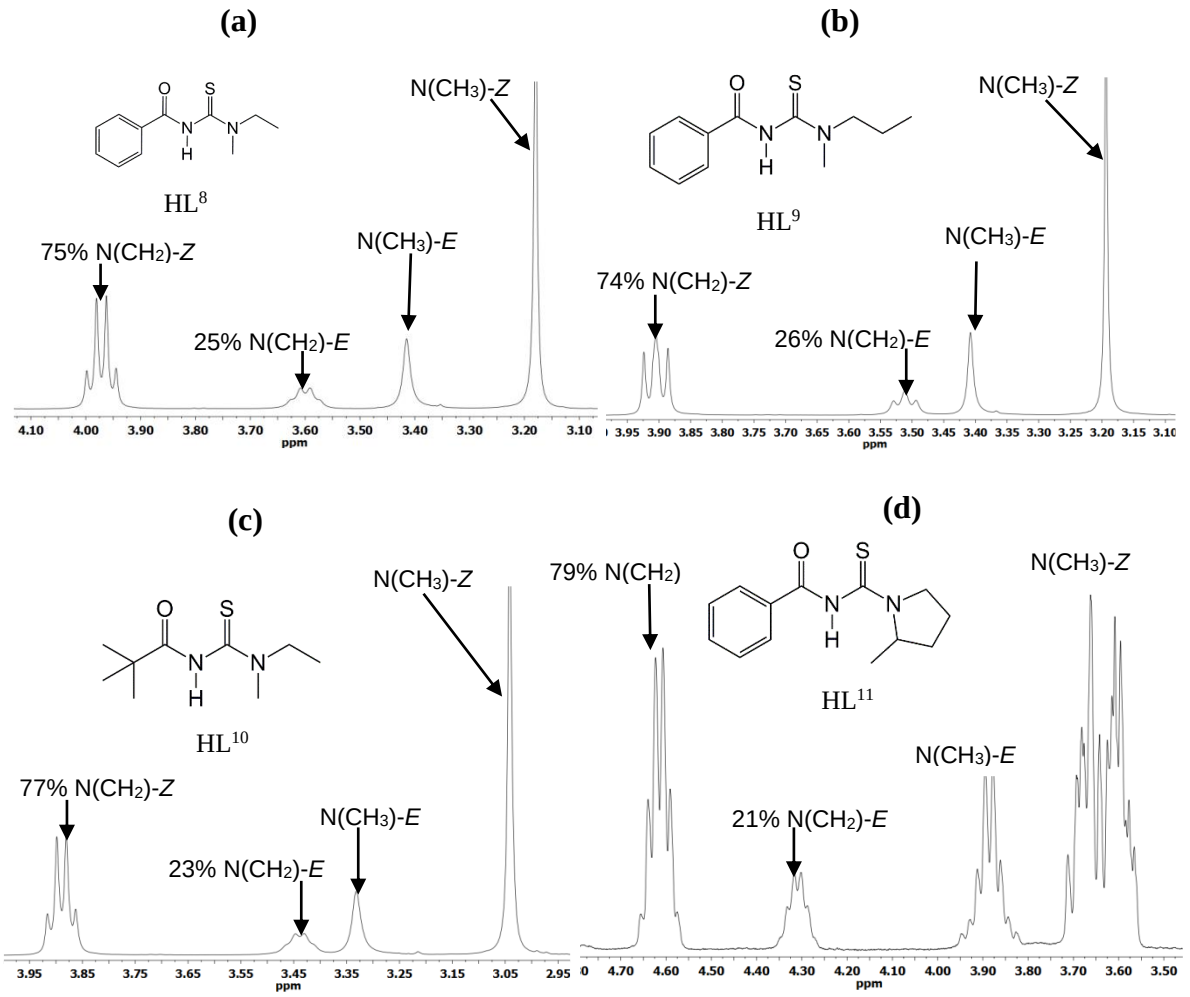

Figure 5.1. Partial ^{1}H NMR spectra of **(a) HL^{8}**, **(b) HL^{9}**, **(c) HL^{10}** and **(d) HL^{11}** in chloroform-*d* at 25°C with distribution of *E*, *Z* isomers in solution.

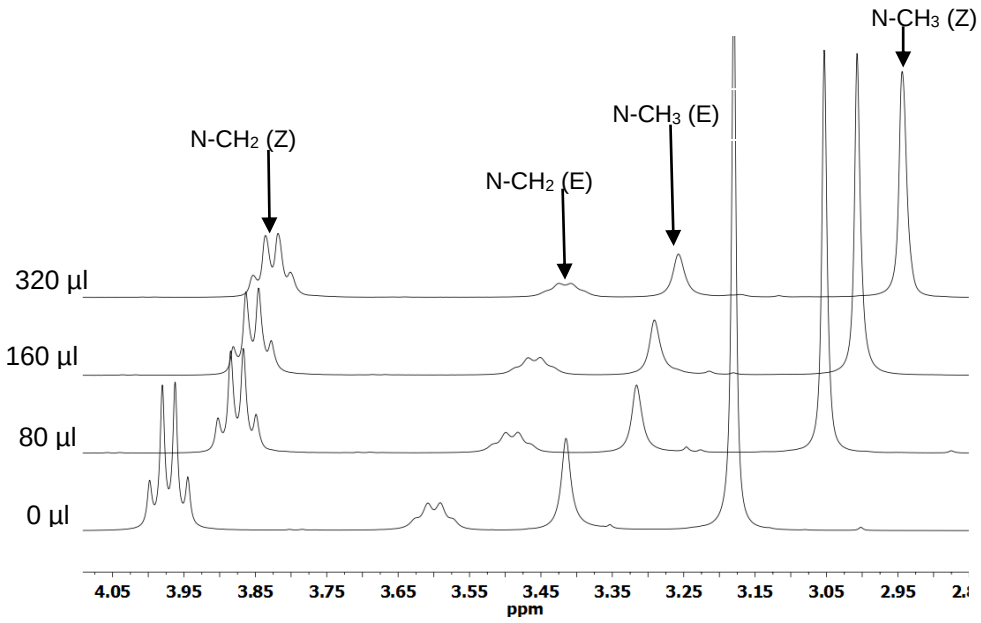

Figure 5.2. Partial ^{1}H NMR spectra of **HL^{8}** showing upfield shifts in N(CH_3) and N(CH_2) resonances after addition of different volumes of benzene-d_6, in chloroform-*d* at 25° C.

Table 5.1. Chemical shifts values of the *E, Z* isomers for the N(CH_3) and N(CH_2) protons of HL^8 in chloroform-*d* obtained from benzene-d_6 titration at 25°C.

Volume of Benzene-d_6 added(µl)	δ N(CH_2)/ppm		δ N(CH_3)/ppm	
	Z	*E*	*Z*	*E*
0	3.97	3.60	3.18	3.41
80	3.88(0.09)	3.49(0.11)	3.05(0.13)	3.32(0.09)
160	3.86(0.02)	3.46(0.03)	3.01(0.04)	3.29(0.03)
320	3.83(0.01)	3.42(0.02)	2.94(0.03)	3.26(0.01)

5.2.2. Characterization of *E, Z* isomers in *cis*-[M(L^n-κ*S,O*)$_2$] (M = Pt(II) or Pd(II)) complexes

5.2.2.1. ^{1}H and ^{13}C NMR characterization

Addition of stoichiometric amounts of the ligands HL^{8-15} to either K_2PdCl_4 or K_2PtCl_4 in acetonitrile/water mixtures produces corresponding *cis*-[M(L^n-κ*S,O*)$_2$] complexes as discussed in chapter 2, section 2.1.1. Evidence of configurational isomerism in the resulting *cis*-[M(L^n-κ*S,O*)$_2$] (M = Pt(II) or Pd(II)) complexes is provided by their ^{1}H NMR spectra. Figure 5.3 shows the partial ^{1}H NMR spectrum of *cis*-[Pd(L^8-κ*S,O*)$_2$] (HL^8 = *N*-methyl,*N*-ethyl-*N*'-benzoylthiourea) at 25 °C and in chloroform-*d*, with only the *N*-alkyl resonances shown for clarity. Two sets of resonances are evident and assigned to the *cis*-[Pd(*ZZ*-L^8-κ*S,O*)$_2$] and *cis*-[Pd(*EE*/*EZ*-L^8-κ*S,O*)$_2$] (due to overlap of *EZ* and *EE*) isomers. The relative distributions of the *ZZ* (δ = 3.41 ppm) and *EZ/EE* (δ = 3.89 ppm) resonances for the N(CH_3) protons are respectively 57.8:42.2 %. The distribution of the N(CH_2) protons centred at δ = 3.45 ppm could not be obtained due to overlap of resonances. The N(CH_3)(ZZ) singlet is shifted slightly upfield relative to its *EZ, EE* resonances. This could be attributed to the magnetic anisotropy of the sulfur atom and its influence on N-CH_2 protons coplanar to it at the *cis-ZZ* configuration.

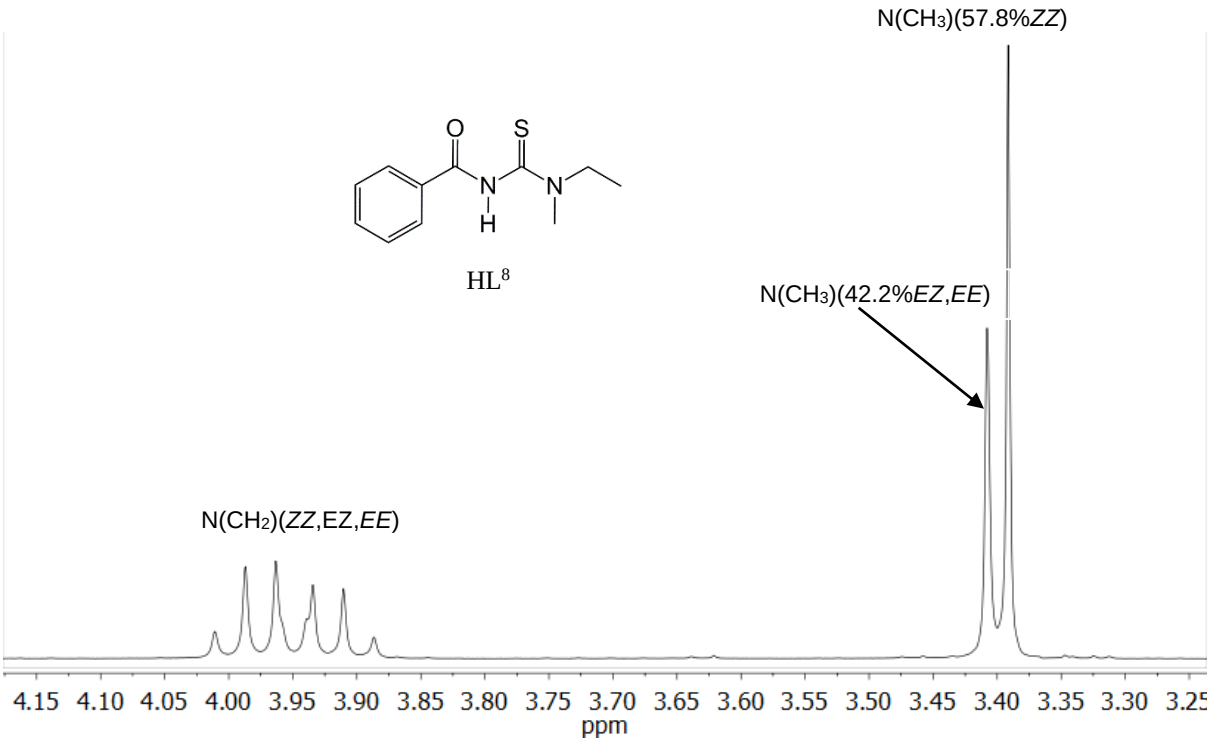

Figure 5.3. Partial ^{1}H NMR spectrum of a mixture of *ZZ*, *EZ* and *EE* configurational isomers of *cis*-[Pd(L^{8}-κ*S*,*O*)$_2$] in chloroform-d at 25 °C.

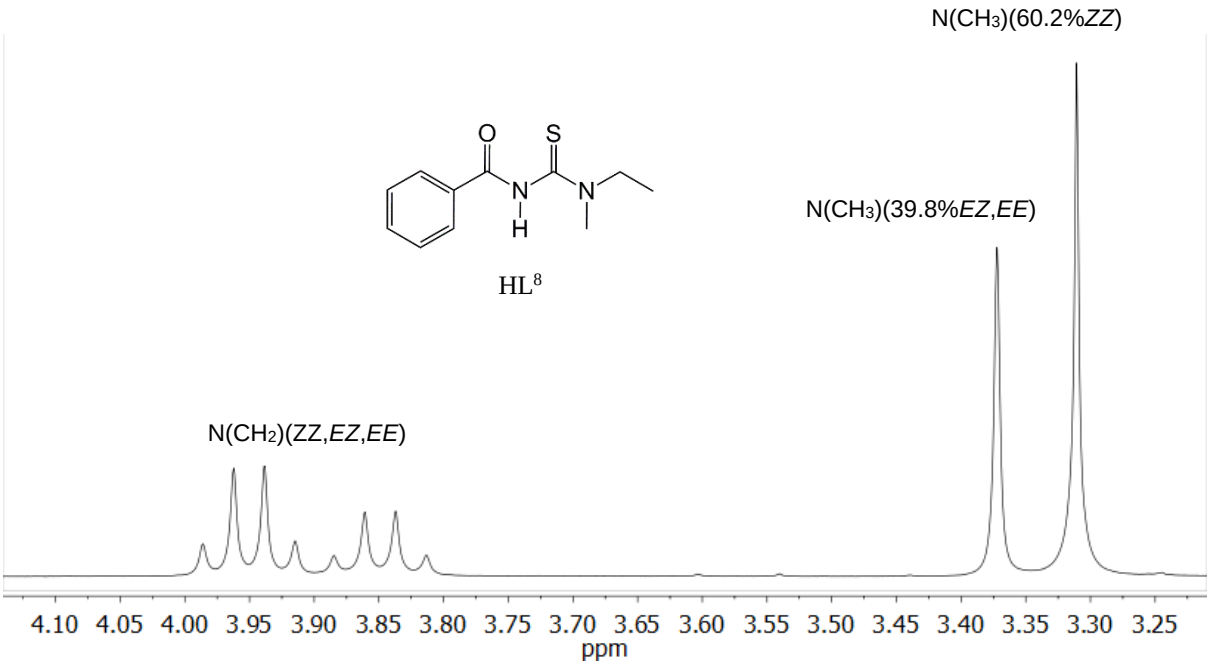

Figure 5.4. Partial ^{1}H NMR spectrum of a mixture of *ZZ*, *EZ* and *EE* configurational isomers of *cis*-[Pt(L^{8}-κ*S*,*O*)$_2$] in chloroform-*d* and at 25°C.

The chemical shift positions of all resonances in the partial ^{1}H NMR spectrum of the *cis*-[Pt(L^{8}-κ*S*,*O*)$_2$] complex (Figure 5.4) are very similar to that of the *cis*-[Pd(L^{8}-κ*S*,*O*)$_2$] complex (Figure 5.3) but with some notable differences. For the *cis*-[Pt(L^{8}-κ*S*,*O*)$_2$] complex, two sets of quartets centred at δ = 3.95 ppm and δ = 3.85 ppm are evident. These are assigned to the *cis*-*ZZ* and *cis*-*EE*/*EZ* (due to overlap of *EZ* and *EE*) isomers respectively. The relative distribution of *ZZ* and *EZ/EE* resonances for both N(CH$_3$) and N(CH$_2$) protons is 60.2:39.8 % respectively. Also for the *cis*-[Pt(L^{8}-κ*S*,*O*)$_2$] complex, the N(CH$_3$)(ZZ) singlet is shifted slightly upfield relative to its *EZ* and *EE* resonances.

The distributions of the *E*, *Z* isomers for some of the *cis*-[M(L^{n}-κ*S*,*O*)$_2$] (M = Pt(II) or Pd(II)) complexes are given in Table 5.2. A higher relative distribution of the configurational isomers is observed for the *cis*-[M(L^{n}-κ*S*,*O*)$_2$] complexes (Table 5.2) compared to their respective HL$^{8\text{-}11}$ ligands (Figure 5.1). This suggests that complex formation results in significant delocalization, consequently leading to a higher barrier of C-N rotation as observed for bis(*N*,*N*-diethyl-*N'*-benzoylthioureato-κ^2*S*,*O*)nickel(II) relative to its free ligand.[64] Table 5.2 further reveals that slightly higher relative distributions of the *EZ/EE* isomers are observed for the *cis*-[Pd(L^{n}-κ*S*,*O*)$_2$] complexes compared to their *cis*-[Pt(L^{n}-κ*S*,*O*)$_2$] counterparts. This is presumably due to a higher kinetic lability of the Pd(II) complexes relative to Pt(II) complexes.

Table 5.2. Distribution of *cis*-*ZZ*, -*EZ*, -*EE* isomers in the *cis*-Pt(L$^{8\text{-}10,15}$-κ*S*,*O*)$_2$] and *cis*-[Pd(L^{8,9,15}-κ*S*,*O*)$_2$] complexes in chloroform-*d* at 25 °C.

Complex	**%*ZZ***	**%*EE/EZ***
***cis*-[Pt(L^{8}-κ*S*,*O*)$_2$]**	60.2	39.8
***cis*-[Pd(L^{8}-κ*S*,*O*)$_2$]**	57.8	42.2
***cis*-[Pt(L^{9}-κ*S*,*O*)$_2$]**	61.7	38.3
***cis*-[Pd(L^{9}-κ*S*,*O*)$_2$]**	59.9	40.1
***cis*-[Pt(L^{10}-κ*S*,*O*)$_2$]**	61.0	39.0
***cis*-[Pt(L^{15}-κ*S*,*O*)$_2$]**	71.9	28.1
***cis*-[Pd(L^{15}-*S*,*O*)$_2$]**	69.4	30.6

The $^{13}C\{^{1}H\}$ NMR spectra of all the *cis*-[M($L^{8\text{-}15}$-κ*S*,*O*)$_2$] (M = Pt(II) or Pd(II)) complexes are characterized by at least two sets of peaks assigned to their *cis*-*ZZ* and *cis*-*EZ*/*EE* isomers. Figure 5.5 shows the partial $^{13}C\{^{1}H\}$ NMR spectrum of the *cis*-[Pt(L^{8}-κ*S*,*O*)$_2$] complex with two resonances observed for the N(CH_3) and N(CH_2) groups. In addition, the $^{13}C\{^{1}H\}$ NMR resonances reveal a ^{4}J (^{195}Pt, ^{13}C) coupling of *ca* 40 Hz for the N(CH_3) resonances assigned to the *cis*-*ZZ* configuration. The observation of a ^{4}J (^{195}Pt, ^{13}C) coupling of this magnitude has been attributed by Koch *et al*.[69] to a favourable 'W' configuration adopted by the larger *N*-alkyl groups relative to the Pt atom. For the *cis*-[Pt($L^{8\text{-}15}$-κ*S*,*O*)$_2$] complexes, there were however no evidence of ^{5}J (^{195}Pt-^{1}H) coupling as these were probably too small for any significant chemical shift anisotropy to have an effect.[69]

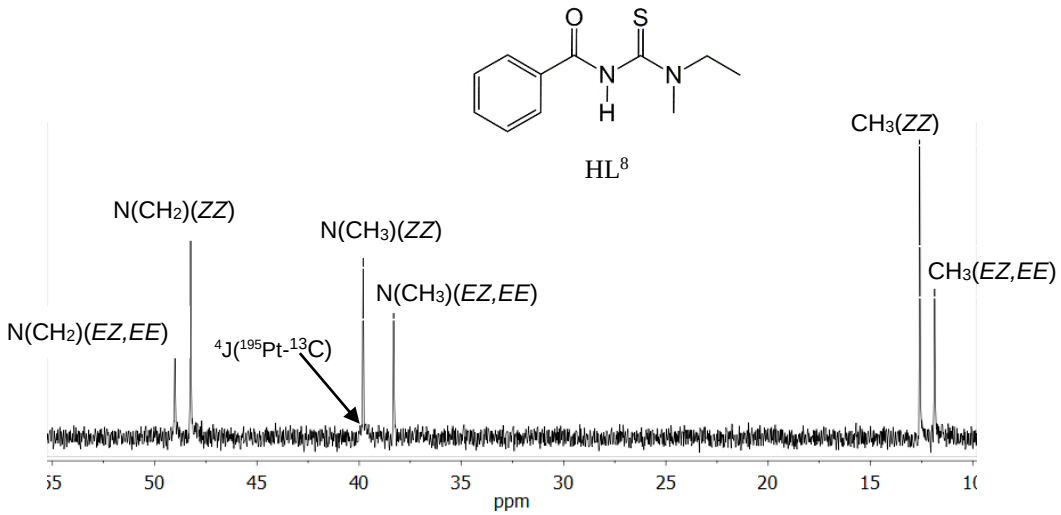

Figure 5.5. Partial $^{13}C\{^{1}H\}$ NMR spectrum of *cis*-[Pt(L^{8}-κ*S*,*O*)$_2$] in chloroform-*d* at 25 °C.

Assignment of the N(CH_2) and N(CH_3) carbons at δ = 48.4 ppm and 39.5 ppm respectively for the *cis*-[Pt(*ZZ*-L^{8}-κ*S*,*O*)$_2$] complex was achieved by means of a one-bond heteronuclear chemical shift correlation spectroscopy (HSQC). This was aided by correlation with their respective assigned protons at δ = 3.94 ppm and 3.29 ppm (Figure 5.6). In a similar manner, correlation of the N(CH_2) δ = 3.83 ppm and N(CH_3), δ = 3.35 ppm protons in the *cis*-[Pt(*EE*-L^{8}-κ*S*,*O*)$_2$] or *cis*-[Pt(*EZ*-L^{8}-κ*S*,*O*)$_2$] conformation leads to assignment of their respective carbons at δ = 49.2 ppm and 38.5 ppm. The peaks at δ = 128.2 ppm, 129.5 ppm and 131.6 ppm each show a $^{1}J_{C\text{-}H}$ correlation with $H^{3,3'}$ (δ = 7.42 ppm), H^{4} (δ = 7.52 ppm) and $H^{2,2'}$ (δ = 8.27 ppm) and are therefore assigned to C(3), C(4) and C(2) respectively. The HQSC shows that no hydrogen is attached to the peak at δ = 137.7 ppm and these are assigned to the ipso carbon C(1).

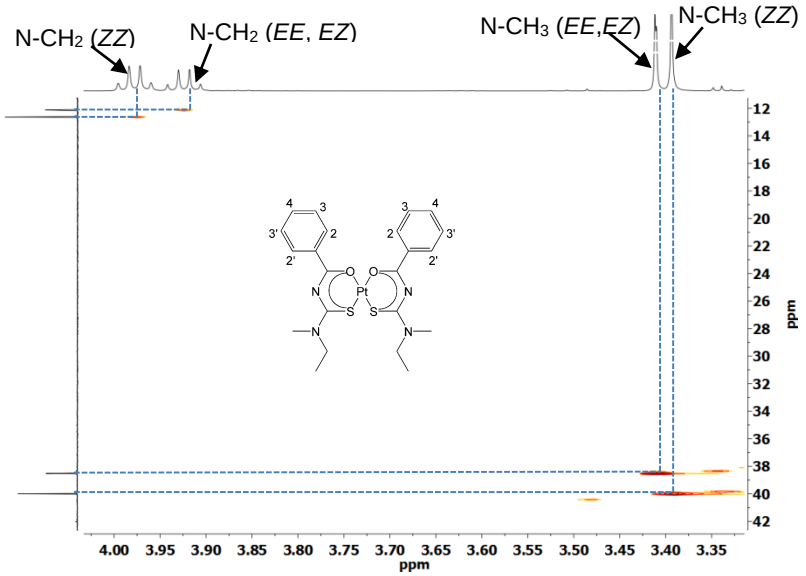

Figure 5.6. Expanded region of the HSQC correlation spectrum of *cis*-[Pt(L^8-κ*S*,*O*)$_2$] in chloroform-*d* at 25 °C.

Further confirmation of the assignment of the *cis*-*ZZ*, *EZ* and *EE* carbons of the *cis*-[Pt(L^8-κ*S*,*O*)$_2$] complex was based on their ^{1}H, ^{13}C HMBC correlation (Figure 5.7). The HMBC spectrum shows the following long range two-bond correlation between C(7) (*cis*-*ZZ*, δ = 12.7 ppm), C(7) (*cis*-*EE/EZ*, δ = 12.0 ppm), and N(CH_3) (*cis*-*ZZ*, δ = 3.94 ppm), N(CH_3) (*cis*-*EE*, *EZ*, δ = 3.83 ppm) protons through the nitrogen atom. A $^3J_{C-H}$ bond correlation through the nitrogen atom is observed between these N(CH_3) resonances and C(5) (*cis*-*ZZ*, δ = 39.9 ppm), C(5) (*cis*-*EZ/EE*, δ = 38.5 ppm) respectively. Also, C(6) (*cis*-*EZ/EE*, δ = 49.2 ppm), C(6) (*cis*-*ZZ*, δ = 48.4 ppm) experience respectively $^2J_{C-H}$ bond correlations with the N(CH_2) (*cis*-*EZ/EE*), N(CH_2) (*cis*-*ZZ*) protons, as well as a $^3J_{C-H}$ bond correlation with the CH_3 (*cis*-*EZ/EE*, δ = 1.32 ppm), CH_3 (*cis*-*ZZ*, δ = 1.27 ppm) protons.

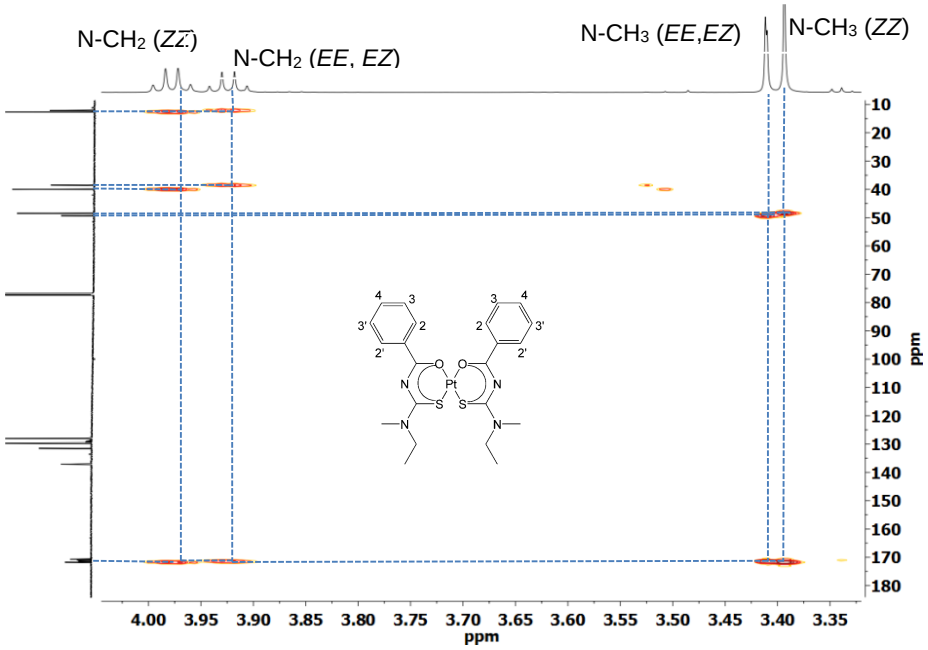

Figure 5.7. $^{1}H/^{13}C$ HMBC correlation spectrum of *cis*-[Pt(L^{8}-κ*S*,*O*)$_2$] in chloroform-*d* at 25°C.

The HMBC correlation was particularly useful for assigning the carbonyl and thiocarbonyl carbons as shown in Figure 5.8. The carbon signals at δ = 167.8 ppm and 167.5 ppm are assigned to C(O) based on a $^{3}J_{C\text{-}H}$ correlation with the phenyl *ortho* protons $H^{2'}$ at δ = 8.27 ppm. The other set of peaks at δ = 168.5 ppm and 168.8 ppm are assigned to C(S) as these correlate to both the N(CH_2) and N(CH_3) protons by a $^{3}J_{C\text{-}H}$ coupling through the nitrogen atom.

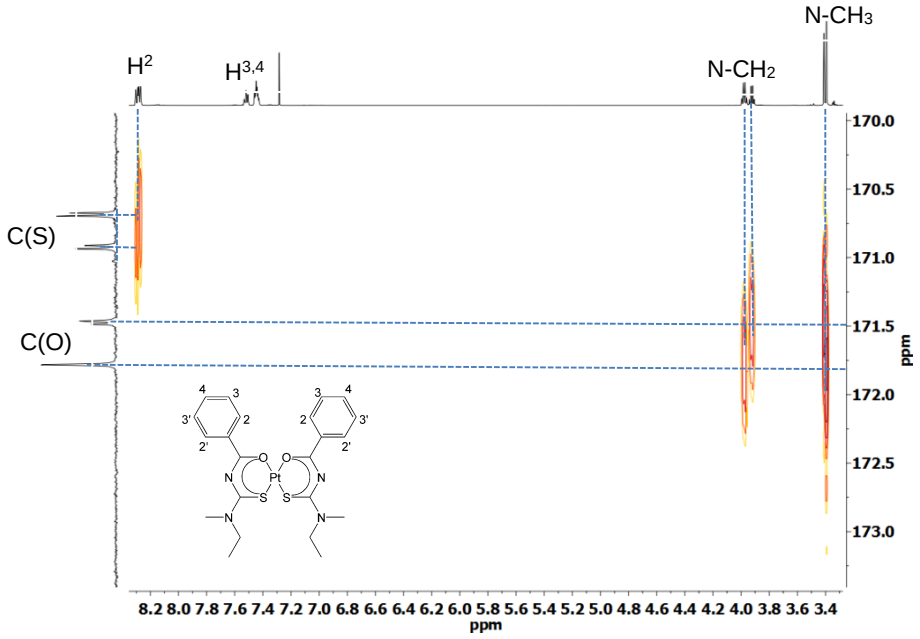

Figure 5.8. $^{1}H/^{13}C$ HMBC correlation spectrum of *cis*-[Pt(L^{8}-κ*S*,*O*)$_2$] in chloroform-*d* at 25 °C; correlation of only C(O) and C(S) shown.

Unambiguous confirmation of the stereochemistry of the *cis*-[M(L^8-κ*S*,*O*)$_2$] (M = Pt(II) or Pd(II)) complexes was achieved on the basis of 1D NOESY assignment. This was aided by correlation with the previously assigned ^{1}H NMR spectrum as shown in Figures 5.9 and 5.10. The *cis*-[Pt(*ZZ*-L^8-κ*S*,*O*)$_2$] conformation was assigned by selective irradiation of the N(CH_3) protons at δ = 3.29 ppm. This leads to a considerable enhancement of the CH_3 (δ = 1.30 ppm), N(CH_2) (δ = 3.94, 3.84 ppm), as well as the phenyl ortho proton $H^{2'}$ at δ = 8.27 ppm. This is consistent with the expected close proximity of the N(CH_3) protons to CH_3, N(CH_2) and $H^{2,2'}$ when in the *cis-ZZ* conformation, resulting in potential dipolar interactions and hence NOE enhancements. This assignment is supported by selectively irradiating the CH_3 protons in the *cis-ZZ* conformation. This produces marked NOE of the nearby N(CH_3) and N(CH_2) resonances, with a lesser enhancement of the phenyl $H^{2,2'}$ protons which have a greater interproton distance in space. The observation of the NOE between this set of protons suggest a short interproton distance between them thereby confirming the *cis-ZZ* configuration.

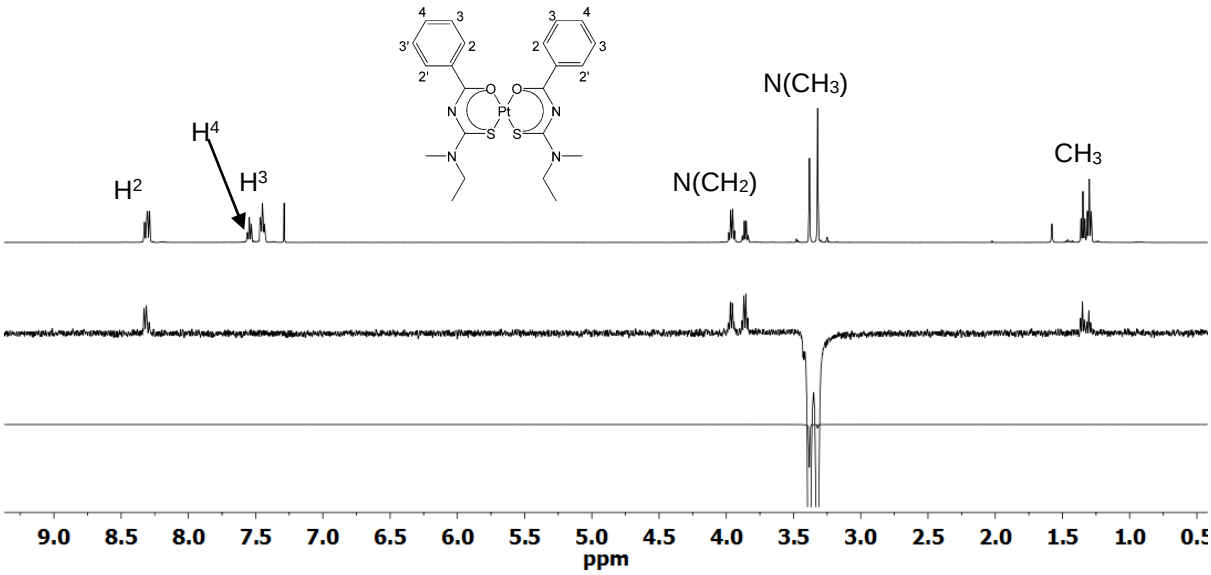

Figure 5.9. 1D NOESY spectrum showing assignment of *cis*-[Pt(*ZZ*-L^8-κ*S*,*O*)$_2$] in chloroform-*d* at 25 °C from irradiation of N(CH_3) protons; ^{1}H NMR spectrum is overlaid to assist assignment.

Although a considerable enhancement was observed for the N(CH_2) and CH_3 peaks upon selective irradiation of the N(CH_3) proton in the *cis-EE/EZ* configuration, no NOE was observed for the ortho $H^{2,2'}$ protons of the phenyl ring. This suggests that the $H^{2,2'}$ protons are too far apart to experience any NOE (Figures A5.1 and A5.2). This can only be accounted for if the N(CH_2) protons are in the *E* configuration. NOE assignment of the *E*, *Z* peaks of the N(CH_2) protons follow the same pattern as that of the N(CH_3) protons. The *E*, *Z* resonances of

the other *cis*-[Pt($L^{9\text{-}15}$-κ*S*,*O*)$_2$] and *cis*-[Pd($L^{9\text{-}15}$-κ*S*,*O*)$_2$] complexes were assigned by analogy to the *cis*-[Pt(L^{8}-κ*S*,*O*)$_2$] complex.

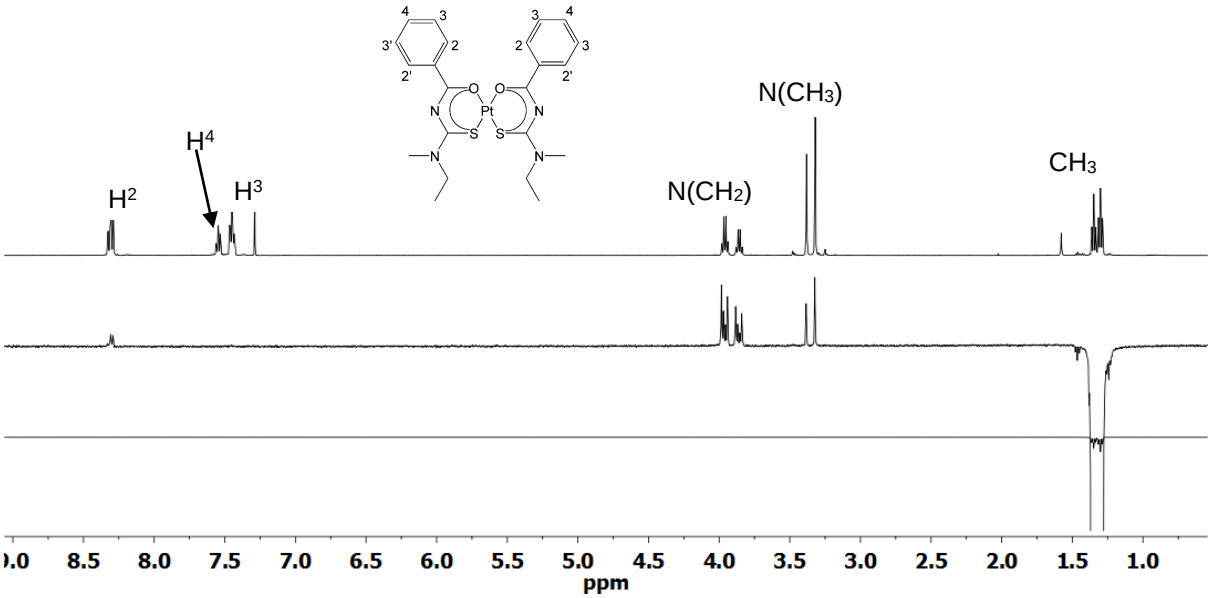

Figure 5.10. 1D NOESY spectrum showing assignment of *cis*-[Pt(*ZZ*-L^{8}-κ*S*,*O*)$_2$] in chloroform-*d* at 25 °C from irradiation of (CH_3) protons; ^{1}H NMR spectrum is overlaid to assist assignment.

5.2.2.2. ^{1}Pt{^{1}H} NMR characterization of configurational *E, Z* isomers

In all the *cis*-[M($L^{8\text{-}15}$-κ*S*,*O*)$_2$] (M = Pt(II) or Pd(II)) complexes studied, the *EZ* and *EE* resonances could not be resolved completely due to overlap of their ^{1}H NMR spectra. Fortunately, all the *cis*-[Pt($L^{8\text{-}15}$-κ*S*,*O*)$_2$] complexes show directly detected and well-resolved ^{195}Pt resonances. These ^{195}Pt{^{1}H} resonances have previously been assigned as the *cis*-[Pt(*ZZ*-L-κ*S*,*O*)$_2$], *cis*-[Pt(*EZ*-L-κ*S*,*O*)$_2$] and *cis*-[Pt(*EE*-L-κ*S*,*O*)$_2$] isomers respectively by Koch and co-workers using ^{1}H detected ^{1}H-(^{195}Pt)-^{13}C correlation spectroscopy.[69] All the ^{195}Pt{^{1}H} resonances observed for the *cis*-[Pt($L^{8\text{-}15}$-κ*S*,*O*)$_2$] complexes were thus assigned with the assumption that the configurational *cis*-[Pt(*ZZ*-L^{n}-κ*S*,*O*)$_2$], *cis*-[Pt(*EZ*-L^{n}-κ*S*,*O*)$_2$] and *cis*-[Pt(*EE*-L^{n}-κ*S*,*O*)$_2$] isomers follow the same chemical shift trends. Hence the most downfield resonance is assigned to the *cis-ZZ* isomer, while the most upfield resonance is assigned to the *cis-EE* isomer. Figure 5.11 shows the ^{195}Pt{^{1}H} spectrum of the *cis*-[Pt(L^{8}-κ*S*,*O*)$_2$] complex. It can be clearly observed that the complex exists in a chloroform-*d* solution as *cis*-[Pt(*ZZ*-L^{8}-κ*S*,*O*)$_2$], *cis*-[Pt(*EZ*-L^{8}-κ*S*,*O*)$_2$] and *cis*-[Pt(*EE*-L^{8}-κ*S*,*O*)$_2$] isomers with well-resolved ^{195}Pt{^{1}H} resonances at δ = -2709, -2713 and -2716 ppm respectively. The ^{195}Pt chemical shift

range of the *cis*-configurational (-2700 to -2720 ppm) isomers is consistent with that observed for *cis*-[Pt(L^n-κ*S*,*O*)$_2$] complexes with symmetrically substituted *N*,*N*-dialkyl-*N*'-acylthioureas.[51] The relative distribution of the configurational isomers of *cis*-[Pt(L^8-κ*S*,*O*)$_2$] (33 % *ZZ* : 47 % *EZ* : 20 % *EE*) were obtained by deconvolution of the ^{195}Pt{^{1}H} spectrum as shown in Figure 5.11.

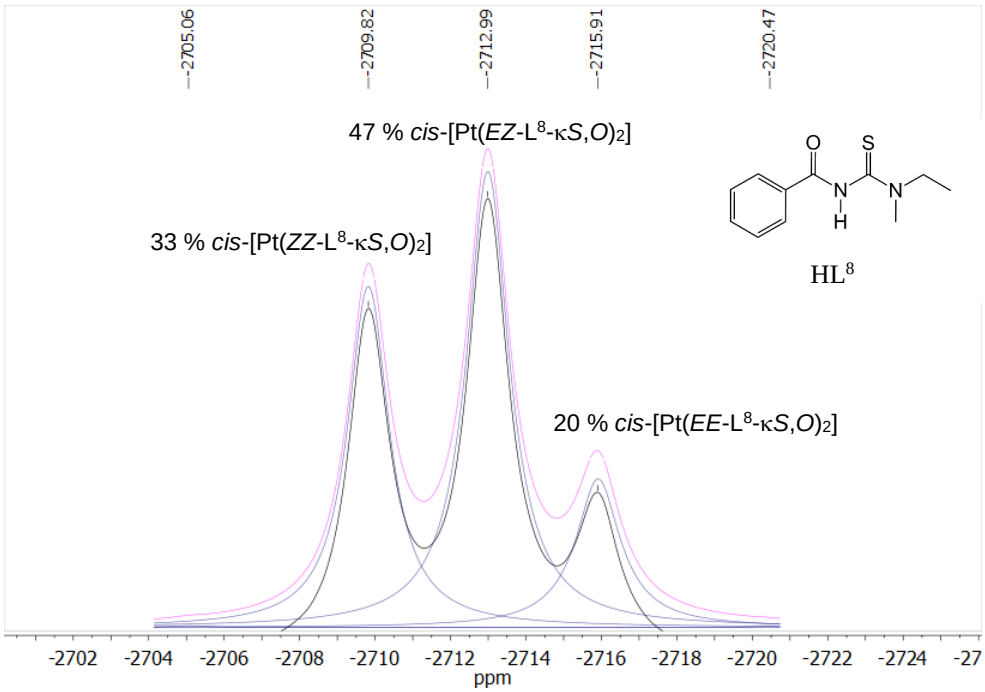

Figure 5.11. ^{195}Pt{^{1}H} NMR spectrum showing chemical shifts and relative distribution (obtained by ^{195}Pt NMR deconvolution analysis and estimated to have an error of ±1) of ZZ, *EZ* and *EE* isomers of *cis*-[Pt(L^8-κ*S*,*O*)$_2$] in chloroform-*d* at 25 °C.

The ^{195}Pt{^{1}H} NMR spectrum of the *cis*-[Pt(L^8-κ*S*,*O*)$_2$] complex was also obatined in acetone-d_6 as depicted in Figure 5.12, in order to determine the effect of another solvent on the chemical shifts and relative distribution of configurational isomers. Only acetone-d_6 was used for this ^{195}Pt{^{1}H} study since the *cis*-[Pt(L^8-κ*S*,*O*)$_2$] complex was insoluble in other organic solvents which were available. It can be observed from Figure 5.12 that the distribution of configurational isomers in acetone-d_6 remained almost invariant (32 % *cis*-[Pt(*ZZ*-L^8-κ*S*,*O*)$_2$], 52 % *cis*-[Pt(*ZE*-L^8-κ*S*,*O*)$_2$] and 16 % *cis*-[Pt(*EE*-L^8-κ*S*,*O*)$_2$]) compared to their relative distribution in chloroform-*d* (33 % *ZZ*, 47 % *EZ*, 20 % *EE*). This suggests that the use of acetone does not significantly influence the C-N rotational barrier and distribution of isomers in solution relative to chloroform. However, a slight downfield shift of *ca* 12 ppm is observed for all the *cis*-[Pt(*ZZ*-L^8-κ*S*,*O*)$_2$], *cis*-[Pt(*ZE*-L^8-κ*S*,*O*)$_2$] and *cis*-[Pt(*EE*-L^8-κ*S*,*O*)$_2$] ^{195}Pt{^{1}H} resonances in acetone-d_6 compared to chloroform-*d*. This can be ascribed to slight differences

in solvation effects experienced by Pt(II) in acetone and chloroform which influences ^{195}Pt chemical shift anisotropy. A comparison of the relative distribution of isomers in acetone-d_6 and chloroform-*d* does not fully represent a solvent effect study on the barrier of C-N restricted rotation and distribution of isomers. The solvent effect on the distribution of *E, Z* isomers will require further studies which are beyond the scope of the present study.

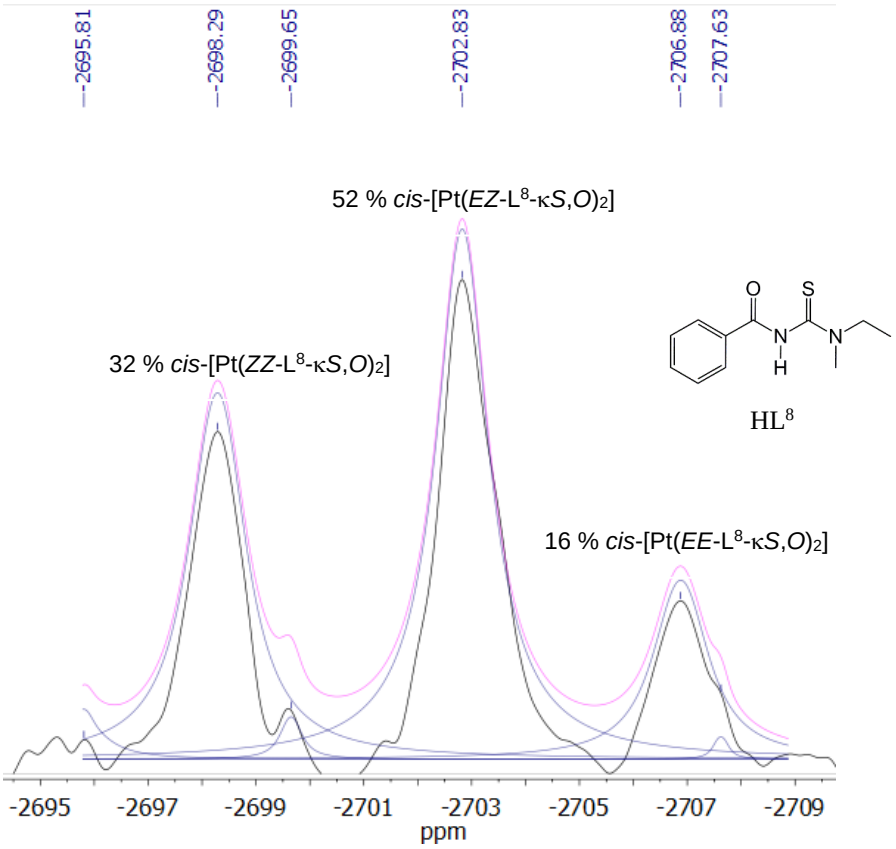

Figure 5.12. ^{195}Pt{^{1}H} NMR spectrum showing chemical shifts and relative distribution (obtained by ^{195}Pt NMR deconvolution analysis and estimated to have an error of ±1) of *E,Z* isomers of *cis*-[Pt(L^8-κ*S,O*)$_2$] in acetone-d$_6$ at 25 °C.

The temperature dependence of the chemical shift positions and distribution of the *E, Z* isomers was also studied for the *cis*-[Pt(L^8-κ*S,O*)$_2$] complex by increasing the temperature of the chloroform-*d* solution in the range 25-45 °C. Temperatures above 50 °C were avoided to prevent boiling of chloroform. Figure 5.13 (a) depicts the effect of temperature on the ^{195}Pt{^{1}H} resonances. It is evident that no significant changes in the relative distribution of the *cis*-[Pt(*ZZ*-L^8-κ*S,O*)$_2$], *cis*-[Pt(*EZ*-L^8-κ*S,O*)$_2$] and *cis*-[Pt(*EE*-L^8-κ*S,O*)$_2$] isomers occur over the range 25-45 °C. Previous reports indicate that at temperatures lower than 25 °C, the *cis-ZZ* isomers are more favoured over the *cis-EE* and *cis-EZ* isomers in chloroform-*d*.[115] A temperature dependence study at lower temperatures (< 25 °C) is beyond the scope of this study.

A linear downfield shift of the three ^{195}Pt resonances is observed with an increase in temperature as shown in Figure 5.13 (b) and with a slope of 0.4 ppm/K obtained. This indicates a linear ^{195}Pt chemical shift dependence upon increasing temperature and demonstrates the sensitivity of ^{195}Pt environment towards subtle changes in temperature.

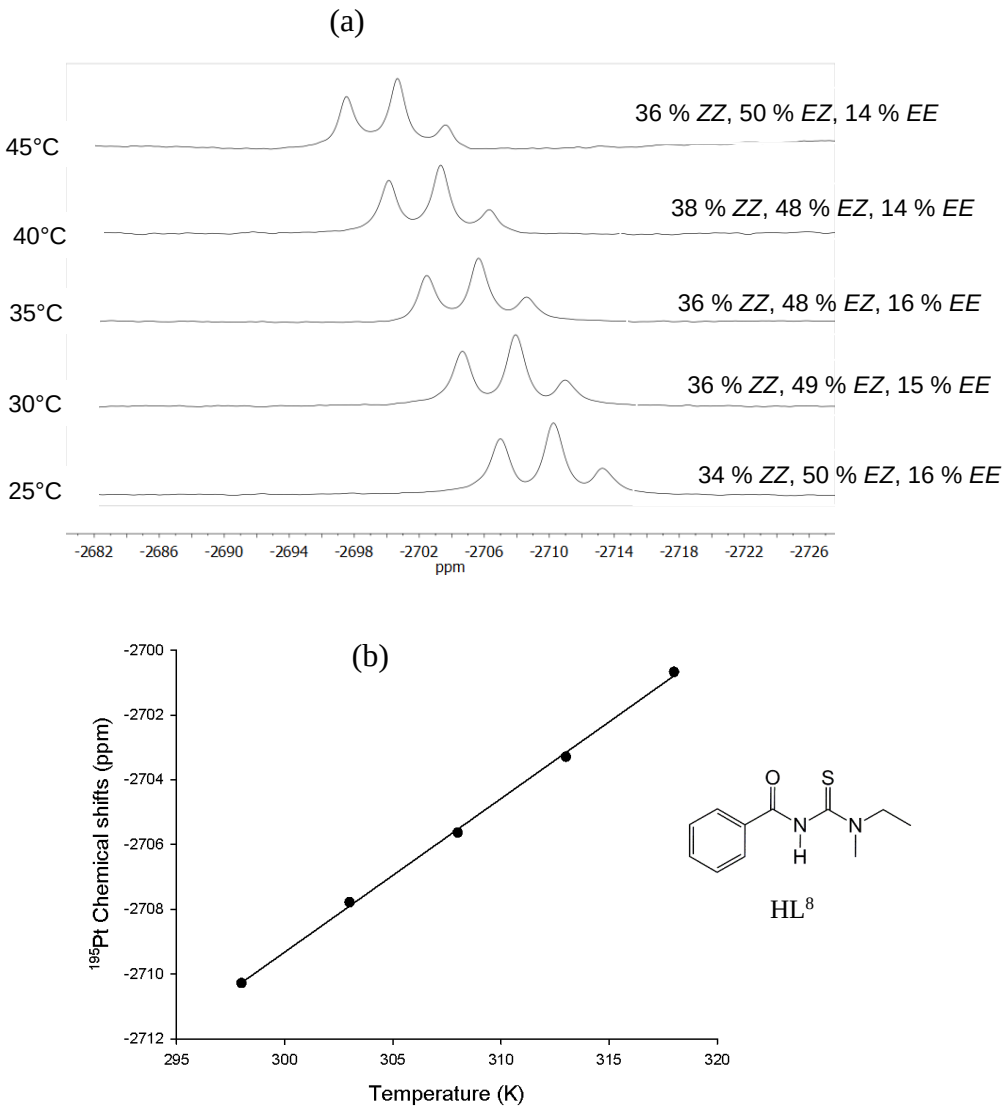

Figure 5.13. Effect of temperature on chemical shift dependence of *cis*-[Pt(L^{8}-κ*S*,*O*)$_2$] in chloroform-*d* at 25 °C.

The effect of ligand structure on the relative distribution of configurational isomers was also investigated in chloroform-*d* for the *cis*-[Pt(L$^{8\text{-}15}$-κ*S*,*O*)$_2$] complexes. The distributions of *E, Z* isomers obtained from the ^{195}Pt{^{1}H} spectra of the complexes are depicted in Table 5.3. The *cis*-[Pt(L^{8}-κ*S*,*O*)$_2$] complex in which the *cis*-*EZ* (47 %) configuration is more favoured relative to the *cis*-*ZZ* (33 %) and *cis*-*EE* (20 %) isomers, can be used as a suitable starting point

to investigate substituent effects on the isomeric distribution. An increase in the alkyl chain length from ethyl to propyl at the thioamido nitrogen in the *cis*-[Pt(L^9-κ*S*,*O*)$_2$] complex increases the distribution of the *cis-ZZ* isomer (42 %), with a corresponding decrease in the *cis-EE* isomer (13 %). A similar effect is also produced by using a pivaloyl group at the carbonyl end in the *cis*-[Pt(L^{11}-κ*S*,*O*)$_2$] complex leading to a relative distribution of 42 % *cis-ZZ*, 46 % *cis-EZ*, and 12 % *cis-EE*. These results indicate that introduction of larger *N*-alkyl substituents either at the thioamido or the carbonyl end leads to lowering the of C-N rotational barrier. This is confirmed by replacing the *N*-propyl group with a bulkier *N*-phenylethylene substituent for the *cis*-[Pt(L^{12}-κ*S*,*O*)$_2$] complex which shows a relative distribution of 57 % *cis-ZZ*, 40 % *cis-EZ* and 3 % *cis-EE*. By introducing a long *n*-pentyl chain as well as a phenyl ring at the thioamido nitrogen, a further increase in the distribution of the *cis-ZZ* isomer (64 %) is obtained in the *cis*-[Pt(L^{13}-κ*S*,*O*)$_2$] complex at the expense of a decrease in the *cis-EZ* (32 %) and *cis-EE* (4 %) isomers. In addition to steric effects, the increase in the C-N rotational barrier in the *cis*-[Pt(L^{13}-κ*S*,*O*)$_2$] complex could also be attributed to competition of the lone pair of electrons between the nitrogen atom and its directly attached phenyl ring. This is seen in the *cis*-[Pt(L^{14}-κ*S*,*O*)$_2$] complex in which the direct attachment of a phenyl group and an isopropyl group to the nitrogen atom produces a 53 % *cis-ZZ*: 43 % *cis-EZ*: 4 % *cis-EE* distribution of isomers. The C-N rotational barrier also decreases presumably due to *para* substitution of an electron-donating methoxy group on a phenyl ring in the *cis*-[Pt(L^{15}-κ*S*,*O*)$_2$] complex. This enhances the distribution of the *cis-ZZ* isomer (69 %) relative to its *cis-EZ* (29 %) and *cis-EE* (2 %) counterparts. The *cis*-[Pt(L^{10}-κ*S*,*O*)$_2$] complex shows only a single ^{195}Pt{^{1}H} resonance which could not be deconvoluted hence the relative distribution of isomers could not be obtained.

From Table 5.3, it is evident that the presence of different ligand substituents at the *N*-alkyl moiety also results in significant ^{195}Pt{^{1}H} chemical shift differences of the configurational isomers. The results indicate that substitution of either the *N*-isopropyl, *N*-phenyl or *N*-pentyl group in the respective *cis*-[Pt($L^{13,14,15}$-κ*S*,*O*)$_2$] complexes produces a notable downfield shift of the ^{195}Pt{^{1}H} resonances by *ca* ± 50 ppm compared to the other *cis*-[Pt($L^{8\text{-}12}$-κ*S*,*O*)$_2$] complexes. This suggests that the presence of either a relatively longer *n*-pentyl group or the *N*-phenyl groups could presumably affect the delocalization of electrons and electron density around the Pt atom. This could have led to increased shielding of the *cis*-[Pt($L^{13,14,15}$-κ*S*,*O*)$_2$] resonances.

Table 5.3. $^{195}Pt\{^{1}H\}$ chemical shifts and relative distributions (obtained by ^{195}Pt NMR deconvolution analysis and estimated to have an error of ±1 %) for non-irradiated $CDCl_3$ solutions of mixtures of *ZZ*, *EZ* and *EE* isomers of *cis*-[Pt($L^{8\text{-}15}$-κ*S*,*O*)$_2$] complexes at 25 °C; The chemical shifts and relative distributions of isomers of *cis*-[Pt(L^{10}-κ*S*,*O*)$_2$] could not be measured since the peaks were not well-resolved at 25 °C.

Structure of Ligand in *cis*-[Pt(L-κ*S*,*O*)$_2$] complex	$^{195}Pt\{^{1}H\}$ NMR Spectrum	$^{195}Pt\{^{1}H\}$ chemical shifts/ppm			Relative ^{195}Pt peak intensities		
		ZZ	***EZ***	***EE***	***ZZ***	***EZ***	***EE***
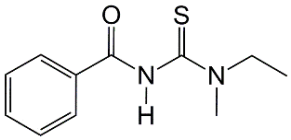 HL[8]	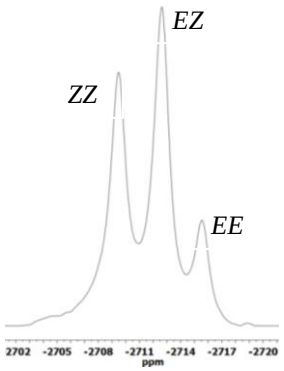	-2710	-2713	-2716	33%	47%	20%
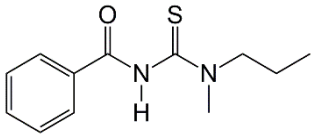 HL[9]	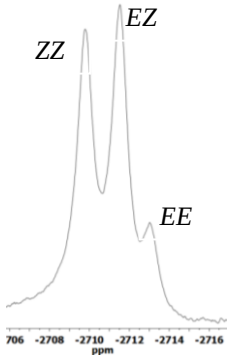	-2710	-2712	-2713	42%	45%	13%

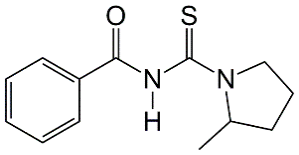 HL[10]	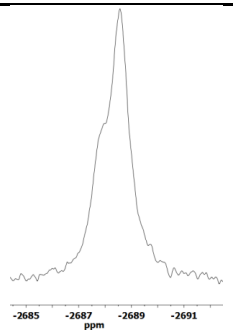	-	-	-	-	-	-
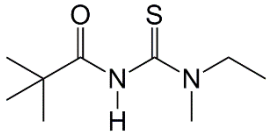 HL[11]	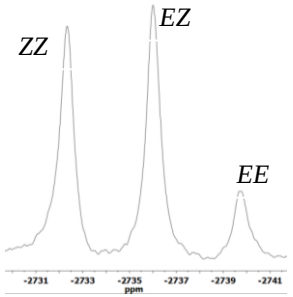	-2732	-2736	-2739	41%	46%	13%
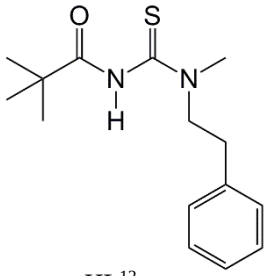 HL[12]	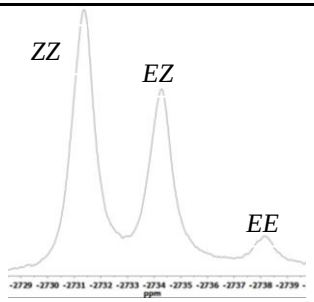	-2731	-2734	-2738	57%	40%	3%

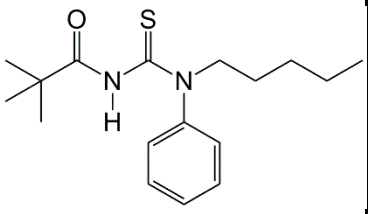 HL[13]	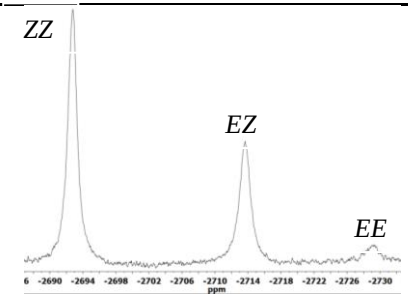	-2692	-2713	-2729	64%	32%	4%
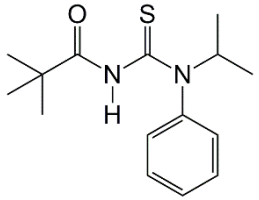 HL[14]	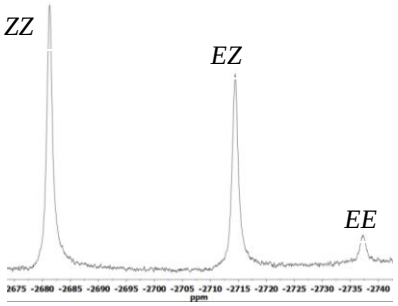	-2681	-2714	-2737	53%	43%	4%
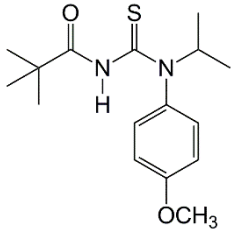 HL[15]	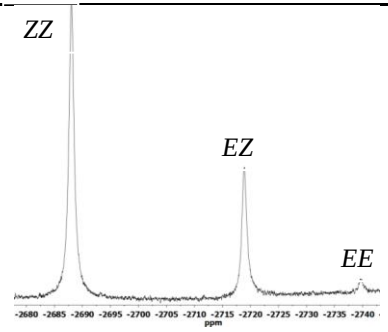	-2688	-2718	-2739	69%	29%	2%

5.2.3. Single-crystal X- structures of *E, Z* isomers of *cis*-[M(L^n-κ*S,O*)$_2$] (M = Pt(II) or Pd(II)) complexes

The *cis*-[Pd(L^8-κ*S,O*)$_2$] (HL^8 = *N*-methyl,*N*-ethyl,-*N*'-benzoylthiourea) and *cis*-[Pt(L^8-κ*S,O*)$_2$] complexes were crystallized in acetonitrile or dichloromethane by slow evaporation in a sealed vial and in the absence of light. Both complexes crystallized as a *cis*-[Pt(L^8-*EE*-*S,O*)$_2$] isomer in both acetonitrile and dichloromethane. The fact that the *cis*-[Pt(L^8-*EE*-*S,O*)$_2$] isomer was isolated in preference to the *cis*-[Pt(L^8-*ZZ*-*S,O*)$_2$] and *cis*-[Pt(L^8-*EZ*-*S,O*)$_2$] isomers suggests that the *cis*-[Pt(L^8-*EE*-*S,O*)$_2$] complex has a relatively lower solubility in both solvents.

The *cis*-[Pt(*EE* -L^8-κ*S,O*)$_2$] structure is shown in Figure 5.14. The compound has a monoclinic space group $P2_1/c$ and confirms a *cis*-κ*S,O* coordination. The structure adopts a *cis*-*EE* conformation in which the *N*-ethyl groups point away from the sulfur atom in the chelate. The average Pd-S (2.2339(1)Å), and Pd-O (2.025(3)Å), N(3)-C(4) 1.344(6)Å bond distances are consistent with the Pd-S and Pd-O bond distances of related Pt(II) complexes.[56] The *cis*-[Pt(*EE*-L^8-κ*S,O*)$_2$] structure deviates slightly from ideal square planarity as represented by S(4)-Pt(1)-O(1) 176.4(1)°, S(5)-Pt(1)-O(2) 176.7(1)° bond angles. This slight deviation could be ascribed to steric hindrance between the *N*-methyl group and the ortho phenyl hydrogen at the *cis*-*EE* configuration. The H27-H1B bond distance of 2.578 Å represents interactions between and the *N*-ethyl and the phenyl proton at the *ortho* position in the *cis*-*EE* conformation. This relatively small H-H interproton distance is in full agreement with the observed NOEs between these protons obtained from the 1D NOESY (Figure 5.9 and 5.10) results and are well below the 4 Å distance required for analysis of such transient NOE intensities.

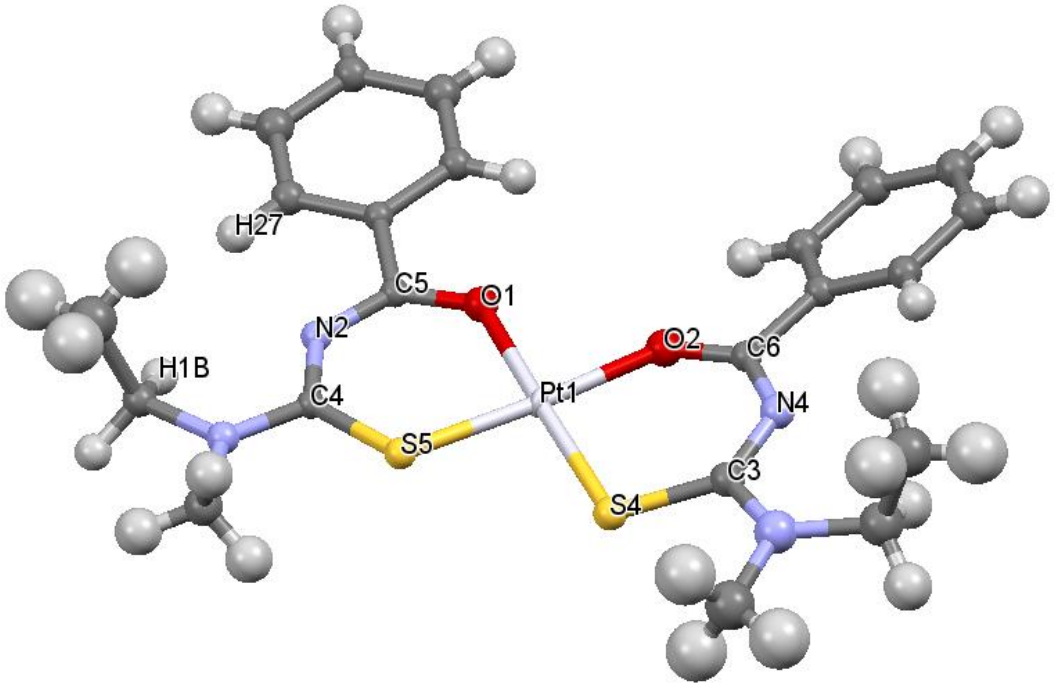

Figure 5.14. Molecular structure from single-crystal X-ray difraction of a *cis*-*EE* isomer of *cis*-bis(*N*-methyl, *N*-ethyl, *N*'-benzoylthioureato-κ^2*S*,*O*)platinum(II), *cis*-[Pt(L^8-κ*S*,*O*)$_2$] isolated from an acetonitrile solution by slow evaporation.

The *cis*-[Pd(*EE*-L^8-κ*S*,*O*)$_2$] structure is given in Figure 5.15 and crystallizes in the monoclinic space group $P2_1/c$. The compound also shows a *cis*-κ*S*,*O* coordination of sulfur and oxygen donor atoms to Pd(II). The average Pd-S and Pd-O bond lengths (2.235(1)Å and 2.025(3)Å respectively), are very similar to that of *cis*-bis(*N*,*N*-diethyl-*N'*-benzoylthioureato-κ^2*S*,*O*)palladium(II) *cis*-[Pd(L^1-κ*S*,*O*)$_2$] [Pd-S 2.231(4)Å, Pd-O 2.022(1)Å].[17] The Pd-S and Pd-O bond lengths are similar to Pt-S 2.233(1)Å and Pt-O 2.025(3)Å) in the analogous *cis*-[Pt(*EE*-L^8-κ*S*,*O*)$_2$] complex (Figure 5.14). This suggests that a change in the metal centre has no significant effect on electron delocalization across the chelate ring. The *cis*-[Pd(*EE*-L^8-κ*S*,*O*)$_2$] structure is slightly distorted from square planarity as represented by the S(2)-Pd(1)-O(5) 176.5(8)Å and S(3)-Pd(1)-O(4) 176.9(8)Å bond angles.

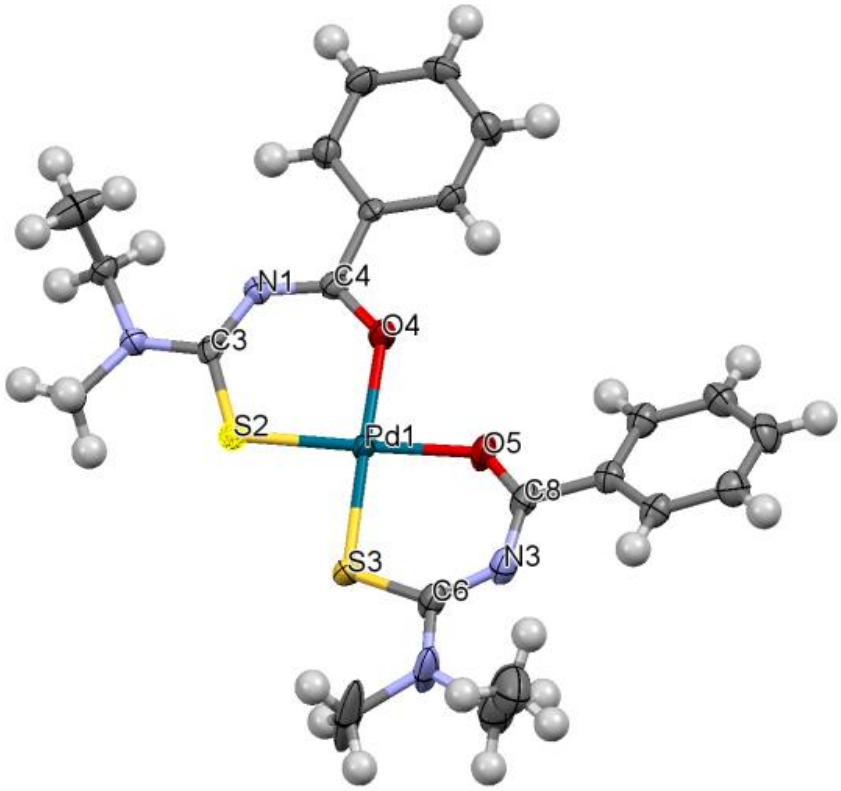

Figure 5.15. Molecular structure from single-crystal X-ray difraction of a *cis*-*EE* isomer of *cis*-bis(*N*-methyl, *N*-ethyl, *N*'-benzoylthioureato-κ^2*S*,*O*)palladium(II), *cis*-[Pd(L^8-κ*S*,*O*)$_2$] isolated from an acetonitrile solution by slow evaporation.

Unlike the *cis*-[Pt(L^8-κ*S*,*O*)$_2$] and *cis*-[Pd(L^8-κ*S*,*O*)$_2$] complexes, slow evaporation of a solution of the *cis*-[Pt(L^{15}-κ*S*,*O*)$_2$] complex in acetonitrile leads to the isolation of a *cis*-[Pt(L^{15}-*ZZ*-κ*S*,*O*)$_2$] (HL^{15} = *N*-isopropyl,*N*-4-methyoxy-phenyl, *N*'-(2,2-dimethyl-propanoyl)thiourea) isomer. The molecular structure of the *cis*-[Pt(L^{15}-*ZZ*-κ*S*,*O*)$_2$] isomer is depicted in Figure 5.16. The structure crystallizes in the triclinic P-1 space group and shows a *cis*-κ*S*,*O* configuration. This represents the first example of a molecular structure of a *cis*-[Pt(*ZZ*-L-κ*S*,*O*)$_2$] complex with the *N*,*N*-disubstituted-acylthioureas. The isolation of the *cis*-[Pt(*ZZ*-L^{15}-κ*S*,*O*)$_2$] isomer is in agreement with the increased *cis*-*ZZ* distribution of ^{195}Pt{^{1}H} resonances observed for the *cis*-[Pt(L^{15}-κ*S*,*O*)$_2$] complex (69 % *ZZ*, 29 % *EZ*, 2 % *EE*). The Pt-S 2.234(3)Å and Pt-O 2.031(8)Å bond distances in the *cis*-[Pt(*ZZ*-L^{15}-κ*S*,*O*)$_2$] complex are similar to those in the *cis*-[Pt(*EE*-L^8-κ*S*,*O*)$_2$] complex (Pt-S 2.234(1)Å and Pt-O 2.025(3)Å). This signifies that the presence of the *N*-phenyl and *N*-isopropyl groups has no significant effect on the delocalization of electrons across the six membered Pt-S-C-N-C-O ring. The C-N 1.35(2)Å bond in the *cis*-

[Pt(*ZZ*-L^{15}-κ*S*,*O*)$_2$] isomer is slightly longer than that of the *cis*-[Pt(*EE*-L^{8}-κ*S*,*O*)$_2$] complex. The steric effect of the *N*-isopropyl and *N*-4-methoxy-phenyl substituents is reflected in a slight decrease in the C(23)-N(8)-C(5) 114(1)° bond angle with a corresponding slight increase in C(23)-N(8)-C(9) 126(1)° compared to the respective bond angles in the *cis*-[Pt(*EE*-L^{8}-κ*S*,*O*)$_2$] C(3)-N(5)-C(9) 121.0(9)° and C(3)-N(5)-C(10) 122.9(5)°.

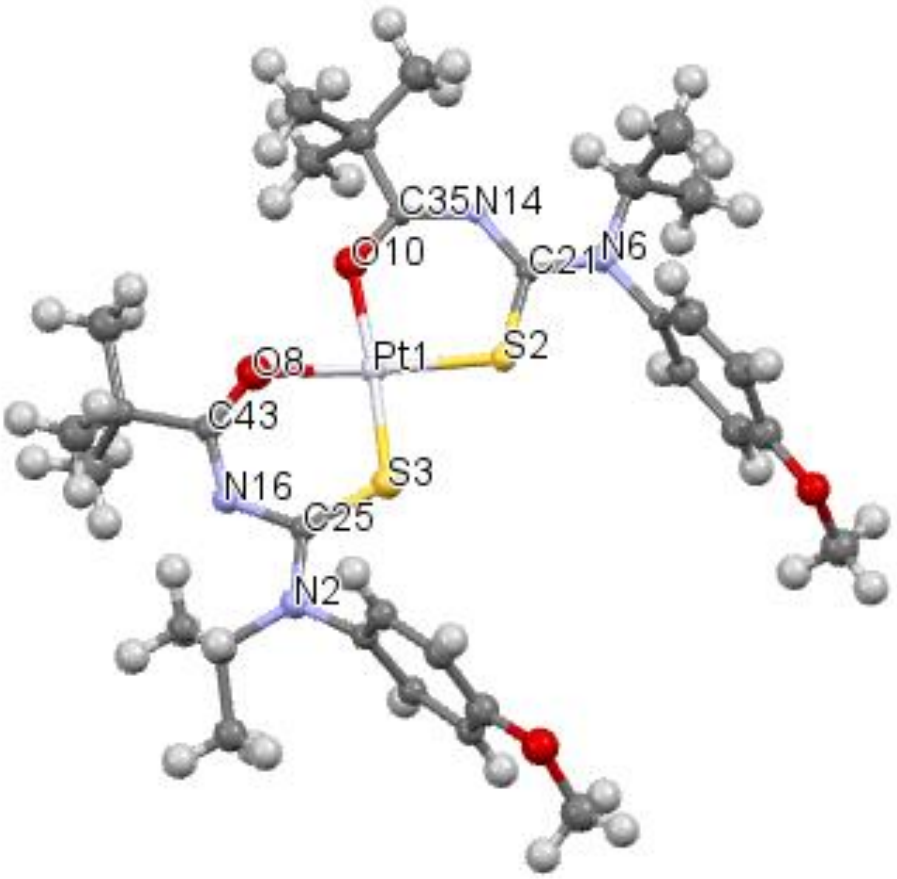

Figure 5.16. Molecular structure from single-crystal X-ray difraction of a *cis-ZZ* isomer of bis(*N*-isopropyl-*N*-4-methyoxy-phenyl, *N*'-(2,2-dimethylpropanoyl)thioureato-κ^2*S*,*O*)platinum(II), *cis*-[Pt(L^{15}-κ*S*,*O*)$_2$] isolated from an acetonitrile solution by slow evaporation.

5.2.4. Photo-induced isomerization of *cis*-[M(L^n-κ*S*,*O*)$_2$] (M = Pt(II), Pd(II)) complexes of asymmetrically substituted *N*,*N*-dialkyl-*N*'-acylthioureas

Irradiation of the *cis*-[M(L$^{8\text{-}15}$-κ*S*,*O*)$_2$] complexes generates *trans* isomers in acetonitrile and chloroform solutions. The *cis*→*trans* isomerism was monitored by RP-HPLC, ^{1}H and ^{195}Pt{^{1}H} NMR spectroscopy. Injection of acetonitrile solutions of all complexes in the absence of light produced only a single RP-HPLC peak, using both a C_{18} column and a mixed mode HILIC column under isocratic as well as gradient elution conditions. Irradiation of a solution of the *cis*-[Pd(L^8-κ*S*,*O*)$_2$] complex (retention time of 13.6 minutes) results in the formation of an additional peak assigned to the *trans*-[Pd(L^8-κ*S*,*O*)$_2$] isomer (retention time of 15.2 minutes) as depicted in Figure 5.17. The *trans*-[Pd(L^8-κ*S*,*O*)$_2$] isomer is more strongly retained on the C_{18} column than the *cis*-[Pd(L^8-κ*S*,*O*)$_2$] isomer. This is consistent with the differences in retention times observed for the geometric isomers of the *cis*-[Pd(L$^{1\text{-}6}$-κ*S*,*O*)$_2$] complexes studied in chapter 3 (section 3.2.1, Figure 3.4, page 58).

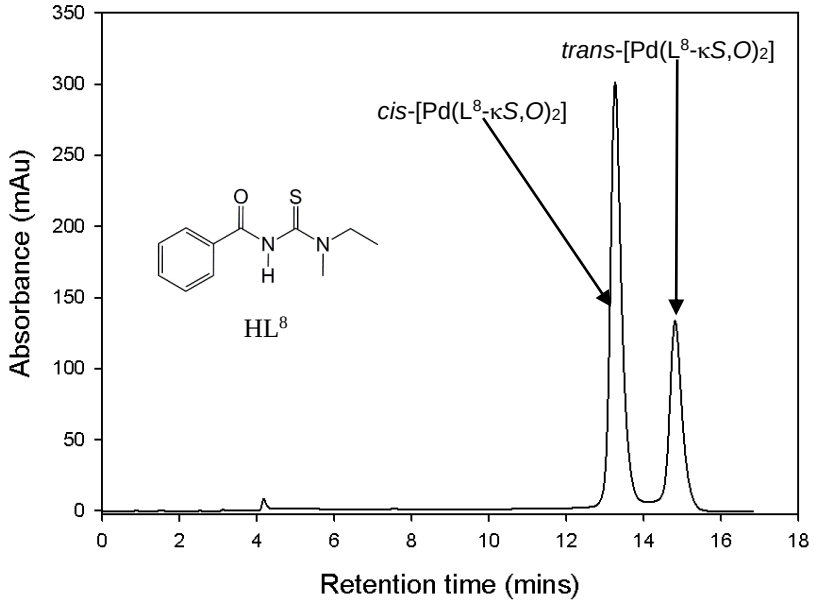

Figure 5.17. Chromatogram showing RP-HPLC separation of an acetonitrile solution of *cis*-[Pd(L^8-κ*S*,*O*)$_2$] after irradiation with polychromatic light from a 5 Watt LED lamp for 10 mins; conditions: mobile phase, acetonitrile:water (90:10 %v/v); GEMINI C_{18}, 5 µm, 250 x 4.6 mm column; 20 µl injection volume; 1 mlmin^{-1} flow rate; 262 nm detection.

Figure 5.18 (b) shows the ^{1}H NMR spectra of a chloroform-*d* solution of the *cis*-[Pt(L^{8}-κ*S*,*O*)$_2$] complex after 30 minutes irradiation with polychromatic light from a 5 Watt LED lamp. The partial ^{1}H NMR spectrum of the unirradiated *cis*-[Pt(L^{8}-κ*S*,*O*)$_2$] solution is provided in Figure 5.18 (a). The formation of an additional *trans*-$H^{2,2}$ resonance at δ = 8.07 ppm indicates *cis*→*trans* isomerization. The difference in chemical shift between the *cis*-*trans* isomers of the protons $H^{2,2'}$ is *ca* 0.21 ppm, consistent with that observed for symmetrically substituted *cis*-[M($L^{1\text{-}6}$-κ*S*,*O*)$_2$] (M=Pt(II), Pd(II)) complexes studied in chapter 3 (section 3.2.1, Figure 3.2, page 55). Two additional singlets are observed at δ = 3.39 ppm and δ = 3.23 ppm. These are assigned to *trans* resonances of N(CH_3) protons. Although unambiguous assignment of the two *trans*-N(CH_3) resonances could not be achieved, it is more likely that the new singlet at δ = 3.39 ppm is due to the *trans*-[Pt(*ZZ*-L^{8}-κ*S*,*O*)$_2$] isomer, while the singlet at δ = 3.23 ppm is due to the N(CH_3) protons of the *trans*-[Pt(*EZ*,*EE*-L^{8}-κ*S*,*O*)$_2$] isomers. This tentative assignment is based on the chemical shift trends observed in the ^{1}H NMR spectrum of the unirradiated *cis*-[Pt(L^{8}-κ*S*,*O*)$_2$] complex (Figure 5.18 (a)).

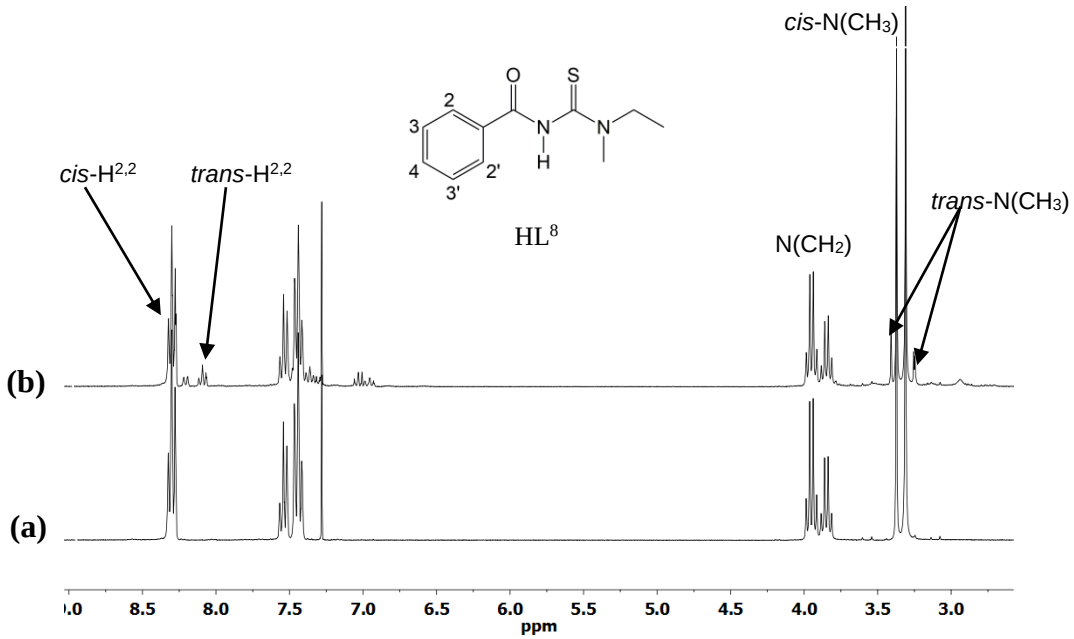

Figure 5.18. ^{1}H NMR spectra of chloroform-*d* solutions of the *cis*-[Pt(L^{8}-κ*S*,*O*)$_2$] complex (a) without irradiation and (b) after irradiation for 30 minutes with polychromatic light from a 5 Watt LED lamp.

It is obvious from Figures 5.17 and 5.18 that the *trans*-[Pt/Pd(*EZ*-L^8-κ*S*,*O*)$_2$], *trans*-[Pt/Pd(*EE*-L^8-κ*S*,*O*)$_2$] and *trans*-[Pt/Pd(*ZZ*-L^8-κ*S*,*O*)$_2$] isomers formed from irradiation of the *cis*-[Pt/Pd(L^8-κ*S*,*O*)$_2$] complexes cannot be separately identified either by ^{1}H NMR spectroscopy or RP-HPLC. With the use of ^{195}Pt{^{1}H} NMR spectroscopy, the *trans*-configurational isomers of all *cis*-[Pt($L^{8\text{-}15}$-κ*S*,*O*)$_2$] complexes were identified as three additional ^{195}Pt{^{1}H} resonances in the range δ(^{195}Pt) -1966 to -2006 ppm (Figures A5.5 to A5.10). In general, the *trans*-^{195}Pt{^{1}H} resonances are significantly shifted more downfield by an average of *ca.* 730 ppm relative to their respective *cis*-^{195}Pt{^{1}H} counterparts. This is consistent with upfield shifts of the ^{195}Pt resonances of *trans*-[Pt(L^n-κ*S*,*O*)$_2$] complexes with the symmetrically substituted *N*,*N*-dialkyl-*N*'-acylthioureas .[58]

Figure 5.19 shows the ^{195}Pt{^{1}H} spectrum of an irradiated solution of the *cis*-[Pt(L^{15}-κ*S*,*O*)$_2$] complex in chloroform-*d*. In the dark, three well-resolved ^{195}Pt{^{1}H} resonances were observed at δ -2688 ppm, -2718 ppm and -2739 ppm assigned to *cis*-[Pt(*ZZ*-L^{15}-κ*S*,*O*)$_2$], *cis*-[Pt(*EZ*-L^{15}-κ*S*,*O*)$_2$] and *cis*-[Pt(*EE*-L^{15}-κ*S*,*O*)$_2$] isomers respectively, with relative distribution of 69 % *ZZ*: 29 % *EZ*: 2 % *EE* (Table 5.3). The ^{195}Pt{^{1}H} spectrum of the irradiated solution shows three additional resonances at δ = -1972 ppm (52 *% ZZ*), -1989 ppm (45 % *EZ*), and -2006 ppm (27 % *EE*). These are tentatively assigned to the respective *trans*-[Pt(*ZZ*-L^{15}-κ*S*,*O*)$_2$], *trans*-[Pt(*EZ*-L^{15}-κ*S*,*O*)$_2$] and *trans*-[Pt(*EE*-L^{15}-κ*S*,*O*)$_2$] isomers with the assumption that the chemical shift trend follows that of their respective *cis*-[Pt(*ZZ*-L^{15}-κ*S*,*O*)$_2$], *cis*-[Pt(*EZ*-L^{15}-κ*S*,*O*)$_2$] and *cis*-[Pt(*EE*-L^{15}-κ*S*,*O*)$_2$] isomers. The ^{195}Pt{^{1}H} spectra representing irradiated solutions of the other *cis*-[Pt($L^{8\text{-}14}$-κ*S*,*O*)$_2$] complexes are provided in Figures A5.5 to A5.10, while the relative distributions of *trans*-isomers are presented in Table 5.4.

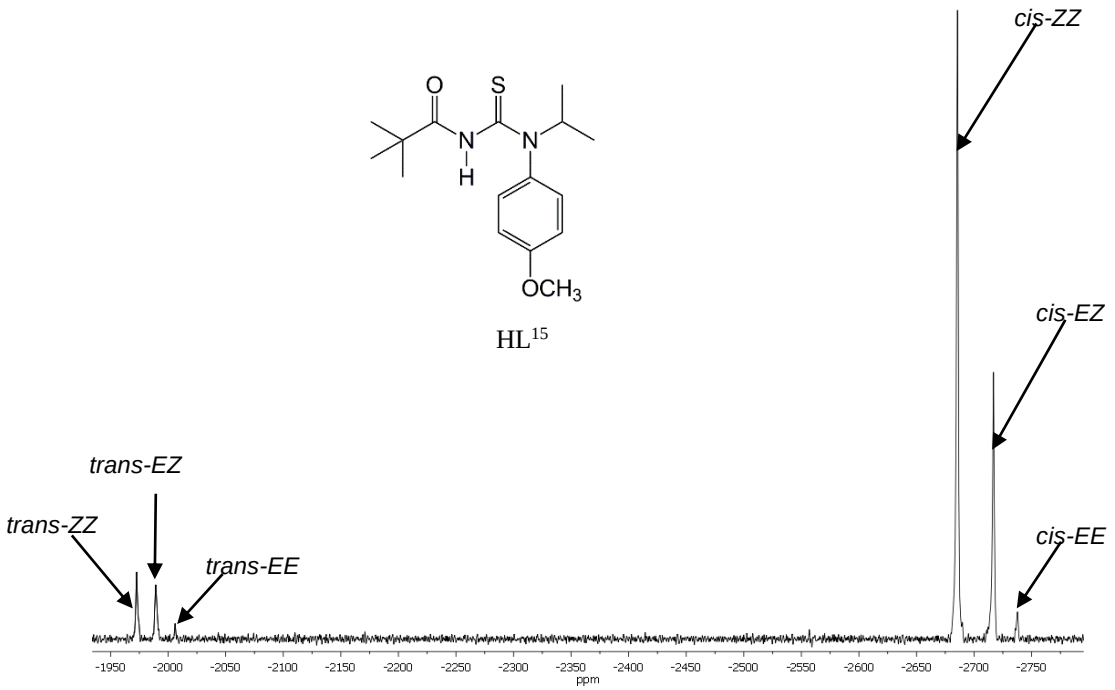

Figure 5.19. $^{195}Pt\{^{1}H\}$ NMR spectrum of a chloroform-*d* solution of a mixture of *ZZ*, *EZ* and *EE* configurational isomers of *cis*-[Pt(L^{15}-κ*S*,*O*)$_2$] after irradiation with polychromatic light from a 5 Watt LED lamp showing the formation of *trans-ZZ*, *trans-EZ* and *trans-EE* isomers by photoirradiation.

The trend in the relative distribution of the *trans-EE*, *trans-EZ* and *trans-ZZ* isomers is similar to that of their *cis*-[Pt($L^{8\text{-}15}$-κ*S*,*O*)$_2$] isomers but for a notable exception. In [Pt(L^{14}-κ*S*,*O*)$_2$] the relative distribution of the *trans-EZ* isomer (52 %) is higher than the *trans-ZZ* (33 %), which is contrary to the trend observed for the *cis*-isomers (43 % *EZ* and 53 % *ZZ*). Also, the distribution of *trans-EE* isomers of the *cis*-[Pt($L^{8\text{-}11}$-κ*S*,*O*)$_2$] complexes are much lower (2-3 %) compared to the relative distribution of their *cis-EE* counterparts (13-20 %). The reverse is true for the *cis*-[Pt($L^{13\text{-}15}$-κ*S*,*O*)$_2$] complexes in which much higher relative distribution of the *trans-EE* isomers (13-27 %) is observed compared to their *cis-EE* isomers (2-4 %). This inconsistency in the distribution of *E*, *Z* isomers suggests that photo-induced isomerization of the *cis*-[Pt($L^{8\text{-}15}$-κ*S*,*O*)$_2$] complexes is more complicated than envisaged. Unambiguous assignment of the new *trans*-[Pt($L^{8\text{-}15}$-κ*S*,*O*)$_2$] resonances formed after photo-induced isomerization of *cis*-[Pt($L^{8\text{-}15}$-κ*S*,*O*)$_2$] will therefore require further studies. When the irradiated *cis*-[Pt($L^{8\text{-}15}$-κ*S*,*O*)$_2$] solutions are left in the dark, all the *trans* $^{195}Pt\{^{1}H\}$ resonances slowly vanish accompanied by growth of their *cis* $^{195}Pt\{^{1}H\}$ resonances.

Table 5.4. The relative distributions of *trans-ZZ*, *trans-EZ* and *trans-EE* isomers (obtained by ^{195}Pt NMR deconvolution analysis and estimated to have an error of ±1 %) from photo-induced isomerization of *cis*-[Pt($L^{8\text{-}15}$-κ*S*,*O*)$_2$] complexes in chloroform-*d* under polychromatic light irradiation with a 5Watt LED lamp at 25 °C determined from ^{195}Pt{^{1}H} resonances.

	cis			***trans***		
	% ZZ	***% EZ***	***% EE***	***% ZZ***	***% EZ***	***% EE***
Pt[L^8-κ*S*,*O*)$_2$]	33	47	20	32	65	3
Pt[L^9-κ*S*,*O*)$_2$]	42	45	13	41	56	3
Pt[L^{11}-κ*S*,*O*)$_2$]	41	46	13	49	49	2
Pt[L^{12}-κ*S*,*O*)$_2$]	57	40	3	-	-	-
Pt[L^{13}-κ*S*,*O*)$_2$]	64	32	4	61	26	13
Pt[L^{14}-κ*S*,*O*)$_2$]	53	43	4	33	52	15
Pt[L^{15}-κ*S*,*O*)$_2$]	69	29	2	52	45	27

5.2.5. Preparation of *trans*-bis(*N*-methyl-*N*'-ethyl-*N*'-benzoylthioureato-κ^2*S*,*O*)palladium(II) by photo-induced isomerization

The *trans*-[Pd(L^8-κ*S*,*O*)$_2$] complex was isolated as a mixture of *trans*-[Pd(*ZZ*-L^8-κ*S*,*O*)$_2$], *trans*-[Pd(*EZ*-L^8-κ*S*,*O*)$_2$] and *trans*-[Pd(*EE*-L^8-κ*S*,*O*)$_2$] isomers after irradiation of a *cis*-[Pd(L^8-κ*S*,*O*)$_2$] solution in acetonitrile with polychromatic light accompanied by slow evaporation. The *trans*-[Pd($L^{9\text{-}15}$-κ*S*,*O*)$_2$] complexes of other ligands $HL^{9\text{-}15}$ could not be isolated since their *cis*-[Pd($L^{9\text{-}15}$-κ*S*,*O*)$_2$] complexes were found to be less soluble in acetonitrile. Isolation of the *trans*-[Pt(L^8-κ*S*,*O*)$_2$] complex was not also successful despite several attempts. After irradiation of an acetonitrile solution of the *cis*-[Pt(L^8-κ*S*,*O*)$_2$] complex for several days, no *trans*-[Pt(L^8-κ*S*,*O*)$_2$] product was obtained. This could be attributed to the fact that *trans*-[Pt(L^n-κ*S*,*O*)$_2$] complexes are known to undergo significant photodecomposition after photoirradiation.[58] Despite several attempts to crystallize the isolated *trans*-[Pd(L^8-κ*S*,*O*)$_2$] complex, single-crystals suitable for X-ray diffraction could not be obtained after photoirradiation of the *cis*-[Pd(L^8-κ*S*,*O*)$_2$] complex in acetonitrile.

The isolated *trans*-[Pd(L^8-κ*S*,*O*)$_2$] complex was soluble in chloroform-*d* hence ^{1}H NMR was used for its characterization. The downfield region of the ^{1}H NMR spectrum of the complex is shown in Figure A5.11 (a) in comparison with its *cis*-[Pd(L^8-κ*S*,*O*)$_2$] isomer (Figure A5.11(b)). The *trans*-$H^{2,2}$ resonance is shifted upfield (δ = 8.07 ppm) relative to the resonance for the *cis*-[Pd(L-κ*S*,*O*)$_2$] isomer at δ = 2.25 ppm. This difference in chemical shift is consistent with that obtained for *cis-trans* complexes of symmetrically substituted *N*,*N*-di-alkyl-*N*'-benzoylthioureas investigated in chapter 3 (section 3.2.2, page 60). Figure 5.20 (a) and (b) show the upfield regions of the ^{1}H NMR spectrum of the *cis*-[Pd(L^8-κ*S*,*O*)$_2$] and isolated *trans*-[Pd(L^1-κ*S*,*O*)$_2$] complexes. The set of multiplets centred at δ = 3.98 ppm are tentatively assigned to *trans-ZZ*(N(CH_2), *trans-EZ*(N(CH_2) and *trans-EE*(N(CH_2) resonances which overlap at 25 °C (Figure 5.20 (a)). This set of *trans*-multiplets are shifted slight downfield relative to their *cis*-counterpart at δ = 3.94 ppm (Figure 5.20 (b)). The two upfield singlets in Figure 5.20 (a) at δ = 3.39 ppm and δ = 3 .23 ppm are ascribed to protons with *trans*-N(CH_3)-*ZZ* and *trans*-N(CH_3)-*EZ/EE* configuration. Unambiguous assignment of the *trans*-resonances is beyond the scope of this study.

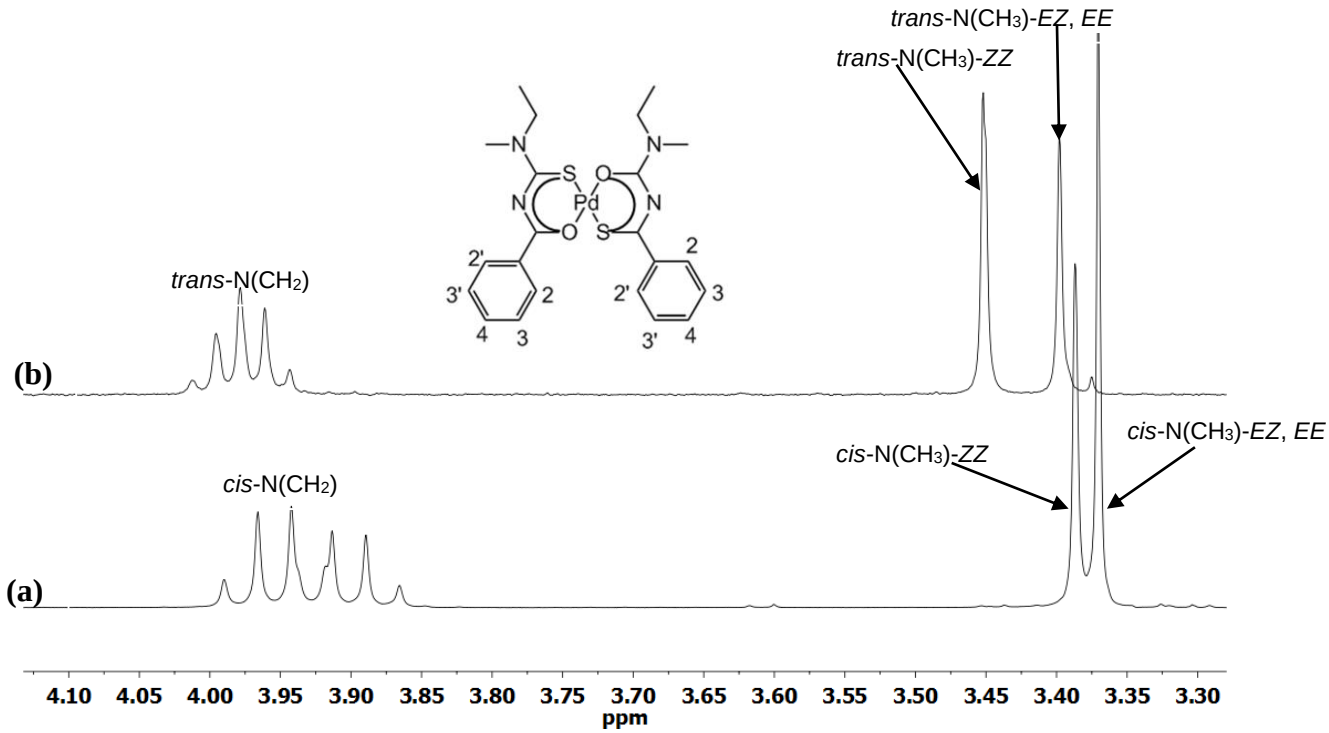

Figure 5.20. Upfield region of ^{1}H NMR spectra for a mixture of *cis-ZZ*, *cis-EZ*, *cis-EE* isomers of **(a)** *cis*-[Pd(L^8-κ*S*,*O*)$_2$] and **(b)** isolated *trans*-[Pd(L^8-κ*S*,*O*)$_2$] in chloroform-*d* at 25 °C.

Further confirmation of the isomeric veracity of the observed *cis*-*trans* resonances is obtained by allowing the solutions of *trans*-[Pd(L^8-κ*S*,*O*)$_2$] in the dark followed by ^{1}H NMR spectra acquisition. All the *trans*-$H^{2,2}$ and -N(CH_3) resonances are seen to slowly diminish with time while their *cis* counterparts increase slowly in intensity until complete *trans*-c*is* reversion is achieved (Figure 5.21 (a) and (b)). This spontaneous *trans*→*cis* isomerization was also observed for the isolated *trans*-[Pd(L^{1-7}-κ*S*,*O*)$_2$] complexes of the symmetrically substituted *N*,*N*-dialkyl-*N*'-acylthioureas (chapter 3 and 4) and will be discussed further in the next chapter.

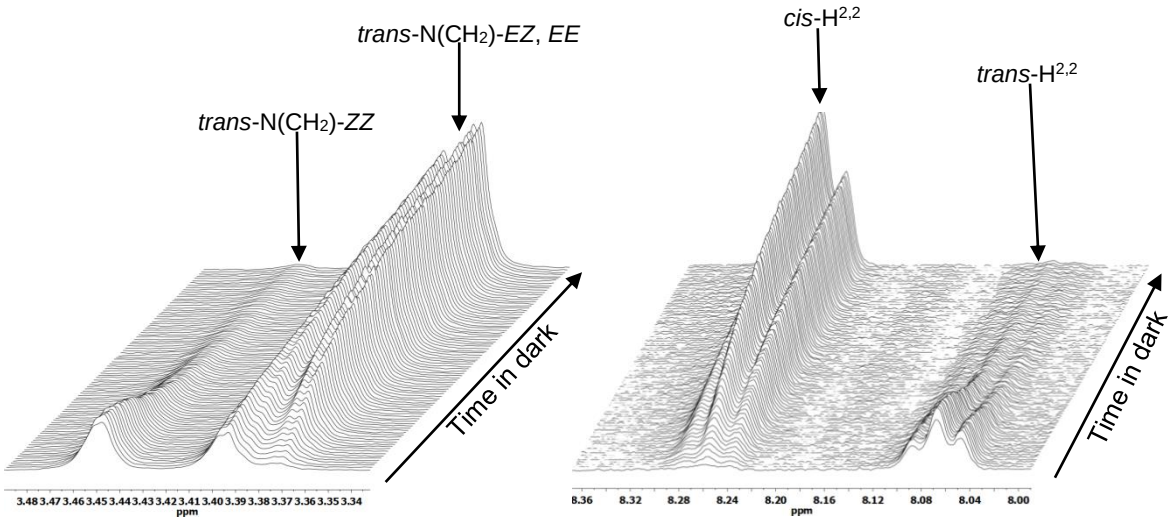

Figure 5.21. ^{1}H NMR spectra showing reversion of *trans*-[Pd(L^8-κ*S*,*O*)$_2$] to *cis*-[Pd(L^8-κ*S*,*O*)$_2$] in chloroform-*d* and in the dark.

5.3. Conclusions

In conclusion, Pt(II) and Pd(II) complexes were successfully prepared from the asymmetrically substituted HL^{8-15} ligands. Both the ligands and complexes were shown to exhibit *E*, *Z* configurational isomers from their ^{1}H NMR, HMBC and HSQC spectra in chloroform-*d*. Unambiguous assignment of the *cis*-[Pt(*ZZ*-L^n-κ*S*,*O*)$_2$], *cis*-[Pt(*EZ*-L^n-κ*S*,*O*)$_2$] and *cis*-[Pt(*EE*-L^n-κ*S*,*O*)$_2$] isomers was assisted with the use of 1D NOESY. Moreover, the ^{195}Pt{^{1}H} spectra of the *cis*-[Pt(L^{8-15}-κ*S*,*O*)$_2$] complexes showed three well-resolved ^{195}Pt{^{1}H} resonances assigned to the *cis*-*ZZ*, *cis*-*EZ* and *cis*-*EE* isomers.

From the ^{195}Pt{^{1}H} NMR data, it was evident that the relative distribution of the *cis*-*ZZ*, *cis*-*EZ* and *cis*-*EE* isomers in solution is dependent on the nature of the ligand substituents. With the two solvents used (chloroform-*d* and acetone-d_6), the effect of solvent appeared to be insignificant in determining which isomer predominates in solution. The chemical shifts of

^{195}Pt{^{1}H} resonances were found to be dependent on the nature of the ligand substituents and showed a linear dependence with increase in temperature of the chloroform-*d* solution. For the first time, the *cis*-[Pt(*EE*-L^{8}-κ*S*,*O*)$_2$] and *cis*-[Pd(*EE*-L^{8}-κ*S*,*O*)$_2$] structures with relatively smaller *N*-ethyl, *N*-methyl substituents were isolated in chloroform and dichloromethane. In contrast, the presence of a relatively larger *N*-4-methoxy-phenyl and *N*-isopropyl substituents resulted in the isolation of the *cis*-[Pt(*ZZ*-L^{15}-κ*S*,*O*)$_2$] complex in chloroform. This can be attributed to the increased relative distribution of the *cis*-ZZ isomer as observed from the ^{195}Pt{^{1}H} NMR spectrum, which is caused by the presence of *N*-4-methoxy-phenyl and *N*-isopropyl substituents on a nitrogen atom. Also, the solubility of the *cis*-[Pt(*ZZ*-L^{15}-κ*S*,*O*)$_2$] isomer might have been lower than that of the *cis*-[Pt(*EZ*-L^{15}-κ*S*,*O*)$_2$] and *cis*-[Pt(*EE*-L^{15}-κ*S*,*O*)$_2$] isomers leading to its selective isolation.

Irradiation of chloroform-*d* solutions of all the *cis*- [M (L$^{8\text{-}15}$-κ*S*, *O*)$_2$] (M = Pt(II) or Pd(II)) complexes with a 5 Watt LED lamp led to their photo-isomerization. The use of RP-HPLC and ^{1}H NMR limited the determination of all *trans-EZ*, *trans-EE* and *trans-ZZ* isomers due to their similar chemical shifts and retention times and hence overlapping of peaks. The ^{195}Pt{^{1}H} NMR spectra of the irradiated chloroform-*d* solutions revealed three additional resonances assigned to the *trans-EE*, *trans-EZ* and *trans-ZZ* isomers. All *trans* ^{195}Pt{^{1}H} resonances were significantly more deshielded by *ca* δ740 ppm relative to their respective *cis-ZZ*, *cis-EZ* and *cis-EE* counterparts. The relative distributions of the photo-isomerised *trans*-[Pt(*ZZ*-L-κ*S*,*O*)$_2$], *trans*-[Pt(*EZ*-L-κ*S*,*O*)$_2$] and *trans*-[Pt(*EE*-L-κ*S*,*O*)$_2$] isomers were found to be dependent on the nature of the ligand substituents.

For the first time, slow evaporation of an acetonitrile solution of the *cis*-[Pd(L^{8}-κ*S*,*O*)$_2$] complex of an asymmetrically substituted *N*,*N*-dialkyl-*N*'-acylthiourea ligand after light irradiation led to isolation of a *trans*-[Pd(L^{8}-κ*S*,*O*)$_2$] isomer. The new *trans*-[Pd(L^{8}-κ*S*,*O*)$_2$] complex was successfully characterized by ^{1}H NMR spectroscopy, although unambiguous assignment of the *trans-E,Z* resonances could not be achieved. In the absence of light in chloroform-*d*, the isolated *trans*-[Pd(L^{8}-κ*S*,*O*)$_2$] complex reverted completely to its *cis*-[Pd(L^{8}-κ*S*,*O*)$_2$] isomer.

6

Towards understanding the spontaneous trans-[M(L-κS,O)$_2$]→cis-[M(L-κS,O)$_2$] (M=Pt(II), Pd(II)) isomerization

Synopsis

This chapter examines the relative rates of spontaneous trans→cis isomerization of isolated trans-[Pd(L^n-κS,O)$_2$] complexes in chloroform and acetonitrile. Significantly higher relative rates of trans→cis isomerization were observed in acetonitrile than in chloroform. The presence of different ligand substituents slightly influenced the relative isomerization rates. The relative rates of trans→cis isomerization were found to increase with increase in temperature, with the activation parameters suggesting association during the reaction. The presence of trace amounts of N,N-dialkyl-N'-acylthioureas catalyses the trans→cis reaction indicative of ligand exchange. Evidence of formation of mixed-ligand complexes during the ligand exchange-mediated trans→cis isomerization is also provided.

6.1. Introduction.

The overwhelming tendency of the *N*,*N*-dialkyl-*N*'-acyl(aroyl)thioureas to form the *cis*-[M(L^n-κ*S*,*O*)$_2$] (M = Pt(II) or Pd(II)) complexes in preference to the *trans*-[M(L^n-κ*S*,*O*)$_2$] complexes is well documented.[10,17,27,30-34,99] The only known means of obtaining the *trans*-[M(L^n-κ*S*,*O*)$_2$] complexes of Pt(II) and Pd(II) is *via* a photo-induced isomerization after irradiation with polychromatic light.[13] When solutions of the *cis*-[Pd(L^n-κ*S*,*O*)$_2$] complexes in acetonitrile are irradiated, the *trans*-[M(L^n-κ*S*,*O*)$_2$] isomers are generated and after continuous light exposure a steady state constituting of a mixture of the *cis*-*trans* complexes is achieved.[13] In the simplest form, the reversible *cis*-*trans* isomerization can be considered as separate forward and reverse reactions as represented below. For both Pt(II) and Pd(II) complexes with the *N*,*N*-di-substituted acylthioureas, the forward process (*cis*→*trans*) is induced by light of wavelength < 480 nm.[13] The reverse reaction (*trans*→*cis*) takes place in the dark and is a thermal process.

$$cis\text{-}[Pd(L^n\text{-}\kappa S,O)_2] \underset{\Delta,\ thermal}{\overset{Light,\ h\upsilon}{\rightleftharpoons}} trans\text{-}[Pd(L^n\text{-}\kappa S,O)_2]$$

The preferential formation of the *cis*-[M(L^n-κ*S*,*O*)$_2$] complexes after coordination of Pt(II) or Pd(II) to the *N*,*N*-dialkyl-*N*'-acylthioureas may be ascribed to the higher *trans*-influence of the sulfur donor atom relative to the oxygen atom.[58] The rareness of the *trans*-[M(L^n-κ*S*,*O*)$_2$] complexes could be associated with small differences in ground state energy of *ca* 2.5 Kcal/mol between the *cis*-*trans* isomers of a bis(*N*,*N*-dimethyl-*N*'-methylthioureato)palladium(II) complex as estimated by DFT calculations (Figure 6.1).[57] The mechanism of the photo-induced *cis*→*trans* isomerization for square *cis*-[M(L^n-κ*S*,*O*)$_2$] complexes of the *N*,*N*-dialkyl-*N*'-acyl(aroyl)thioureas (HL) is not yet fully understood. DFT calculations suggest that photo-induced isomerization of *cis*-bis(*N*,*N*-dimethyl-*N*'-methylthioureato)palladium(II) involves an electron excitation from the Highest Occupied Molecular Orbital (HOMO) of the *cis* conformation to the Lowest Unoccupied Molecular Orbital (LUMO) leading to weakening of either the Pd-O or Pd-S bond in the complex.[57] This theoretical study also proposed that the singlet excited state, triplet excited state and doubly excited singlet state pathways may all be involved after photo-induced excitation leading to isomerization of the *cis*-[Pd(L-κ*S*,*O*)$_2$] complex. In addition, the DFT results suggest that in acetonitrile, the intermediates from photo-induced *cis*→*trans* isomerization are formed by

intramolecular twisting and initial cleavage of either the Pd-S or Pd-O bond in the complex.[57] A trigonal bipyramidal transition state of the complex in acetonitrile was also postulated. The photo-induced *cis→trans* process reportedly ends up with transition to the ground state of the *trans*-[Pd(L-κ*S*,*O*)$_2$] isomer by thermal relaxation.[57]

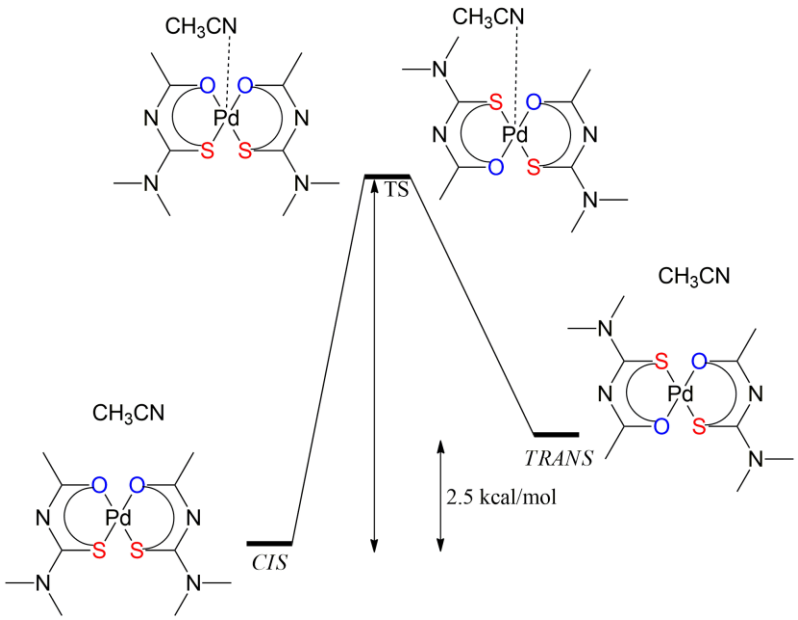

Figure 6.1. Representation of relative energies of *cis*-*trans* isomers involved during photo-induced isomerization of *cis*-bis(*N*,*N*-dimethyl-*N*'-methylthioureato)palladium(II) as obtained from DFT studies.[57]

The spontaneous and thermal *trans→cis* isomerization of Pt(II) and Pd(II) complexes of the *N*,*N*-dialkyl-*N*'-acylthioureas is reminiscent of the thermal isomerization of *cis*-Pt(gly-κ*N*,*O*)$_2$(gly = glycinato) complexes reported by Balzani and co-workers.[91-93] These authors found that the presence of free glycine ligands acts as a catalyst for the *cis→trans* isomerization. A ligand exchange mechanism was proposed for the reaction as one which involves substitution of the *cis*-Pt(gly-κ*N*,*O*)$_2$ complex with a free labelled glycine ligand thereby yielding *trans* and *cis* isomers. For the photo-induced *cis→trans* isomerization of the *cis*-Pt(gly-κ*N*,*O*)$_2$ (gly = glycinato) complexes, an intramolecular twisting mechanism was proposed.[91] This was supported by DFT calculations performed by Richardson and co-workers.[94]

In chapters 3, 4 and 5 isolation of the *trans*-[Pd(L$^{1-8}$-κ*S*,*O*)$_2$] complexes of the *N*,*N*-dialkyl-*N*'-acylthioureas was described. The structures and names of the HL$^{1-8}$ ligands were given in chapter

2, Figure 2.2 (page 20). The isolated *trans*-[Pd(L^{1-8}-κ*S*,*O*)$_2$] isomers were also shown to undergo slow *trans→cis* reversion in chloroform-*d*. In a non-coordinating solvent such as chloroform, one would expect that *trans→cis* isomerization would not proceed assuming that the reactions would occur only in coordinating solvents such as acetonitrile. This poses the question as to what other solution factors are responsible for the spontaneous *trans→cis* isomerization. In this chapter, some factors influencing the relative rate of *trans→cis* isomerization will be examined, leading to a ligand exchange study for the thermal isomerization process.

6.2. Results and discussion

6.2.1. Relative rates of spontaneous *trans*-[Pd(L^n-κ*S*,*O*)$_2$]→*cis*-[Pd(L^n-κ*S*,*O*)$_2$] isomerization in the absence of light

6.2.1.1. Rates of *trans→cis* isomerization in chloroform as monitored by ^{1}H NMR spectroscopy

The relative rate of spontaneous *trans→cis* isomerization of the isolated *trans*-[Pd(L^{1-8}-κ*S*,*O*)$_2$] complexes in chloroform-*d* was studied using ^{1}H NMR spectroscopy. The rate constants were estimated from relative peak intensities of ^{1}H NMR resonances as discussed in chapter 2, section 2.3.5 (page 46). ^{1}H NMR analysis was carried out by preparing a 5 mg/mL solution of the isolated *trans*-[Pd(L^{1-8}-κ*S*,*O*)$_2$] complexes in chloroform-*d* followed by ^{1}H NMR data acquisition. Figure 6.2 (a) shows the high-field region of an array of the ^{1}H NMR spectra of the *trans*-[Pd(L^2-κ*S*,*O*)$_2$] complex (HL^2 = *N*,*N*-diethyl-*N*'-4-methoxy-benzoylthiourea) as a function of time in the dark. Only the resonances of the $H^{2,2'}$ protons are shown for the sake of simplicity. The *trans*-$H^{2,2}$ resonances at δ = 8.02 ppm slowly diminish in intensity with time at the expense of the *cis*-$H^{2,2}$ resonances at δ = 8.20 ppm which slowly increase. After *ca* 6 hours in the dark, complete reversion to the *cis* complex occurred.

The order of the *trans→cis* reaction was examined by analysing the plots of the relative peak intensity (Figure 6.2 (b)), and the natural logarithm of relative peak intensity (Figure 6.3) versus time in the dark. If the reaction is zero-order, the rate should be independent of the concentration of reactants. Hence the plot of concentration of the *trans*-[Pd(L^2-κ*S*,*O*)$_2$] complex versus time should be linear. If the reaction is first-order, then the plot of the natural logarithm of concentration versus time in the dark should be linear. If the reaction is second-order, a plot of 1/[reactants]

versus time should give a straight line. From the linear plot of the natural logarithm of relative peak intensity versus time (Figure 6.3), it is evident that the *trans→cis* isomerization of the *trans*-[Pd(L^2-κ*S*,*O*)$_2$] complex is most likely a first-order reaction.

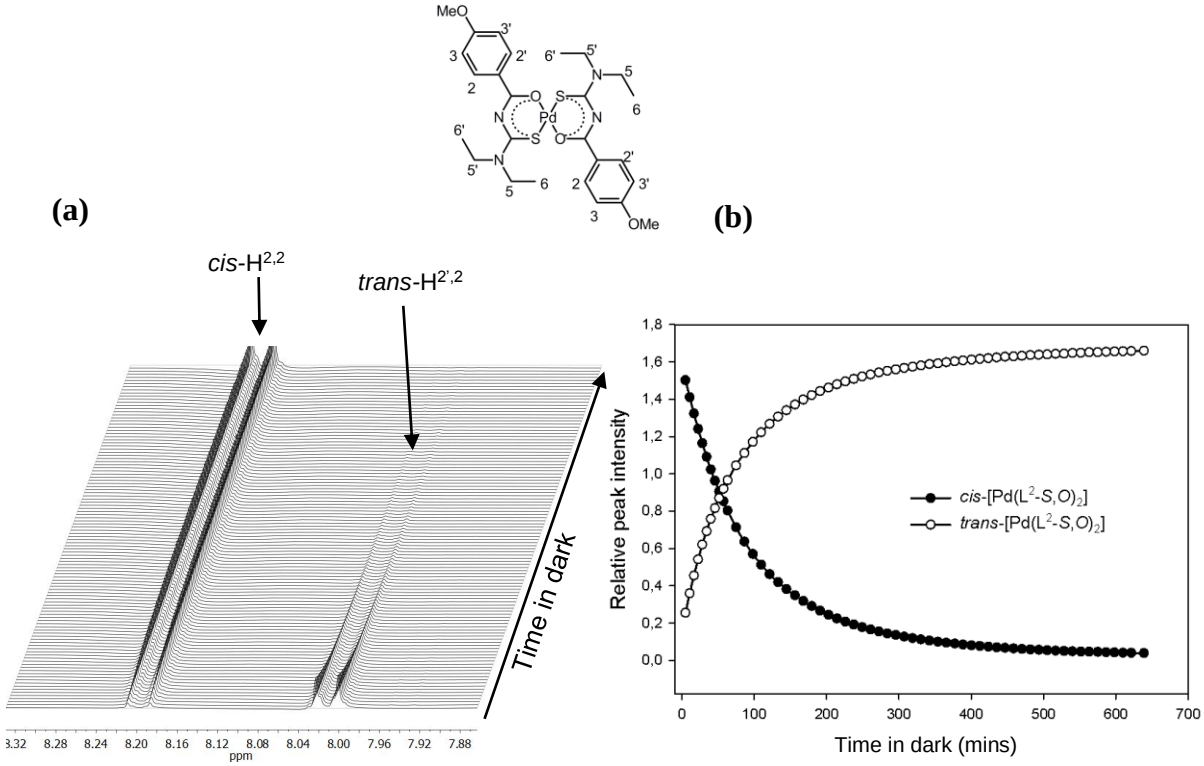

Figure 6.2. **(a)** Changes in $H^{2,2'}$ resonance intensity with time for *cis* and *trans* isomers; and **(b)** plot of relative peak area *vs.* time in dark; for *trans→cis* isomerization of isolated *trans*-[Pd(L^2-κ*S*,*O*)$_2$] complex in chloroform-*d* at 25 °C.

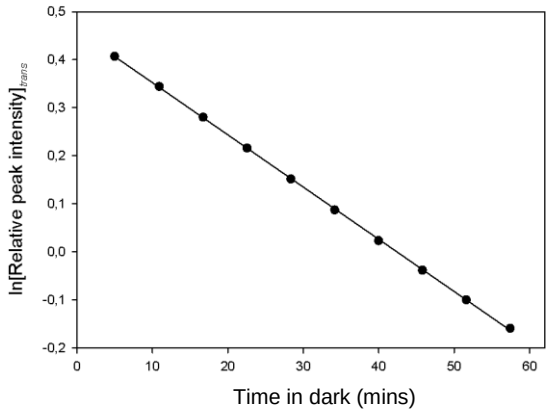

Figure 6.3. **(a)** Plot of natural logarithm of relative peak intensity *vs*. time in dark for *trans→cis* isomerization of *trans*-[Pd(L^2-κ*S*,*O*)$_2$] in chloroform-*d* at 25 °C.

The effect of ligand substituents on the relative rates of *trans→cis* isomerization was investigated using ^{1}H NMR spectroscopy. The arrayed ^{1}H NMR spectrum representing the spontaneous *trans→cis* isomerization of the isolated *trans*-[Pd(L^{1}-κ*S*,*O*)$_2$] complex was provided in chapter 3, Figure 3.12 (page 65), while the arrayed spectra of the isolated *trans*-[Pd($L^{3,4-6}$-κ*S*,*O*)$_2$] complexes are provided in Figure A6.1. The normalized plots of relative peak intensity versus time in the dark for the isolated *trans*-[Pd(L^{1-8}-κ*S*,*O*)$_2$] complexes is given in Figure 6.4. The *trans→cis* reversion for most of the isolated *trans*-[Pd(L^{n}-κ*S*,*O*)$_2$] complexes was achievable within 6 hours in chloroform-*d*. This is indicative of the slow nature of the *trans→cis* isomerization in chloroform.

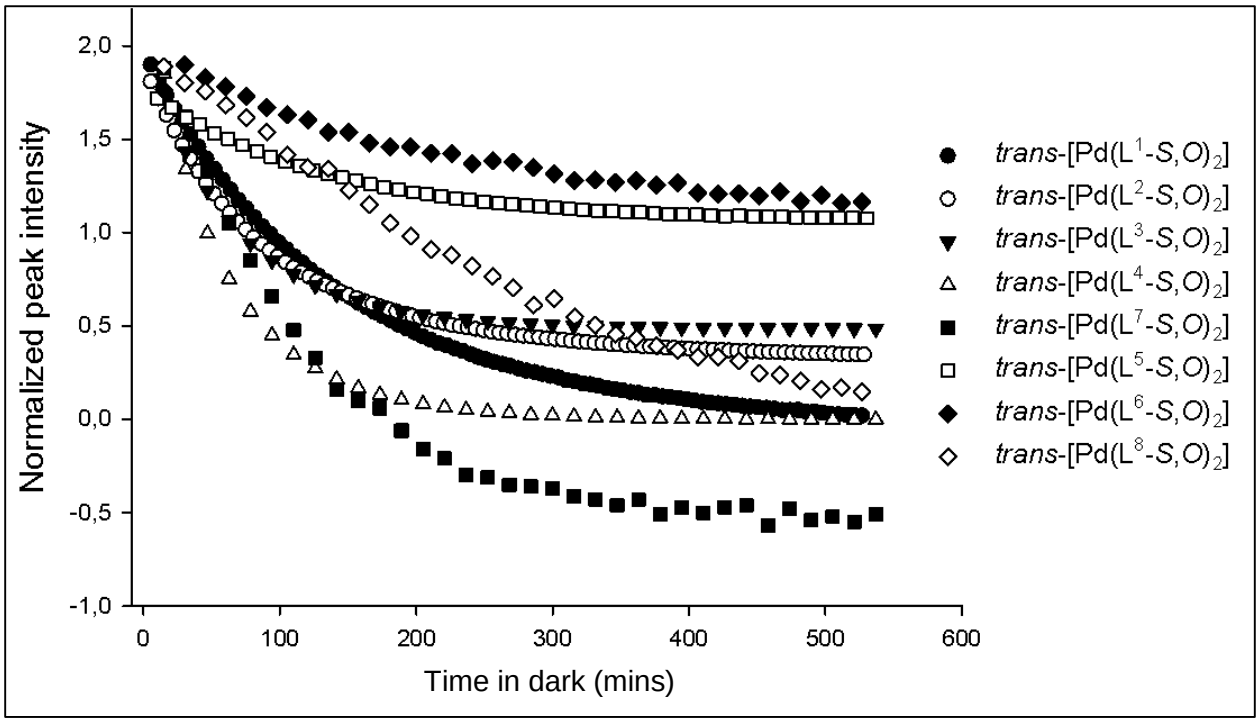

Figure 6.4. Plots of normalized relative peak intensity of *trans*-$H^{2,2}$ resonances versus time in dark, following *trans→cis* isomerization of isolated *trans*-[Pd(L^{1-8}-κ*S*,*O*)$_2$] complexes in chloroform-*d* at 25°C.

Figure 6.5 shows the plots of natural logarithm of relative peak intensity versus time in the dark for the *trans*-[Pd(L^{1-8}-κ*S*,*O*)$_2$] complexes in chloroform-*d*. The rate constants estimated from the slopes of these plots are given in Table 6.1. The linear plots (Figure 6.5) indicate that the spontaneous *trans→cis* isomerization in chloroform is a first-order reaction.

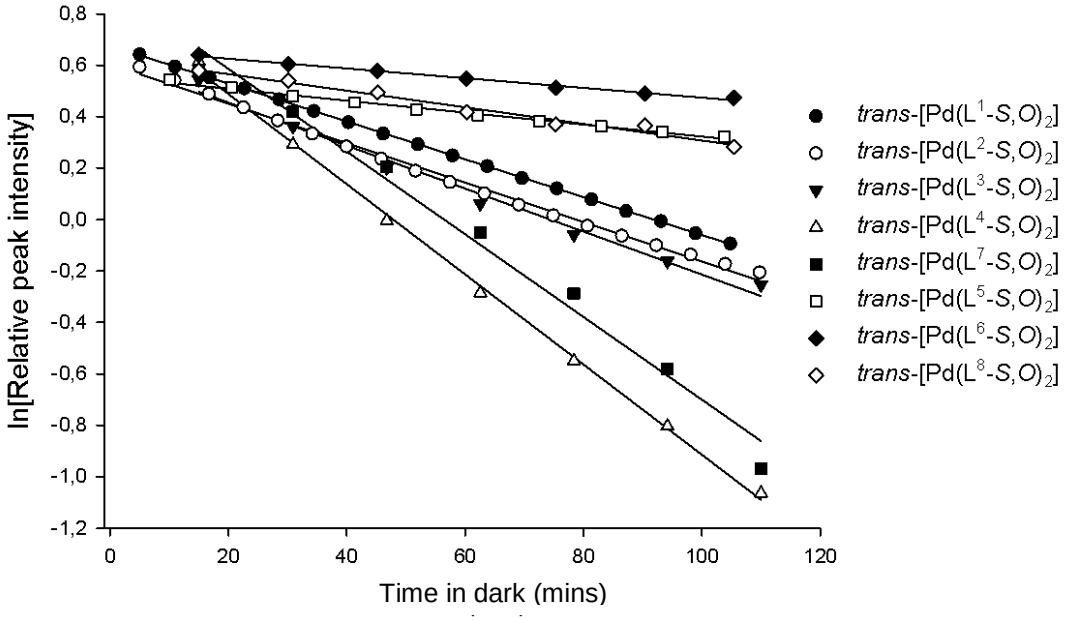

Figure 6.5. First-order plots of ln[peak area of *trans*] *vs* time in dark, for *trans→cis* isomerization of isolated *trans*-[Pd(L^{1-8}-κ*S*,*O*)$_2$] complexes in the dark, in chloroform-*d* at 25 °C.

Table 6.1. Relative rates of *trans→cis* isomerization of isolated *trans*-[Pd(L^{1-8}-κ*S*,*O*)$_2$] complexes in the dark, in chloroform-*d* at 25 °C obtained from changes in relative peak area for $H^{2,2'}$ protons.

Complex	**Chemical shift of $H^{2,2'}$ (ppm)**		**k x 10^{-2} (min^{-1})**
	cis	***trans***	
[Pd(L^1-κ*S*,*O*)$_2$]	8.25	8.06	0.85(±0.08)
[Pd(L^2-κ*S*,*O*)$_2$]	8.20	8.02	0.72(±0.05)
[Pd(L^3-κ*S*,*O*)$_2$]	7.55	7.36	0.95(±0.08)
[Pd(L^4-κ*S*,*O*)$_2$]	8.15	7.97	1.20(±0.04)
[Pd(L^5-κ*S*,*O*)$_2$]	8.13	7.94	0.23(±0.04)
[Pd(L^6-κ*S*,*O*)$_2$]	8.28	8.08	0.18(±0.04)
[Pd(L^7-κ*S*,*O*)$_2$]	8.95	8.63	0.74(±0.07)
[Pd(L^8-κ*S*,*O*)$_2$]	8.25	8.07	0.38(±0.06)

Inspection of Table 6.1 reveals that the relative rates of *trans→cis* isomerization for *trans*-[Pd(L^5-κ*S*,*O*)$_2$], HL^5 = *N*,*N*-diethyl-*N*'-4-methyl-benzoylthiourea (k = 0.23 x 10^{-2} min^{-1}), *trans*-[Pd(L^6-κ*S*,*O*)$_2$], HL^6 = *N*,*N*-dimethyl-*N*'-4-methyl-benzoylthiourea (k = 0.18 x 10^{-2} min^{-1}), and *trans*-[Pd(L^8-κ*S*,*O*)$_2$], HL^8 = *N*-methyl, *N*-ethyl,-*N*'-benzoylthiourea (k = 0.38 x 10^{-2} min^{-1}) are slightly lower than that of *trans*-[Pd(L^1-κ*S*,*O*)$_2$], HL^1 = *N*,*N*-diethyl-*N*'-benzoylthiourea (k = 0.85 x 10^{-2} min^{-1}). The relative rates of *trans→cis* isomerization for *trans*-[Pd(L^3-κ*S*,*O*)$_2$], HL^3 = *N*,*N*-diethyl-*N*'-3,4,5-tri-methoxy-benzoylthiourea (k = 0.95 x 10^{-2} min^{-1}), *trans*-[Pd(L^4-κ*S*,*O*)$_2$], HL^4 = *N*,*N*-diethyl-*N*'-4-chloro-benzoylthiourea (1.20 x 10^{-2} min^{-1}), *trans*-[Pd(L^2-κ*S*,*O*)$_2$], HL^2 = *N*,*N*-diethyl-*N*'-4-methoxy-benzoylthiourea (k = 0.72 x 10^{-2} min^{-1}) and *trans*-[Pd(L^7-κ*S*,*O*)$_2$], HL^7 = *N*,*N*-diethyl-*N*'-1-naphthoylthiourea (k = 0.74 x 10^{-2} min^{-1}) are very similar to that of *trans*-[Pd(L^1-κ*S*,*O*)$_2$].

The difference in relative rates of isomerization between the *trans*-[Pd(L^{1-8}-κ*S*,*O*)$_2$] complexes is not overwhelming. Moreover, no consistent trend in the estimated rate constants was observed based on electronic effect of ligand substituents. Intuitively, it is possible to assume that the presence of electron withdrawing groups on the phenyl ring could make the palladium centre more positive thereby weakening the Pd-O bond. This could increase the rate of Pd-O bond cleavage and consequently increase the rates of isomerization. In the same manner, the presence of electron-donating groups could render the palladium centre more negative, increasing the Pd-O bond strength and thereby decreasing the rate of *trans→cis* isomerization.

The effect of concentration on the relative rate of *trans→cis* isomerization was studied at two concentrations namely 5 mg/mL and 10 mg/mL for the *trans*-[Pd(L^4-κ*S*,*O*)$_2$] complex (HL^4 = *N*,*N*-diethyl-*N*'-4-chloro-benzoylthiourea). At concentrations higher than 10 mg/mL, the *trans*-[Pd(L^4-κ*S*,*O*)$_2$] complex was insoluble in chloroform-*d*, hence concentration dependence studies at higher concentrations could not be investigated. The *trans*-[Pd(L^4-κ*S*,*O*)$_2$] complex was selected for this study because it was easier to isolate compared to the other *trans*-[Pd($L^{1,2,3-8}$-κ*S*,*O*)$_2$] complexes. The arrayed ^{1}H NMR spectra representing changes in *trans*-$H^{2,2}$ resonance intensities for the 10 mg/mL solution of the *trans*-[Pd(L^4-κ*S*,*O*)$_2$] complex are depicted in Figure A6.2 (a). Figure 6.6 shows the changes in relative peak intensity versus time in the dark at the two concentrations studied. The relative rate of *trans→cis* isomerization is similar for the two concentrations (k = 1.20

x 10^{-2} (± 0.04) min^{-1} at 5 mg/mL, and k = 1.31 x 10^{-2} (± 0.1) min^{-1} at 10 mg/mL). This further suggests that the *trans→cis* reaction is first-order.

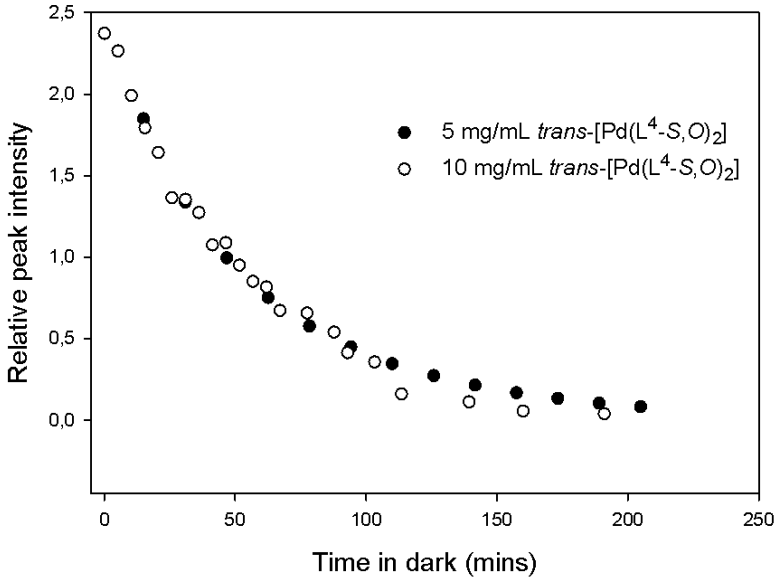

Figure 6.6. Plots of normalized peak area of *trans*-$H^{2,2}$ resonances as a function of time in dark, representing *trans→cis* isomerization of isolated *trans*-[Pd(L^4-κ*S*,*O*)$_2$] at different concentration in chloroform-*d* at 25 °C.

6.2.1.2. Effects of temperature on relative rates of *trans→cis* isomerization in chloroform

The effect of temperature on the relative rates of *trans→cis* isomerization for the *trans*-[Pd(L^4-κ*S*,*O*)$_2$] complex was studied in chloroform-*d* in the range 25-55 °C, by keeping all other variables constant. Higher temperatures were avoided to prevent chloroform from boiling. The reactions were carried out by rapidly dissolving 5 mg of the isolated *trans*-[Pd(L^4-κ*S*,*O*)$_2$] complex in chlroform-*d* and monitroing the dissapearance of the $H^{2,2'}$ resonances by ^{1}H NMR spectroscopy at the different temperatures. The changes in *trans*-$H^{2,2}$ resonance intensities of the *trans*-[Pd(L^4-κ*S*,*O*)$_2$] complex at the three different temperatures are depicted in Figures A6.2 (b-d). The activation parameters namely $\Delta H^{\#}$ and $\Delta S^{\#}$ which are presented in Table 6.2 for the *trans→cis* isomerization were calculated using the Eyring equation ($\ln(k/T) = -\Delta H^{\#}/RT + \Delta S^{\#}/R + 23.8$). It is evident from the results that an increase in temperature increases the rate of *trans→cis* isomerization.

Table 6.2. Kinetic and activation parameters for *trans→cis* isomerization of *trans*-[Pd(L^4-κ*S*,*O*)$_2$] in chloroform-*d* at different temperatures.

Complex	T (K)	k x 10^{-4} (s^{-1})	$\Delta H^{\#}$ ($kJmol^{-1}$)	$\Delta S^{\#}$ ($JK^{-1}mol^{-1}$)
trans-[Pd(L^4-κ*S*,*O*)$_2$]	298	1.30(±0.04)	48.9(±1)	-117.7(±1)
	308	3.03(±0.1)		
	318	5.02(±0.06)		
	328	9.43(±0.1)		

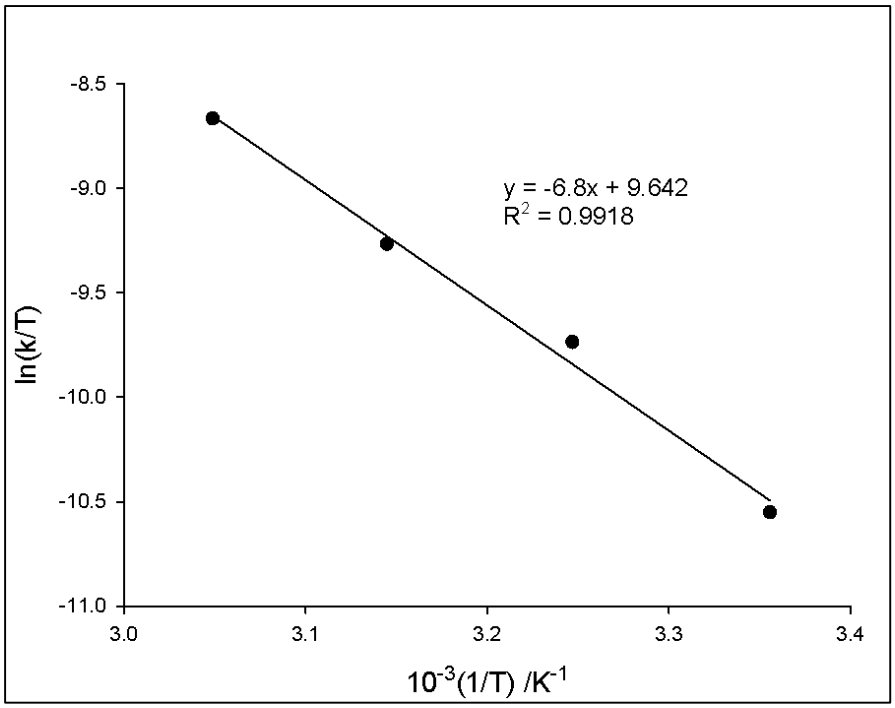

Figure 6.7. Eyring plot for *trans→cis* isomerization of *trans*-[Pd(L^4-κ*S*,*O*)$_2$] in chloroform-*d* in the temperature range 25-55 °C.

Figure 6.7 shows that a linear Eyring plot is obtained for the *trans*-[Pd(L^4-*S*,*O*)$_2$] complex in the temperature range 25-55 °C. A low value for $\Delta H^{\#}$ (48.9 $kJmol^{-1}$) and the large negative $\Delta S^{\#}$ value (-117.7 $JK^{-1}mol^{-1}$) suggest a significant associative character during the spontaneous *trans→cis* isomerization. This association could involve the *trans*-[Pd(L^n-κ*S*,*O*)$_2$] complexes with free *N*,*N*-dialkyl-*N*'-acylthioureas in solution. Hence it is possible that the free ligands in solution

could act as proton donors coordinating to the *trans*-[Pd(L^n-κ*S*,*O*)$_2$] isomers and forcing the chelate ring opening presumably by a Pd-S or Pd-O bond cleavage. The high negative $\Delta S^{\#}$ value is concurrent with the suggestion that both the displaced and entering HL^4 ligand are attached in the transition state, leading to a more compact transition state and hence a decrease in disorder of the system.

The ^{1}H NMR results presented so far in this chapter indicate that in chloroform-*d*, the relative rates of *trans→cis* isomerization are too slow in view of the long NMR acquisition times required for analysis. This could be because the chloroform molecule is unlikely to coordinate to any vacant coordination site on Pd if either Pd-O or Pd-S bond breaking occurs. Also, the relatively high concentrations of the *trans*-[Pd(L^n-κ*S*,*O*)$_2$] complexes (5 mg/mL) limits their ^{1}H NMR analysis. In the next section, the effect of a coordinating solvent acetonitrile on the relative rates of *trans→cis* isomerization at lower concentrations will be discussed.

6.2.1.3. Rates of *trans→cis* isomerization in acetonitrile as monitored by RP-HPLC

The relative rates of *trans→cis* isomerization were also examined in acetonitrile and monitored by RP-HPLC since the *cis* and *trans* isomers have different retention times. This was achieved by dissolving 2 mg of the *cis*-[Pd(L^{1-8}-κ*S*,*O*)$_2$] complexes in 10 ml acetonitrile. The *trans*-[Pd(L^{1-8}-κ*S*,*O*)$_2$] isomers were then generated *in-situ* by irradiation of the solution of the *cis*-[Pd(L^{1-8}-κ*S*,*O*)$_2$] complexes for 30 minutes with a 5 Watt LED lamp, during which a steady state between the *cis*-*trans* isomers was achieved. The irradiated sample was then rapidly injected onto the C_{18} column in the dark at intervals of *ca* 13 minutes with RP-HPLC detection at 262 nm using a photodiode array detector. The chromatographic trace obtained from the irradiated solution exhibits two peaks assigned to the *cis* and *trans* isomer as shown in Figure 6.8 for the *cis*-[Pd(L^1-κ*S*,*O*)$_2$] complex (HL^1 = *N*,*N*-diethyl-*N*'-benzoylthiourea). The changes in peak intensity as a function of time in the dark reveal that the peak corresponding to the *trans*-[Pd(L^1-κ*S*,*O*)$_2$] complex (elutes after 12.3 minutes), decreases with time at the expense of the *cis*-[Pd(L^1-κ*S*,*O*)$_2$] complex (which elutes at 11.3 minutes). After *ca* 2 hours in the dark, the *trans*-[Pd(L^1-κ*S*,*O*)$_2$] isomer completely vanishes. A plot of the natural logarithm of the relative peak area versus time in the dark (Figure 6.9) gives a straight, consistent with a first-order transformation.

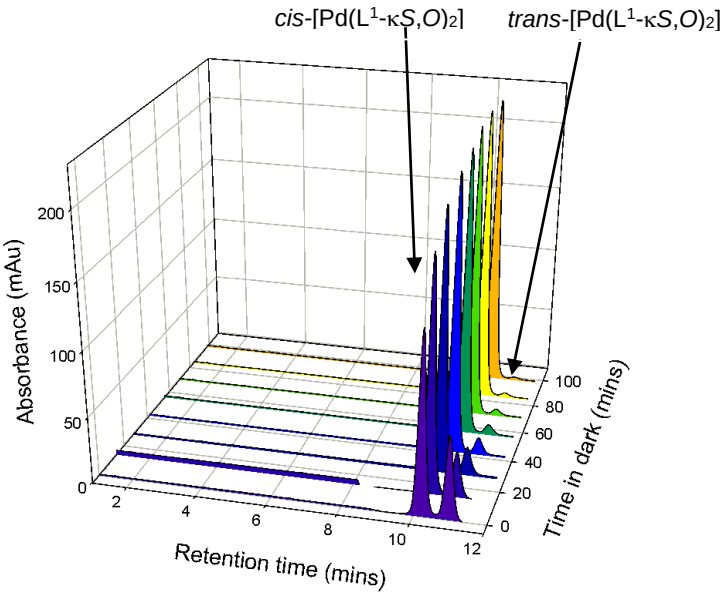

Figure 6.8. Overlaid chromatograms showing *trans→cis* isomerization in acetonitrile for solutions of *cis*-[Pd(L^1-κ*S*,*O*)$_2$] pre-irradiated with a 5Watt LED lamp and left in the dark; conditions: mobile phase, 95:5 % v/v acetonitrile:water; GEMINI C_{18}, 5 µm, 250 x 4.6 mm column; 20 µl injection volume; 1 $mlmin^{-1}$ flow rate; 262 nm detection.

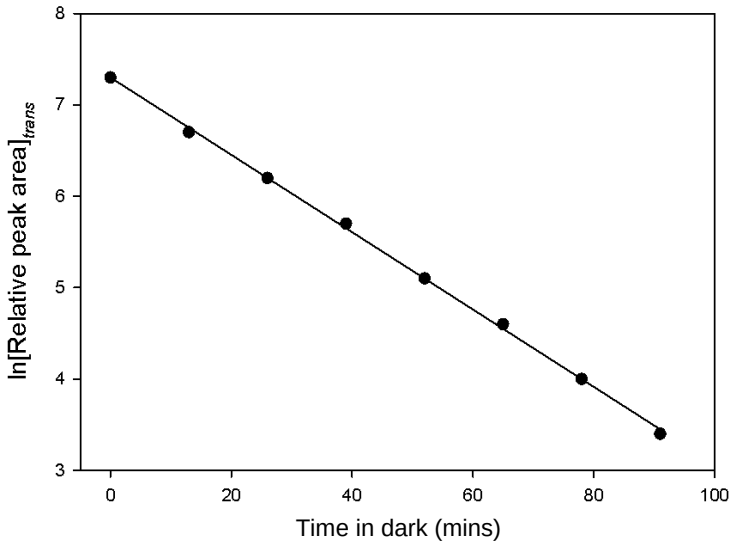

Figure 6.9. Plot of ln[Relative peak intensity] *vs*. time in the dark for the *trans→cis* isomerization of *cis*-[Pd(L^1-κ*S*,*O*)$_2$] in acetonitrile.

The RP-HPLC chromatograms obtained after irradiating acetonitrile solutions of the other *cis*-[Pd(L^{2-8}-κ*S*,*O*)$_2$] complexes are given in Figure A6.3. The percentage of the *cis*-[Pd(L^{1-8}-κ*S*,*O*)$_2$] isomers formed during *trans*→*cis* isomerization in acetonitrile is depicted in Figure 6.10. Due to significantly higher retention time of *cis*-[Pd(L^4-κ*S*,*O*)$_2$] (retention time of 36 minutes at 95:5 % v/v acetonitrile:water), the relative rates of *trans*→*cis* isomerization for the irradiated *cis*-[Pd(L^4-κ*S*,*O*)$_2$] (*N*,*N*-diethyl-*N*'-4-chloro-benzoylthiourea) complex in acetonitrile could not be determined using RP-HPLC.

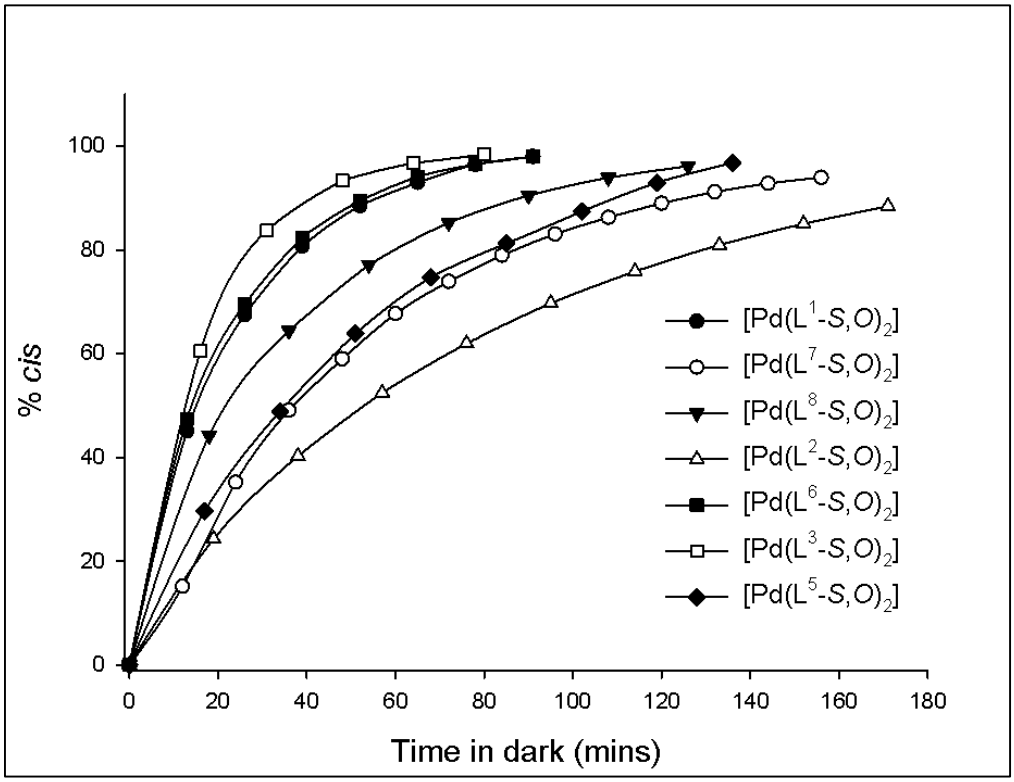

Figure 6.10. Plots of % *cis* isomers versus time in dark, for *trans*→*cis* isomerization of *cis*-[Pd(L^{1-7}-κ*S*,*O*)$_2$] complexes in acetonitrile at 25 °C.

Analysis of the linear kinetic plots obtained from relative peak areas (Figure 6.11) indicate that the *trans*→*cis* isomerization of the *trans*-[Pd(L^{1-8}-κ*S*,*O*)$_2$] isomers is first-order in acetonitrile. The plot of natural logarithm of peak area versus time in the dark for the *trans*-[Pd(L^7-κ*S*,*O*)$_2$] complex is given in Figure A6.4. The rates constants were estimated from the slopes of these plots and presented in Table 6.3. From the results, it is evident that lower rate constants are obtained for the *trans*-[Pd(L^2-κ*S*,*O*)$_2$] (HL^2 = *N*,*N*-diethyl-*N*'-4-methoxy-benzoylthiourea, k = 1.26 x 10^{-2} min^{-}

^{1}), *trans*-[Pd(L^5-κ*S*,*O*)$_2$] (HL^5 = *N*,*N*-diethyl-*N*'-4-methyl-benzoylthiourea, k = 2.58 x 10^{-2} min^{-1}), *trans*-[Pd(L^7-κ*S*,*O*)$_2$] (HL^7 = *N*,*N*-diethyl-*N*'-1-naphthoylthiourea, k = 1.5 x 10^{-2} min^{-1}) and *trans*-[Pd(L^8-κ*S*,*O*)$_2$] (HL^8 = *N*-*m*ethyl, *N*-ethyl,-*N*'-benzoylthiourea, k = 2.78 x 10^{-2} min^{-1}) complexes compared to the *trans*-[Pd(L^1-κ*S*,*O*)$_2$] (k = 4.20 x 10^{-2} min^{-1}) complex. The relative rates of isomerization obtained for the *trans*-[Pd(L^3-κ*S*,*O*)$_2$], HL^3 = *N*,*N*-diethyl-*N*'-3,4,5-tri-methoxy-benzoylthiourea (k = 5.17 x 10^{-2} min^{-1}) and *trans*-[Pd(L^6-κ*S*,*O*)$_2$], HL^6 = *N*,*N*-dimethyl-*N*'-benzoylthiourea, (k = 4.95 x 10^{-2} min^{-1}) complexes are slightly higher than that of the *trans*-[Pd(L^1-κ*S*,*O*)$_2$] complex.

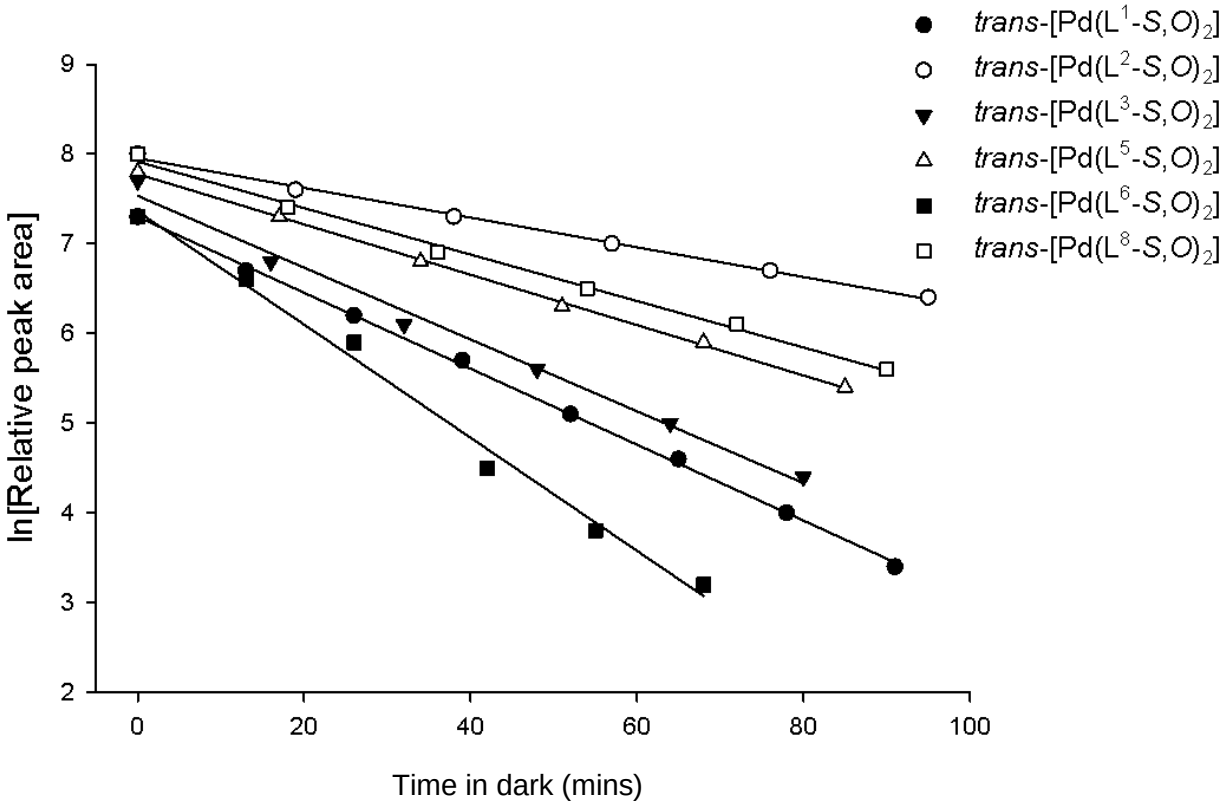

Figure 6.11. First-order plots of ln[relative peak area] vs time in dark for *trans*→*cis* isomerization of *cis*-[Pd(L^{1-7}-κ*S*,*O*)$_2$] complexes in acetonitrile at 25 °C.

Table 6.3. Kinetic data for *trans→cis* isomerization of *trans*-[Pd(L^{1-7}-κ*S*,*O*)$_2$] complexes in the dark, in acetonitrile and at room temperature.

Complex	Retention time (mins)		k x 10^{-2} (min^{-1})
	cis	*trans*	
[Pd(L^1-κ*S*,*O*)$_2$]	11.6	12.6	4.20 (± 0.1)
[Pd(L^2-κ*S*,*O*)$_2$]	16.0	16.9	1.26 (± 0.04)
[Pd(L^3-κ*S*,*O*)$_2$]	12.6	13.7	5.17 (± 0.09)
[Pd(L^5-κ*S*,*O*)$_2$]	13.3	14.8	2.58 (± 0.06)
[Pd(L^6-κ*S*,*O*)$_2$]	9.4	10.5	4.95 (± 0.07)
[Pd(L^7-κ*S*,*O*)$_2$]	9.5	6.2	1.50 (± 0.05)
[Pd(L^8-κ*S*,*O*)$_2$]	13.4	15.0	2.78 (± 0.04)

The effect of acetonitrile solvent on the relative rates of isomerization can be investigated by comparing the rate constants in Table 6.3 (in acetonitrile) with those in Table 6.1 (in chloroform-*d*). The results indicate that the rate of *trans→cis* isomerization for the *trans*-[Pd(L^6-κ*S*,*O*)$_2$], *trans*-[Pd(L^4-κ*S*,*O*)$_2$] and *trans*-[Pd(L^8-κ*S*,*O*)$_2$] complexes are significantly higher in acetonitrile by factors of *ca* 27, 11 and 7 respectively. The rates of isomerization of the *trans*-[Pd(L^1-κ*S*,*O*)$_2$] and *trans*-[Pd(L^3-κ*S*,*O*)$_2$] complexes are *ca* 5 times higher in acetonitrile compared to chloroform. The isomerization of *trans*-[Pd(L^2-κ*S*,*O*)$_2$] and *trans*-[Pd(L^7-κ*S*,*O*)$_2$] complexes are *ca* 2 times faster in acetonitrile than in chloroform. The higher relative rates of isomerization in acetonitrile suggests that the reaction could involve coordination of an acetonitrile molecule to a vacant coordination site on the Pd atom after a potential Pd-O or Pd-S bond cleavage.

The semi-quantitative kinetic results presented so-far indicate that temperature and the nature of the solvent influences the relative rates of *trans→cis* isomerization of Pd(II) complexes of the *N*,*N*-dialkyl-*N*'-acylthioureas. Although slight changes in the rates of isomerization were observed for some of the complexes studied, there was no obvious trend in the rate *trans→cis* isomerization in both acetonitrile and chloroform based on the electronic effects of ligand substituents. The results also showed that the *trans→cis* isomerization is a first-order reaction in both chloroform and acetonitrile solvents. The rate of isomerization was however found to be independent of the concentration of the *trans*-[Pd(L^4-κ*S*,*O*)$_2$] complex in chloroform. The activation parameters

obtained from the temperature dependence study suggest that the *trans→cis* isomerization involves association between the *trans*-[Pd(L^{1-8}-κ*S*,*O*)$_2$] complexes and another compound present in solution. Balzani and co-workers found out that the presence of free glycine ligands in solution catalyses the thermal *cis→trans* isomerization of *cis*-Pt(gly-κ*N*,*O*)$_2$ complexes.[92] It is therefore possible that the presence of trace amounts of free ligands in solution might have triggered the isomerization of the *trans*-[Pd(L^{1-8}-κ*S*,*O*)$_2$] complexes to their *cis* counterparts. It is on this basis that a ligand exchange study was conducted and this will be presented in the following sections.

6.2.2. Ligand exchange leading to spontaneous *trans→cis* isomerization

6.2.2.1. Ligand exchange between *cis*-[Pd(L^n-κ*S*,*O*)$_2$] complexes

The addition of a *cis*-[Pd(L^A-κ*S*,*O*)$_2$] complex to another *cis*-[Pd(L^B-κ*S*,*O*)$_2$] complex forms a mixed-ligand complex *cis*-[Pd($L^{A,B}$-κ*S*,*O*)$_2$] by ligand exchange. Mixed ligand complexes of the type *cis*-[Pd($L^{A,B}$-κ*S*,*O*)$_2$] can be formed either by exchanging of ligands between *cis*-[Pd(L^A-κ*S*,*O*)$_2$] and *cis*-[Pd(L^B-κ*S*,*O*)$_2$] complexes (Figure 6.12) or by exchanging between a bound ligand HL^A in *cis*-[Pd(L^A-κ*S*,*O*)$_2$] complex and a free unbound HL^B ligands (Figure 6.13)).

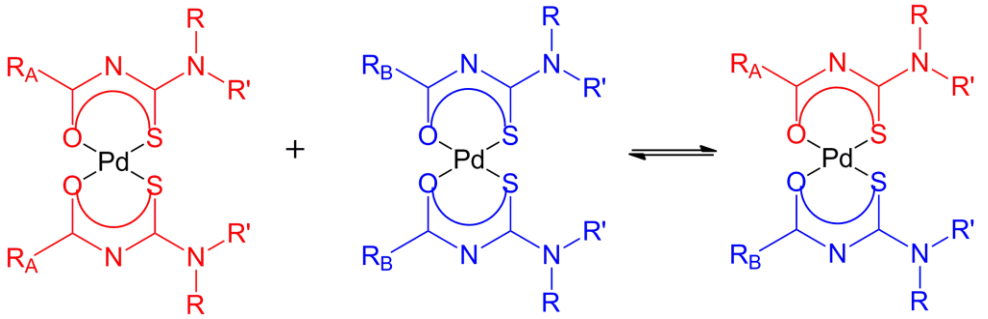

cis-[Pd(L^A-κ*S*,*O*)$_2$] *cis*-[Pd(L^B-κ*S*,*O*)$_2$] *cis*-[Pd($L^{A,B}$-κ*S*,*O*)$_2$]

Figure 6.12. Representation of ligand exchange between *cis*-[Pd(L^A-κ*S*,*O*)$_2$] and *cis*-[Pd(L^B-κ*S*,*O*)$_2$] leading to the formation of mixed ligand complexes in acetonitrile.

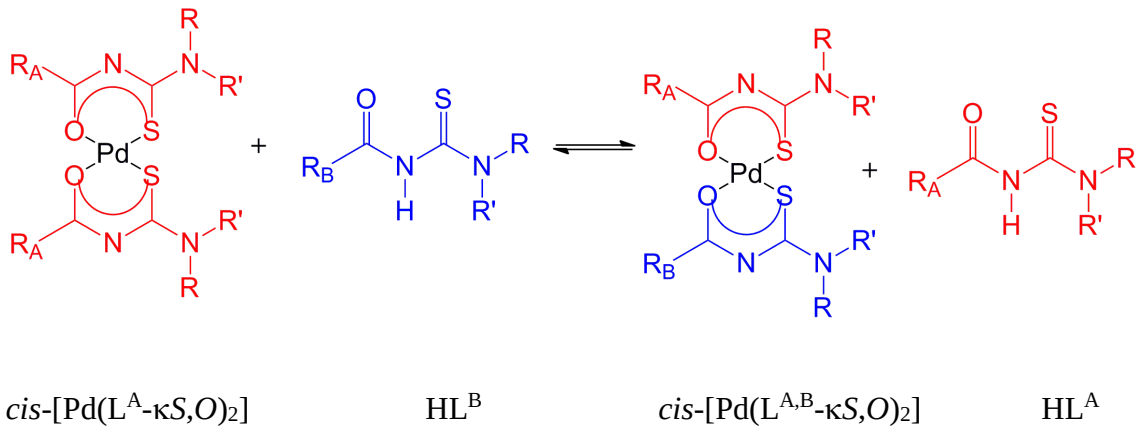

Figure 6.13. Representation of ligand exchange between unbound ligand HL^A and *cis*-[$Pd(L^B$-κ*S*,*O*)$_2$] leading to the formation of mixed ligand complexes in acetonitrile.

The formation of the mixed-ligand complex *cis*-[$Pd(L^{1,6}$-κ*S*,*O*)$_2$] was studied using RP-HPLC by adding equimolar acetonitrile solutions of the *cis*-[$Pd(L^1$-κ*S*,*O*)$_2$] and *cis*-[$Pd(L^6$-κ*S*,*O*)$_2$] complexes followed by injection for RP-HPLC analysis. Figure 6.14 shows the overlaid chromatograms of a mixture of the *cis*-[$Pd(L^1$-κ*S*,*O*)$_2$] and *cis*-[$Pd(L^6$-κ*S*,*O*)$_2$] complexes. The retention times of the pure *cis*-[$Pd(L^1$-κ*S*,*O*)$_2$] and *cis*-[$Pd(L^6$-κ*S*,*O*)$_2$] complexes are 11.3 and 6.9 minutes respectively (Figure 6.14 (a)). After *ca* 10 minutes in the dark, a new peak elutes at retention time of 8.7 minutes and is assigned to the mixed-ligand *cis*-[$Pd(L^{1,6}$-κ*S*,*O*)$_2$] complex. This *cis*-[$Pd(L^{1,6}$-κ*S*,*O*)$_2$] peak could have been formed due to a rapid exchanging of the HL^1 and HL^6 ligands between the *cis*-[$Pd(L^1$-κ*S*,*O*)$_2$] and *cis*-[$Pd(L^6$-κ*S*,*O*)$_2$] complexes. Over a period of time, this peak is observed to grow in intensity with concurrent decreases in the intensities of the *cis*-[$Pd(L^1$-κ*S*,*O*)$_2$] and *cis*-[$Pd(L^6$-κ*S*,*O*)$_2$] peaks, and eventually reaches a steady state after *ca* 8 hours. During this time, a steady state mixture between the *cis*-[$Pd(L^1$-κ*S*,*O*)$_2$], *cis*-[$Pd(L^{1,6}$-κ*S*,*O*)$_2$] and *cis*-[$Pd(L^6$-κ*S*,*O*)$_2$] peaks is obtained in the ratio of 1:2:1 (Figure 6.14 (b)). This relative peak area ratio is consistent with the expected statistical ratio of 1:2:1 for the *cis*-[$Pd(L^1$-κ*S*,*O*)$_2$], *cis*-[$Pd(L^{1,6}$-κ*S*,*O*)$_2$] and *cis*-[$Pd(L^6$-κ*S*,*O*)$_2$] complexes.

The photo-induced isomerization of the mixed-ligand complex *cis*-[$Pd(L^{1,6}$-κ*S*,*O*)$_2$] was then studied by irradiating a mixture of the *cis*-[$Pd(L^1$-κ*S*,*O*)$_2$] and *cis*-[$Pd(L^6$-κ*S*,*O*)$_2$] complexes with polychromatic light from a 5 Watt LED lamp for 30 minutes, followed by injection onto a C_{18} column for RP-HPLC analysis. The observed chromatographic trace for the irradiated mixture

presented in Figure 6.14 (c) clearly evinces the appearance of three additional peaks at 12.3 minutes, 9.4 minutes and 7.5 minutes assigned to *trans*-[Pd(L^1-κ*S*,*O*)$_2$], *trans*-[Pd($L^{1,6}$-κ*S*,*O*)$_2$] and *trans*-[Pd(L^6-κ*S*,*O*)$_2$] respectively. As the irradiation time increases, the peaks representing the three *trans* isomers increase in intensity at the expense of their *cis* counterparts. At steady state, the ratio of the peaks is 1:2:1, consistent with the composition of their *cis* complexes in the unirradiated mixture. When the irradiated mixture was left in the dark, the *trans*-[Pd($L^{1,6}$-κ*S*,*O*)$_2$], *trans*-[Pd(L^1-κ*S*,*O*)$_2$] and *trans*-[Pd(L^6-κ*S*,*O*)$_2$] peaks decrease in intensity at the expense of their *cis* counterparts (Figure A6.5).

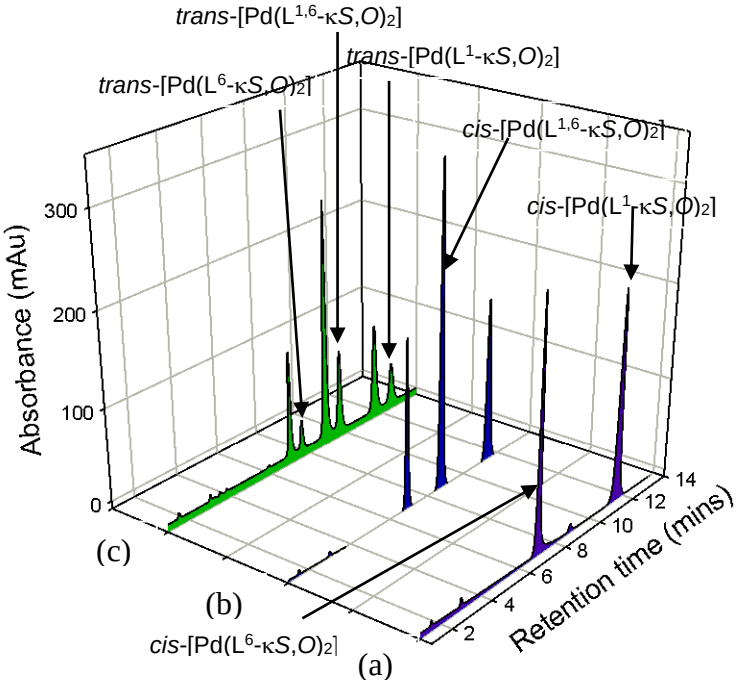

Figure 6.14. Comparison of RP-HPLC chromatograms representing (a) pure *cis*-[Pd(L^1-κ*S*, *O*)$_2$] and *cis*-[Pd(L^6-κ*S*,*O*)$_2$] complexes, (b) ligand exchange in the dark, and (c) *cis*→*trans* isomerization of the mixed-ligand complex *cis*-[Pd($L^{1,6}$-κ*S*,*O*)$_2$]; conditions: mobile phase, 95:5% v/v acetonitrile:water; GEMINI C_{18}, 5 µm, 250 x 4.6 mm column; 20 µl injection volume; 1 $mlmin^{-1}$ flow rate; 262 nm detection; photo-irradiation with a 5 Watt LED lamp.

6.2.2.2. Ligand exchange between *trans*-[Pd(L-κ*S*,*O*)$_2$] and free *N*,*N*-dialkyl-*N*'-acylthioureas studied using ^{1}H NMR spectroscopy

A ligand exchange study was carried out on the isolated *trans*-[Pd(L^4-κ*S*,*O*)$_2$] complex in the presence of the free *N*,*N*-diethyl-*N*'-4-chloro-benzoylthiourea ligand using ^{1}H NMR spectroscopy. The *trans*-[Pd(L^4-κ*S*,*O*)$_2$] complex was selected for this study because it was easier to isolate compared to the other *trans*-[Pd(L^n-κ*S*,*O*)$_2$] complexes. Figure 6.15 shows the changes in relative peak intensity of the H^{2,2} resonances in the *trans*-[Pd(L^4-κ*S*,*O*)$_2$] complex in chloroform-*d* with and without the addition of 1 mol % the HL^4 ligand as a function of time in the dark. This highlights the profound effect of the presence of free ligands on the rates of *trans*→*cis* isomerization. It is evident that the *trans* resonances immediately collapse at the expense of the *cis*-resonances upon addition of 1 mol % of the ligand. This indicates that the HL^4 ligand initially bound to the *trans*-[Pd(L^4-κ*S*,*O*)$_2$] complex is expelled by the free added HL^4 ligand in solution during the course of the reaction. A rapid decrease in the intensity of the *trans*-H$^{2',2}$ resonances occurs upon addition of 1 mol % of the HL^4 ligands and within 10 minutes, the *trans*-[Pd(L^4-κ*S*,*O*)$_2$] complex was completely converted to its *cis*-[Pd(L^4-κ*S*,*O*)$_2$] isomer. A similar rapid decrease in rate was observed when 1 mol % of another ligand *N*,*N*-diethyl-*N*'-4-methoxy-benzoylthiourea was added to the solution of *trans*-[Pd(L^4-κ*S*,*O*)$_2$] in the absence of light (Figure A6.6). This suggests that the primary role of the added ligands is to act as a proton donor leading to a chelate ring opening and consequently higher *trans*→*cis* reaction rates. Confirmation of the role of free ligands was achieved by the addition of *N*,*N*,*N*',*N*'-tetramethyl-1,8-naphthalenediamine (TMND) which acts as a 'proton sponge' and should decrease the amount of free ligands or protons in the chloroform-*d* solution. Addition of an excess of the 'proton sponge' solution in chloroform-*d* to a solution of the *trans*-[Pd(L^4-κ*S*,*O*)$_2$] complex leads to a significant decrease in the relative rates of *trans*→*cis* isomerization as shown in Figure 6.15.

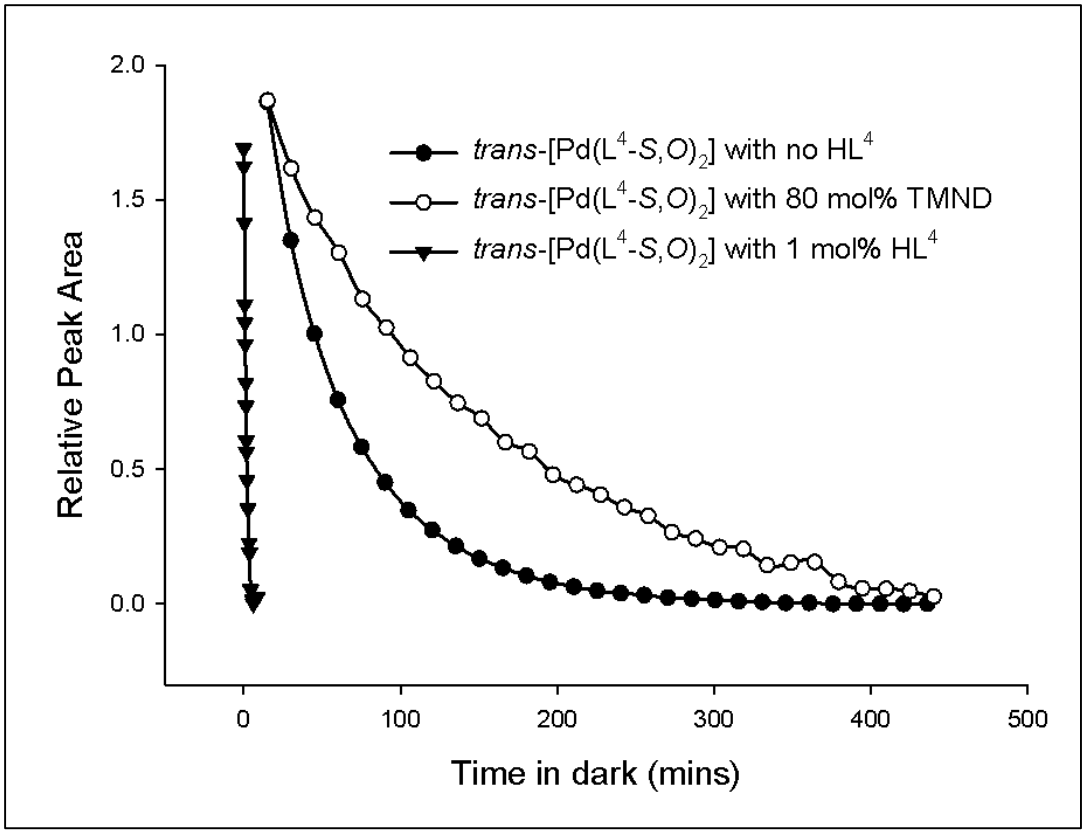

Figure 6.15. Plots of relative peak area versus time in the dark, for *trans*→*cis* isomerization of *trans*-[Pd(L^4-κ*S*,*O*)$_2$] without and with the additions of HL^4 and *N*,*N*,*N*',*N*'-tetramethyl-1,8-naphthalenediamine (TMND) in chloroform-*d* at 25 °C.

The effect of concentration of the added *N*,*N*-dialkyl-*N*-acylthioureas on the relative rates of *trans*→*cis* isomerization was further investigated while keeping all other factors constant. To achieve this, three samples of the *trans*-[Pd(L^4-κ*S*,*O*)$_2$] complex with the same concentration (11.06 mM) were prepared in chloroform while varying concentration of the *N*,*N*-diethyl-*N*'-4-chloro-benzoylthiourea (HL^4) ligand at 25 °C, as shown in Table 6.4. Ligand concentrations > 0.12 mM could not be used as the *trans*→*cis* reactions were too fast under these conditions to be monitored by ^{1}H NMR spectroscopy. The reaction was followed by monitoring the decrease in intensity of the ^{1}H NMR signals. The changes in *trans*-$H^{2,2}$ resonance intensities of the *trans*-[Pd(L^4-κ*S*,*O*)$_2$] complex at different ligand concentrations are depicted in the arrayed ^{1}H NMR spectra provided in Figure A6.7. The estimated rate constants representing the relative rates of ligand-catalysed *trans*→*cis* isomerization are presented in Table 6.4, while the representative changes in relative peak intensity of the *trans*-$H^{2,2}$ resonances associated with the process are given

in Figure 6.16. It is evident from the rate constant values that the relative rates of *trans→cis* isomerization increase linearly with increase in concentration of HL^4 ligand. This indicates that the reaction is first-order with respect to the concentration of the added ligands. This first order increase in rate with increase in ligand concentration is consistent with a direct attack by free ligands on the *trans*-[Pd(L^4-κ*S*,*O*)$_2$] complex and supports an associative ligand exchange process during *trans→cis* isomerization.

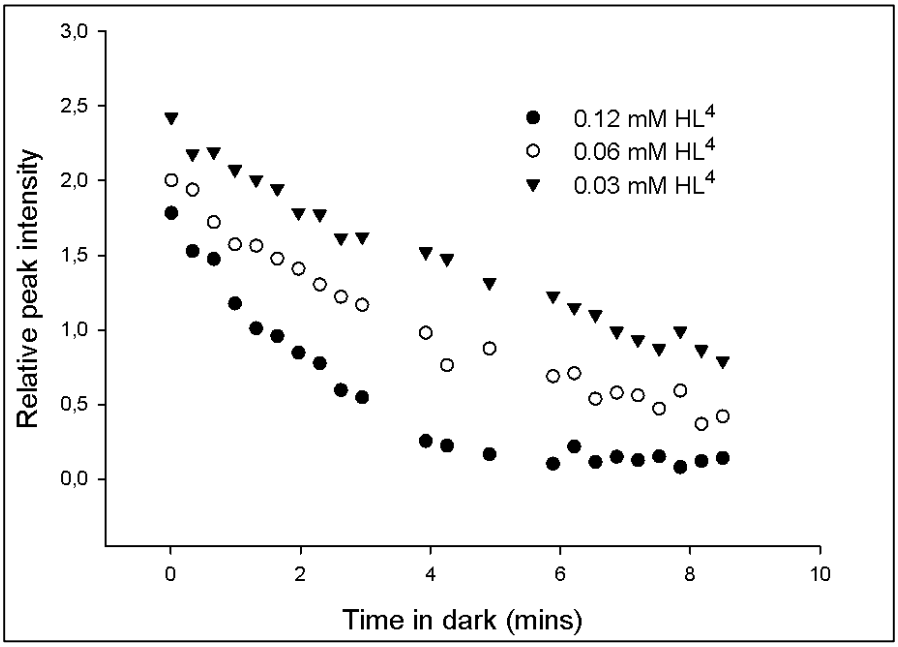

Figure 6.16. Plots of relative peak intensity versus time in dark for *trans→cis* isomerization of *trans*-[Pd(L^4-κ*S*,*O*)$_2$ in chloroform-*d*, at different concentrations of *N*,*N*-diethyl-*N*'-4-chlro-benzoylthiourea (HL^4) at 25 °C.

Table 6.4. Rate constants for *trans→cis* isomerization of *trans*-[Pd(L^4-κ*S*,*O*)$_2$] in chloroform-*d* after addition of different concentrations of HL^4 ligand at 25°C.

Ligand	**[*trans*-[Pd(L^4-κ*S*,*O*)$_2$]] (mM)**	**[HL^4] (mM)**	**k x 10^{-1} (s^{-1})**
HL^4	11.06	0.12	4.0 (±0.3)
	11.06	0.06	2.1 (±0.8)
	11.06	0.03	1.0 (±0.4)

6.2.2.3. Ligand exchange between *trans*-[Pd(L-κ*S*,*O*)$_2$] and free *N*,*N*-dialkyl-*N*'-acylthioureas studied using RP-HPLC

In order to provide further evidence on ligand exchange during *trans→cis* isomerization, the ligand catalysed reactions were also studied using RP-HPLC in acetonitrile. This was carried out be dissolving 2 mg of each *cis*-[Pd(L$^{1\text{-}8}$-κ*S*,*O*)$_2$] complex in 10 ml acetonitrile. After this, 1 ml of the solution of each complex was irradiated for 30 minutes with a 5 Watt LED lamp in order to allow sufficient time for a steady state to be attained. 250 µl of a solution containing 1.6 mg of the *N*,*N*-dialkyl-*N*'-acylthiourea ligands in 10 ml acetonitrile was then added to the irradiated solution. The resulting mixture was rapidly injected onto a C_{18} column at intervals of *ca* 12-16 minutes in the absence of light. Figures 6.17 (a) and (b) show the overlaid chromatograms representing irradiated acetonitrile solutions of *cis*-[Pd(L^1-κ*S*,*O*)$_2$] and *cis*-[Pd(L^7-κ*S*,*O*)$_2$] respectively to which solutions of excess *N*,*N*-diethyl-*N*'-benzoylthiourea (HL^1) and *N*,*N*-diethyl-*N*'-1-napthoylthiourea (HL^7) ligands were respectively added. It is evident from both chromatograms that the peaks corresponding to either the *trans*-[Pd(L^1-κ*S*,*O*)$_2$] or *trans*-[Pd(L^7-κ*S*,*O*)$_2$] isomer rapidly vanishes within 10 minutes upon addition of both HL ligands. Without the addition of free ligands, complete reversion of the *trans*-[Pd(L-κ*S*,*O*)$_2$] complexes in acetonitrile occurred after *ca* 2 hours (Figures 4.6 and 6.8). The resulting chromatograms (Figure 6.16 (a) and (b)) obtained from addition of the free ligands show only peaks of added ligands and the *cis*-[Pd(L^1-κ*S*,*O*)$_2$] or *cis*-[Pd(L^7-κ*S*,*O*)$_2$] isomer. For both *cis*-[Pd(L^1-κ*S*,*O*)$_2$] and *cis*-[Pd(L^7-κ*S*,*O*)$_2$] complexes, the relative rates of collapse of the *trans*-isomers were too rapid to be monitored by RP-HPLC. In comparison, the relative rate of collapse of *trans*-[Pd(L^7-κ*S*,*N*)$_2$] isomer is much lower.

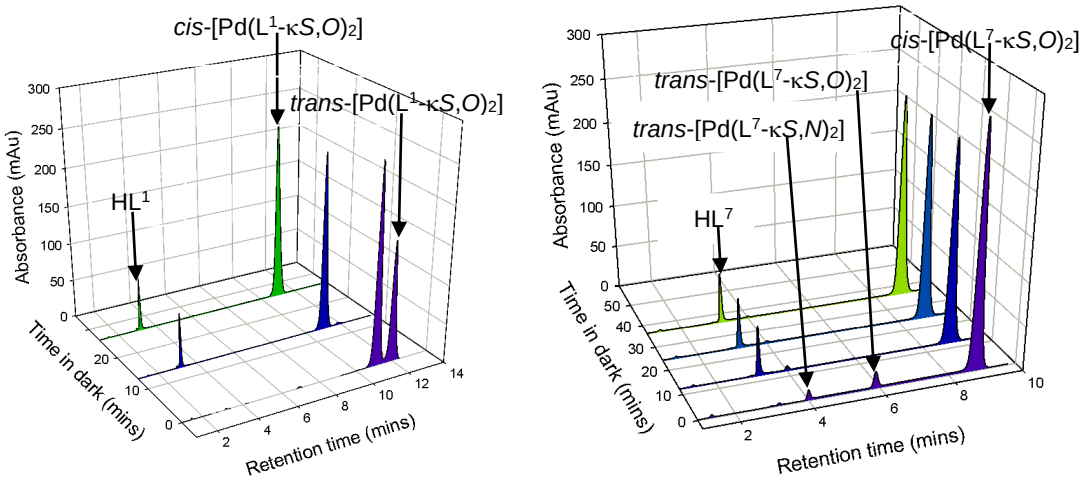

Figure 6.17. Overlaid chromatograms showing ligand exchange during *trans→cis* isomerization for solutions of (a) *cis*-[Pd(L^1-κ*S*,*O*)$_2$] and (b) *cis*-[Pd(L^7-κS,O)$_2$], to which solutions of HL^1 and HL^7 are respectively added; solutions pre-irradiated with a 5Watt LED lamp and allowed in the dark for subsequent time periods; conditions: mobile phase, 95:5% v/v acetonitrile:water; GEMINI C_{18}, 5 µm, 250 x 4.6 mm column; 20 µl injection volume; 1 $mlmin^{-1}$ flow rate; 262 nm detection.

Tables 6.5 and A6.1 show the changes in peak areas for *trans*-[Pd(L^7-κ*S*,*N*)$_2$] and *trans*-[Pd(L^1-κ*S*,*O*)$_2$] complexes respectively after additions of solutions of the HL^7 and HL^1 ligands. An interesting observation can be made by closer inspection of the changes in peak intensities. It is evident that with time, both the *cis*-[Pd(L^1-κ*S*,*O*)$_2$] and *cis*-[Pd(L^7-κ*S*,*O*)$_2$] complexes initially experience a slight decrease during the first 12 minutes of the reaction, after which their peak intensity almost remain invariant over time as the reaction goes to completion. The initial decrease in peak intensity of the *cis*-[Pd(L^n-κ*S*,*O*)$_2$] complexes is consistent with a mutual exchange of the HL ligands in the *cis*-*trans* complexes. It is thus possible that the free ligand initially reacts with the *trans*-[Pd(L^a-κ*S*,*O*)$_2$] isomer in the irradiated mixture to rapidly form the *cis*-[Pd(L^a-κ*S*,*O*)$_2$] isomer. This could then undergo ligand exchange with the other *cis*-[Pd(L^b-κ*S*,*O*)$_2$] complex.

Table 6.5. Changes in peak areas for the ligand catalysed *trans→cis* isomerization of *trans*-[Pd(L^7-κ*S*,*O*)$_2$] complexes in the dark, following pre-irradiation in acetonitrile with a 5 Watt LED lamp at 25 °C.

Time(mins)	Peak area of HL^7	Peak area of *trans*-[Pd(L^7-κ*S*,*N*)$_2$]	Peak area of *trans*-[Pd(L^7-κ*S*,*O*)$_2$]	Peak area of *cis*-[Pd(L^7-κ*S*,*O*)$_2$]
0	-	72.053	151.731	3794.428
12	69.876	69.534	20.387	2930.793
24	67.173	42.298	-	3042.412
36	66.600	24.397	-	3088.591
48	66.205	14.588	-	3103.511
60	65.697	9.380	-	3116.914

(a) (b)

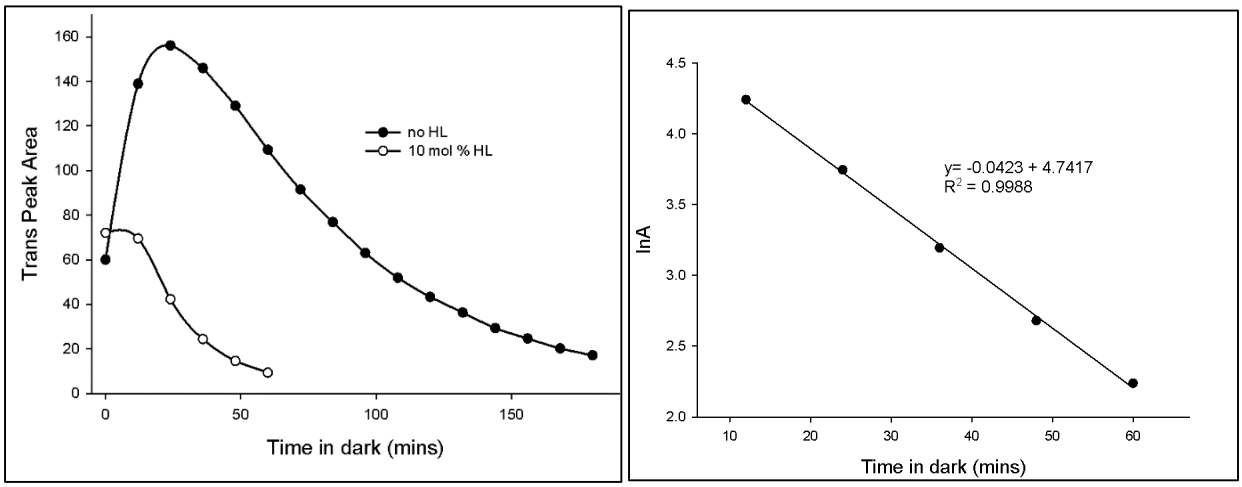

Figure 6.18. Plots of (a) relative peak area (A) and (b) natural logarithm of relative peak area (A) *vs.* time in dark for the *trans→cis* isomerization of *trans*-[Pd(L^7-κ*S*,*N*)$_2$] in acetonitrile at 25 °C, with and without addition of solutions of HL^7 ligand; photodiode array detection at 262 nm.

The relatively lower rate of ligand-catalysed *trans→cis* isomerization of the *trans*-[Pd(L^7-κ*S*,*N*)$_2$] complex in acetonitrile after addition of the HL^7 ligand enabled monitoring of disappearance of the *trans*-[Pd(L^7-κ*S*,*N*)$_2$] peaks as a function of time in dark as shown in Figure 6.18 (a). The slope of the plot of the natural logarithm of the peak areas versus time in the dark

(Figure 6.17 (b)) gives a rate constant k value of 4.23 x 10^{-2} min^{-1} with addition of the HL^7 ligand. This is more than 4 times higher than the rate of *trans→cis* isomerization of the *trans*-[Pd(L^7-κ*S*,*N*)$_2$] complex in the absence the HL^7 ligand (k = 1.01 x 10^{-2} min^{-1}).

The RP-HPLC results observed so far indicate that the addition of excess *N*,*N*-dialkyl-*N*'-acylthioureas to a pre-irradiated mixture of the *cis-trans* isomers rapidly consumes the *trans*-[Pd(L^n-κ*S*,*O*)$_2$] isomers, leaving behind only its *cis* counterpart, while the ligand itself is regenerated at the end of the process. These results suggest that the added ligands act as proton donors to assist in a potential Pd-O or Pd-S bond cleavage. Further confirmation of the possible role of the ligand as a proton donor was provided by repeating the experiment in a protic solvent methanol without the addition of excess ligand. Irradiation of *ca* 2 mg of the *cis*-[Pd(L^1-κ*S*,*O*)$_2$] complex in 10 ml of methanol was carried after which the solution was injected for RP-HPLC analysis. The irradiated solution was then left in the dark with subsequent RP-HPLC injection after every 12 minutes, yielding the overlaid chromatograms in Figure 6.19. It is evident that rapid collapse of the *trans*-[Pd(L^1-κ*S*,*O*)$_2$] peak was also observed within 12 minutes even without the addition of excess HL ligands. This suggests that methanol catalyses the *trans→cis* isomerization by donating a proton to the *trans*-[Pd(L^1-κ*S*,*O*)$_2$] complex, leading to dechelating of the *trans*-[Pd(L^1-κ*S*,*O*)$_2$] complex in the same way as when the free *N*,*N*-dialkyl-*N*'-acylthiourea ligands were added. Methanol has a slight higher donor number (19 kcal/mol) than acetonitrile (14.1 kcal/mol). Hence it is also possible that the rapid collapse of the RP-HPLC could have been as a result of increased donor ability of methanol to coordinate to the Pd(II) ion.

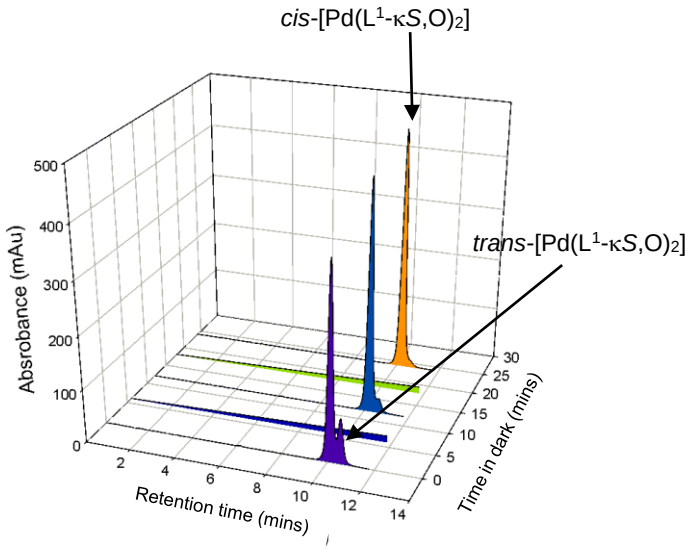

Figure 6.19. Overlaid RP-HPLC chromatograms showing *trans→cis* isomerization of *cis*-[Pd(L^1-κ*S*,*O*)$_2$] in methanol; solution pre-irradiated with a 5Watt LED lamp and allowed in the dark for subsequent time periods; conditions: mobile phase, 95:5% v/v methanol:water; GEMINI C_{18}, 5 µm, 250 x 4.6 mm column; 20 µl injection volume; 1 mlmin^{-1} flow rate; 262 nm detection.

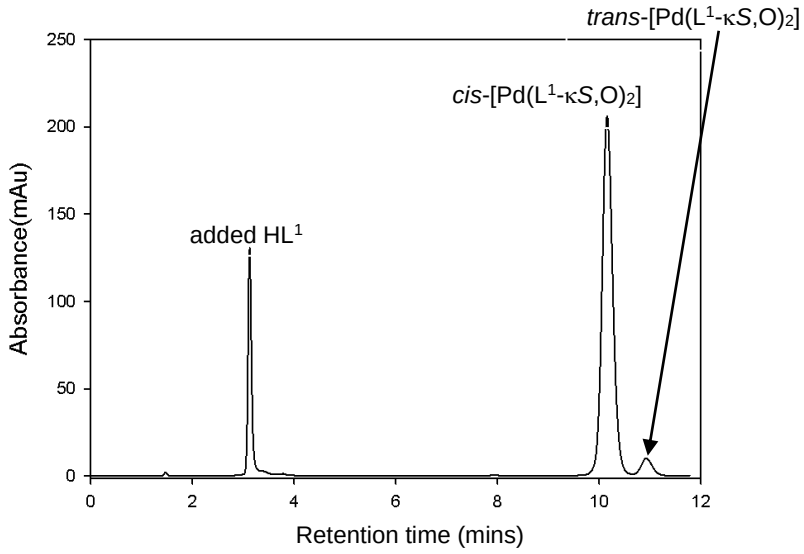

Figure 6.20. RP-HPLC chromatogram a solution of *cis*-[Pd(L^1-κ*S*,*O*)$_2$] pre-irradiated with a 5 Watt LED lamp for 30 min in the presence of excess HL^1 ligand; conditions: mobile phase, 95:5% v/v acetonitrile:water; GEMINI C_{18}, 5 µm, 250 x 4.6 mm column; 20 µl injection volume; 1 mlmin^{-1} flow rate; 262 nm detection.

Further evidence of a ligand catalysed *trans→cis* isomerization was provided by irradiating an acetonitrile mixture of the *cis*-[Pd(L^1-κ*S*,*O*)$_2$] complex and excess the HL^1 ligand (70 mol %) with polychromatic light. By comparing the resulting RP-HPLC chromatogram (Figure 6.20) with that of the irradiated *cis*-[Pd(L^1-κ*S*,*O*)$_2$] complex in the absence of ligands (Figure 6.8), it is evident that a relatively small proportion of the *trans*-[Pd(L^1-κ*S*,*O*)$_2$] isomer (*ca* 5%) is present in the irradiated solution of the *cis*-[Pd(L^1-κ*S*,*O*)$_2$] complex after addition of the HL^1 ligand even after 30 minutes of irradiation with polychromatic light. This indicates that the presence of the excess ligand inhibits the formation of the *trans*-[Pd(L^1-κ*S*,*O*)$_2$] isomer from photo-induced isomerization of its *cis*-[Pd(L^1-κ*S*,*O*)$_2$] counterpart.

6.2.3. RP-HPLC evidence of formation of mixed-ligand complexes

From the previous sections, it has been shown that ligand exchange caused by free ligands in solution could assist in the spontaneous *trans→cis* isomerization for the *trans*-[Pd(L^{1-8}-κ*S*,*O*)$_2$] complexes. If this is so, then a catalysed *trans*-[Pd(L^{1-8}-κ*S*,*O*)$_2$] reversion to *cis*-[Pd(L^{1-8}-κ*S*,*O*)$_2$] should still occur irrespective of which HL^n ligand is used. This was investigated by adding 10 mol % solutions of other HL^n ligands to the pre-irradiated acetonitrile solutions of the *cis*-[Pd(L^1-κ*S*,*O*)$_2$] complex and monitoring the reaction by RP-HPLC as a function of time in the dark. Figure 6.21 (a) shows the RP-HPLC chromatogram obtained from addition of *N*,*N*-dimethyl-*N*'-benzoylthiourea (HL^6) to a pre-irradiated solution of the *cis*-[Pd(L^1-κ*S*,*O*)$_2$] complex. It is evident that the reactions taking place between the added HL^6 ligand and the irradiated *trans*-[Pd(L^1-κ*S*,*O*)$_2$] complex conform with formation of a stable mixed-ligand complex. Upon addition of the HL^6 ligand to the irradiated solution of the *cis*-[Pd(L^1-κ*S*,*O*)$_2$] complex, the *trans*-[Pd(L^1-κ*S*,*O*)$_2$] isomer which was seen to elute at 11.8 minutes (Figure 6.8 (a)) quickly vanishes after 12 minutes in the dark. In addition to the *cis*-[Pd(L^1-κ*S*,*O*)$_2$] and *cis*-[Pd(L^6-κ*S*,*O*)$_2$] peaks, a new peak assigned to the mixed-ligand complex *cis*-[Pd($L^{1,6}$-κ*S*,*O*)$_2$] appears in the chromatogram after addition of the free HL^6 ligand. The added HL^6 ligand which elutes after 2.8 minutes therefore exchanges with the HL^1 ligand bound to the *trans*-[Pd(L^1-κ*S*,*O*)$_2$] complex forming HL^1 (retention time of 3.3 minutes), *cis*-[Pd(L^6-κ*S*,*O*)$_2$] (retention time of 7.1 minutes), and the mixed-ligand complex *cis*-[Pd($L^{1,6}$-κ*S*,*O*)$_2$] (retention time of 8.9 minutes), while the HL^6 ligand is regenerated.

The ligand-exchange product *cis*-[Pd($L^{1,6}$-κ*S*,*O*)$_2$] was identified by comparison of its retention time with that observed in Figure 6.14 for the reaction of *cis*-[Pd(L^1-κ*S*,*O*)$_2$] and *cis*-[Pd(L^6-κ*S*,*O*)$_2$] complexes. Also, the UV spectra of the ligands and complexes present in the representative RP-HPLC chromatograms (Figure 6.21 (b)) were compared with those of pure authentic HL ligands and *cis*-[Pd(L-κ*S*,*O*)$_2$] complexes.

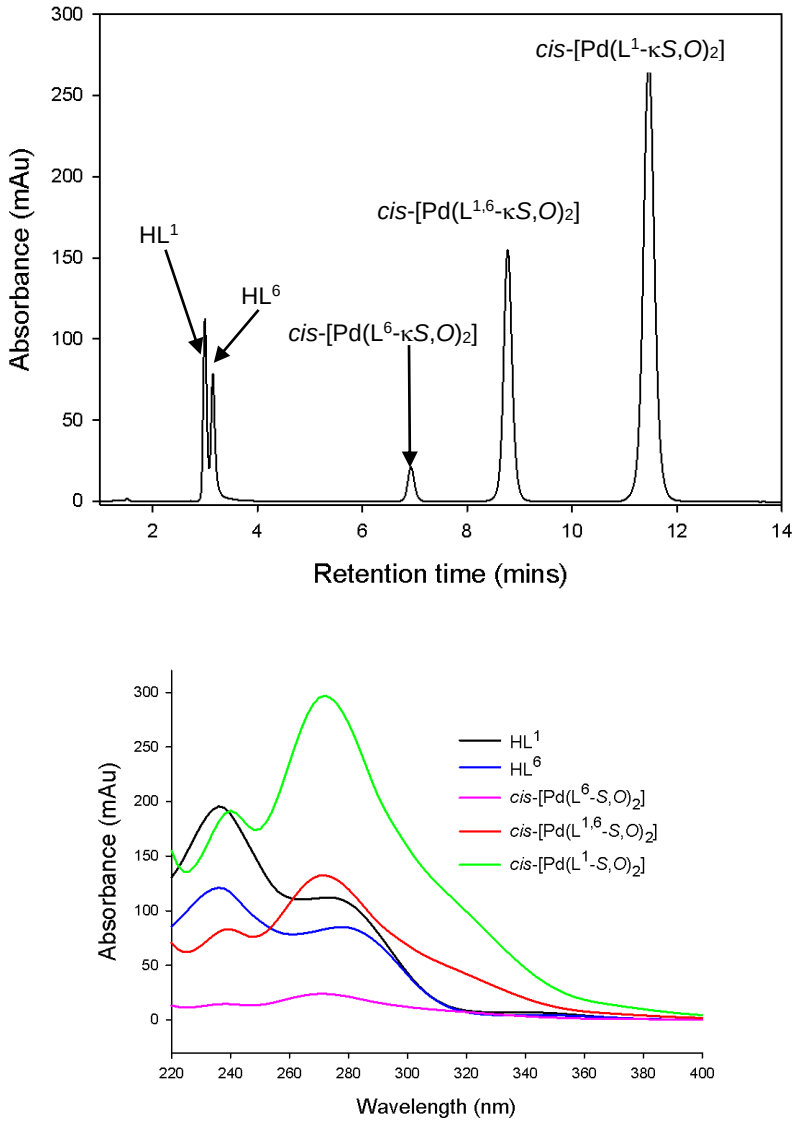

Figure 6.21. **(a)** Representative RP-HPLC chromatogram showing products of ligand exchange following addition of acetonitrile for solution HL^6 to a solution of *cis*-[Pd(L^1-κ*S*,*O*)$_2$] pre-irradiated with a 5Watt LED lamp; conditions: mobile phase, 95:5 %v/v acetonitrile:water; GEMINI C_{18}, 5 µm, 250 x 4.6 mm column; 20 µl injection volume; 1 mlmin^{-1} flow rate; 262 nm detection; **(b)** UV-Vis spectra from photodiode array detection at 262nm for ligand exchange products from addition of HL^6 to a pre-irradiated solution of *trans*-[Pd(L^1-κ*S*,*O*)$_2$] in acetonitrile at room temperature.

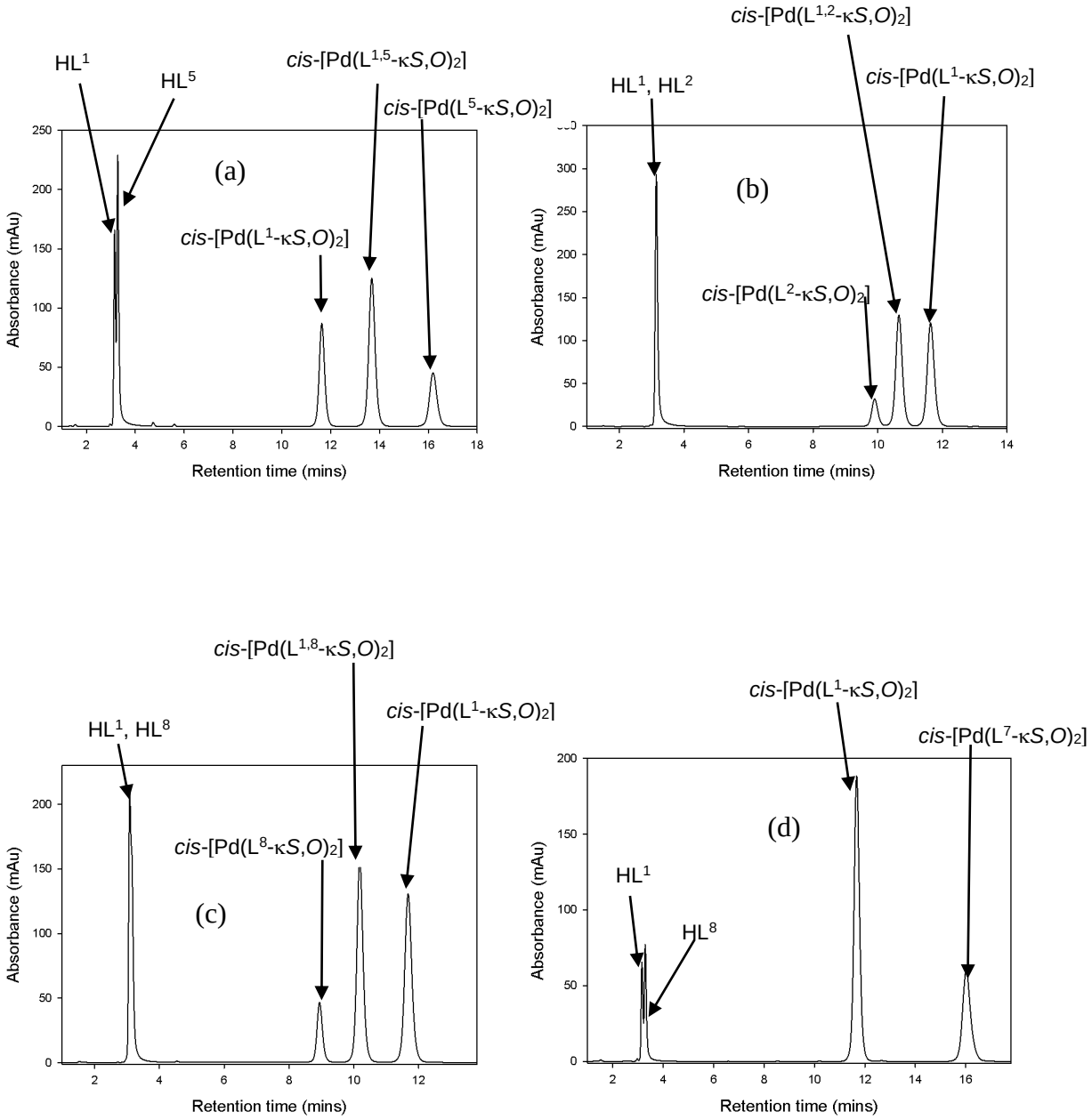

Figure 6.22. RP-HPLC chromatograms showing peaks from formation of ligand exchange products when acetonitrile solutions of (a) HL^2, (b) HL^5, (c) HL^8 and (d) HL^7 were added to solutions of *cis*-[Pd(L^1-κ*S*,*O*)$_2$] pre-irradiated with a 5Watt LED lamp; conditions: mobile phase, 95:5% v/v acetonitrile:water; GEMINI C_{18}, 5 µm, 250 x 4.6 mm column; 20 µl injection volume; 1 $mlmin^{-1}$ flow rate; 262 nm detection.

The catalysed *trans*-*cis* isomerization was also studied in acetonitrile with addition of the other *N*,*N*-dialkyl-*N*'-acylthioureas ($HL^{2,5,7,8}$) to the irradiated mixture of the *cis*-[Pd(L^1-κ*S*,*O*)$_2$] complex. A 0.385 mM solution of the *cis*-[Pd(L^1-κ*S*,*O*)$_2$] complex was irradiated for 30 minutes with polychromatic light after which 10 µl of solutions of the ligands HL^2, HL^5, HL^7 and HL^8 were separately added. Figures 6.22 (a)-(d) show the representative chromatograms for the resulting ligand-exchange products obtained. The UV-Vis spectra used for assigning the peaks are provided in Figure A6.8. A common feature in all the chromatographic traces is the presence of peaks for both the HL^1 and the added HL^n ligands between 2-3 minutes retention time. These peaks overlap for the HL^2 and HL^8 ligands which are closely retained to the HL^1 ligand on the C_{18} column. With the exception of the HL^7 ligand, peaks corresponding to mixed-ligand complexes are seen in all the chromatograms between the peaks of the two initial *cis* complexes. The mixed-ligand complex *cis*-[Pd($L^{1,8}$-κ*S*,*O*)$_2$] elutes after 10.2 minutes (Figure 6.21 (c)) between the *cis*-[Pd(L^1-κ*S*,*O*)$_2$] and *cis*-[Pd(L^8-κ*S*,*O*)$_2$] complexes (retention time of 8.9 minutes). Figure 6.21 (d) shows that no mixed-ligand complex *cis*-[Pd($L^{1,7}$-κ*S*,*O*)$_2$] is formed between *cis*-[Pd(L^1-κ*S*,*O*)$_2$] and *cis*-[Pd(L^7-κ*S*,*O*)$_2$] (retention time of 16.0 minutes). This exceptional behaviour observed for the *cis*-[Pd(L^7-κ*S*,*O*)$_2$] complex can be ascribed to steric or electronic influence of the presumably bulky naphthyl group. This could also be associated with the unprecedented formation of a *trans*-[Pd(L^7-κ*S*,*N*)$_2$] isomer from photo-induced isomerization of the *cis*-[Pd(L^7-κ*S*,*O*)$_2$] complex as was observed in chapter 4.

6.3. Conclusions

In conclusion, the *trans*-[Pd(L^{1-8}-κ*S*,*O*)$_2$] complexes isolated in chapters 3 and 4 were successfully utilized to study the relative rates of thermal *trans→cis* isomerization in chloroform-*d*. While there appear to be some influence of ligand substituents particular for *p*-substituted groups on the phenyl rings, the effect is not particularly overwhelming. Slight decreases in rates of isomerization were observed by the introduction of electron releasing methoxy and methyl substituents at the *para* position of the phenyl ring. The relative rates of *trans→cis* isomerization were also successfully studied using RP-HPLC after irradiation of the *cis*-[Pd(L^{1-8}-κ*S*,*O*)$_2$] complexes. Three main factors namely temperature, solvent and presence of trace amounts of ligands were found to influence the relative rate of conversion of the *trans*-[Pd(L^{1-8}-κ*S*,*O*)$_2$] complexes into their more thermodynamically stable *cis*-[Pd(L^{1-8}-κ*S*,*O*)$_2$] isomers. The relative rates of first-order *trans→cis* isomerization were significantly higher in acetonitrile compared to chloroform. This can be attributed to the ability of acetonitrile to coordinate to the Pd atom thereby assisting either the Pd-O or Pd-S bond cleavage and leading to faster reaction rates. An increase in temperature in the range 25 to 55 °C also resulted in an increase in rate of *trans→cis* isomerization. Large negative entropy of activation and positive enthalpy of activation values were obtained for the *trans→cis* reaction of the *trans*-[Pd(L^4-κ*S*,*O*)$_2$] complex indicative of association between the complex and free HL^4 ligands in solution.

The addition of trace amounts of free HL ligands to solutions of the *trans*-[Pd(L^{1-8}-κ*S*,*O*)$_2$] complexes was found to catalyse the *trans→cis* isomerization, resulting in a rapid collapse of the *trans*-H^1 NMR and RP-HPLC peaks. In addition, a first-order increase in the rates of *trans→cis* isomerization was observed with increase in ligand concentration. The results revealed that the free ligands in solution presumably act as a proton donor coordinating to the nitrogen atom and presumably resulting in ring opening of the six-membered chelate. These results were supported by the fact that addition of *N*,*N*,*N*',*N*'-tetramethyl-1,8-naphthalene diamine used as a 'proton sponge' led to a decrease in the rates of *trans→cis* isomerization. In a protic solvent methanol, the *trans→cis* isomerization was faster compared to acetonitrile without the addition of excess ligand solution. Evidence of ligand exchange following *trans→cis* isomerization was also provided by the formation of mixed-ligand complexes of the type *cis*-[Pd($L^{a,b}$-κ*S*,*O*)$_2$] from representative RP-HPLC chromatograms and LC-UV spectra.

7

Concluding remarks and discussions

The results compiled in this thesis reveal that the direct addition of Pt(II) or Pd(II) to the *N*,*N*-dialkyl-*N*'-acyl(aroyl)thioureas form exclusively *cis*-[M(L^{1-15}-κ*S*,*O*)$_2$] (M = Pt(II) or Pd(II)) complexes. It was evident that the *trans*-[M(L^{1-8}-κ*S*,*O*)$_2$] isomers can only be reliably prepared by photo-induced isomerization of their *cis*-[M(L^{1-8}-κ*S*,*O*)$_2$] counterparts after irradiation in acetonitrile with polychromatic light. Photo-induced isomerization of the *cis*-[Pd($L^{1-6,8}$-κ*S*,*O*)$_2$] complexes with the *N*,*N*-di-substituted benzoylthioureas ($HL^{1-6,8}$) formed only the *trans*-[Pd($L^{1-6,8}$-κ*S*,*O*)$_2$] isomers. Irradiation of *cis*-bis(*N*,*N*-diethyl-*N*'-1-naphthylthioureato-κ^2*S*,*O*)palladium(II) with polychromatic light uniquely produced a four-membered *trans*-[Pd(L^7-κ*S*,*N*)$_2$] complex in addition to the *trans*-[Pd(L^7-κ*S*,*O*)$_2$] isomer. To the best of our knowledge, this *trans*-[Pd(L^7-κ*S*,*N*)$_2$] isomer represents the first example of a *trans*-κ*S*,*N* complex of the *N*,*N*-dialkyl-*N*'-acylthioureas with Pd(II). The reactions that led to the formation of the *trans*-[Pd(L^{1-8}-κ*S*,*O*)$_2$] and *trans*-[Pd(L^7-κ*S*,*N*)$_2$] complexes are summarized in Figure 7.1.

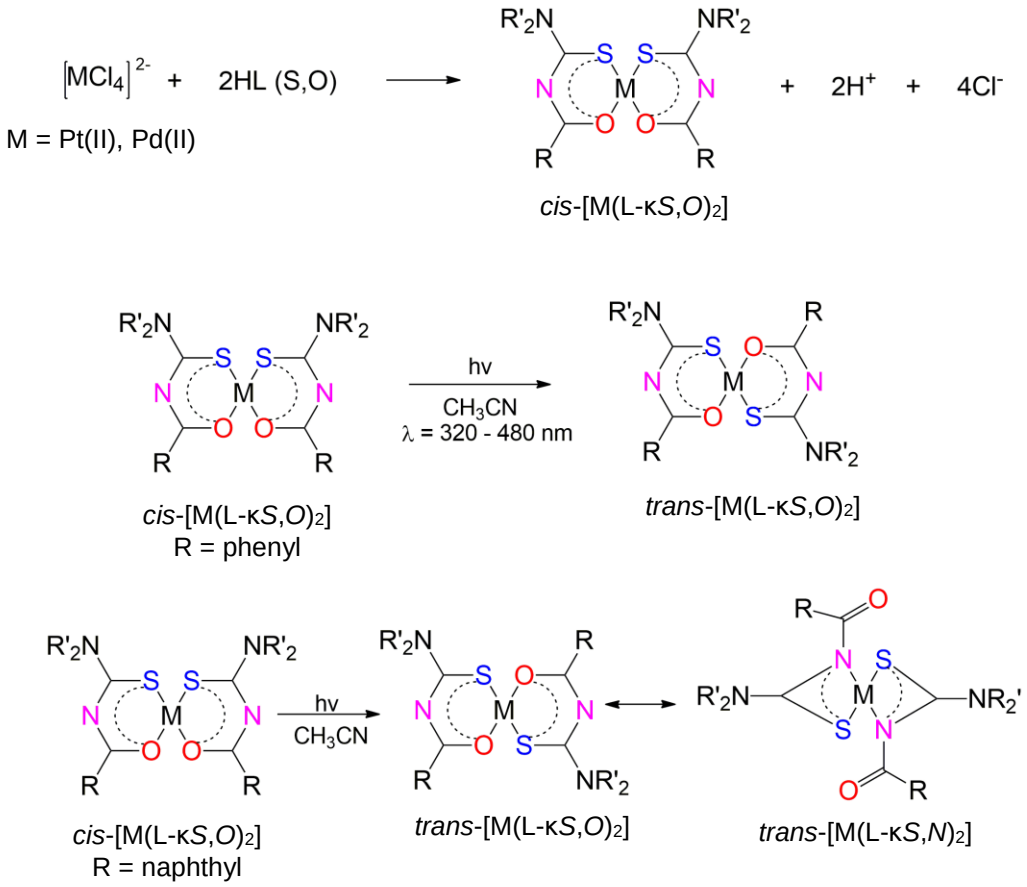

Figure 7.1. General scheme for the preparation of *cis*-[M(L^{1-8}-κ*S*,*O*)$_2$], *trans*-[M(L^{1-8}-κ*S*,*O*)$_2$] and *trans*-[Pd(L^7-κ*S*,*N*)$_2$] complexes.

The results further showed that solid forms of the *trans*-[Pd(L^{1-8}-κ*S*,*O*)$_2$] and *trans*-[Pd(L^7-κ*S*,*N*)$_2$] complexes of the *N*,*N*-di-substituted acylthioureas can be isolated in high yields by photo-induced *cis*→*trans* isomerization accompanied by vapour diffusion or slow evaporation. The isolated *trans*-[Pd(L^{1-8}-κ*S*,*O*)$_2$] complexes were found to be less soluble in both acetonitrile and chloroform. Hence it is more likely that the difference in solubility of the *cis*-*trans* isomers in acetonitrile accounts for the isolation of the *trans*-[Pd(L^{1-8}-κ*S*,*O*)$_2$] complexes in preference to the *cis*-[Pd(L^{1-8}-κ*S*,*O*)$_2$] complexes upon continuous light exposure. Significantly higher melting points were obtained for the isolated *trans*-[Pd(L^{1-8}-κ*S*,*O*)$_2$] complexes compared to their *cis*-[Pd(L^{1-8}-κ*S*,*O*)$_2$] counterparts. This could be indicative of a higher solvation energy of the *trans*-[Pd(L^{1-8}-κ*S*,*O*)$_2$] isomers compared to the *cis*-[Pd(L^{1-8}-κ*S*,*O*)$_2$] isomers and is supported by a lower relative solubility in acetonitrile observed for the *trans*-[Pd(L^{1-8}-κ*S*,*O*)$_2$] complexes. The unusual photo-induced formation of the *trans*-[Pd(L-κ*S*,*N*)$_2$] isomer only for *cis*-bis(*N*,*N*-diethyl-*N*'-1-naphthylthioureato-κ^2*S*,*O*)palladium(II) is presumably caused by the steric or electronic effect of the naphthyl groups although it remains unclear which of these factors dominate. An inspection of the single-crystal X-ray structure of the *cis*-bis(*N*,*N*-diethyl-*N*'-1-naphthylthioureato-κ^2*S*,*O*)palladium(II) complex suggests that its unprecedented photochemical behaviour is more likely influenced by steric effects of the naphthyl groups. The ability of nitrogen atom in the chelate to act as a potential donor atom presumably increases by the presence of these groups. Hence the sterically hindered naphthyl groups could have enhanced the donor capacity of the nitrogen atom and consequently its ability to re-coordinate to the Pd(II) ion in preference to the oxygen atom during the photo-induced *cis*→*trans* isomerization. On electronic grounds, the naphthyl groups could have increased the nucleophilicity of the nitrogen atom relative to the oxygen atom leading to preferential coordination of the Pd(II) nitrogen and leaving the oxygen donor atom free in the resulting *trans*-[Pd(L^7-κ*S*,*N*)$_2$] complex. For monosubstituted acylthioureas, the formation of structures similar to *trans*-[Pd(L^7-κ*S*,*N*)$_2$] are influenced by the presence of intramolecular hydrogen bonding.[44]

This study also revealed that ^{195}Pt{^{1}H} NMR spectroscopy can be used to identify separate ^{195}Pt resonances of the configurational *trans*-[Pd(*EE*-L^n-κ*S*,*O*)$_2$], *trans*-[Pd(*EZ*-L^n-κ*S*,*O*)$_2$] and *trans*-[Pd(*ZZ*-L^n-κ*S*,*O*)$_2$] isomers formed from photo-induced isomerization of the *cis*-[Pt(L^n-κ*S*,*O*)$_2$] complexes with asymmetrically substituted *N*,*N*-dialkyl-*N*'-acyl(aroyl)thioureas (HL^{8-15}).

Downfield shifts of *ca* 750 ppm were recorded for the *trans* ^{195}Pt resonances relative to their *cis* counterparts consistent with ^{195}Pt chemical shifts differences of *cis*-*trans* isomers reported in the literature.[51] Attempted isolation of the *trans* configurational isomers led to a mixture of *ZZ*, *EZ* and *EE* isomers of *trans*-bis(*N*-methyl-*N*-ethyl-*N*'-benzoylthioureato-κ^2*S*,*O*)palladium by slow evaporation in acetonitrile after irradiation with polychromatic light. The results further indicated that the most prominent factor influencing the relative distribution and chemical shifts of configurational isomers is the electronic or steric effect of ligand substituents. This explains why the introduction of *N*-pentyl and *N*-phenyl ligand substituents led to an increase in the relative distribution of *cis*-[Pt(*ZZ*-L-κ*S*,*O*)$_2$] isomer in the representative complexes. In contrast, significantly higher distributions of *cis*-[Pt(*EE*-L-κ*S*,*O*)$_2$] isomers were obtained for *cis*-complexes with relatively smaller *N*-ethyl and *N*-methyl substituents. These trends could partially explain the isolation of the *cis*-[Pd(*EE*-L^8-κ*S*,*O*)$_2$] and *cis*-[Pt(*EE*-L^8-κ*S*,*O*)$_2$] isomers for HL = *N*-methyl-*N*-ethyl-*N'*-benzoylthiourea, while the *cis*-[Pt(*ZZ*-L^{15}-κ*S*,*O*)$_2$] isomer was isolated for HL = *N*-isopropyl-*N*-4-methoxy-phenyl-*N*'-(2,2-dimethylpropanoyl)thiourea. Since the *cis*-[Pt(L^{15}-κ*S*,*O*)$_2$] complex showed a higher relative distribution of the *cis*-[Pt(*ZZ*-L^{15}-κ*S*,*O*)$_2$] isomer in solution (69 % ZZ, 29 % *EZ*, 2 % *EE*), it is likely that the combined effects of the higher relative distribution and solubility might have resulted in the isolation of the *cis*-[Pt(*ZZ*-L^{15}-κ*S*,*O*)$_2$] isomer in preference to the *cis*-[Pt(*EZ*-L^{15}-κ*S*,*O*)$_2$] and *cis*-[Pt(*EE*-L^{15}-κ*S*,*O*)$_2$] isomers.

The *trans*-[Pd(L$^{1\text{-}8}$-κ*S*,*O*)$_2$] and *trans*-[Pd(L^7-κ*S*,*N*)$_2$] complexes isolated in this study were found to undergo a spontaneous *trans*→*cis* isomerization in the dark in both chloroform and acetonitrile as summarized in Figure 7.2. It was evident that the *trans*→*cis* isomerization of platinum(II) and palladium(II) complexes with the *N*,*N*-dialkyl-*N*'-acyl(aroyl)thioureas is catalysed by the presence of trace amounts of ligands in solution. For most of the complexes, the relative rates of *trans*→*cis* isomerization were significantly higher in acetonitrile compared to chloroform but did not show any consistent trend based on electronic effects of ligand substituents. The increase in relative rate of isomerization in acetonitrile suggests that a coordinating solvent assists the *trans*→*cis* isomerization by probably coordinating to any vacant coordination site on the Pd atom in the *trans*-[Pd(L^n-κ*S*,*O*)$_2$] complexes.

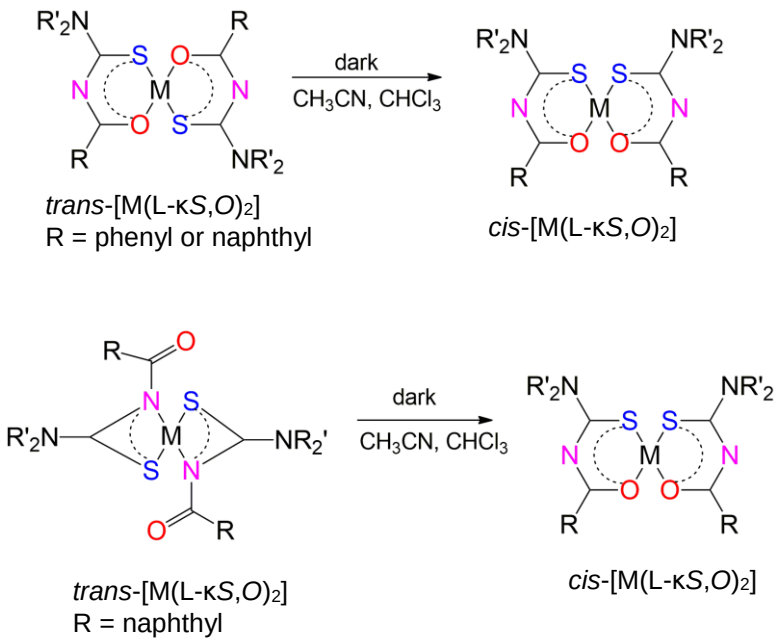

Figure 7.2. General scheme for the spontaneous *trans*→*cis* isomerization of *trans*-[Pd(L^{1-8}-κ*S*,*O*)$_2$] and *trans*-[Pd(L^{7}-κ*S*,*N*)$_2$] complexes in the dark.

The relative rates of *trans*→*cis* isomerization increased linearly with increase in concentration of the free ligands indicative of the occurrence of ligand exchange between *cis*-*trans* isomers and traces of the *N*,*N*-di-substituted acylthioureas in solution. Further support of association between the ligands and complexes was provided by temperature dependence experiments which showed large negative activation entropy for the *trans*→*cis* isomerization of the *trans*-[Pd(L^{4}-κ*S*,*O*)$_2$] complex. Confirmation of the occurrence of ligand exchange was provided from evidence of the formation of mixed-ligand *cis*-[Pd($L^{a,b}$-κ*S*,*O*)$_2$] complexes after addition of acetonitrile solutions of free ligands to irradiated mixtures of *cis*-*trans* isomers. The ligand exchange process during the *trans*→*cis* isomerism of palladium(II) complexes is similar to that proposed by Balzani and co-workers[91-93] for the *cis*→*trans* isomerization of *cis*-(gly-κ*N*,*O*)$_2$ complexes in the presence of free glycine ligands.

From the above mentioned findings, the mechanism presented in Figure 7.3 is proposed for the *trans*→*cis* isomerization of Pt(II) and Pd(II) complexes of the *N*,*N*-di-substituted acylthioureas. According to the results, a consecutive displacement assisted by prior association of the free HL

ligands is most likely to occur during the *trans*→*cis* isomerization. This is confirmed by the first-order dependence of the isomerization rates on the concentration of the ligand and supported by the high negative activation entropy. Also, the ligand catalysed *trans*→*cis* isomerization occurs irrespective of the nature of the *N*,*N*-dialkyl-*N'*-acyl(aroyl)thiourea used. This supports the fact that the ligands act as proton donors for coordination to the nitrogen in the chelate ring of the *trans* complexes. Further support for this statement is provided by the fact that the *trans*→*cis* isomerization was also catalysed in the presence of a protic solvent methanol without the addition of free ligands. Coordination of the nitrogen atom in the *trans*-[Pd(L^n-κ*S*,*O*)$_2$] complexes presumably weakens the Pd-O or Pd-S bonds thereby facilitating its cleavage and subsequent displacement by the free ligands in solution. Evidence of a potential Pd-O or Pd-S bond cleavage leading to a chelate ring-opening during *cis*-*trans* isomerization of bis(*N*,*N*-dimethyl-*N*'-methylthioureato)palladium(II) has been provided by DFT calculations.[57] After the Pd-O or Pd-S bond cleavage, coordination sites would become vacant and made available for free HL ligands as well as solvent molecules to coordinate to the Pd metal centre. The next step in the *trans*→*cis* process may possibly involve a five coordinate intermediate in which the acetonitrile solvent is coordinated to the metal centre. This solvent-assisted pathway might have led to the higher relative rates of *trans*→*cis* isomerization obtained in acetonitrile compared to chloroform. The overall consequence of the ligand exchange mediated *trans*→*cis* isomerization is the displacement of a ligand attached to the *trans*-[Pd(L^n-κ*S*,*O*)$_2$] complexes by the entering free ligand assisted by acetonitrile solvent. In the final chelation step of the process, the strong *trans*-influence of a sulfur donor atom would then presumably lead to coordination of the oxygen atom to Pd(II) forming the *cis*-[Pd(L^n-κ*S*,*O*)$_2$] products. Alternatively, the solvent-assisted *trans*→*cis* isomerization may involve the displacement of a ligand HL^a which is bound to a *trans*-[Pd(L^a-κ*S*,*O*)$_2$] complex by another free HL^b ligand in solution. This would result in the formation of the mixed-ligand complex *cis*-[Pd($L^{a,b}$-κ*S*,*O*)$_2$], with subsequent release of the displaced HL^a ligand.

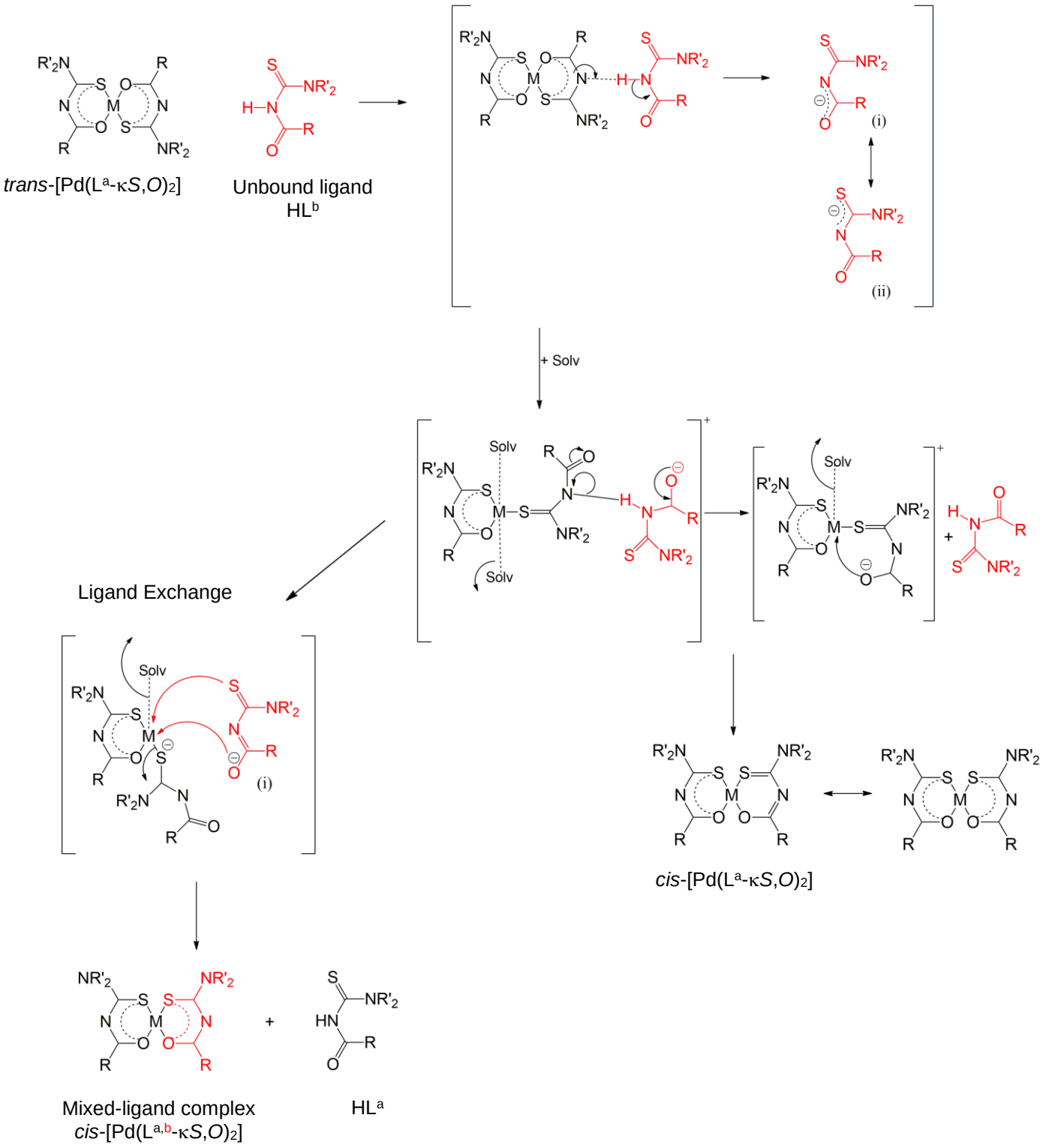

Figure 7.3. Proposed mechanism for *trans*→*cis* isomerization of Pt^{II} and Pd^{II} complexes of the *N*,*N*-dialkyl-*N*'-acyl(aroyl)thioureas in the presence of trace amounts of ligands; Solv = solvent.

It should be noted that from this study, no ^{1}H NMR evidence of the intermediates in the proposed mechanism (Figure 7.3) was obtained. This could presumably be due to the unstable nature of the intermediates as well as their short lifetimes in acetonitrile or chloroform. The mechanism proposed in Figure 7.3 therefore remains speculative. Also, this study did not investigate the relative rates and mechanism of photo-induced *cis*→*trans* isomerization. Whenever a steady state was achieved from the irradiated *cis*-[M(L^{n}-κ*S*,*O*)$_2$], the *trans*-[M(L^{n}-κ*S*,*O*)$_2$] isomers in solution were observed to slowly revert back to their *cis* isomers when the light source for irradiation was switched off. This served as a limitation for performing a kinetic study on the photo-induced process using either ^{1}H NMR spectroscopy or RP-HPLC. A better understanding of the mechanism of both photo-induced (*cis*→*trans*) and thermal (*trans*→*cis*) processes will require further studies some of which are proposed here. More insights on the mechanism of photo-induced *cis*→*trans* isomerization could be achieved by developing an *in-situ* laser-NMR setup with a possibility of online light irradiation and ^{1}H NMR detection. This will not only enable accurate determination of rates of photo-induced *cis*→*trans* isomerization but could also identify certain unstable intermediates and photo-products formed after photo-irradiation. Further insights into the mechanisms of both the photo-induced (*cis*→*trans*) and the thermal (*trans*→*cis*) isomerization of the *cis*-[M(L^{n}-κ*S*,*O*)$_2$] (M = Pt(II) or Pd(II)) complexes will require DFT studies. In particular, DFT calculations will likely explain which of the electronic or steric factors in the *N*,*N*-diethyl-*N*'-1-naphthoylthiourea ligand caused the unprecedented formation of the *trans*-[Pd(L^{7}-κ*S*,*N*)$_2$] isomer in addition to the *trans*-[Pd(L^{7}-κ*S*,*O*)$_2$] isomer during photo-induced isomerization of the *cis*-[Pd(L^{7}-κ*S*,*O*)$_2$] complex. A final recommendation from this study is that the vapour diffusion or slow evaporation methods developed for isolating the *trans*-[Pd(L^{1-8}-κ*S*,*O*)$_2$] complexes could be extended to Pd(II) complexes with longer *N*-alkyl chains. This could potentially lead to preparation of novel *trans*-[Pd(L^{n}-κ*S*,*O*)$_2$] complexes with liquid crystalline properties.

References.

1. R. G. Cawthorn, *Platinum Metals Rev.*, 2010, **54**, 205-215.
2. C. R. M. Rao, G. S. Reddi, *Trends Anal. Chem*., 2000, **19**, 565-586.
3. T. Bossi, J. Gediga, *Johnson Matthey Technol. Rev*., 2017, **61**, 111-121.
4. O. T. Holton, J. W. Stevenson, *Platinum Metals Rev*., 2013, **57**, 259-271.
5. H. Connor, *Platinum Metals Rev*., 1967, **11**, 2-9.
6. C. Couderc, *Platinum Metals Rev*., 2010, **54**, 186-191.
7. A. Cowley, B. Woodward, *Platinum Metals Rev*., 2011, **55**, 98-107.
8. C. F. J. Barnard, *Platinum Metals Rev*., 1989, **33**, 162-167.
9. Y. Wang, X. Li, *Procedia Engineering*, 2012, **45**, 1005-1009.
10. A. N. Mautjana, J. D. Miller, A. Gie, S. A. Bourne and K. R. Koch, *J. Chem. Soc. Dalton Trans.*, 2003, 1952.
11. F. Z. El Aamrani, A. Kumar, J. L. Cortina, A. M. Sastre, *Anal. Chim. Acta*, 1999, **382**, 205-213.
12. M. Dominguez, E. Antico, L. Beyer, A. Aguirre, S. Garcia-Granda, V. Salvado, *Polyhedron*, 2002, **21**, 1429-1437.
13. D. Hanekom, J. M. McKenzie, N. M. Derix and K. R. Koch, *Chem. Commun.*, 2005, 767-769.
14. W. R. Rocha, W. B. de Almeida, *J. Braz. Chem. Soc*., 2000, **11**, 112-120.
15. K. Neucki, *Ber. Dtsch. Chem. Ges.*, 1873, **6**, 598.
16. L. Beyer, E. Hoyer, H. Hartman, J. Liebscher, *Z. Anorg. Allg. Chem*., 1981,**21**, 81.
17. N. Selvakumaran, S. W. Ng, E. R. T. Tiekink, R. Karvembu, *Inorg. Chim. Acta*, 2011, **376**, 278-284.
18. N. Selvakumaran, A. Pratheepkumar, S. W. Ng, E. R. T. Tiekink, R. Karvembu, *Inorg. Chim. Acta*, 2013, **404**, 82-87.
19. A. M. Plutin, R. Mocelo, A. Alvarez, R. Ramos, E. E. Castellano, M. R. Cominetti, A. E. Graminha, A. G. Ferreira, A. A. Batista, *J. Inorg. Biochem*., 2014, **134**, 76-82.
20. S. Yaseen, M. K. Rauf, S. Zaib, A. Badshah, M. N. Tahir, M. I. Ali, I. Ud-Din, M. Sahid, J. Iqbal, *Inorg. Chim. Acta*, 2016, **443**, 69-77.

21. W. Yang, L. Huanhuan, L. Mengying, F. Wang, Z. Weiqun, F. Jianfen, *J. Inorg. Biochem*., 2012, **116**, 97-105.
22. Z. Weiqun, W. Yang, X. Liqun, C. Xianchen, *J. Inorg. Biochem*., 2005, **99**, 1314-1319.
23. A. Saeed, U. Flörke, M. F. Erben, *J. Sulf. Chem*., 2014, **35**, 318-355.
24. K. H. Konig, M. Schuster, B. Steinbrech, G. Schneeweis, R. Sclodder, *Fres. Z. Anal. Chem.*, 1985, **321**, 457.
25. M. Schuster, E. Unterreitmaier, *Fres. J. Anal. Chem*., 1993, **346**, 630.
26. W. Henderson, C. Evans, B. K. Nicholson, J. Fawcett, *Dalton Trans*., 2003, 2691-2697.
27. A. Mohamadou, I. Dechamps-Olivier, J-P. Barbier, *Polyhedron*, 1994, **13**, 1363-1370.
28. K. R. Koch, C. Sacht, S. Bourne, *Inorg. Chim. Acta*, 1995, **232**, 109-115.
29. J. E. Spenceley, W. Henderson, J. R. Lane, G. C. Saunders, *Inorg. Chim. Acta*, 2015, **425**, 83-91.
30. R. A. Bailey, K. L. Rothaupt, R. K. Kulling, *Inorg. Chim. Acta*, 1988, **147**, 233-236.
31. H. Mandal, D. Ray, *Inorg. Chim. Acta*, 2014, **414**, 127-133.
32. D. S. Mansuroglu, H. Arslan, U. Florkes, N. Kulku, *J. Coord. Chem*., 2008, **61**, 3134-3146.
33. H. Arslan, N. Kulcu, U. Florke, *Transit. Metal Chem*., 2003, **28**, 816-819.
34. N. Gunasekaran, P. Jerome, S. N. Weng, E. R. T. Tiekink, R. Karvembu, *J. Mol. Catal. A: Chem.*, 2012, **353-354**, 156-162.
35. C. Viorel, A. S. Mocanu, R. Constantin, D. Manaila-Maximean, D. Florea, *J. Therm. Anal. Calorim*., 2012, **107**, 877-886.
36. C. Viorel, I. Mihaela, I. Monica, D. Florea, I. Neagoe, P. Simona, *Polyhedron*, 2009, **28**, 3739-3746.
37. A. S. Mocanu, I. Monica, D. Florea, M. Ilie, C. Viorel, *Inorg. Chim. Acta*, 2010, **363**, 729-736.
38. I. Monica, M. Bucos, D. Florea, C. Viorel, *J. Mol. Struct*., 2011, **987**, 1-6.
39. A. C. Tenchiu, I Monica, D. Florea, A. C. Whitwood, C. Viorel, *Polyhedron*, 2008, **27**, 3537-3544.
40. M. Micutz, I. Monica, T. Staicu, D. Florea, L. Pasuk, Y. Molard, T. Roisnel, C. Viorel, *Dalton Trans*., 2014, **43**, 1151-1160.
41. A. N. Westra, S. A. Bourne, C. Esterhuysen, and K. R. Koch**,** *Dalton Trans*., 2005, 2162-2172.

42. K. R. Koch, S. A. Bourne, A. Coetzee, *J. Miller, J. Chem. Soc., Dalton Trans.*, 1999, 3157-3161.
43. A. N. Westra, S. A. Bourne, K. R. Koch, *Dalton Trans*., 2005, 2916-2924.
44. K. R. Koch, *Coord. Chem. Rev.*, 2001, **216**, 473.
45. K. R. Koch, Y. Wang, A. Coetzee, *J. Chem. Soc. Dalton Trans*., 1999, 1013-1016.
46. M. G. Babashkina, D. A. Safin, M. Bolte, M. Srebro, M. Mitoraj, A. Uthe, A. Klein, M. Köckerling, *Dalton Trans*., 2011, **40**, 3142-3153.
47. M. G. Babashkina, D. A. Safin, M. Bolte, A. Klein, *Inorg. Chem. Commun.*, 2009, **12**, 678-681.
48. F. D. Sokolov, S. V. Baranov, D. A. Safin, F. E. Hahn, M. Kubiak, T. Pape, M. G. Babashkina, N. G. Zabirov, J. Galezowska, H. Kozlowski, R. A. Cherkasov, *New J. Chem*., 2007, **31**, 1661-1667.
49. M. G. Babashkina, D. A. Safin, M. Srebro, P. Kubisiak, M. P. Mitoraj, M. Bolte, Y. Garcia, *Eur. J. Inorg. Chem*., 2013, 545-555.
50. A. Irving, K. R. Koch, M. Matoetoe, *Inorg. Chimica Acta*, 1993, **206**, 193-199.
51. K. R. Koch, T. Grimmbacher, C. Sacht, *Polyhedron*, 1998, **17**, 267-274.
52. K. R. Koch. S. Bourne, *J. Mol. Struct*., 1998, **441**, 11-16.
53. H. Arslan, U. Florke, N. Kulcu, M. F. Emen, *J. Coord. Chem*., 2006, **59**, 223.
54. W. Hernandez, E. Spodine, A. Vega, R. Richter, J. Griebel, R. Kirmse, U. Schroder, L. Beyer, *Z. Anorg. Allg. Chem*., 2004, **630**, 1381.
55. K. Ramasamy, M. A. Malik, P. O'Brien, J. Raftery, *Dalton Trans*., 2010, **39**, 1460-1463.
56. K. R. Koch, J. Du Toit, M. R. Caira and C. Sacht, *J. Chem. Soc. Dalton Trans*., 1994, 785-786.
57. M. R. Burger, *PhD Thesis, Stellenbosch University*, 2008.
58. H. A. Nkabyo, D. Hannekom, J. McKenzie, K. R. Koch, *J. Coord. Chem.*, 2014, **76**, 4039-4060.
59. I. Ledneczki, P. Forgo, J. T. Kiss, A. Molnar, I. Palinko, *J. Mol. Struct*., 2007, **834-836**, 349-356.
60. L. A. M. Fontoura, I. J. R. da Cruz, C. R. D. Correia, *J. Mol. Struct*., 2002, **609**, 73-81.
61. B. Galabov, S. Ilieva, B. Hadjieva, E. Dinchova, *J. Phys. Chem. A*, 2003, **107**, 5854-5861.
62. L. Isbrandt, W. C-T. Tung, M. T. Rogers, *J. Magn. Reson*., 1973, **9**, 461-466.

63. T. Ozawa, Y. Isoda, H. Watanabe, T. Yuzuri, H. Suezawa, K. Sakakibara, M. Hirota, *Magn. Reson. Chem*., 1997, **35**, 323-332.
64. M. Tafazzoli, A. Ziyaei-Halimjani, M. Ghiasi, M. Fattahi, M. R. Saidi, *J. Mol. Struct*., 2008, **886**, 24-31.
65. N. G. Vassilev, V. S. Dimitrov, *J. Mol. Struct*., 1999, **484**, 39-47.
66. S. Behrendt, L. Beyer, F. Dietze, E. Kleinpeter, E. Hoyer, E. Ludwig, E. Uhlemann, *Inorg. Chim. Acta*., 1980, **43**, 141-144.
67. A. Gryf-Keller, P. Szczecinski, H. Koziel, *J. Organomet. Chem*., 1989, **372**, 225-230.
68. E. Klienpeter, A. Schulenburg, I. Zug, H. Hartmann, *J. Org. Chem*., 2005, **70**, 6592-6602.
69. D. Argyropoulos, E. Hoffmann, S. Mtongana, K. R. Koch, *Magn. Reson. Chem*., 2003, **41**, 102-106.
70. K. R. Koch, C. Sacht, T. Grimmbacher, S. Bourne, *S. Afr. J. Chem*., 1995, 71-77.
71. G. K. Anderson, R. J. Cross, *J. Chem. Soc. Rev*., 1980, **9**, 185.
72. S. P. Babailov, Y. G. Kriger, I. K. Igunenov, *Russ. Chem. Bull*., 1997, **46**, 1038-1039
73. R. Sakamoto, S. Kume, M. Sugimoto, H. Nishihara, *Chem. Eur. J*., 2009, **15**, 1429-1439.
74. E. A. Allen, J. Del Gaudio, W. Wilkinson, *Thermochim. Acta*, 1975, **11**, 197-203.
75. D. A. Redfield, L. W. Cary, J. H. Nelson, *Inorg. Chem*., 1975, **14**, 50-59.
76. R. A. Al-Balushi, A. Haque, M. Jayapal, M. K. Al-Suti, J. Husband, M. S. Khan, J. M. Skelton, K. C. Molloy, P. R. Raithby, *Inorg. Chem*., 2016, **55**, 10955-10967.
77. W. E. Hill, D. M. A. Minahan, J. G. Taylor, C. A. McAuliffe, *J. Am. Chem. Soc.*, 1982, **104**, 6001-6005.
78. B. L. Shaw, *J. Am. Chem. Soc*., 1975, **97**, 3856.
79. D. A. Redfield, J. H. Nelson, *Inorg. Chem.*, 1973, **12**, 15-19.
80. A. W. Verstuyft, J. H. Nelson, *Inorg. Chem*., 1975, **14**, 1501-1505.
81. R. Romeo, D. Minniti, S. Lanza, *Inorg. Chem*., 1980, **19**, 3668-3673.
82. T. Yutaka, I. Mori, M. Kurihara, J. Mizutani, N. Tamai, T. Kawai, M. Irie, H. Nishihara, *Inorg. Chem.*, 2002, **41**, 7143-7150.
83. F. D. Lewis, A. M. Miller, G. D. Salvi, *Inorg. Chem*., 1995, **34**, 3171-3181.
84. C. Y. Mok, S. G. Tan, G. C. Chan, *Inorg. Chim. Acta*, 1990, **176**, 43-48.
85. H. Nishihara, M. Nihei, A. Hirooka, M. Kurihara, *Macromol. Symp*., 2002, **186**, 93-98.
86. D. G. Cooper, J. Powell, *Can. J. Chem*., 1973, **51**, 1634-1644.

87. J. Powell, D. G. Cooper, *J.C.S. Chem. Comm*., 1974, 749-750.

88. W. J. Louw, *J.C.S. Chem. Comm.*, 1974, 353.

89. W. J. Louw, *Inorg. Chem*., 1977, **16**, 2147-2160.

90. W. J. Louw, R. van Eldik, *Inorg. Chem*., 1981, **20**, 1939-1941.

91. V. Balzani, V. Carassiti, *J. Phys. Chem*., 1968, **72**, 383-388.

92. F. Scandola, O. Traverso, V. Balzani, G. L. Zucchini, V. Carassiti, *Inorg. Chim. Acta*, 1967, **1**, 76.

93. V. Balzani, V. Carassiti, L. Moggi, F. Scandola, *Inorg. Chem*., 1965, **4**, 1243-1246.

94. F. S. Richardson, D. D. Shiallady, A. Waltrop, *Inorg. Chim. Acta*, 1971, **5**, 279-289.

95. I. B. Douglass and F. B. Dains, *J. Am. Chem. Soc*., 1934, **56**, 719.

96. A. Takamizawa, K. Hira, K. Matsui, *Bull. Chem. Soc. Japan*., **36**, 1963, 1214.

97. D.T Elmore, R. J. Ogle, *J. Chem. Soc.* 1958, 1141-1145.

98. H. Marquez, A. Plutin, Y. Rodriquez, E. Perez, A. Loupy, *Synt. Commun*., 2000, **30**, 1067-1073.

99. S. Saeed, N. Rashid, N. Rashid, M. Ali, R. Hussain, *Eur. J. Chem*., 2010, **1**, 200-205.

100. A. A. Al-abbasi, M. I. M. Tahir, M. B. Kassim, *Acta Crystallogr., Sect. E*, 2011, **67**, 3414.

101. J. M. McKenzie, K. R. Koch, *Acta Crystallogr., Sect. E*, 2006, **62**, 4263.

102. A. M. Plutin, H. Marquez, E. Ochoa, M. Morales, M. Sosa, L. Moran, Y. Rodriguez, M. Suarez, M. Martin, C. Seoane, *Tetrahedron*, 2000, **56**, 1533.

103. H. Perez, R. S. Correa, A. M. Plutin, A. A. Alvarez, Y. Mascarenhas, *Acta Crystallogr., Sect*. E, 2011, **67**, 647.

104. G. M. Sheldrick, *Acta Crystallogr., Sect. A.: Found. Crystallogr*., 2008, **64**, 112.

105. L. J. Barbour. *J. Supramol. Chem*., 2003, **1**, 189.

106. POV-Ray™ for windows, Persistence of vision Raytracer Pty. Ltd., Williamstown, Australia, 2004.

107. W. Su-Yun, Z. Xiao-Ya, L. Hai-Pu, Y. Ying, H. W. Roesky, *Z. Anorg. Allg. Chem*., 2015, **641**, 883-889.

108. D. J. Che, X. L. Yao, G. Li, Y. H. Li, *J. Chem. Soc., Dalton Trans*., 1998, 1853-1856.

109. Y. Jean, I. Demache, A. Lledos, F. Maseros, *J. Mol. Str.(Theochem).*, 2003, **632**, 131-144.

110. B. D. Smith, D. M. Goodenough-Lashua, C. J. E. D'Souza, K. J. Norton, L. M. Schmidt, J. C. Tung, *Tetrahedron Lett*., 2004, **45**, 2747-2749.
111. E. A Basso, P. R. Oliveir, F. Weictzycoski, R. M. Pontes, B. C. Fiorin, *J. Mol. Struct*., 2005, **753**, 139-146.
112. A. R. Modarresi-Alam, A. Nowroozi, P. Najafi, F. Movahedifar, H. Hajiabadi, *J. Mol. Struct.*, 2014, **1076**, 299-307.
113. C. Suarez, E. J. Nicholas, M. R. Bowman, *J. Phys. Chem*. A, 2003, **107**, 3024-3029.
114. W. E. Stewart, T. H. Siddall, *Chem. Rev*., 1970, **70**, 517-551.
115. S. Mtongana, *PhD Thesis, Stellenbosch University*, 2006.

Appendix A- Additional NMR, FT-IR, RP-HPLC and X-ray data

Table A2.1. Selected bond lengths (Å) and angles (°) for *cis*-[Pd(L^2-κ*S*,*O*)$_2$] and *cis*-[Pd(L^7-κ*S*,*O*)$_2$].

	cis-[Pd(L^2-κ*S*,*O*)$_2$]	*cis*-[Pd(L^7-κ*S*,*O*)$_2$]
Pd(1)-S(1A)	2.2364(4)	2.241(10)
Pd(1)-S1(B)	2.2351(4)	2.2458(9)
Pd(1)-O(1A)	2.009(1)	2.015(2)
Pd(1)-O(1B)	2.015(1)	2.032(2)
S(1A)-C(9A)	1.744(2)	1.735(4)
S(1B)-C(12B)	1.743(2)	1.738(3)
O(1A)-C(8A)	1.264(2)	1.275(4)
O(1B)-C(11B)	1.264(2)	1.270(4)
N(1A)-C(8A)	1.337(2)	1.326(4)
N(1A)-C(9A)	1.335(2)	1.348(5)
N(1B)-C(11B)	1.330(2)	1.326(4)
N(1B)-C(12B)	1.339(2)	1.350(4)
S(A1)-Pd(1)-S(1B)	86.62(1)	86.93(3)
S(1A)-Pd(1)-O(1A)	94.16(3)	93.98(8)
S(1A)-Pd(1)-O(1B)	178.94(3)	177.99(7)
S(1B)-Pd(1)-O(1A)	177.52(3)	179.08(8)
S(1B)-Pd(1)-O(1B)	94.44(3)	92.57(6)
O(1A)-Pd(1)-O(1B)	84.78(5)	86.53(9)
Pd(1)-S(1A)-C(9A)	107.92(5)	108.14(12)
Pd(1)-S(1B)-C(9B)	107.53(3)	104.66(11)
Pd(1)-O(1A)-C(8A)	131.3(1)	130.5(2)
Pd(1)-O(1B)-C(8B)	129.7(1)	128.6(2)
C(11A)-N(1A)-C(12A)	126.6(1)	126.1(3)
C(11B)-N(1B)-C(12B)	126.8(1)	125.7(3)

Table A2.2. Selected bond lengths (Å) and angles (°) for *cis*-[Pd(L^4-κ*S*,*O*)$_2$], *cis*-[Pd(L^5-κ*S*,*O*)$_2$] and *cis*-[Pd(L^6-κ*S*,*O*)$_2$].

	cis-[Pd(L^4-κ*S*,*O*)$_2$]	*cis*-[Pd(L^5-κ*S*,*O*)$_2$]	*cis*-[Pd(L^6-κ*S*,*O*)$_2$]
Pd(1)-S(1A)	2.246(1)	2.242(2)	2.2388(9)
Pd(1)-S1(B)	2.241(1)	2.248(2)	2.2325(9)
Pd(1)-O(1A)	2.016(5)	2.020(6)	2.028(3)
Pd(1)-O(1B)	2.013(3)	2.021(5)	2.025(2)
S(1A)-C(9A)	1.744(5)	1.757(7)	1.743(4)
S(1B)-C(12B)	1.744(4)	1.720(7)	1.738(4)
O(1A)-C(8A)	1.266(6)	1.272(9)	1.266(4)
O(1B)-C(11B)	1.269(6)	1.257(8)	1.272(4)
N(1A)-C(8A)	1.325(6)	1.33(1)	1.343(5)
N(1A)-C(9A)	1.346(7)	1.35(1)	1.325(4)
N(1B)-C(11B)	1.330(7)	1.38(1)	1.339(4)
N(1B)-C(12B)	1.341(7)	1.34(1)	1.335(4)
S(A1)-Pd(1)-S(1B)	89.07(4)	89.12(7)	86.92(3)
S(1A)-Pd(1)-O(1A)	92.7(1)	93.0(2)	93.39(7)
S(1A)-Pd(1)-O(1B)	176.8(1)	175.7(2)	176.07(7)
S(1B)-Pd(1)-O(1A)	178.2(1)	176.8(2)	176.97(7)
S(1B)-Pd(1)-O(1B)	94.0(1)	94.6(2)	94.53(7)
O(1A)-Pd(1)-O(1B)	84.2(2)	83.2(2)	85.4(1)
Pd(1)-S(1A)-C(9A)	106.8(2)	107.7(2)	106.9(1)
Pd(1)-S(1B)-C(9B)	107.3(2)	107.1(3)	107.9(1)
Pd(1)-O(1A)-C(8A)	129.2(3)	127.8(5)	129.5(2)
Pd(1)-O(1B)-C(8B)	129.3(3)	127.2(5)	129.0(2)
C(11A)-N(1A)-C(12A)	126.4(4)	124.2(6)	126.1(3)
C(11B)-N(1B)-C(12B)	125.6(4)	126.6(7)	125.7(3)

Table A3.1. Selected bond lengths (Å) and angles (°) for *trans*-[Pd(L^1-κ*S*,*O*)$_2$], *trans*-[Pd(L^5-κ*S*,*O*)$_2$] and *trans*-[Pd(L^6-κ*S*,*O*)$_2$].

	trans-[Pd(L^1-κ*S*,*O*)$_2$]	*trans*-[Pd(L^5-κ*S*,*O*)$_2$]	*trans*-[Pd(L^6-κ*S*,*O*)$_2$]
Pd(1)-S(1)	2.283(11)	2.282	2.297
Pd(1)-O(1)	1.992(2)	1.975	1.989
S(1)-C(8)	1.713(4)	1.689(6)	1.727(3)
O(1)-C(7)	1.286(5)	1.256(6)	1.280(3)
N(1)-C(8)	1.321(5)	1.30296)	1.345(4)
N(1)-C(7)	1.344(5)	1.348(7)	1.359(4)
S(1)-Pd(1)-S(1_a)	180.00	180.00	180.00
S(1)-Pd(1)-O(1)	94.23(7)	94.0	94.51
S(1)-Pd(1)-O(1_a)	85.77(7)	86.0	85.49
S(1_a)-Pd(1)-O(1)	85.77(7)	86.0	85.49
S(1_a)-Pd(1)-O(1_a)	94.23(14)	94.0	94.51
O(1)-Pd(1)-O(1_a)	180.00	180.00	180.00
Pd(1)-S(1)-C(8)	107.20(2)	106.7	107.47
Pd(1)-O(1)-C(8)	128.8(2)	129.4	129.8
C(7)-N(1)-C(8)	126.9(3).	127.3(5)	127.2(2)

Table A4.1. Selected bond lengths (Å) and angles (°) for *trans*-[Pd(L^7-κ*S*,*O*)$_2$], *trans*-[Pd(L^7-κ*S*,*N*)$_2$]

	trans-[Pd(L^7-κ*S*,*O*)$_2$]	*trans*-[Pd(L^7-κ*S*,*N*)$_2$]
Pd(1)-S(1A)	2.283(11)	2.3252(10)
Pd(1)-O(1A)	1.978(2)	-
S(1A)-C(9A)	1.70(3)	1.741(3)
O(1A)-C(8A)	1.281(2)	1.225(4)
N(1A)-C(8A)	1.321(5)	1.384(4)
N(1A)-C(9A)	1.344(5)	1.366(4)
N(1B)-C(11B)		-
N(1B)-C(12B)		-
S(A1)-Pd(1)-S(1B)	180.00	
S(1A)-Pd(1)-O(1A)	94.23(7)	
S(1A)-Pd(1)-O(1B)	85.77(7)	-
S(1B)-Pd(1)-O(1A)	85.77(7)	-
S(1B)-Pd(1)-O(1B)	94.23(14)	-
O(1A)-Pd(1)-O(1B)	180.00	-
Pd(1)-S(1A)-C(9A)	107.20(2)	-
Pd(1)-S(1B)-C(9B)		79.94(9)
Pd(1)-O(1A)-C(8A)	128.8(2)	-
Pd(1)-O(1B)-C(8B)		-
C(11A)-N(1A)-C(12A)	126.9(3).	-
C(11B)-N(1B)-C(12B)		121.5(2)

Table A4.1. Selected bond lengths (Å) and angles (°) for *cis*-[Pd(*EE*-L^8-κ*S*,*O*)$_2$], *cis*-[Pt(*EE*-L^8-*S*,*O*)$_2$] and *cis*-[Pt(*ZZ*-L^{15}-κ*S*,*O*)$_2$].

	***cis*-[Pd(*EE*-L^8-κ*S*,*O*)$_2$]**	***cis*-[Pt(*EE*-L^8-κ*S*,*O*)$_2$]**	***cis*-[Pd(*ZZ*-L^{15}-κ*S*,*O*)$_2$]**
Pd(1)/Pt(1)-S(1)	2.233(1)	2.235(1)	2.234(4)
Pd(1)/Pt(1)-S(1_a)	2.237(1)	2.230(1)	2.234(4)
Pd(1)/Pt(1)-O(1)	2.018(3)	2.020(3)	2.03(1)
Pd(1)/Pt(1)-O(1_a)	2.032(3)	2.031(3)	1.993(9)
S(1)-C(3)	1.743(4)	1.728(5)	1.73(2)
O(1)-C(5)	1.272(4)	1.323(6)	1.26(2)
N(1)-C(3)	1.343(4)	1.323(6)	1.38(2)
N(1)-C(4)	1.321(4)	1.344(6)	1.31(2)
S(1)-Pd(1)/Pt(1)-S(1_a)	87.58(3)	88.21(4)	88.6(1)
S(1)-Pd(1)/Pt(1)-O(1)	176.45(8)	176.4(1)	176.3(3)
S(1)-Pd(1)/Pt(1)-O(1_a)	93.63(8)	93.6(1)	93.7(3)
S(1_a)-Pd(1)/Pt(1)-O(1)	92.88(8)	94.3(1)	96.0(3)
S(1_a)-Pd(1)/Pt(1)-O(1_a)	176.89(8)	176.7(1)	171.4(3)
O(1)-Pd(1)/Pt(1)-O(1_a)	86.1(1)	84.0(1)	81.4(4)
Pd(1)/Pt(1)-S(4)-C(3)	107.9(1)	107.6(3)	108.7(5)
Pd(1)/Pt(1)-O(1)-C(5)	130.3(2)	129.3(3)	109.0(5)
C(5)-N(1)-C(4)	126.5(3).	126.7(4)	129.0(1)

Table A6.1. Changes in peak areas for ligand catalyzed *trans* →*cis* isomerization of *trans*-[Pd(L^1-κ*S*,*O*)$_2$] complexes in the dark, following pre-irradiation in acetonitrile with a 5Watt LED lamp at 25°C.

Time(mins)	*trans*-[Pd(L^1-κ*S*,*O*) (no HL added)	*trans*-[Pd(L^1-κ*S*,*O*)$_2$](HL added)	*cis*-[Pd(L^1-κ*S*,*O*)$_2$] (HL added)
0	1483.551	3016.892	4596.654
13	815.078	42.177	4070.564
26	482.716	-	4135.236
39	286.153	-	-
52	170.696	-	-
65	104.137	-	-
78	52.642	-	-
91	29.833	-	-

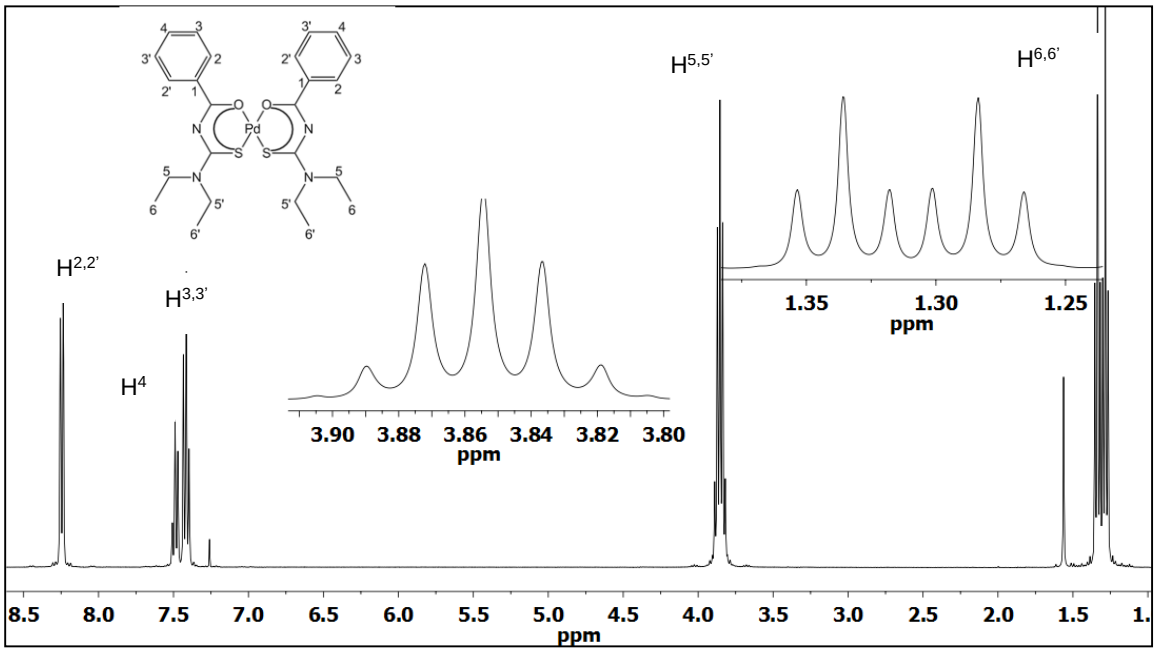

Figure A2.1. ^{1}H NMR spectrum of *cis*-bis(*N*,*N*-diethyl-*N*'-benzoylthioureato)palladium(II) *cis*-[Pd(L^1-κ*S*,*O*)$_2$] in chloroform-*d* at 25 °C.

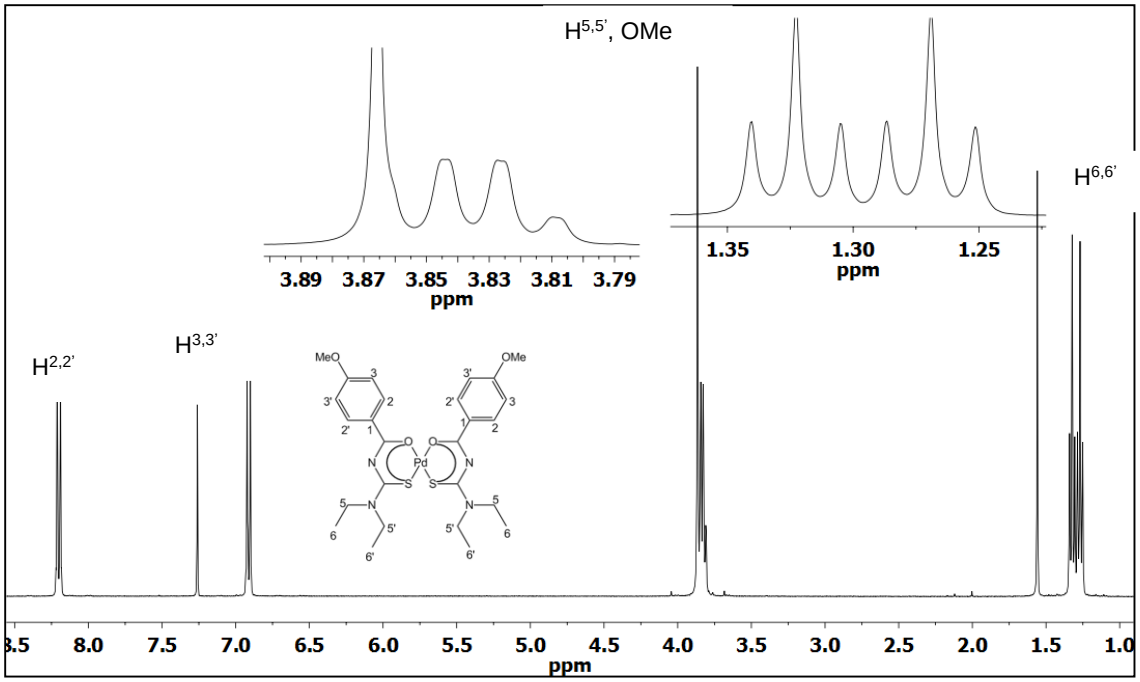

Figure A2.2. ^{1}H NMR spectrum of *cis*-bis(*N*,*N*-diethyl-*N*'-4-methoxy-benzoylthioureato)palladium(II) *cis*-[Pd(L^{2}-κ*S*,*O*)$_2$] in chloroform-*d* at 25 °C.

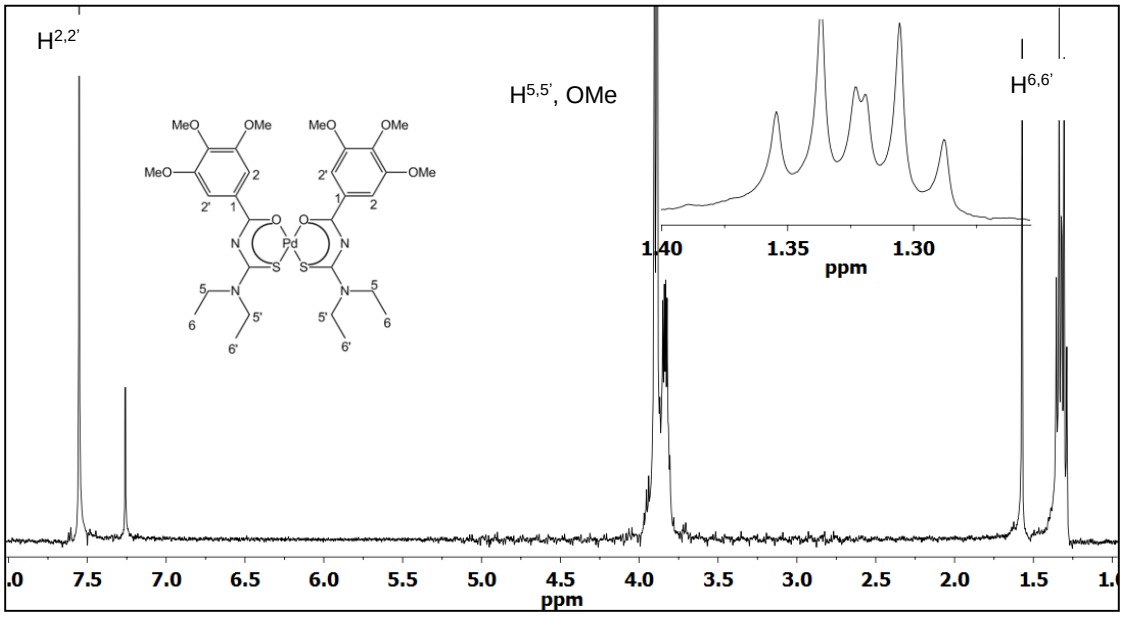

Figure A2.3. ^{1}H NMR spectrum of *cis*-bis(*N*,*N*-diethyl-*N*'-3,4,5-trimethoxy-benzoylthioureato)palladium(II) *cis*-[Pd(L^{3}-κ*S*,*O*)$_2$] in chloroform-*d* at 25 °C.

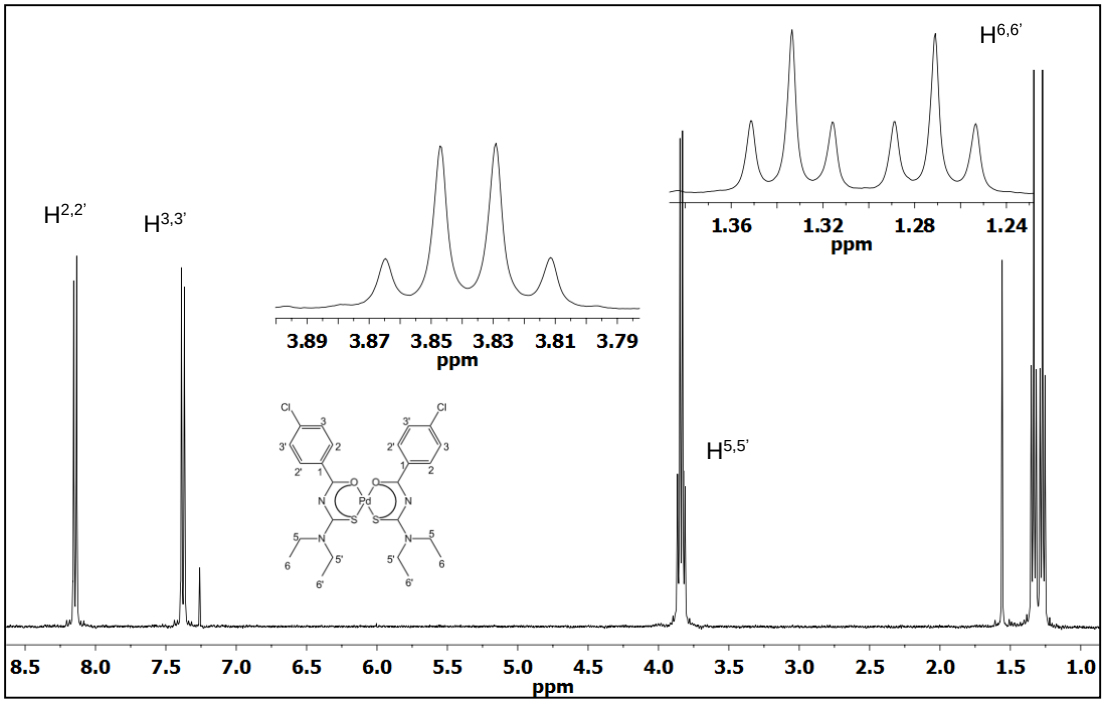

Figure A2.4. ^{1}H NMR spectrum of *cis*-bis(*N*,*N*-diethyl-*N*'-4-chloro-benzoylthioureato)palladium(II) *cis*-[Pd(L^4-κ*S*,*O*)$_2$] in chloroform-*d* at 25 °C.

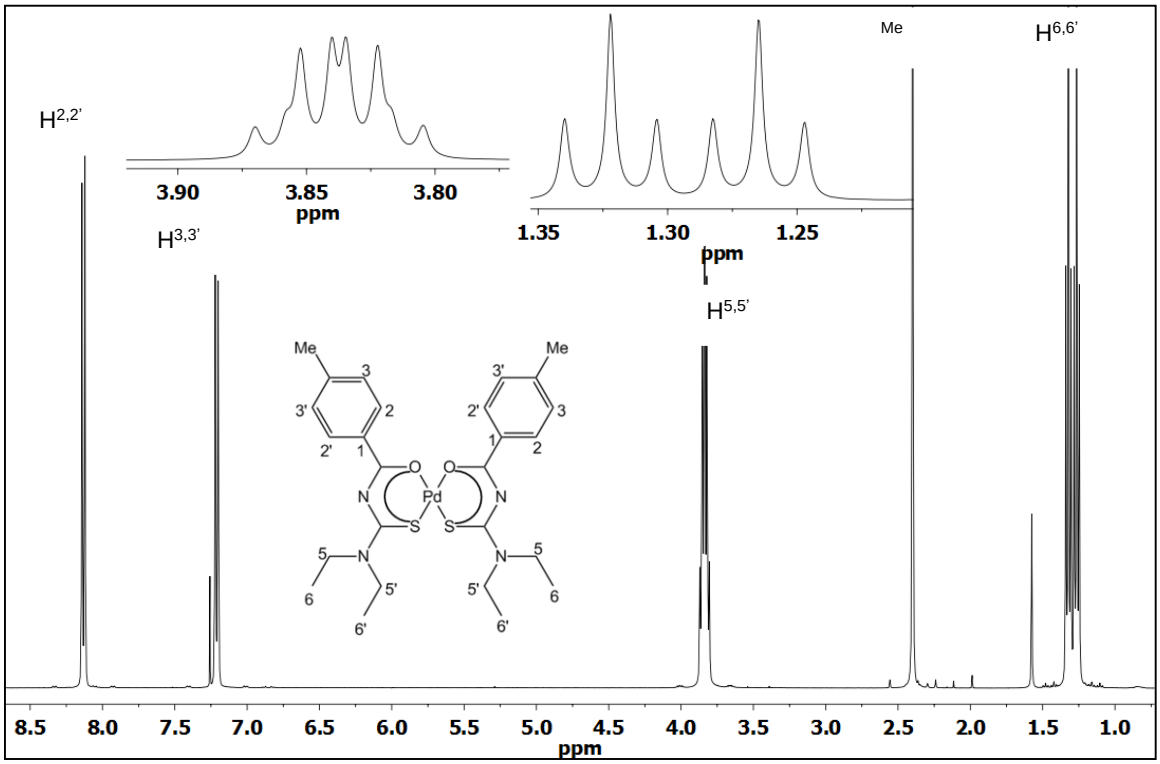

Figure A2.5. ^{1}H NMR spectrum of *cis*-bis(*N*,*N*-diethyl-*N*'-4-methyl-benzoylthioureato)palladium(II) *cis*-[Pd(L^5-κ*S*,*O*)$_2$] in chloroform-*d* at 25 °C.

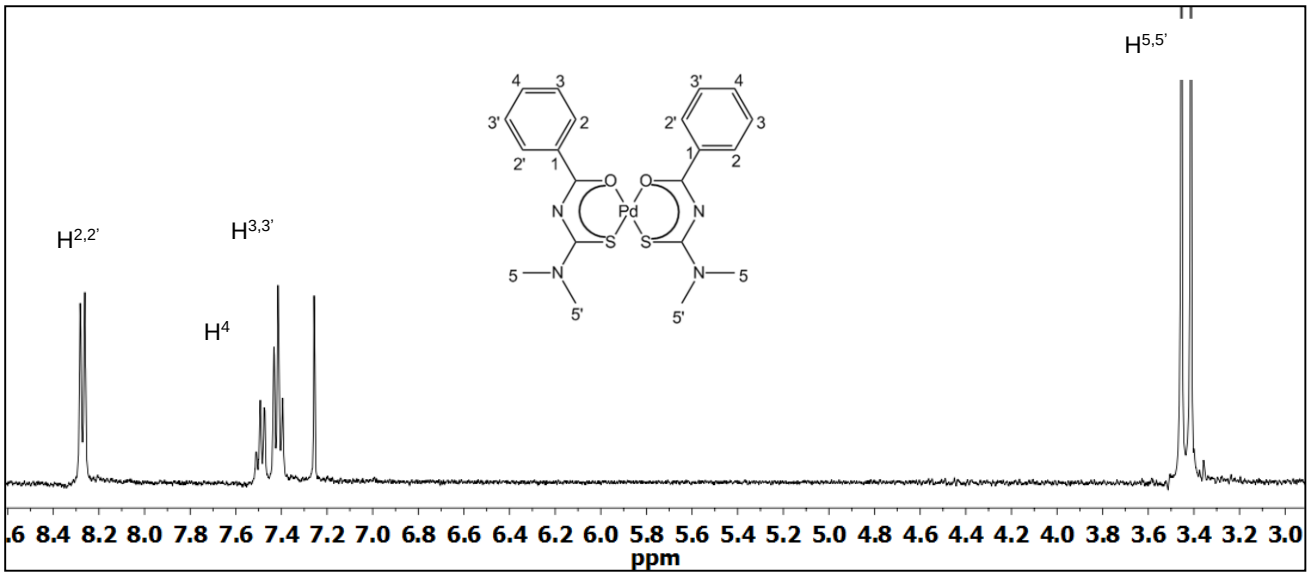

Figure A2.6. ^{1}H NMR spectrum of *cis*-bis(*N*,*N*-dimethyl-*N*'-benzoylthioureato)-palladium(II) *cis*-[Pd(L^{6}-κ*S*,*O*)$_2$] in chloroform-*d* at 25 °C.

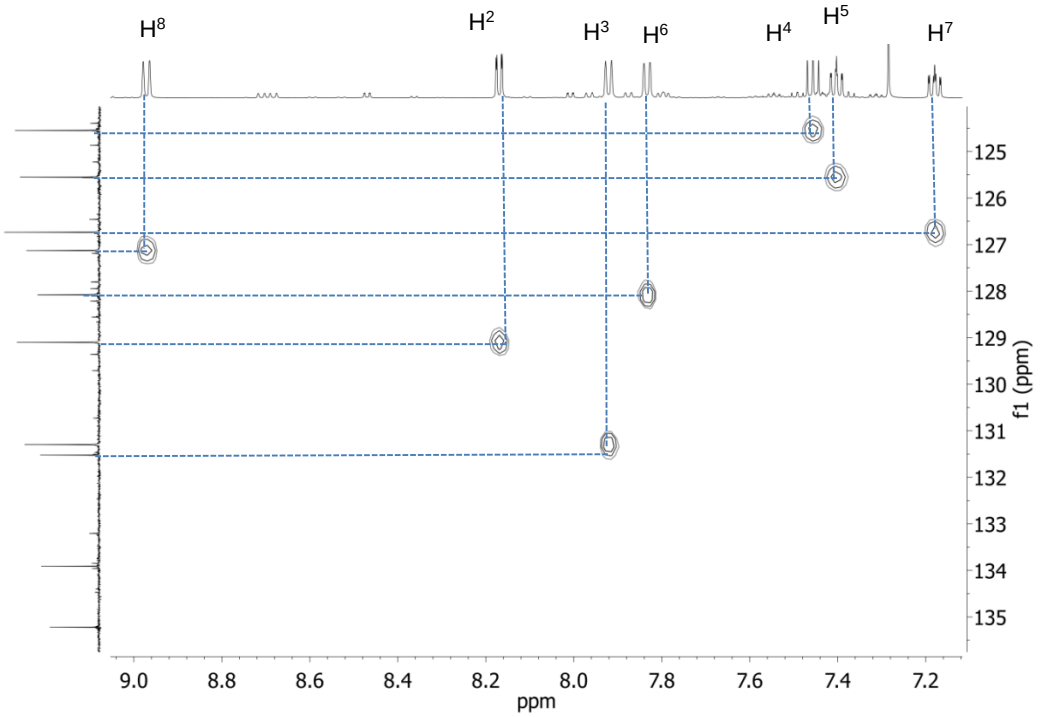

Figure A2.7. Full ^{1}H/^{13}C HSQC assignment of naphthyl region of *cis*-bis(*N*,*N*-diethyl-*N*'-1-naphthoylthioureato)palladium(II) *cis*-[Pd(L^{7}-κ*S*,*O*)$_2$] in chlroform-*d* at 25 °C.

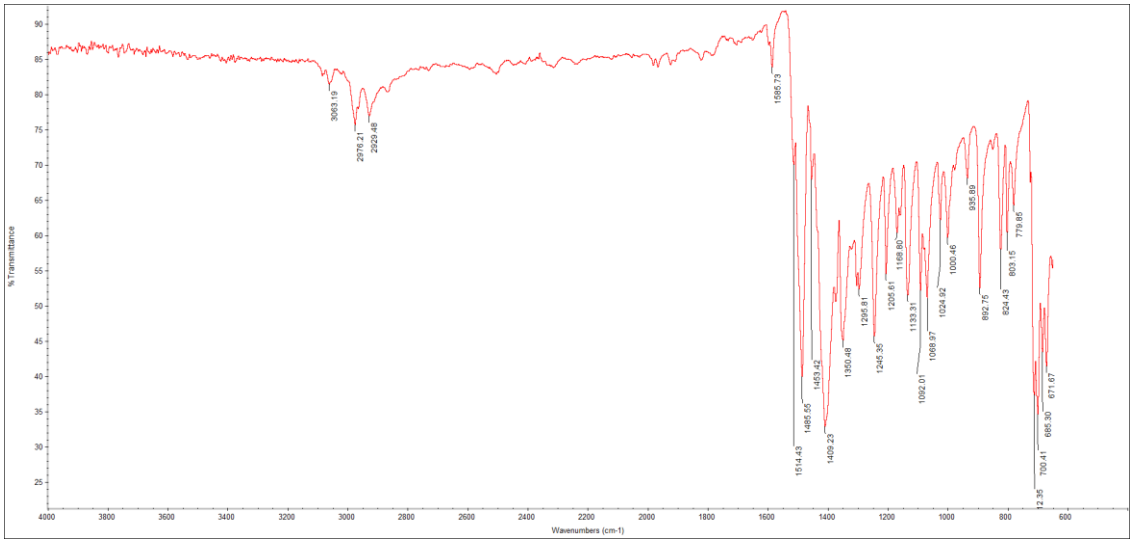

Figure A2.8. FT-IR spectrum of *cis*-bis(*N*,*N*-diethyl-*N*'-benzoylthioureato-κ^2*S*,*O*)palladium(II).

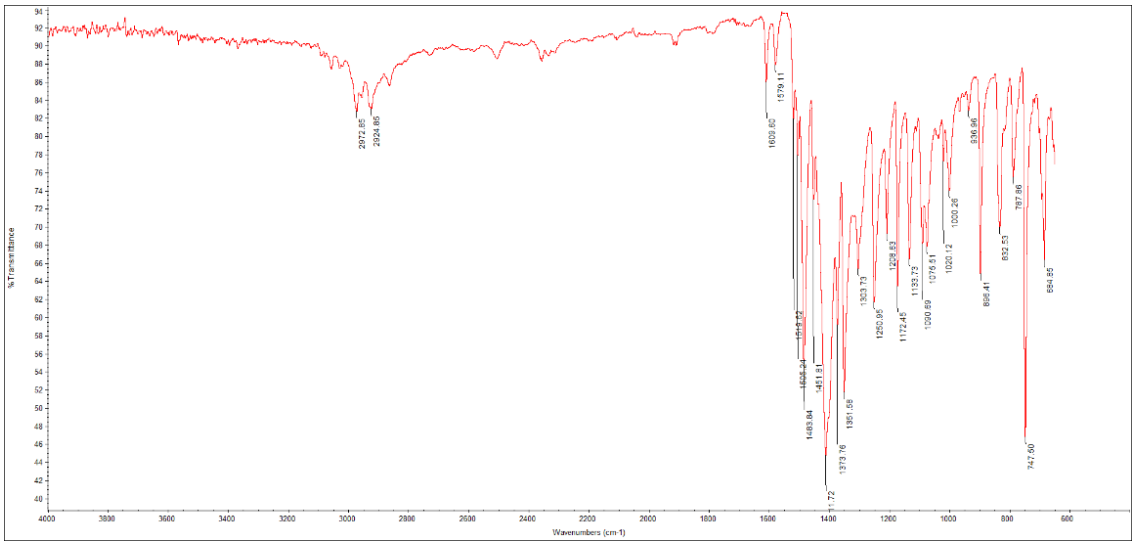

Figure A2.9. FT-IR spectrum of *cis*-bis(*N*,*N*-diethyl-*N*'-*p*-methyl-benzoylthioureato-κ^2*S*,*O*)palladium(II).

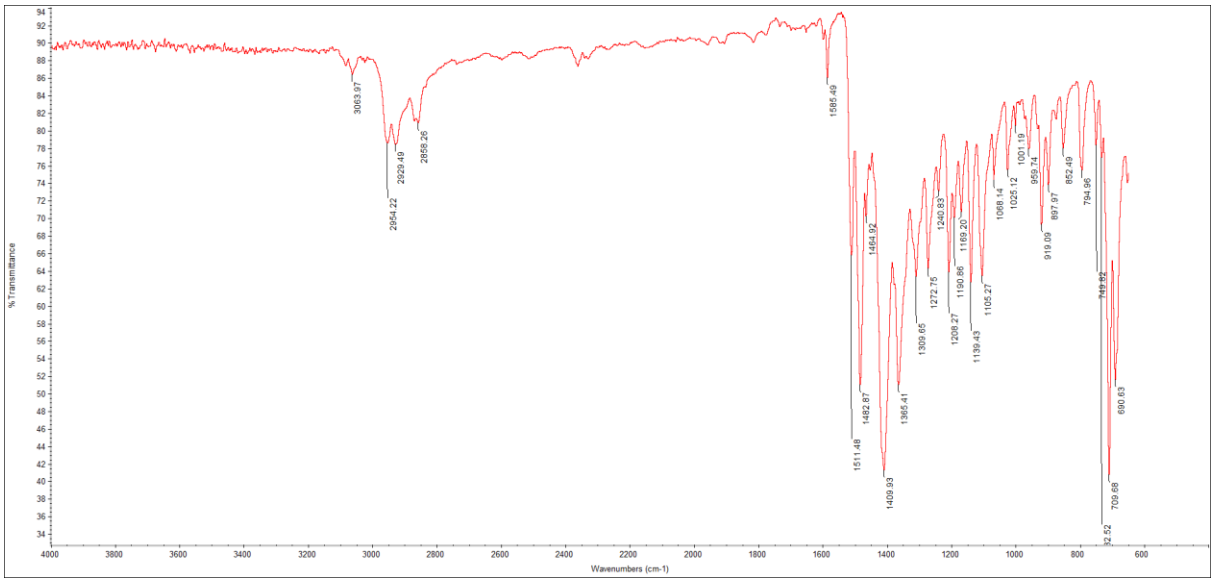

Figure A2.10. FT-IR spectrum of *cis*-bis(*N*,*N*-diethyl-*N*'-*p*-chloro-benzoylthioureato-κ^2*S*,*O*)palladium(II).

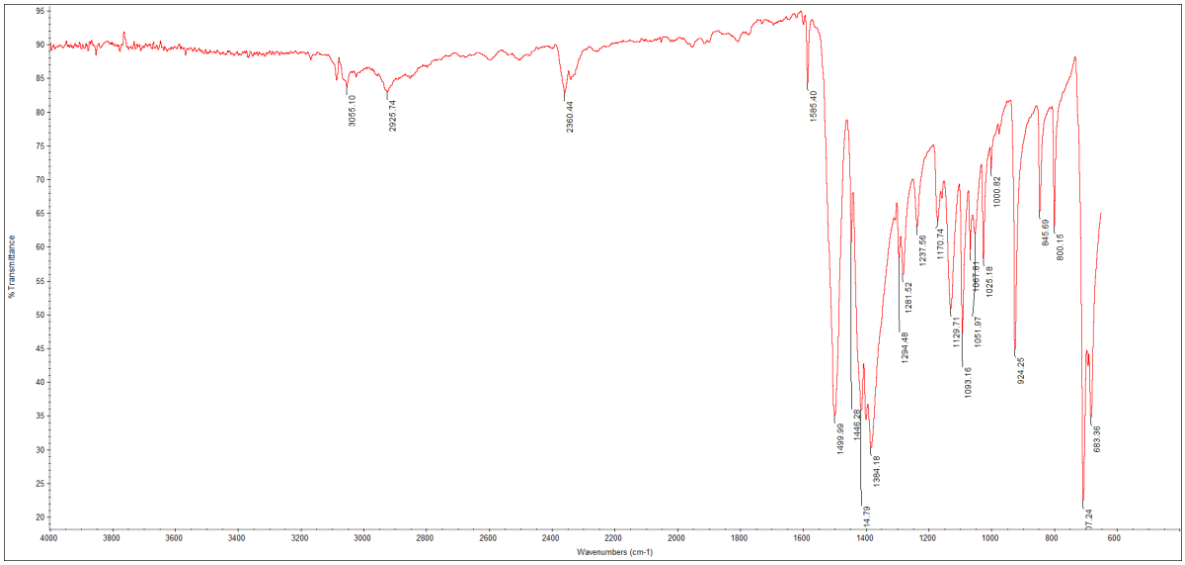

Figure A2.11. FT-IR spectrum of *cis*-bis(*N*,*N*-dimethyl-*N*'-benzoylthioureato-κ^2*S*,*O*)palladium(II).

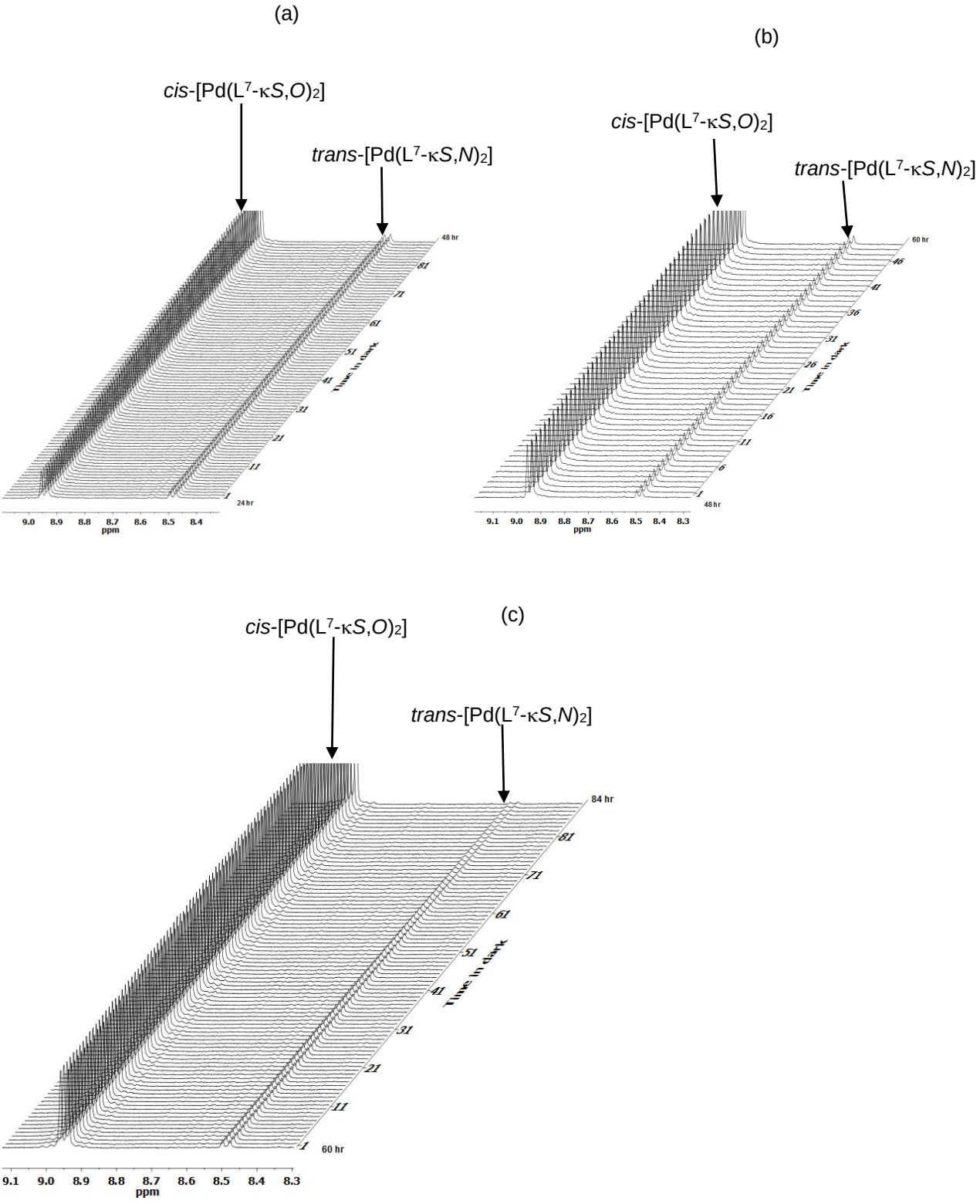

Figure A4.1. An array of ^{1}H NMR spectra representing spontaneous *trans* → *cis* isomerization for isolated *trans*-[Pd(L^{7}-κ*S*,*O*)$_2$] and *trans*-[Pd(L^{7}-κ*S*,*N*)$_2$] to *cis*-[Pd(L^{7}-κ*S*,*O*)$_2$] after (a) 48hr, (b) 60hr, and (c) 80hr in the dark in chloroform-*d* at 25 °C.

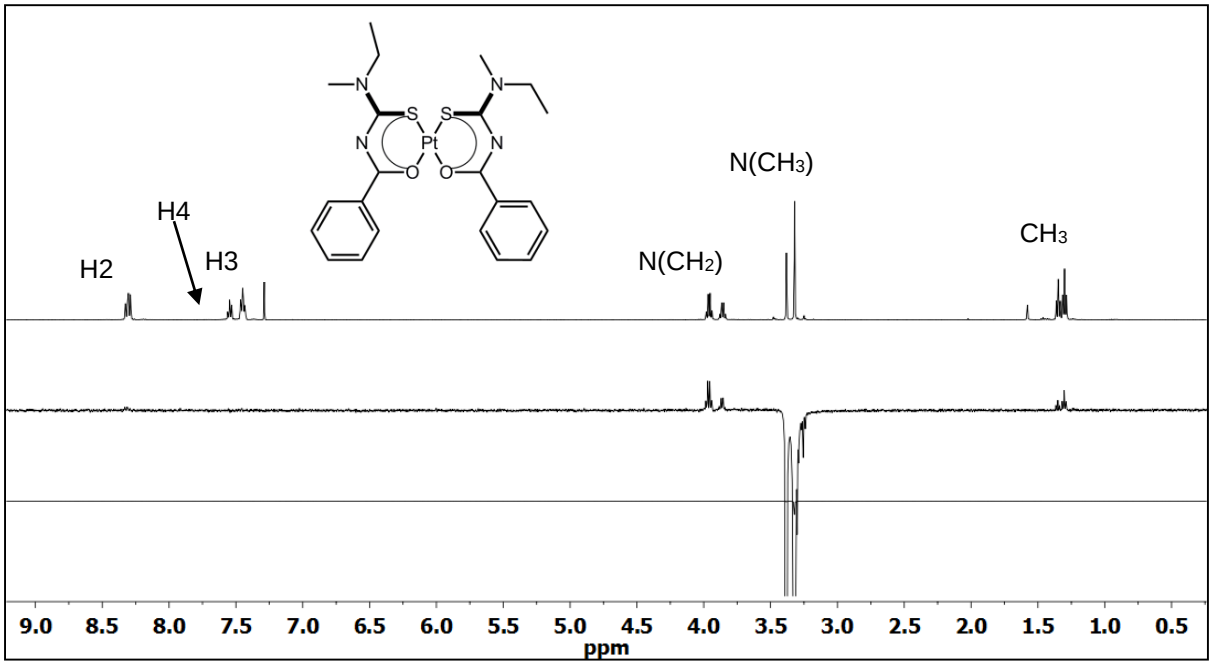

Figure A5.1. 1D NOESY spectrum showing assignment of *cis*-[Pt(*EZ/EE*-L^9-κ*S*,*O*)$_2$] in chloroform-*d* at 25 °C from irradiation of N-(CH_3) protons; ^{1}H NMR spectrum is overlaid to assist assignment of peaks.

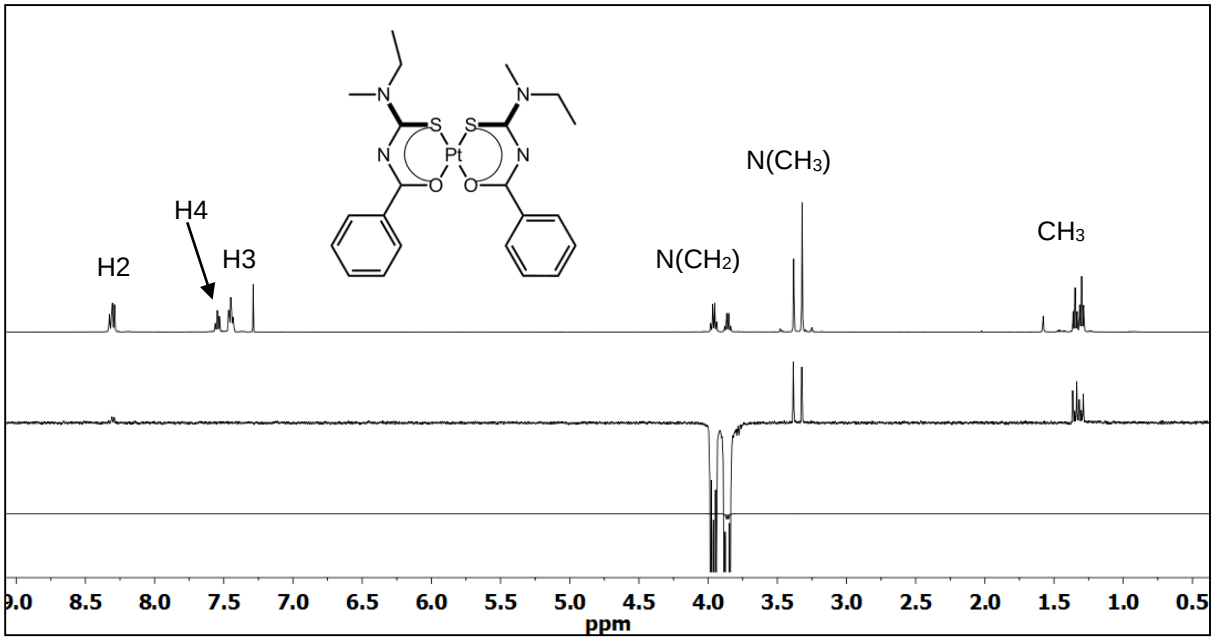

Figure A5.2. 1D NOESY spectrum showing assignment of *cis*-[Pt(*EZ/EE*-L^9-κ*S*,*O*)$_2$] in chloroform-*d* at 25 °C from irradiation of *N*-(CH_2) protons; ^{1}H NMR spectrum is overlaid to assist assignment of peaks.

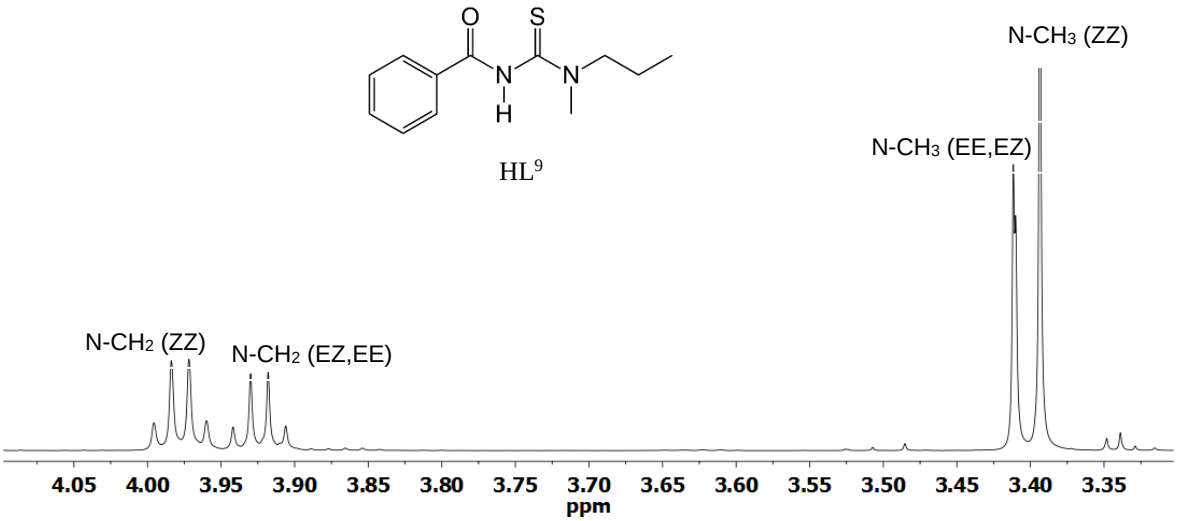

Figure A5.3. Partial ^{1}H NMR spectrum of *cis*-bis(*N*-methyl, *N*'-propyl-*N*'-benzoylthioureato)platinum(II) *cis*-[Pt(L^{9}-κ*S*,*O*)$_2$] in chloroform-*d* at 25 °C.

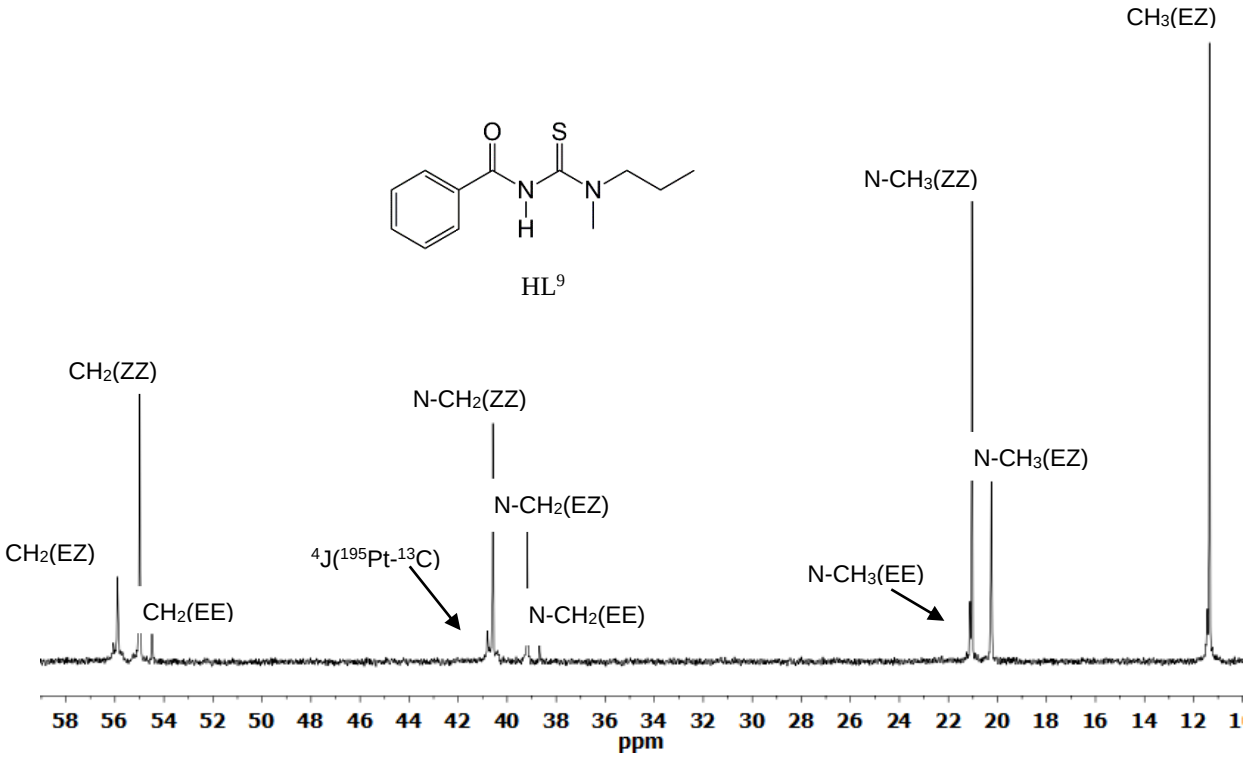

Figure A5.4. Partial ^{13}C{^{1}H} NMR spectra of *cis*-bis(*N*-methyl, *N*-propyl-*N*'-benzoylthioureato)-platinum(II) *cis*-[Pt(L^{9}-κ*S*,*O*)$_2$] in chloroform-*d* at 25 °C.

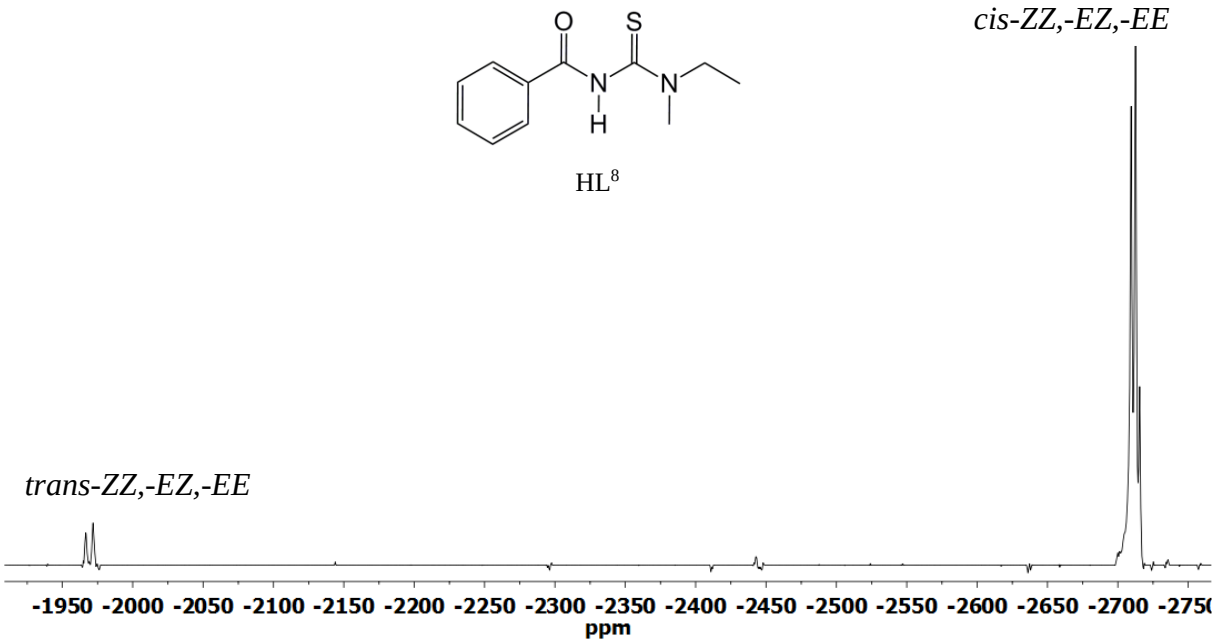

Figure A5.5. $^{195}Pt\{^{1}H\}$ NMR spectrum of a chloroform-*d* solution of *cis*-[Pt(L^{9}-κ*S*,*O*)$_2$] irradiated with polychromatic light from a 5Watt LED lamp for 30 mins at 25 °C, showing *trans-ZZ*, *trans-EZ* and *trans-EE* isomers isomers formed from photo-induced isomerization.

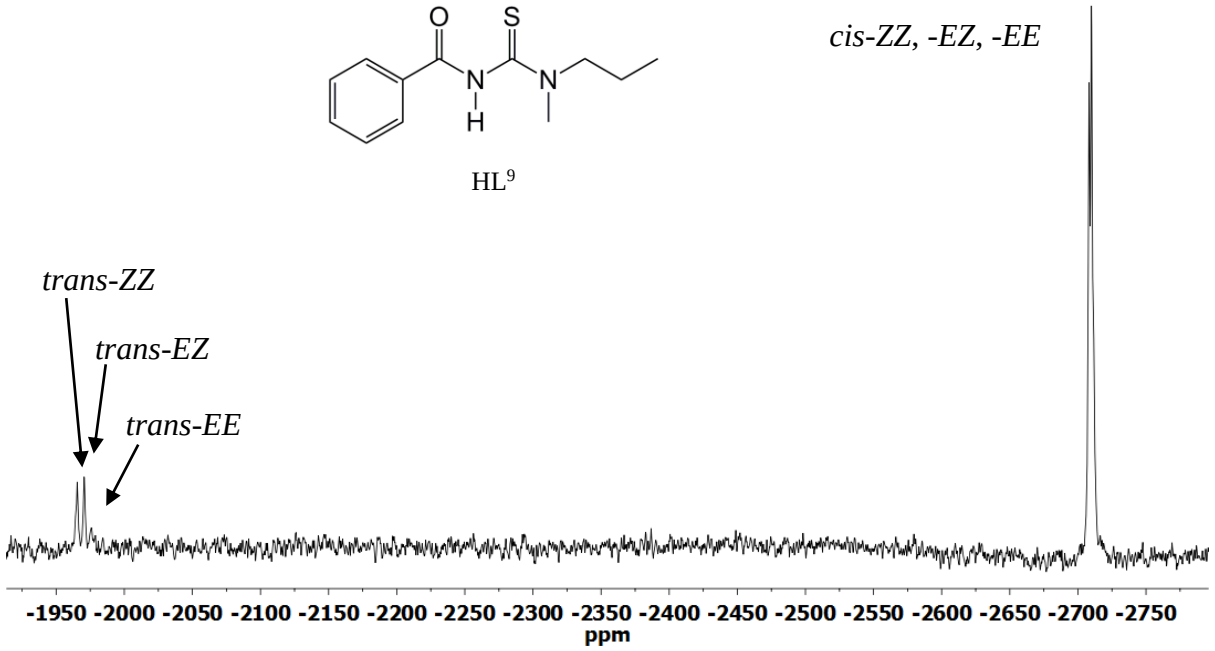

Figure A5.6. $^{195}Pt\{^{1}H\}$ NMR spectrum of a chloroform-*d* solution of *cis*-[Pt(L^{10}-κ*S*,*O*)$_2$] irradiated with polychromatic light from a 5Watt LED lamp for 30 mins at 25 °C, showing *trans-ZZ*, *trans-EZ* and *trans-EE* isomers formed from photo-induced isomerization.

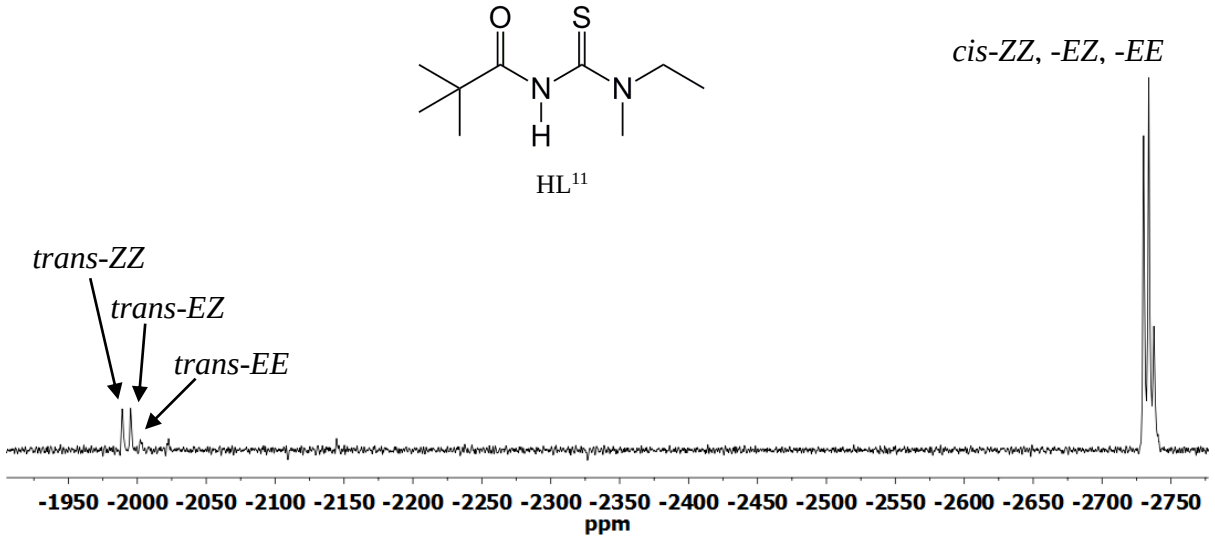

Figure A5.7. $^{195}Pt\{^{1}H\}$ NMR spectrum of a chloroform-*d* solution of *cis*-[Pt(L^{11}-κ*S*,*O*)$_2$] irradiated with polychromatic light from a 5Watt LED lamp for 30 mins at 25 °C, showing *trans-ZZ*, *trans-EZ* and *trans-EE* isomers formed from photo-induced isomerization.

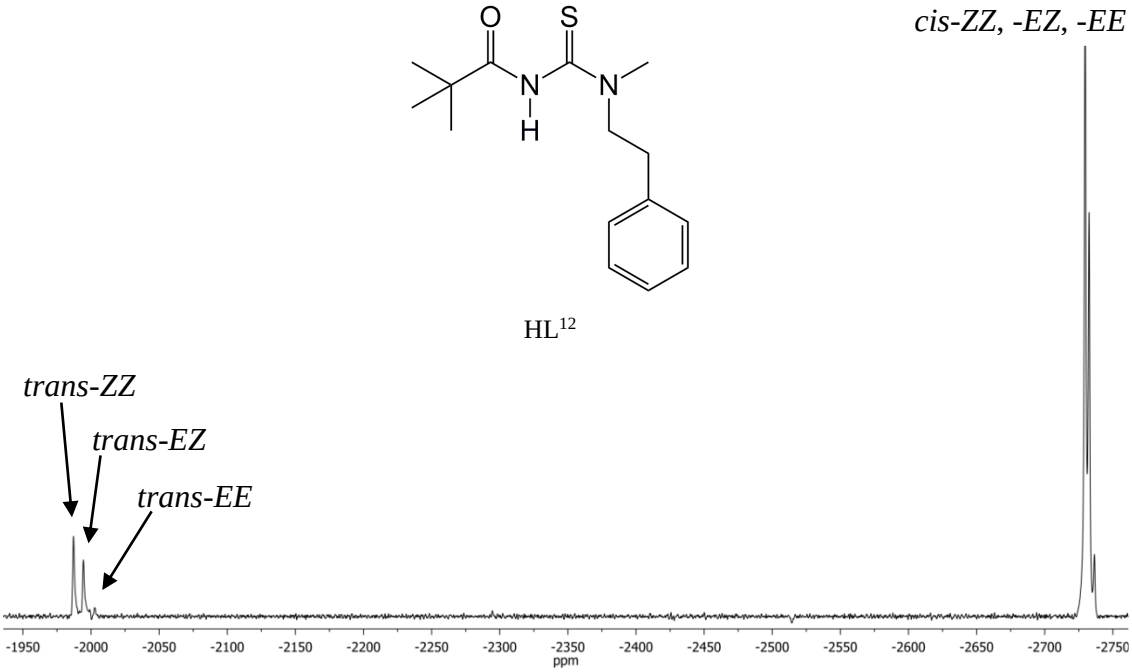

Figure A5.8. $^{195}Pt\{^{1}H\}$ NMR spectrum of a chloroform-*d* solution of *cis*-[Pt(L^{13}-κ*S*,*O*)$_2$] irradiated with polychromatic light from a 5Watt LED lamp for 30 mins at 25 °C, showing *trans-ZZ*, *trans-EZ* and *trans-EE* isomers formed from photo-induced isomerization.

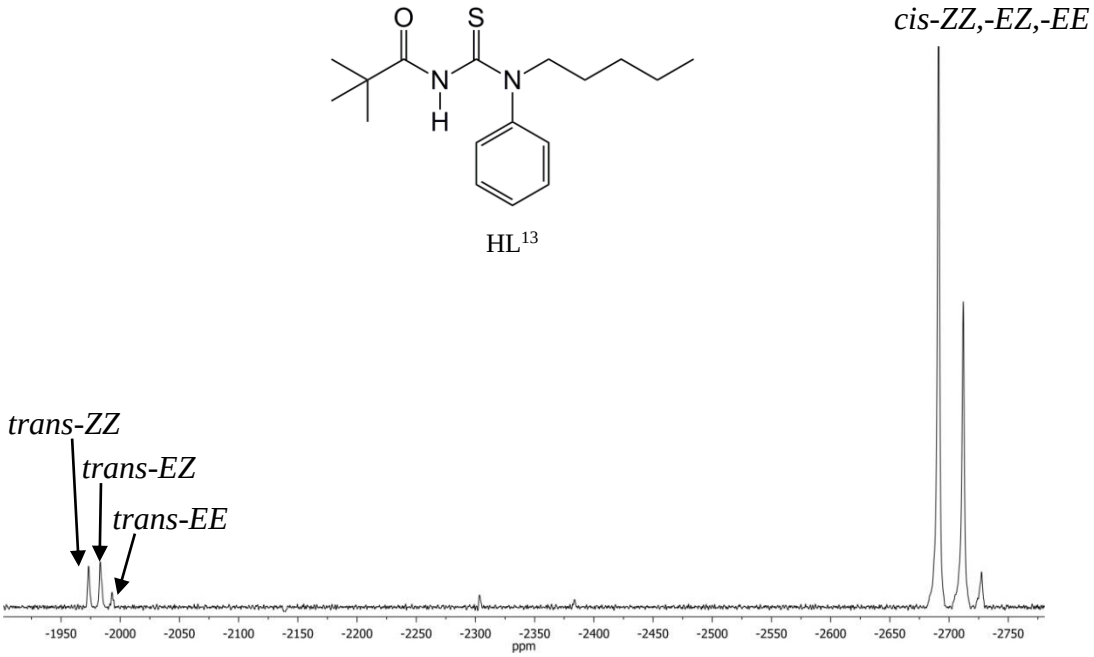

Figure A5.9. $^{195}Pt\{^{1}H\}$ NMR spectrum of a chloroform-*d* solution of *cis*-[Pt(L^{14}-κ*S*,*O*)$_2$] irradiated with polychromatic light from a 5Watt LED lamp for 30 mins at 25 °C, showing *trans-ZZ*, *trans-EZ* and *trans-EE* isomers formed from photo-induced isomerization.

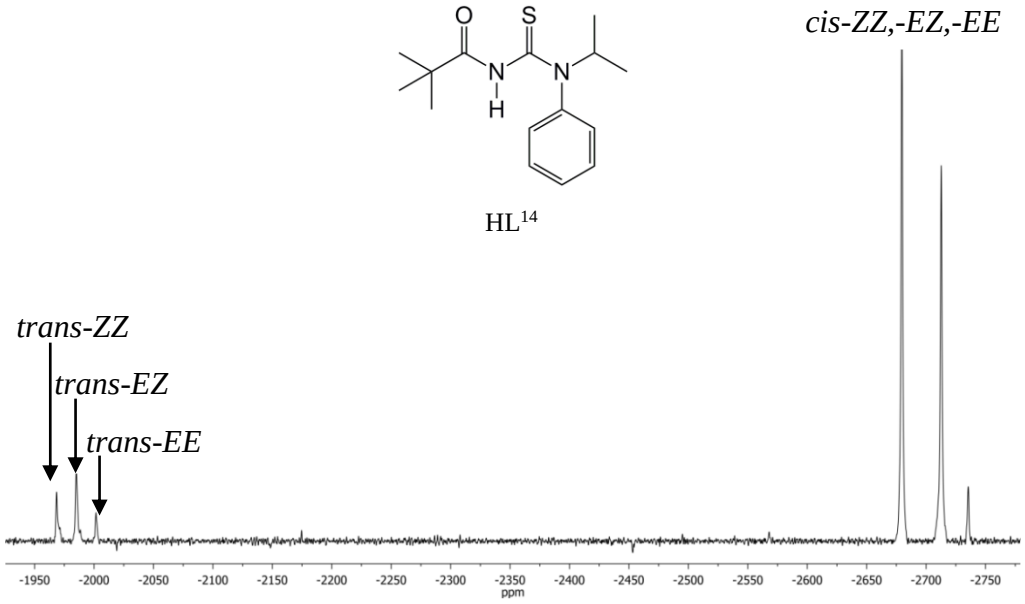

Figure A5.10. $^{195}Pt\{^{1}H\}$ NMR spectrum of a chloroform-*d* solution of *cis*-[Pt(L^{15}-κ*S*,*O*)$_2$] irradiated with polychromatic light from a 5Watt LED lamp for 30 mins at 25 °C, showing *trans-ZZ*, *trans-EZ* and *trans-EE* isomers formed from photo-induced isomerization.

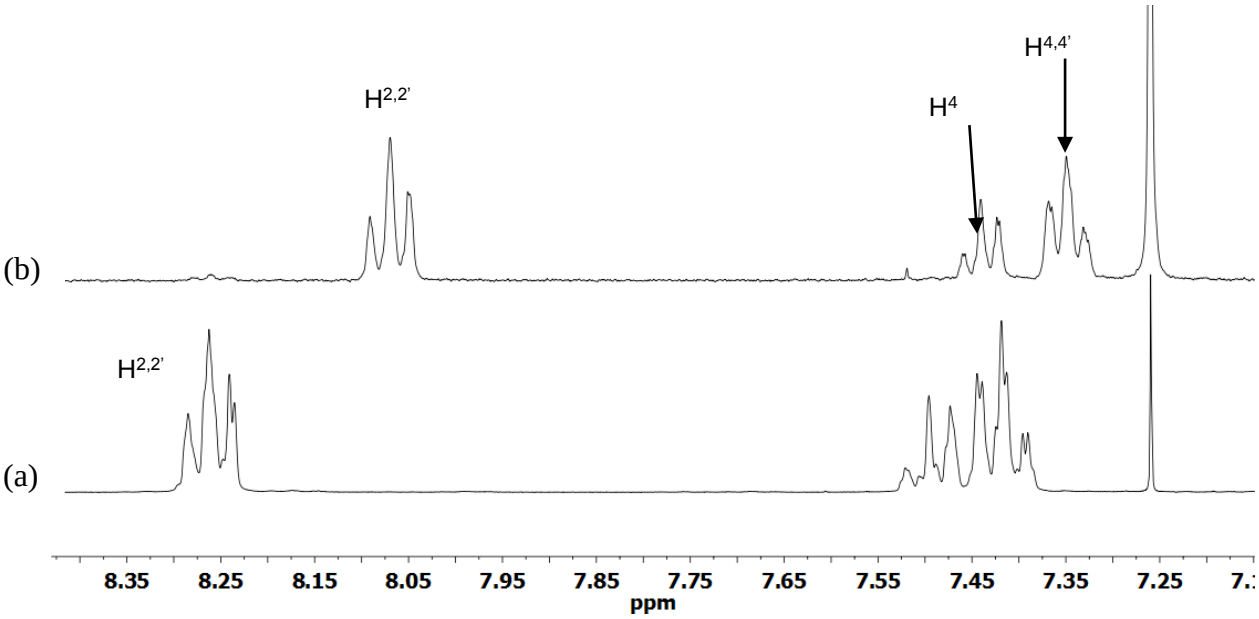

Figure A5.11. Downfield region of ^{1}H NMR spectra of **(a)** *cis*-[Pd(L^{8}-*S*,*O*)$_2$] and **(b)** isolated *trans*-[Pd(L^{8}-*S*,*O*)$_2$] in chloroform-*d* at 25 °C.

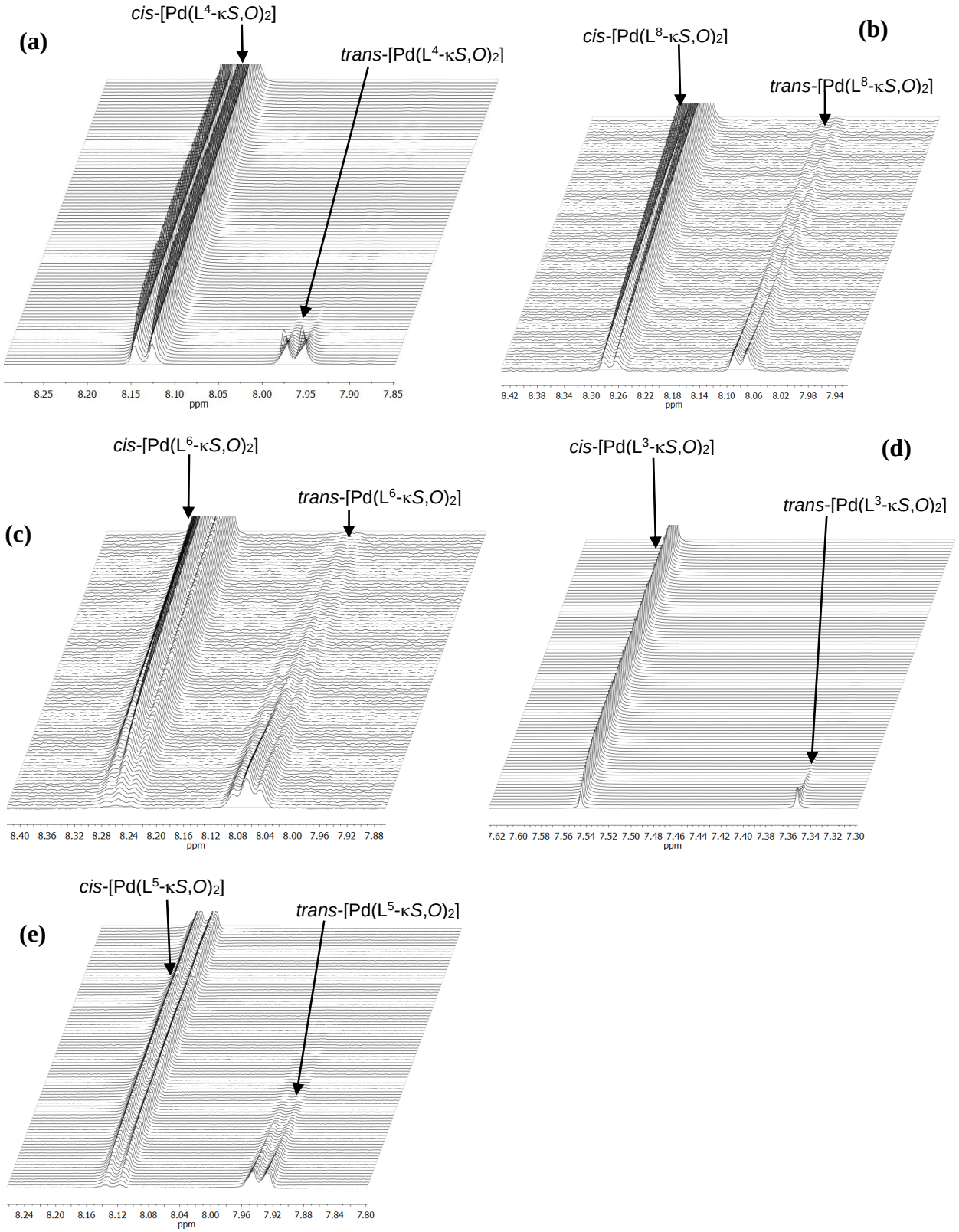

Figure A6.1. An array of ^{1}H NMR spectra representing spontaneous *trans*→*cis* isomerization for isolated (a) *trans*-[Pd(L^{4}-κ*S*,*O*)$_2$], (b) *trans*-[Pd(L^{8}-κ*S*,*O*)$_2$], (c) *trans*-[Pd(L^{6}-κ*S*,*O*)$_2$], (d) *trans*-[Pd(L^{3}-κ*S*,*O*)$_2$], *trans*-[Pd(L^{5}-κ*S*,*O*)$_2$] in chloroform-*d* at 25 °C.

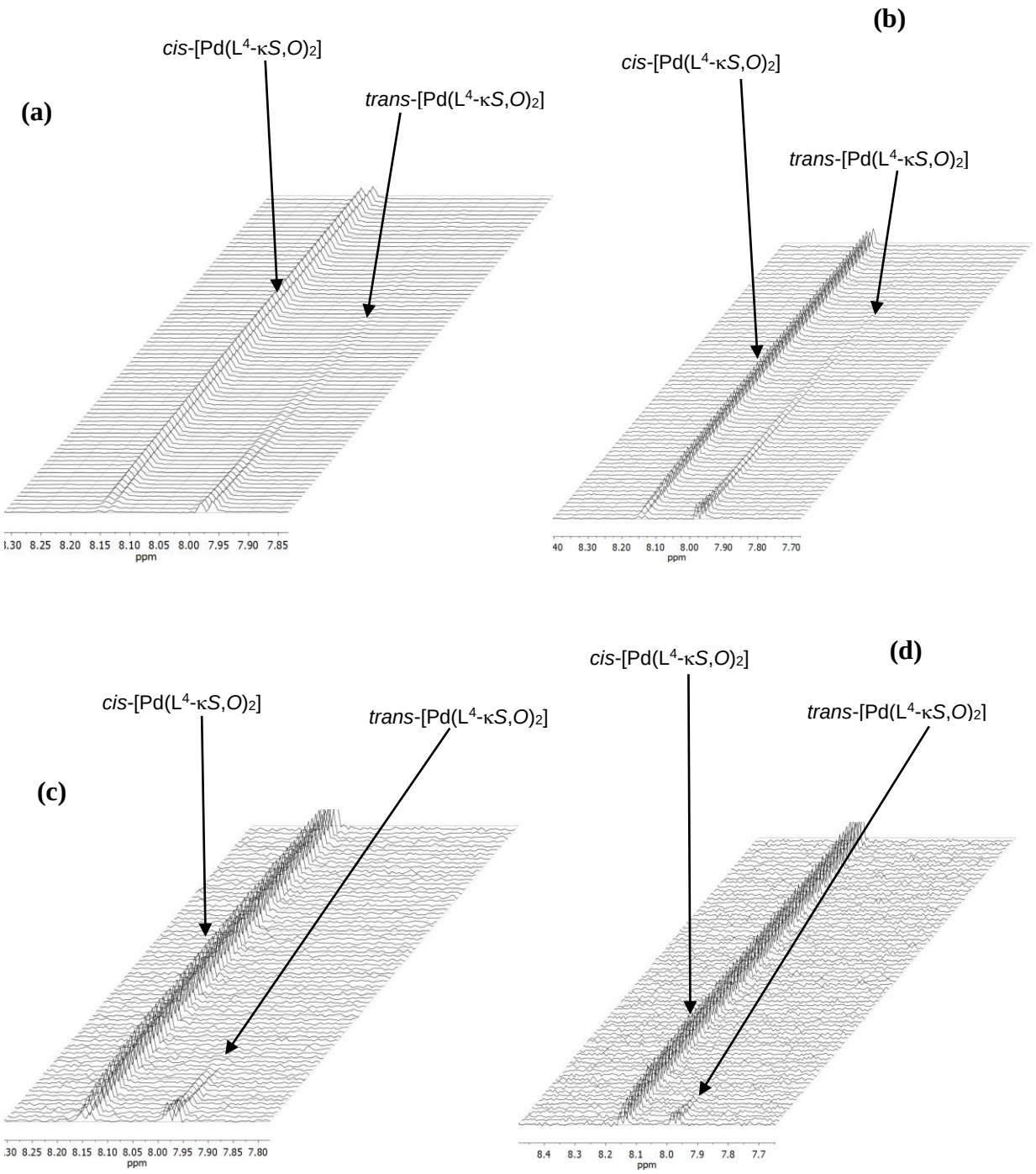

Figure A6.2. An array of ^{1}H NMR spectra representing spontaneous *trans*→*cis* isomerization for isolated *trans*-[Pd(L^{4}-κ*S*,*O*)$_2$] (a) using 10 mg/mL complex at 25 °C (b) using 5 mg/mL complex at 35 °C (c) using 5 mg/mL complex at 45 °C, (d) using 5 mg/mL complex at 55 °C in chloroform-*d*; Each spectrum in the array represents ^{1}H NMR data acquisition after every 5 minutes seconds in the dark.

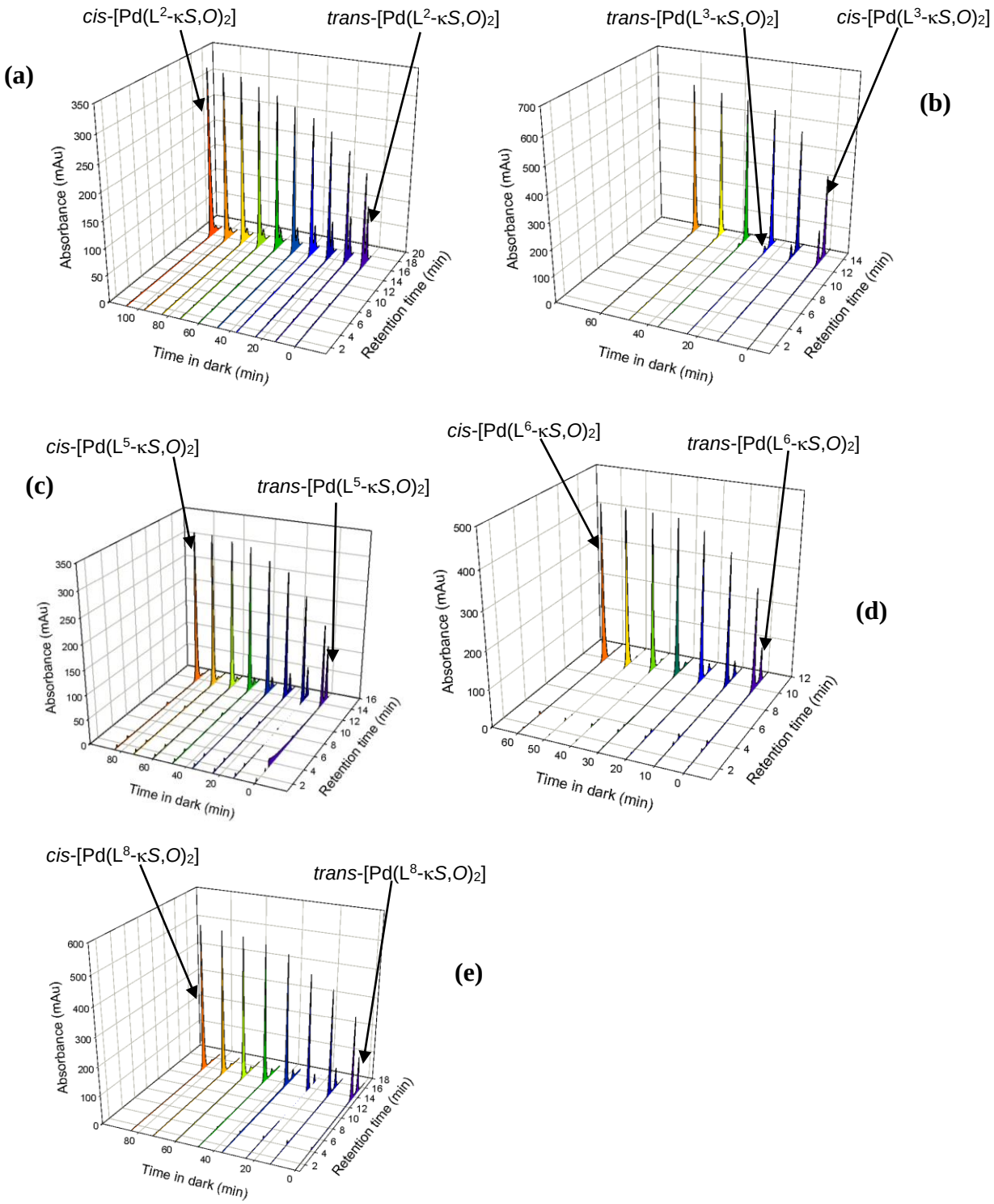

Figure A6.3. Overlaid RP-HPLC chromatograms representing spontaneous *trans*→*cis* isomerization of (a) [Pd(L^2-κ*S*,*O*)$_2$], (b) [Pd(L^3-κ*S*,*O*)$_2$], (c) [Pd(L^5-κ*S*,*O*)$_2$], (d) [Pd(L^6-κ*S*,*O*)$_2$], [Pd(L^8-κ*S*,*O*)$_2$] in acetonitrile after irradiation with polychromatic light from a 5 Watt LED lamp for 30 mins.

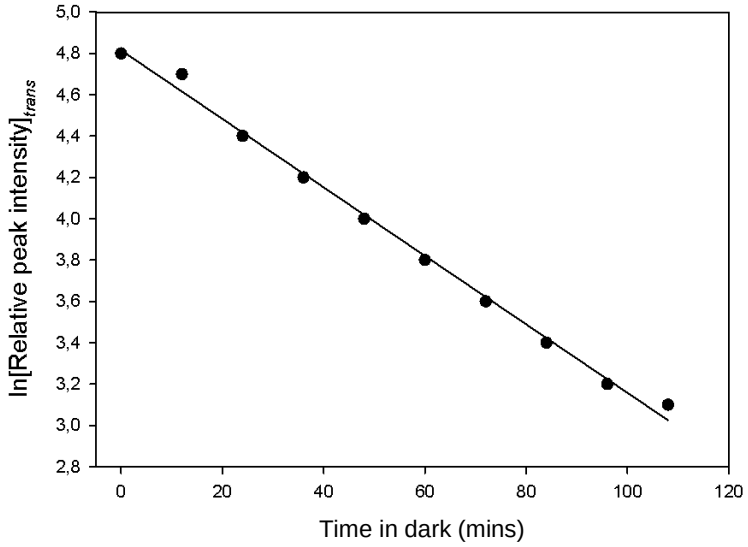

Figure A6.4. Plot of the natural logarithm of relative peak intensity versus time in the dark for the *trans*→*cis* isomerization of *cis*-[Pd(L^7-κ*S*,*O*)$_2$] in acetonitrile at 25 °C.

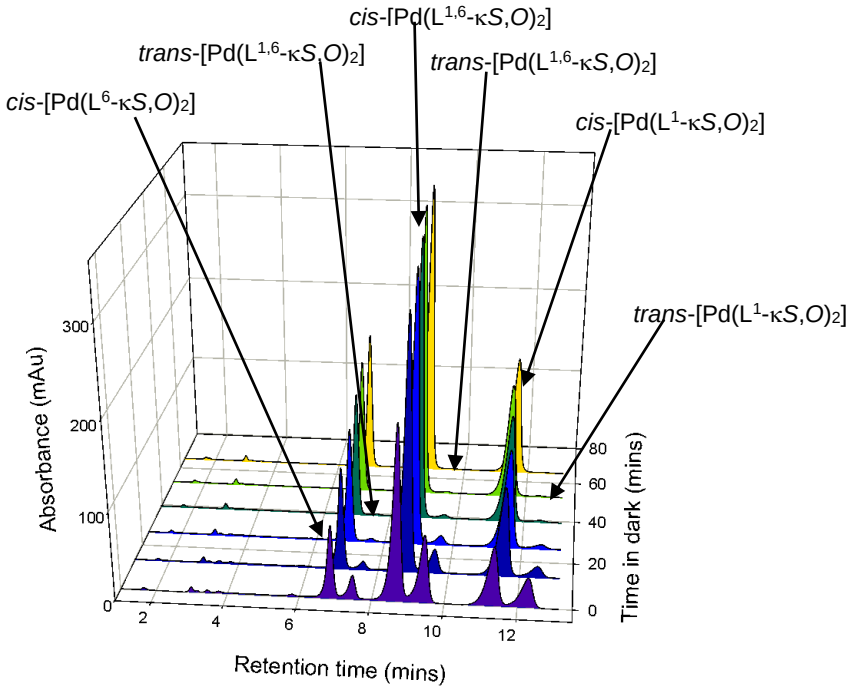

Figure A6.5. Overlaid chromatograms representing *trans*→*cis* isomerization in acetonitrile for mixed solutions of *cis*-[Pd(L^1-κ*S*, *O*)$_2$] and *cis*-[Pd(L^6-κ*S*,*O*)$_2$]; conditions: mobile phase, 95:5% v/v acetonitrile:water; GEMINI C_{18}, 5 µm, 250 x 4.6 mm column; 20 µl injection volume; 1 mlmin^{-1} flow rate; 262 nm detection; photo-irradiation with polychromatic light from a 5Watt LED lamp.

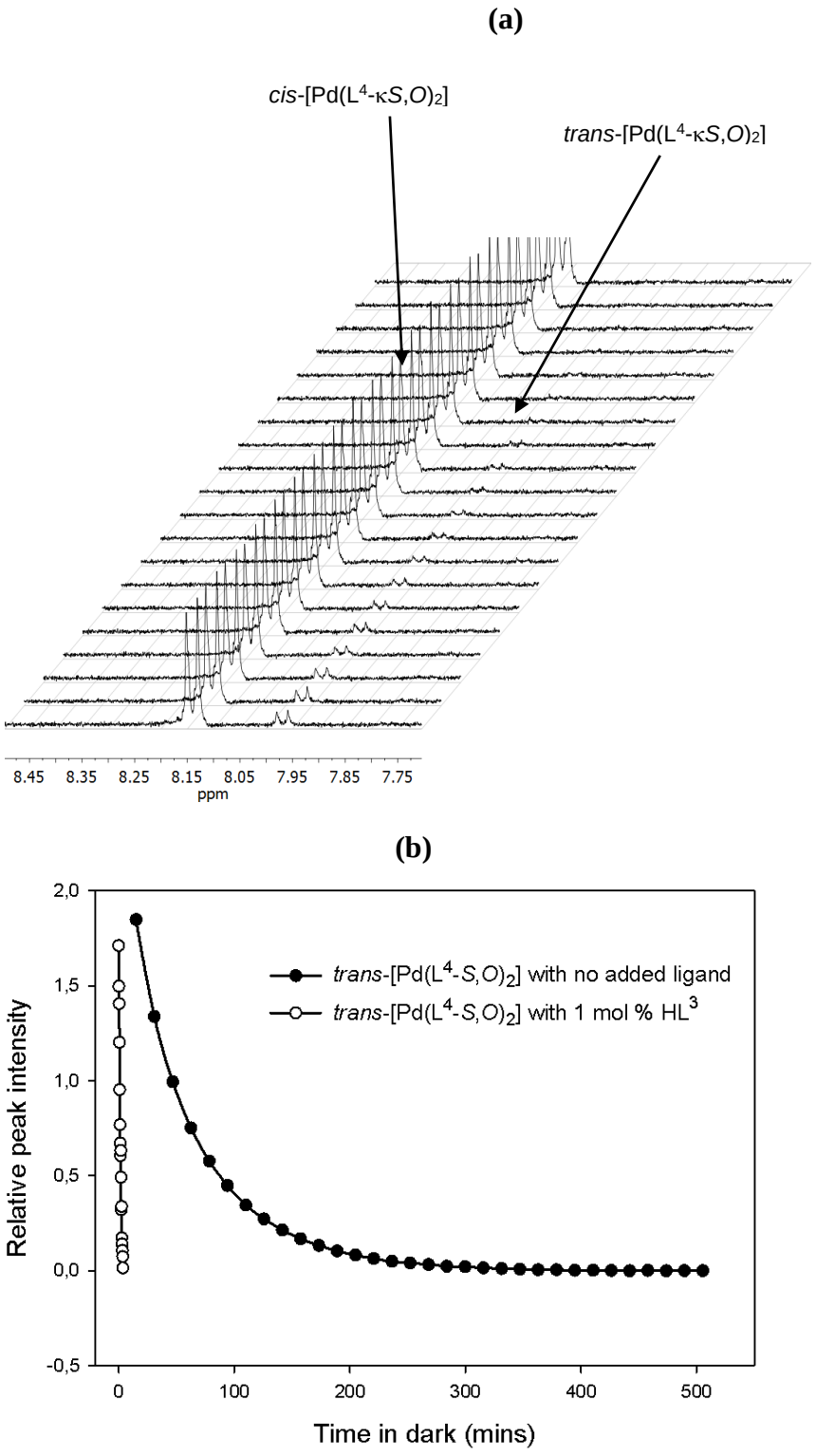

Figure A6.6. (a) An array of ^{1}H NMR spectra; and (b) comparison of plots of relative peak intensity; representing spontaneous *trans*→*cis* isomerization for isolated *trans*-[Pd(L^{4}-κ*S*,*O*)$_2$] after the addition of 1 mol % HL^{3}.

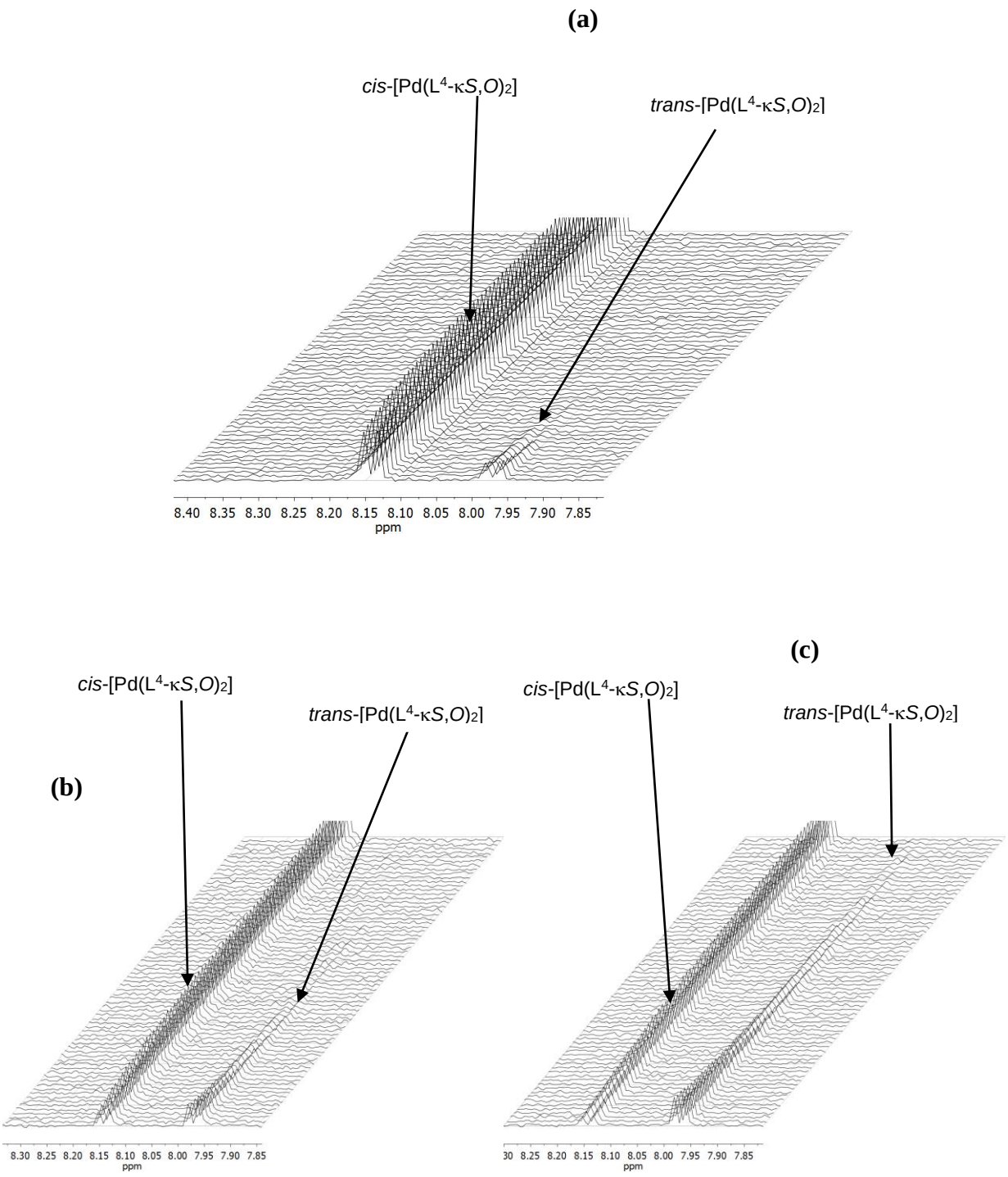

Figure A6.7. An array of ^{1}H NMR spectra representing spontaneous *trans*→*cis* isomerization for isolated *trans*-[Pd(L^{4}-κ*S*,*O*)$_2$] after the addition (a) 0.12 mM HL^{4}, (b) 0.06 mM HL^{4}, and (c) 0.03 mM HL^{4} in chloroform-*d* at 25 °C; Each spectrum in the array represents ^{1}H NMR data acquisition after every 20 seconds in the dark.

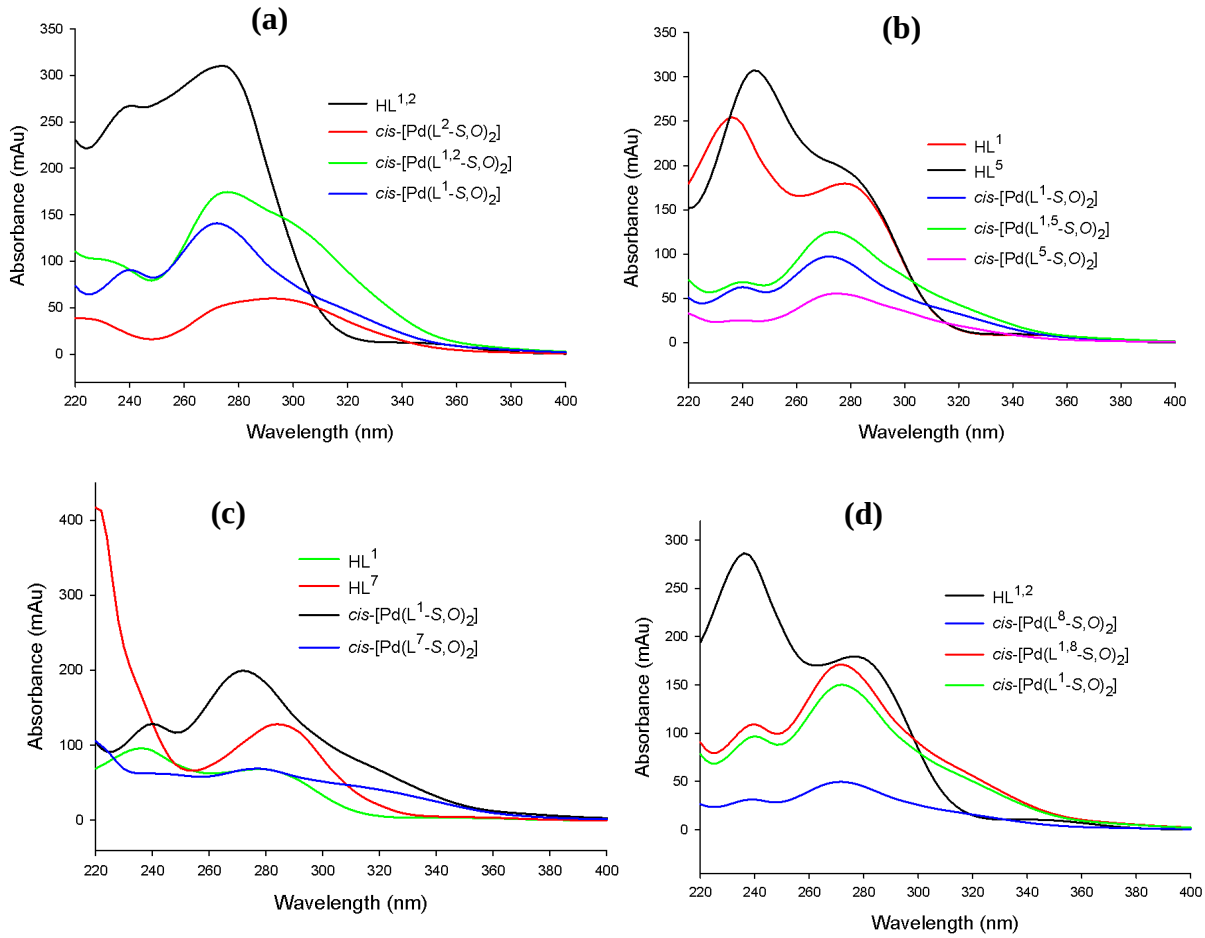

Figure A6.8. Overlaid UV-Vis spectra from photodiode array detection at 262 nm for ligand exchange products from addition of (a) HL^2, (b) HL^5, (c) HL^7, and (d) HL^8 to a pre-irradiated solution of *trans*-[Pd(L^1-κ*S*,*O*)$_2$] in acetonitrile and at room temperatur

Appendix B-Publication

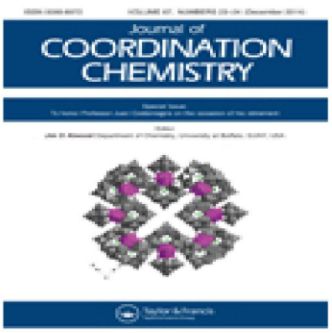

Journal of Coordination Chemistry
Publication details, including instructions for authors and subscription information:
http://www.tandfonline.com/loi/gcoo20

Light-induced cis/trans isomerization of cis-[Pd(L-S,O)$_2$] and cis-[Pt(L-S,O)$_2$] complexes of chelating N,N-dialkyl-N′-acylthioureas: key to the formation and isolation of trans isomers

Henry A. Nkabyo[a], D. Hannekom[a], Jean McKenzie[a] & Klaus R. Koch[a]
[a] Department of Chemistry and Polymer Science, University of Stellenbosch, Stellenbosch, South Africa
Accepted author version posted online: 08 Oct 2014.Published online: 06 Nov 2014.

To cite this article: Henry A. Nkabyo, D. Hannekom, Jean McKenzie & Klaus R. Koch (2014) Light-induced cis/trans isomerization of cis-[Pd(L-S,O)$_2$] and cis-[Pt(L-S,O)$_2$] complexes of chelating N,N-dialkyl-N′-acylthioureas: key to the formation and isolation of trans isomers, Journal of Coordination Chemistry, 67:23-24, 4039-4060, DOI: 10.1080/00958972.2014.974584

To link to this article: http://dx.doi.org/10.1080/00958972.2014.974584

Journal of Coordination Chemistry, 2014
Vol. 67, Nos. 23–24, 4039–4060, http://dx.doi.org/10.1080/00958972.2014.974584

Light-induced *cis/trans* isomerization of *cis*-[Pd(L-*S*,*O*)$_2$] and *cis*-[Pt(L-*S*,*O*)$_2$] complexes of chelating *N*,*N*-dialkyl-*N*′-acylthioureas: key to the formation and isolation of *trans* isomers

HENRY A. NKABYO, D. HANNEKOM, JEAN MCKENZIE and KLAUS R. KOCH*

Department of Chemistry and Polymer Science, University of Stellenbosch, Stellenbosch, South Africa

(*Received 22 September 2014; accepted 26 September 2014*)

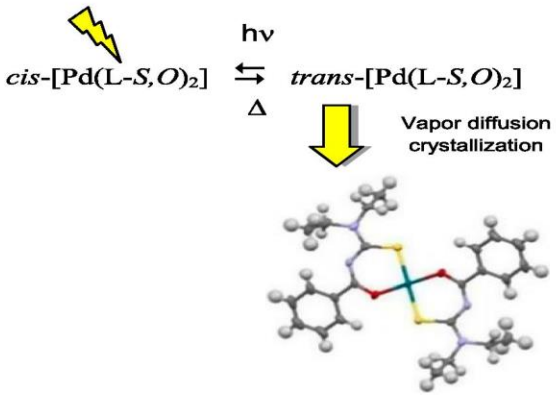

The dominantly formed *cis*-[M(L-*S*,*O*)$_2$] (M = Pt^{II} or Pd^{II}) complexes from *N*,*N*-dialkyl-*N*′-acyl-thioureas in solution undergo a facile *cis* → *trans* isomerization on irradiation with visible light at room temperature, allowing the predictable formation and isolation of the elusive *trans*-[Pd(L-*S*,*O*)$_2$] complexes.

Irradiation *cis*-[M(L″-*S*,*O*)$_2$] complexes (M = Pt^{II}, Pd^{II}) derived from *N*,*N*-dialkyl-*N*′-benzoylthioureas (HL″) with various sources of intense visible polychromatic or monochromatic light with $\lambda < 500$ nm leads to light-induced *cis* → *trans* isomerization in organic solvents. In all cases, white light derived from several sources or monochromatic blue-violet laser 405 nm light, efficiently results in substantial amounts of the *trans* isomer appearing in solution, as shown by ^{1}H NMR and/or reversed-phase HPLC separation in dilute solutions at room temperature. The extent and relative rates of *cis/trans* isomerization induced by *in situ* laser light (λ = 405 nm) of *cis*-[Pd(L^2-*S*,*O*)$_2$] was

*Corresponding author. Email: krk@sun.ac.za

directly monitored by ^{1}H NMR and ^{195}Pt NMR spectroscopy of selected *cis*-[Pt(L-*S*,*O*)$_2$] compounds in chloroform-*d*; both with and without light irradiation allows the $\delta(^{195}Pt)$ chemical shifts *cis/trans* isomer pairs to be recorded. The *cis/trans* isomers appear to be in a photo-thermal equilibrium between the thermodynamically favored *cis* isomer and its *trans* counterpart. In the dark, the *trans* isomer reverts back to the *cis* complex in what is probably a thermal process. The light-induced *cis/trans* process is the key to preparing and isolating the rare *trans* complexes which cannot be prepared by conventional synthesis as confirmed by the first example of *trans*-[Pd(L-*S*,*O*)$_2$] characterized by single-crystal X-ray diffraction, deliberately prepared after photo-induced isomerization in acetonitrile solution.

Keywords: Photo-induced *cis/trans* isomerization; *cis* → *trans* Isomerization; *N,N*-dialkyl-*N*′-benzoyl-thiourea complexes of Pt(II) and Pd(II); *In situ* laser ^{1}H NMR spectroscopy; ^{195}Pt NMR shifts of *cis/trans*-[Pt(L-*SO*)$_2$]; Separation with *rp*-HPLC; Molecular structure of *trans*-bis (*N,N*-diethyl-*N*′-benzoylthioureato)-palladium(II)

1. Introduction

Ligands of the general type *N,N*-dialkyl-*N*′-acyl(aroyl)thioureas (HL; $R^1{}_2NC(S)NHC(O)R^2$, R^1 = alkyl, R^2 = alkyl or aryl groups), first prepared more than 80 years ago [1], have long been known to readily form stable, uncharged coordination compounds with numerous transition metal ions as shown by the studies of Hoyer and Beyer more than three decades ago [2, 3], and later by *inter alia* Konig and Schuster [4–7]. We have been interested in fundamental aspects of the coordination chemistry of *N,N*-dialkyl-*N*′-acyl(aroyl)thioureas with some members of the platinum group metals (PGMs) in view of their potential application in solvent extraction, pre-concentration, separation, and even trace analytical determination of the PGMs [8]. A recent review for 2007–2013 on the coordination chemistry and the potential applications of this class of ligands attests to considerable growth in interest in these molecules worldwide [9].

Our focus on the coordination chemistry and use of this class of deceptively simple ligands arises in part from the relative ease of their synthesis, which together the favorable physiochemical properties of *N,N*-dialkyl-*N*′-acyl(aroyl)thioureas, allows for their selective *in situ* coordination of Pt^{II}, Pd^{II}, and Rh^{III} in acidic chloride-rich solutions, followed by easy quantification of the resultant complexes using reversed-phase high performance liquid chromatography (*rp*-HPLC) illustrates a practically useful application of such molecules [10]. Generally *N,N*-dialkyl-*N*′-acylthioureas show a marked tendency to coordinate to d^8 metal ions to give stable *cis*-[M(L-*S*,*O*)$_2$]-type complexes (M = Pt^{II}, Pd^{II}) upon loss of a proton; in the case of M^{III} transition metal ions, the corresponding *fac*-[M(L-*S*,*O*)$_3$] complexes are usually obtained, in which all sulfurs are coordinated *trans* to O donors [8, 10, 11]. The dominant tendency to form the *cis*-[M(L-*S*,*O*)$_2$] isomer of both Pt(II) and Pd (II) complexes may be exploited to design and prepare exclusively either the 2 : 2 *cis*-[$Pt_2(L^m$-*S*,*O*)$_2$] or the 3 : 3 *cis*-[$Pt_3(L^p$-*S*,*O*)$_3$] metallamacrocyclic Pt(II) complexes from bipodal ligands HL^m (3,3,3′,3′-tetraethyl-1,1-isophthaloylbis(thiourea) and HL^p (3,3,3′,3′-tetra(*n*-butyl)-1,1-terephthaloyl-bis(thiourea), essentially based on whether the two chelating *S,O* moieties are bound *meta* to each other in the bipodal ligand HL^m, or *para* in the HL^p ligand [11]. Moreover, the 2 : 2 *cis*-[$Pt_2(L^m$-*S*,*O*)$_2$] and 3 : 3 *cis*-[$Pt_3(L^p$-*S*,*O*)$_3$] readily react with halogens generated *in situ* electrochemically from halide ions to give the corresponding Pt(IV) analogs *cis*-[$Pt^{IV}{}_2(L^m$-*S*,*O*)$_2Br_4$], *cis*-[$Pt^{IV}{}_2(L^m$-*S*,*O*)$_2Cl_4$], and *cis*-[$Pt^{IV}{}_3I_6(L^p$-*S*,*O*)$_3$], not easily accessible by other means [12]. In this context, the

overwhelming tendency to form *cis* complexes of the numerous complexes of divalent transition metal ions with simple *N*,*N*-dialkyl-*N*′-acyl(aroyl)thioureas which have been structurally characterized is striking [9]. A search of the Cambridge Structural Database shows that of 40 single-crystal X-ray diffraction structures of Pt(II), Pd(II), Ni(II), and Cu(II) complexes from *N*,*N*-dialkyl-*N*′-acyl(aroyl)thiourea ligands which have been characterized in the solid state [13], at least 20 of them are d^8 Pt(II) and Pd(II) complexes. Remarkably out of all these, only one *trans*-bis(*N*,*N*-di(n-butyl)-*N*′-naphthoylthioureato)–platinum(II) complex, isolated serendipitously by us in ca. 15% yield two decades ago, has been characterized by single-crystal X-ray diffraction to date [14]. Only two other examples of *trans*-*S*,*O* chelated Cu(II) complexes have been unambiguously characterized to our knowledge [15, 16].

Despite considerable effort, we have not been able to predictably prepare substantial quantities of *trans*-[Pt(L-*S*,*O*)$_2$] or *trans*-[Pd(L-*S*,*O*)$_2$] complexes with *N*,*N*-dialkyl-*N*′-aroylthioureas by any conventional synthetic route. While intuitively it is not unreasonable to expect that the *cis*-[M(L-*S*,*O*)$_2$] (M = Pt^{II}, Pd^{II}) complexes are likely to be thermodynamically favored in view of the higher *trans* effect/influence of the *S* donor as compared to the *O* donor [17]. The corresponding *trans*-[M(L^n-*S*,*O*)$_2$] (M = Pt^{II}, Pd^{II}) isomers may be expected to be only of slightly higher energy overall. This is confirmed by the small energy difference of 10.1 kJ mol^{-1} for *cis*-[Pt(L-*S*,*O*)$_2$] and *trans*-[Pt(L-*S*,*O*)$_2$] with *N*,*N*-dimethyl-*N*′-methylacylthiourea in vacuum, based on DFT gas-phase calculations. Similar calculations using the conductor-like screening (COSMO) model for chloroform and acetonitrile show these energy differences range from 13.4 to 18.4 kJ mol^{-1}, respectively [18].

We have for some time been interested in the question of why *trans*-*S*,*O* chelated complexes are so rare compared with their *cis* analogs; of particular interest is the question how the *trans*-[M(L-*S*,*O*)$_2$] (M = Pt^{II}, Pd^{II}) complexes may reliably be prepared and isolated in reasonable yields. Recently, we discovered that the key to obtaining *trans*-[M(L-*S*,*O*)$_2$] (M = Pt^{II}, Pd^{II}) complexes in solution appears to be a facile photo-induced isomerization of the *cis*-[M(L^3-*S*,*O*)$_2$] complexes (HL^3 = *N*,*N*-diethyl-*N*′-3,4,5-trimethoxybenzoylthiourea) in acetonitrile solutions, as confirmed by RP-HPLC and ^{1}H NMR spectroscopy [19]. Irradiation of solutions of pure *cis*-[M(L^3-*S*,*O*)$_2$] in acetonitrile with intense white light results in substantial amounts of *trans*-[M(L^3-*S*,*O*)$_2$] appearing in solution at room temperature. The relative (conditional) rate of isomerization of the Pd(II) complexes was found to be significantly higher than that of the corresponding Pt(II) complexes (as might be expected). Interestingly, the *trans*-[Pd(L^3-*S*,*O*)$_2$] isomer formed by photo-induced isomerization was shown to readily revert back to the *cis* complex in the absence of light as schematically indicated below [19].

$$cis\text{-}[M(L^n\text{-}S,O)_2] \underset{\Delta}{\overset{h\nu}{\rightleftarrows}} trans\text{-}[M(L^n\text{-}S,O)_2]$$

This type of light-induced isomerization is reminiscent of the early work of Balzani *et al.* several decades ago, involving isomerization of a bis-chelated glycine complex of platinum (II), *cis*-[Pt(gly-*N*,*O*)$_2$], which readily undergoes *cis* → *trans* isomerization under the influence of light in dilute aqueous solutions [20, 21]. There are relatively few other systematic studies of photo-induced phenomena with Pt(II) and Pd(II) complexes in the literature.

In this paper, we report more detailed investigations of the facile photo-induced *cis*/*trans* isomerization of a series of *cis*-[M(L^n-*S*,*O*)$_2$] (M = Pd(II) and Pt(II)) complexes derived from several HL^n (n = 1–6) ligands shown in scheme 1 below, with the aim of understanding the

possible factors which may influence this reversible process in organic solvents. We examined the effect of differing light sources, as well as a preliminary assessment of the effects of ligand structure on the relative extent of *cis* → *trans* isomerization to steady state, using ^{1}H and ^{195}Pt NMR spectroscopy in relatively concentrated solutions of some *cis*-[M(L^{n}-*S*,*O*)$_2$] (M = Pd(II) and Pt(II)) complexes. Moreover, the photo-induced *cis*/*trans* isomerization of particularly *cis*-[Pd(L^{n}-*S*,*O*)$_2$] complexes in more dilute acetonitrile solutions can conveniently be monitored by *rp*-HPLC, leading to a semi-quantitative estimate of the extent of isomerization as indicated by a *trans* : *cis* ratio at steady state at room temperature.

We now demonstrate that *trans*-[Pd(L^{n}-*S*,*O*)$_2$] complexes can reliably be prepared and isolated from pure *cis*-[Pd(L^{n}-*S*,*O*)$_2$] in acetonitrile in the solid state under intense white light irradiation using a simple vapor diffusion crystallization technique. We believe this simple procedure to be more generally applicable, as illustrated by the first example of a *trans*-bis(*N*,*N*-diethyl-*N*′-benzoylthioureato)–palladium(II) complex characterized by single-crystal X-ray diffraction, deliberately prepared and isolated from its *cis* isomer, using a photo-induced isomerization process. Such a process was presumably responsible for the "accidental" isolation of a *trans*-bis(*N*,*N*-di(n-butyl)-*N*′-naphthoylthioureato)-platinum(II) complex by one of us, two decades ago [14].

2. Experimental setup

2.1. *Materials and general methods*

All chemicals used for the synthesis of ligands and complexes were commercially available from Sigma Aldrich SA and used without purification, while the platinum and palladium salts K_2PdCl_4 and K_2PtCl_4 of >99% purity were obtained from Johnson Matthey PLC. ^{1}H and ^{13}C NMR spectra of ligands and complexes were recorded at 25 °C in $CDCl_3$ solutions using various spectrometers, Varian VNMRS 300 MHz, or Varian UNITY INOVA 400 MHz or 600 MHz NMR spectrometers. All ^{195}Pt NMR spectra were recorded at 30 °C in the given solvents, usually $CDCl_3$ using a Varian INOVA 600 MHz spectrometer operating at 128 MHz. All ^{195}Pt chemical shifts are quoted for convenience relative to external H_2PtCl_6 (500 mg mL^{-1} in 30% v/v D_2O/1 M HCl) at $\delta(^{195}Pt) = 0$ ppm at 30 °C [or at ca + 4522 ppm relative to Ξ at 21.496 Hz], and are estimated to be accurate to ± 2 ppm.

Melting points were obtained using an Electrothermal IA 9000 series digital melting point apparatus. FT-IR analyses were performed on a Thermo Nicolet Avatar 330 Smart Performer ATR instrument using a ZnSe crystal. Thin layer chromatography (TLC) was carried out using silica plates (Merck) with dichloromethane/hexane mixtures of varying compositions as eluents, with visualization using either molecular iodine vapor or UV light.

2.2. *General procedure for synthesis of ligands and complexes*

2.2.1. Synthesis of ligands and complexes [M(L^{n}-S,O)$_2$] (M = Pt(II), Pd(II)). All ligands were prepared by the simple "one-pot" Douglass and Dains method [1] and characterized by standard procedures using melting points, elemental analyses, IR, ^{1}H, and ^{13}C

{^{1}H} NMR spectra in $CDCl_3$. The Pd(II) and Pt(II) complexes were prepared as previously described [10], from K_2PdCl_4 or K_2PtCl_4 as starting material.

A typical procedure for the Pd(II) complexes follows. Solutions containing 40 mg of K_2PdCl_4 (*ca* 0.12 mM Pd(II)) in 15 cm^3 water and 10 cm^3 acetonitrile were added dropwise to a stirred solution of 0.25 mM ligand HL^n in a mixture of 15 cm^3 acetonitrile and 10 cm^3 water containing ~0.25 mM of sodium acetate. The resulting mixture was stirred for 1 h at room temperature, during which a yellow precipitate was formed. Addition of *ca* 100 mL distilled water completed the precipitation, while dissolving excess soluble salts such as K/NaCl and sodium acetate. The precipitates were collected by centrifugation, rinsed with water, followed by drying at *ca* 60–70 °C in vacuum. Recrystallization of complexes from mixtures of chloroform and ethanol afforded yellow/orange crystals in good yields typically >80% of the expected, apart from mechanical losses.

2.2.1.1. *Ligand synthesis.* ***N,N*-diethyl-*N*′-benzoylthiourea (HL^1)**: Yield of 6.3 g (86.3%); m.p. 98–100 °C; (Found: C, 61.15; H, 6.93; N, 12.00; S, 13.61%; calculated for $C_{12}H_{16}N_2OS$: C, 60.98; H, 6.82; N, 11.85; S, 13.57%); IR (ATR, cm^{-1}): ν(N–H) 3258.84 cm^{-1} (br, sh), ν(C=O) 1649.35 cm^{-1} (vs); ^{1}H NMR (300 MHz, $CDCl_3$)/ppm δ 8.34 (singlet, 1H, N–H), 7.82 (doublet, 2H, Ar–H), 7.56 (triplet, 1H, Ar–H), 7.46 (triplet, 2H, Ar–H), 3.81 (doublet, 4H, N–CH_2), 1.32 (triplet, 6H, CH_3); ^{13}C NMR (75 MHz, $CDCl_3$)/ppm δ 11.3, 13.1, 47.5, 50.6, 129.2, 131.7, 134.1, 137.9, 164.2, 180.0.

***N,N*-diethyl-*N*′-(4-methoxybenzoyl)thiourea (HL^2)**: Yield of 3.12 g (78%); m.p. 134–135 °C; (Found: C, 59.12; H, 7.45; N, 10.74; S, 11.74%; calculated for $C_{13}H_{18}N_2O_2S$: C, 56.73; H, 6.80%; ^{1}H NMR (300 MHz, $CDCl_3$)/ppm δ 1.27 (unresolved, 6H, CH_3), 3.57 (unresolved, 2H, CH_2), 3.84 (singlet, 3H, Ar–H), 6.93 (doublet, 2H, Ar–H), 8.21 (singlet, 1H, N–H); ^{13}C{^{1}H} NMR (75 MHz, $CDCl_3$)/ppm δ 11.3, 12.9, 47.7, 51.4, 114.2, 125.0, 130.0, 163.6, 179.9.

***N,N*-diethyl-*N*′-(3,4,5-trimethoxybenzoy)thiourea (HL^3)**: Yield of 80%; m.p. 143–145 °C; (Found: C, 55.30; H, 7.16; N, 8.62; S, 9.37%; calculated for $C_{15}H_{22}N_2O_4S$: C, 55.19; H, 6.79; N, 8.58; S, 9.82%); ^{1}H NMR (300 MHz, $CDCl_3$)/ppm δ 1.31 (unresolved, 6H, CH_3), 3.55 (unresolved, 2H, CH_2), 3.85 (singlet, 3H, CH_3), 3.87 (singlet, 6H, CH_3), 7.05 (singlet, 2H, Ar-H), 8.82 (singlet, 1H, N–H); ^{13}C{^{1}H} NMR (75 MHz, $CDCl_3$)/ppm δ 11.4, 13.3, 47.7, 56.4, 60.9, 105.2, 127.4, 142.1, 153.1, 163.3, 179.6.

***N,N*-diethyl-*N*′-(4-chlorobenzoyl)thiourea (HL^4)**: Yield of 83%; m.p. 163–165 °C; (Found: C, 48.00; H, 4.89; N, 9.42; S, 10.7%; calculated for $C_{12}H_{15}N_2OSCl$: C, 47.78; H, 48.68; N, 9.29; S, 10.63; Cl, 11.76%; ^{1}H NMR (600 MHz, $CDCl_3$)/ppm δ 1.33 (triplet, 6H, CH_3), 3.80 (quartet, 4H, CH_2), 7.44 (doublet, 2H, Ar–H), 7.77 (doublet, 2H, Ar–H), 8.35 (singlet, 1H, N-H); ^{13}C{^{1}H} NMR (125 MHz, $CDCl_3$)/ppm δ 11.7, 13.5, 48.0, 48.3, 112.8, 129.3, 131.3, 139.6, 163.1, 179.3.

***N*-piperidyl-*N*′-benzoylthiourea (HL^5)**: Yield of 41.8%; m.p. 124–126 °C; (calculated for $C_{13}H_{16}N_2OS$: C, 62.86; H, 6.51; N, 11.28; S, 12.91%; Found: C, 62.86; H, 6.67; N, 11.39; S, 12.72%); ^{1}H NMR (600 MHz, $CDCl_3$)/ppm δ 1.71 (unresolved, 6H, CH_3), 3.87 (doublet, 4H, CH_2), 7.47 (triplet, 2H, Ar–H), 7.57 (unresolved, 1H, Ar–H), 7.83 (dd, 2H, Ar–H), 8.42 (singlet, 1H, N–H); ^{13}C{^{1}H} NMR (125 MHz, $CDCl_3$)/ppm δ 23.9, 25.2, 52.8, 127.8, 128.9, 132.6, 132.9, 163.1, 178.2.

***N,N*-diethyl-*N*′-(3,5-dimethoxybenzoyl)thiourea (HL^6)**: Yield of 80%; m.p. 122–124 °C; (calculated for $C_{14}H_{20}N_2O_3S$: C, 56.73; H, 6.80; N, 9.45; S, 10.82%; Found: C, 57.06; H, 6.89; N, 9.51; S, 10.49%); ^{1}H NMR (300 MHz, $CDCl_3$)/ppm δ 1.27 (unresolved, 6H, 2 x CH_3), 3.55 and 4.00 (doublet, 4H, 2 × CH_2), 3.79 (singlet, 2 × OCH_3), 6.61 (1H,

triplet, H_4), 6.93 (2H, doublet, $H_{2/6}$), 8.38 (1H, singlet, N–H); $^{13}C\{^1H\}$ NMR (75 MHz, $CDCl_3$)/ppm 11.2, 13.0, 47.5, 55.4, 105.3, 105.4, 134.8, 161.2, 163.8, 179.5.

2.3.1.2. *Pd(II) and Pt(II) complex synthesis.* ***cis*-bis(*N,N*-diethyl-*N′*-(benzoylthioureato) palladium(II), *cis*-[Pd(L^1-*S,O*)$_2$]**: Yield of 0.106 g (88.3%); m.p. 159–163 °C; IR (ATR, cm^{-1}): ν(C=O) 1583.74 cm^{-1} (w); ^1H NMR (400 MHz, $CDCl_3$)/ppm δ 8.26 (doublet, 2H, Ar–H), 7.50 (unresolved, 1H, Ar–H), 7.44 (unresolved, 2H, Ar–H), 3.85 (quartet, 4H, N–CH_2), 3.50 (quartet, 4H, CH_2), 1.33 (unresolved, 4H, CH_2), 1.23 (triplet, 6H, CH_3); $^{13}C\{^1H\}$ NMR (100 MHz, $CDCl_3$)/ppm δ 12.6, 13.1, 15.3, 46.1, 47.2, 65.9, 127.9, 129.7, 131.4, 137.1, 170.6, 171.1.

***cis*-bis(*N,N*-diethyl-*N*-(4-methoxybenzoylthioureato)palladium(II), *cis*-[Pd(L^2-*S,O*)$_2$]**: Yield of 0.069 g (86.5%); m.p. 138–140 °C; IR (ATR, cm^{-1}): ν(C=O) 1579.25 cm^{-1} (w); ^1H NMR (600 MHz, $CDCl_3$)/ppm δ 1.33 (dt, 6H, CH_3), 3.84 (unresolved, 4H, CH_2), 3.87 (singlet, 3H, O–CH_3), 7.29 (unresolved, 2H, Ar–H), 7.03 (unresolved, 2H, Ar–H); $^{13}C\{^1H\}$ NMR (125 MHz, $CDCl_3$)/ppm δ 12.6, 13.1, 46.1, 47.2, 55.2, 114.3, 117.8, 122.1, 128.8, 138.6.

***cis*-bis(*N,N*-diethyl-*N′*-(3,4,5-trimethoxybenzoylthioureato)palladium(II), *cis*-[Pd(L^3-*S,O*)$_2$]**: Yield of 0.081 g (85.3%); m.p. 198–202 °C; IR (ATR, cm^{-1}): ν(C=O) 1589.40 cm^{-1} (w); ^1H NMR (300 MHz, $CDCl_3$)/ppm, δ 1.28 (triplet, 6H, CH_3), 1.32 (triplet, 6H, CH_3), 3.82 (quartet, 4H, CH_2), 3.83 (singlet, 12H, CH_3), 6.85 (triplet, 2H, Ar–H), 7.44 (doublet, 4H, Ar–H); $^{13}C\{^1H\}$ NMR (300 MHz, $CDCl_3$)/ppm δ 12.3, 13.1, 46.2, 47.23, 55.3, 103.9, 107.4, 139.2, 160.2, 170.0, 171.2.

***cis*-bis(*N,N*-diethyl-*N′*-(4-chlorobenzoylthioureato)palladium(II), *cis*-[Pd(L^4-*S,O*)$_2$]**: Yield of 0.072 g (88.9%); m.p. 179–181 °C; IR (ATR, cm^{-1}): ν(C=O) 1577.73 cm^{-1} (w); ^1H NMR (600 MHz, $CDCl_3$)/ppm δ 1.30 (dt, 6H, CH_3), 3.83 (quarter, 4H, CH_2), 7.38 (unresolved, 2H, Ar–H), 8.14 (unresolved, 2H, Ar–H); $^{13}C\{^1H\}$ NMR (125 MHz, $CDCl_3$)/ppm δ 12.6, 13.1, 46.1, 47.3, 128.2, 131.0, 135.6, 137.7, 169.6, 171.2.

***cis*-bis(*N*-piperidyl-*N′*-(benzoylthioureato)palladium(II), *cis*-[Pd(L^5-*S,O*)$_2$]**: Yield of 0.062 g (82.7%); m.p. 130–134 °C; IR (ATR, cm^{-1}): ν(C=O) 1583.89 cm^{-1} (w); ^1H NMR (600 MHz, $CDCl_3$)/ppm δ 1.72 (unresolved, 6H, CH_2), 4.11 (unresolved, 4H, CH_2), 7.41 (triplet, 2H, Ar–H), 7.48 (triplet, 1H, Ar–H), 8.23 (unresolved, 2H, Ar–H); $^{13}C\{^1H\}$ NMR (125 MHz, $CDCl_3$)/ppm δ 24.5, 26.1, 48.6, 51.1, 127.9, 129.7, 131.5, 131.1, 171.1, 171.4.

***cis*-bis(*N,N*-diethyl-*N′*-(benzoylthioureato)platinum(II), *cis*-[Pt(L^1-*S,O*)$_2$]**: Yield of 0.1025 g (63%); m.p. 152–156 °C; (Found: C, 43.57; H, 4.48; N, 8.91; S, 9.32%; calculated for $C_{28}H_{30}N_4O_2PtS_2$: C, 43.30; H, 4.54; N, 8.42; S, 9.63%); ^1H NMR (600 MHz, $CDCl_3$)/ppm δ 1.28 (6H, triplet, CH_3), 1.34 (6H, triplet, CH_3), 3.77 (4H, quartet, CH_2), 3.83 (4H, quartet, CH_2), 7.42 (4H, triplet, Ar–H), 7.51 (2H, triplet, Ar–H), 8.26 (4H, doublet, Ar–H); $^{13}C\{^1H\}$ (400 MHz, $CDCl_3$)/ppm δ 12.3, 13.1, 46.0, 128.1, 129.3, 131.3, 137.6, 167.0, 168.4. $\delta(^{195}Pt$, 128 MHz, $CDCl_3$)/ppm, −2720.1 (*cis*), −1980.8 (*trans*, post irradiation; white Quartz Halogen light).

***cis*-bis(*N,N*-diethyl-*N′*-(4-methoxybenzoylthioureato)platinum(II), *cis*-[Pt(L^2-*S,O*)$_2$]**: Yield of 0.1444 g (82%); m.p. 198–200 °C; (Found: C, 43.57; H, 4.58; N, 8.91; S, 7.82%; calculated for $C_{28}H_{34}N_4O_4PtS_2$: C, 42.79; H, 5.25; N, 7.68; S, 8.79%); ^1H NMR (600 MHz, $CDCl_3$)/ppm δ 1.27 (6H, triplet, CH_3), 1.33 (6H, triplet, CH_3), 3.77 (4H, quartet, NCH_2), 3.81 (4H, quartet, NCH_2), 3.87 (6H, singlet, O–CH_3), 6.92 (4H, doublet, Ar–H), 8.22 (4H, doublet, Ar–H). $\delta(^{195}Pt$ 128 MHz, $CDCl_3$)/ppm, −2733.8 (*cis*), −1991.0 (*trans*, post irradiation; white Quartz Halogen light).

***cis*-bis(*N,N*-diethyl-*N′*-(3,4,5-trimethoxybenzoylthioureato)platinum(II), *cis*-[Pt(L^3-*S,O*)$_2$]**: Yield of 0.1617 g (79%); m.p. 218–221 °C (decomposition); (Found: C, 42.43; H, 4.88; N, 6.55; S, 7.00; calculated for $C_{30}H_{46}N_4O_8PtS_2$: C, 42.39; H, 5.46; N, 6.59; S, 7.55); ^{1}H NMR (600 MHz, $CDCl_3$)/ppm δ 1.29 (6H, triplet, CH_3), 1.32 (6H, triplet, CH_3), 3.75 (4H, quartet, NCH_2), 3.80 (4H, quartet, NCH_2), 3.87 (12H, singlet, O-CH_3), 3.88 (6H, singlet, CH_3), 7.55 (4H, singlet Ar–H); ^{13}C{^{1}H} NMR (400 MHz, $CDCl_3$)/ppm δ 12.4, 13.1, 30.8, 47.1, 107.4, 132.9, 141.6, 152.6, 166.9, 167.9. δ(^{195}Pt 128 MHz, $CDCl_3$)/ppm, −2723.5 (*cis*), −1982.5 (*trans*, post irradiation; white Quartz Halogen light).

***cis*-bis(*N,N*-diethyl-*N′*-3,5-dimethoxybenzoylthioureato)platinum(II), *cis*-[Pt(L^6-*S,O*)$_2$]**: Yield of 0.1758 g (88%); m.p. 211–212 °C; (Found: C, 42.96; H, 4.47; N, 7.06; S, 7.82; calculated for $C_{28}H_{42}N_4O_6PtS_2$: C, 42.58; H, 5.36; N, 7.09; S, 8.17); ^{1}H NMR (600 MHz, $CDCl_3$)ppm: 1.29 (6H, triplet, CH_3), 1.33 (6H, triplet, CH_3), 3.75 (4H, quartet, NCH_2), 3.81 (4H, quartet, NCH_2), 3.84 (12H, singlet, H_1), 6.61 (2H, singlet, H_2), 7.47 (4H, singlet, H_3) ^{13}C{^{1}H} (75 MHz, $CDCl_3$)ppm: 12.4, 13.1, 46.1, 47.1, 55.4, 103.7, 107.2, 139.7, 160.4, 167.0, 167.7. δ(^{195}Pt 128 MHz, $CDCl_3$)/ppm −2706.7 (*cis*), −1974.5 (*trans*, post irradiation; white Quartz Halogen light).

2.3. *Photo-induced isomerization experiments and rp-HPLC separation of Pt and Pd complexes*

Photo-induced isomerization experiments were performed with several light sources, including an intense white light quartz-halogen lamp (150 Watt), a low-heat (5 Watt OSRAM superstar) white light-emitting diode (LED) lamp, as well as a hand-held blue–violet laser diode (100 mW, λ = 405 nm). Irradiation of complexes prior to *rp*-HPLC was achieved with a homemade pre-column "photo-reactor", constructed using a commercially available Hg UV/visible (PHILIPS TL 4 W/05 4 Watt, 112 × 15 mm) cylindrical lamp as shown schematically in figure S1 (see online supplemental material at http://dx.doi.org/10.1080/00958972.2014.974584) of the electronic supplementary data. This device allows for direct on-line pre-column irradiation of an injected sample aliquot of [M(L^n-*S,O*)$_2$] (M = Pt(II), Pd(II)) complexes, passing through a Teflon tube (61.6 cm, 3 μm ID) coiled around the air-cooled Hg UV/visible lamp *ca* 110 cm long, which is transparent to a large portion of the spectrum of Hg-vapor generated UV/visible light. In this way, a sample aliquot may be exposed to light irradiation prior to entering the analytical *rp*-HPLC column, at a constant flow rate. The relative time of light exposure may be controlled as a function of the effective coil length at a given flow rate. Typical Teflon coil lengths used ranged from 9.4 to 61.6 cm, the longest of which resulted in sufficient exposure time to allow for steady state to be reached (*vide infra*). A disadvantage of this simple but effective device is that the actual spectrum of light that the sample is exposed to is not well known, since it is difficult to estimate the effective photon flux to which a sample is subjected to. Nevertheless, the pre-column photochemical reactor allows for a semi-quantitative estimation of the distribution of *cis/trans* isomers of [M(L^n-*S,O*)$_2$] (M = Pt(II), Pd(II)) generated at steady state, from their subsequent separation and quantification by means of *rp*-HPLC. However, we find that presumably the high energy UV component of Hg-vapor light spectrum results in evidence of some photochemical decomposition after longer exposure times, particularly for the *cis*-[Pt(L^n-*S,O*)$_2$] complexes, although this is not evident for the corresponding palladium complexes, under similar conditions (figure S2, electronic supplementary data).

We find that the photo-induced *cis/trans* isomerization of the [M(L^n-*S,O*)$_2$] complexes can also conveniently be achieved using a simple hand-held AC-powered blue–violet laser

diode (100 mW, 405 nm). This allows the use of monochromatic light to be investigated, immediately prior to manual sample injection onto the analytical *rp*-HPLC column. Interestingly, the laser light generally results in clean and efficient *cis/trans*-isomerization (*vide infra*) of complexes. Since we could not estimate accurately the photon flux which the sample aliquot is exposed to using a hand-held laser, no absolute rates of isomerization can be inferred although semi-quantitative estimates of the conditional steady-state *trans : cis* ratio (K_e = [*trans*-(M(L″-*S,O*)$_2$)]/[*cis*-(M(L″-*S,O*)$_2$)] for a given injected [M(L″-*S,O*)$_2$] complex is possible. Surprisingly, reproducible steady-state *trans : cis* ratios were obtained with the monochromatic laser light irradiation using a hand-held blue–violet laser diode (100 mW, 405 nm) at room temperature. Finally, some *in situ* irradiation experiments using an optical fiber to direct blue–violet laser light directly into an NMR tube containing samples of selected [M(L″-*S,O*)$_2$] (M = Pt(II), Pd(II)) in several solvents were also carried out, allowing for simultaneous recording the ^{1}H NMR spectra of such samples as a function of irradiation time. Moreover for the more soluble *cis*-[Pt(L″-*S,O*)$_2$] complexes in $CDCl_3$, we also obtained the 128 MHz ^{195}Pt{^{1}H} NMR spectra, resulting in the chemical shifts $\delta(^{195}\text{Pt})$ of several *cis*-[Pt(L″-*S,O*)$_2$] and those of their *trans* isomers for the first time.

Reversed-phase HPLC was performed using an Agilent system with Quaternary pump equipped with automatic sample injector; typically, 20 µL aliquots consisting of [M(L″-*S,O*)$_2$] (M = Pt(II), Pd(II)) solutions in acetonitrile at typical concentrations of 100–200 mg L^{-1} gave good separations. A GEMINI 150 × 4.6 mm column packed with "end-capped" 5 µm C_{18}-ODS particles was used throughout together with photometric detection using a UV150 Photo-diode array (PDA) detector; generally maximum sensitivity is obtained by monitoring peaks at 262 nm. A mobile phase of variable composition from 85 : 15 to 90 : 10 (v/v%) acetonitrile:0.1 M acetate buffer (pH 6) using isocratic elution gave optimum separations at room temperature for most complexes. Only de-ionized water and HPLC grade acetonitrile filtered through a 0.45 µm was used to make up the mobile phase. Off-line UV–vis absorption spectra of *cis*-[M(L″-*S,O*)$_2$] (M = Pt(II), Pd(II)) solutions in acetonitrile were recorded using a Varian Cary 50 Bio single-beam spectrophotometer (figure S3, supplementary material).

2.4. *Single-crystal X-ray diffraction*

Crystals suitable for single-crystal X-ray diffraction of *cis*-[Pd(L^2-*S,O*)$_2$] and *cis*-[Pd(L^3-*S,O*)$_2$] were grown from a solvent mixture of a ~80 : 20 (v/v%) acetonitrile–chloroform in a glass vial sealed with a perforated wax-film under slow evaporation of the solvent at room temperature without protection from ambient light.

Crystals of *trans*-[Pd(L^1-*S,O*)$_2$] were prepared from authentic *cis*-bis(*N,N*-diethyl-*N*′-(benzoylthioureato)palladium(II) dissolved in acetonitrile, subjected to intense polychromatic LED white light irradiation in a specially designed two-chamber closed glass vessel interconnected by means of a Teflon tap, to allow for slow vapor diffusion of diethyl ether from one chamber into the chamber containing the solution of *cis*-[Pd(L^1-*S,O*)$_2$] at room temperature. Over a period of several hours at room temperature, pale yellow needle-shaped crystals of *trans*-[Pd(L^1-*S,O*)$_2$] suitable for X-ray diffraction analysis were formed. Significantly, the melting point of *trans*-[Pd(L^1-*S,O*)$_2$] is at 194–196 °C, significantly higher than that of the starting *cis*-[Pd(L^1-*S,O*)$_2$] compound.

X-ray diffraction intensity data were collected on a Bruker SMART APEX single-crystal X-ray diffractometer equipped with a Mo fine-focus sealed tube, Monocap collimator, and

an APEXII detector with Incoatec IμS molybdenum and copper micro-focus X-ray sources and an APEXII detector. The temperature in both systems was regulated using an Oxford Cryosystem. Data were reduced using SAINT [22] and empirical corrections were performed where necessary using multi-scan SADABS [23]. The crystal structures were solved and refined using the SHELX-97 [24] suite of programs and mainly from direct methods. X-seed software [25] was used as a graphic interface for SHELX. All non hydrogen atoms were refined anisotropically by means of full-matrix least-squares calculations for F^2 using SHELXL-97, which is incorporated into the X-seed software package. Hydrogens were placed using a riding model and isotropic thermal parameters were assigned values of 1.2–1.5 times the *U*eq of their parent atoms. Molecular graphics were generated using X-seed.

3. Results and discussion

3.1. *Preparation and configuration of cis-[M(L^n-S,O)$_2$] (M = Pt^{II}, Pd^{II}), HL^n (n = 1–6)*

The preparation of pure *cis*-[M(L^n-*S*,*O*)$_2$] (M = Pt^{II}, Pd^{II}) complexes derived from the series of HL^n (R$^1{}_2$NC(S)NHC(O)R^2, R^1 = alkyl or aryl groups, n = 1–6) ligands as shown in scheme 1 was carried out as described previously based on literature methods [8, 10]. All ligands and complexes were fully characterized by conventional means, including melting points, elemental analysis, IR and ^{1}H and ^{13}C{^{1}H} NMR spectroscopy as indicated in the experimental section. The purity and particularly the isomeric homogeneity of the recrystallized [M(L^n-*S*,*O*)$_2$] (M = Pt^{II}, Pd^{II}) complexes from chloroform/ethanol/methanol under ambient light conditions is confirmed by the narrow melting point range found for these [M(L^n-*S*,*O*)$_2$] (M = Pt^{II}, Pd^{II}) complexes, as well as their chromatographic homogeneity on TLC plates, showing only a single spot on elution (Merck silica-gel) with chloroform as the eluent.

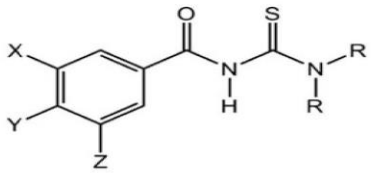

Scheme 1.

HL^1: R = ethyl; X, Y, Z = H; **HL^2**: R = ethyl; X, Z = H, Y = MeO; **HL^3**: R = ethyl; X, Y, Z = MeO; **HL^4**: R = ethyl; X, Z = H, Y = Cl; **HL^5**: R = piperidyl; X, Y, Z = H; **HL^6**: R = ethyl; X, Z = MeO; Y = H.

^{1}H and ^{13}C{^{1}H} NMR spectra of all recrystallized [M(L^n-*S*,*O*)$_2$] (M = Pt(II), Pd(II)) complexes (under low light conditions) recorded in $CDCl_3$ or acetonitrile-d_6 where solubility permits, confirm that these complexes where exclusively the *cis* isomers. These spectra did not contain any trace of peaks ascribable to the *trans* isomers. In the case of soluble Pt(II) complexes in $CDCl_3$, the ^{195}Pt{^{1}H} NMR spectra recorded from freshly prepared solutions under subdued light, showed only a single ^{195}Pt NMR resonance in the ^{195}Pt chemical shift range −2700 ± 100 ppm, characteristic of *cis*-[Pt(L^n-*S*,*O*)$_2$] complexes in $CDCl_3$ (relative to external H_2PtCl_6 (500 mg mL^{-1} in 30% v/v D_2O/1 M HCl) at $\delta(^{195}Pt) = 0$ ppm) [8].

For completeness, particularly for Pd(II) complexes, the single-crystal structure of two representative examples of *cis*-[Pd(L^2-*S*,*O*)$_2$] (figure 1) and *cis*-[Pd(L^3-*S*,*O*)$_2$] (figure S4 in supplementary electronic data) complexes derived from the *N*,*N*-diethyl-*N*′-(4-methoxy-benzoyl)thiourea (HL^2) and *N*,*N*-diethyl-*N*′-(3,4,5-trimethoxybenzoy)thiourea (HL^3), respectively, were determined. The *cis*-[Pd(L^2-*S*,*O*)$_2$] complex crystallizes in a monoclinic space group $P2_1/c$, while *cis*-[Pd(L^3-*S*,*O*)$_2$] crystallizes in the $P2_1/n$ space group, with relevant crystal data given in table S1. The structure of *cis*-[Pd(L^3-*S*,*O*)$_2$] unfortunately displays some slight crystallographic disorder in one of the ethyl moieties over two positions in this complex, although this does not compromise the isomeric veracity of the structure. As anticipated in both cases, the Pd(II) coordinates to two deprotonated *N*,*N*-diethyl-*N*′-benzoylthioureato anions with the *S*- and *O*-donors mutually *cis* to each other forming a square planar complex. The *cis*-[Pd(L^2-*S*,*O*)$_2$] and *cis*-[Pd(L^3-*S*,*O*)$_2$] structures are essentially isostructural with numerous other examples of similar Pt(II), and relatively fewer Pd(II) complexes with related ligands in the Cambridge crystallographic database (CCD) [13], including those described in the recent review [9].

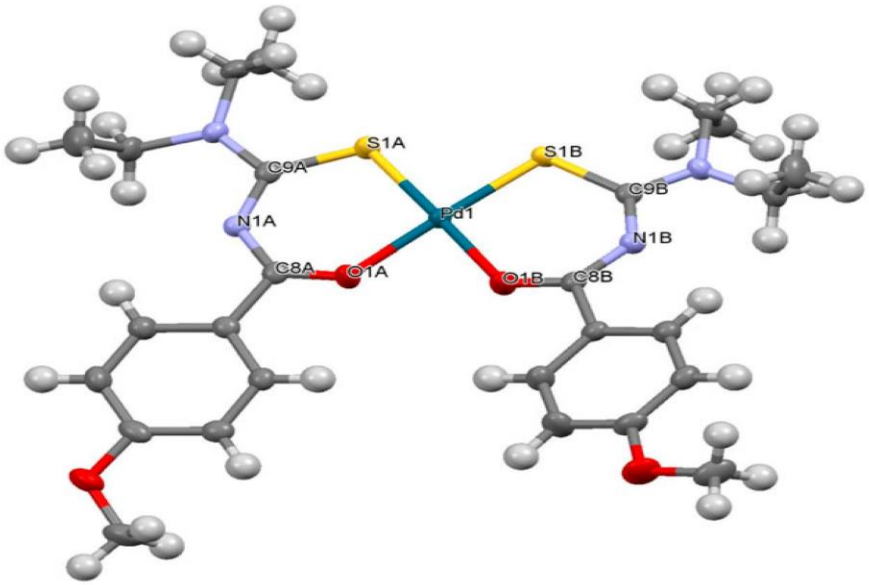

Figure 1. Molecular structure of *cis*-bis(*N*,*N*-diethyl-*N*′-4-methoxy-benzoylthioureato)-palladium(II), *cis*-[Pd(L^2-*S*,*O*)$_2$] with selected bond lengths (Å) and angles (°): Pd(1)–S(1A) 2.2364(4), Pd(1)–O(1A) 2.0085(11), Pd(1)–S(1B) 2.2351(4), Pd(1)–O(1B) 2.0147(12), S(1A)–C(9A) 1.7441(16), O(1A)–C(8A) 1.2636(18), N(1A)–C(8A) 1.3371 (19), N(1A)–C(9A) 1.3354(19); S(1A)–Pd(1)–S(1B) 86.62(1), S(1A)–Pd(1)–O(1A) 94.16(3), S(1A)–Pd(1)–O(1B) 178.94(3), S(1B)–Pd(1)–O(1A) 177.52(3), S(1B)–Pd(1)–O(1B) 94.44(3), O(1A)–Pd(1)–O(1B) 84.78(5), Pd1–S (1A)–C(9A) 107.92(5), Pd(1)–S(1B)–C(9B) 107.53(3), Pd(1)–O(1A)–C(8A) 131.28(10), Pd(1)–O(1B)–C(8B) 129.69(10).

3.2. *Photo-induced cis → trans isomerization of [M(L^n-S,O)$_2$] (M = Pt(II), Pd(II)): ^{1}H and ^{195}Pt NMR studies*

Given the limited scope of our previous communication on the photo-induced *cis/trans* isomerism of *cis*-[Pd(L-*S,O*)$_2$] complexes in solution [19], we specifically examined the photo-induced *cis* → *trans* phenomenon to include several *cis*-[Pd(L^n-*S,O*)$_2$] and *cis*-[Pt (L^n-*S,O*)$_2$] complexes from a selection of *N,N*-dialkyl-*N'*-aroylthiourea ligands HL^n (n = 1–6) by means of NMR spectroscopy in more detail. As a precaution, solutions of all complexes examined by means of ^{1}H NMR (and *rp*-HPLC see below) were freshly prepared under subdued light, and solutions were always stored in the dark. Irradiation of solutions of *cis*-[Pd(L^n-*S,O*)$_2$] complexes in organic solvents such as chloroform or acetonitrile in normal glass vessels with one of several sources of visible light, including intense white light quartz-halogen (150 Watt lamp) light, a low-heat 5 Watt LED source, a Hg UV/visible lamp (4 Watt), and a 100 mW blue–violet laser (λ = 405 nm) *all* result in some degree of *cis* → *trans* isomerization, as conveniently monitored by ^{1}H NMR spectroscopy in reasonably concentrated solutions. This can be illustrated by the partial ^{1}H NMR spectrum of the representative *cis*-[Pd(L^1-*S,O*)$_2$] complex of *N,N*-diethyl-*N'*-benzolythiourea of *ca* 10 mg mL^{-1} in acetonitrile-d$_6$ shown in figure 2(a), confirming that only a single compound is present in solution not subjected to intense light. On irradiation with intense white LED light of a solution of *cis*-[Pd(L^1-*S,O*)$_2$] directly in an NMR tube for 20 and 30 min, followed by the rapid acquisition of a ^{1}H NMR spectrum shows clear evidence of *cis* → *trans* photo-induced isomerization of this complex by the appearance of additional peaks ascribed to the *trans* isomer [figure 2(b) and (c)]. Similar results are obtained for all other soluble palladium(II) complexes. Moreover, on allowing the sample to stand in the dark for sufficiently long, these additional peaks vanish from the ^{1}H NMR spectrum on reacquisition of the ^{1}H NMR spectrum.

The reversion of the *trans* isomer back to the *cis* isomer in the dark takes place for all Pd as well as Pt(II) complexes in either chloroform or acetonitrile solution (see below).

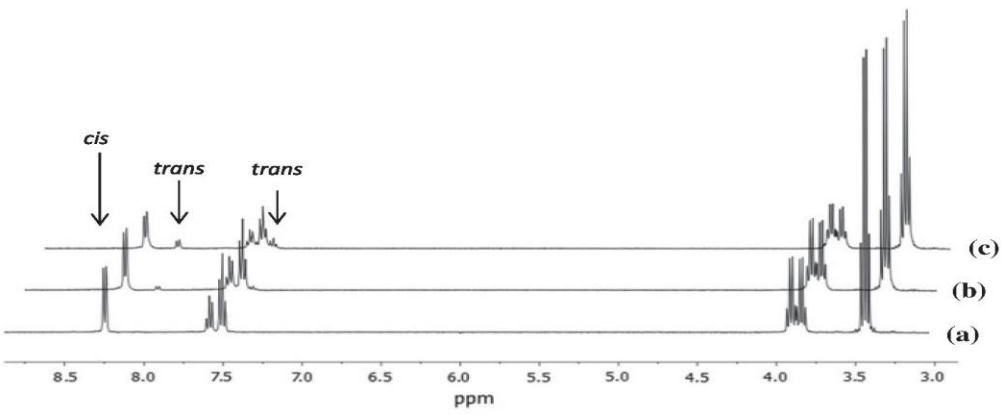

Figure 2. ^{1}H NMR spectra of aromatic region of *cis*-[Pd(L^1-*S,O*)$_2$] in acetonitrile-d$_6$ (400 MHz, 298 K): (a) (in dark); (b) (after irradiation with white light for 20 min); (c) (after irradiation with white light for 30 min).

The extent of conversion to the *trans* isomer as measured by the *trans:cis* ratio (K_e = [*trans*-(Pd(L^n-*S,O*)$_2$)]/[*cis*-(Pd(L^n-*S,O*)$_2$)] at steady state varies significantly for these complexes, depending on the structure of HL^n examined, as well as the solvent acetonitrile-d_6 or $CDCl_3$ used (*vide infra*). For *cis*-[Pd(L^n-*S,O*)$_2$] complexes in acetonitrile-d_6, the relative rate of isomerization takes place on a timescale suitable to be readily measurable by means of ^{1}H NMR. In the case of the corresponding *cis*-[Pt(L^n-*S,O*)$_2$] complexes, however, the relative rates of photo-induced *cis* → *trans* isomerization are generally very much lower (including the reverse reaction in the dark). Moreover, for the generally less soluble *cis*-[Pt(L^n-*S,O*)$_2$] complexes in acetonitrile, prolonged irradiation by polychromatic light sources used in this work (particularly with a strong UV component) indicates some photochemical decomposition in solution after irradiation.

Nevertheless for the most soluble *cis*-[Pt(L^n-*S,O*)$_2$] (n = 1–3,6) complexes in $CDCl_3$ at concentrations of ~50 mg mL^{-1}, we recorded the 128.8 MHz ^{195}Pt{^{1}H} NMR spectra both with and without prior irradiation with intense white light directly in the NMR tube. In the absence of light irradiation, clean single resonance ^{195}Pt{^{1}H} NMR spectra are obtained with δ(^{195}Pt) in the characteristic range of the *cis*-[Pt(L^n-*S,O*)$_2$] complexes typically at −2700 (±30) ppm, depending on the structure of coordinated ligand (table 1). Irradiation of these Pt(II) complexes with intense white light for approximately 30–40 min (but avoiding sample heating), followed by rapid ^{195}Pt{^{1}H} NMR spectral acquisition (ca 15–20 min) results in one additional ^{195}Pt{^{1}H} peak of lower intensity appearing in each spectrum; the major peak corresponds to the *cis*-[Pt(L^n-*S,O*)$_2$] isomer as obtained before, while the minor peak at δ(^{195}Pt) at *ca* −1980 (±15 ppm) is assigned to the *trans*-[Pt(L^n-*S,O*)$_2$] isomer. This is illustrated for *cis*-[Pt(L^3-*S,O*)$_2$] in $CDCl_3$ in figure 3. The ^{195}Pt{^{1}H} chemical shift data similarly recorded for the most soluble *cis/trans*-[Pt(L^n-*S,O*)$_2$] (n = 1–3,6) complexes is listed in table 1. To our knowledge, this is the first ^{195}Pt NMR shielding data corresponding to *trans*-[Pt(L^n-*S,O*)$_2$] (n = 1–3,6) complexes available.

Interestingly, the ^{195}Pt{^{1}H} NMR chemical shifts of *trans*-[Pt(L^n-*S,O*)$_2$] (n = 1–3,6) are significantly less shielded than the corresponding *cis*-[Pt(L^n-*S,O*)$_2$] complexes by an average of some 748 ± 5 ppm (table 1). This difference in shielding between *cis* and *trans* isomers of [Pt(L^n-*S,O*)$_2$] complexes is substantially larger than for similar differences observed in other four-coordinate square planar Pt(II) complexes, based on available data in the literature [26–27]. In the case of *cis* and *trans* PtX_2Cl_2 complexes with X being monodentate ligands with relatively "harder" donors (e.g. N or O) [17] compared with "softer" donor ligands such as phosphines or arsines, similar shielding differences between the *cis* and

Table 1. ^{195}Pt NMR chemical shifts relative to external reference of selected *cis*- and *trans*-[Pt(L^n-*S,O*)$_2$] complexes in $CDCl_3$ at 303 K after irradiation of samples with intense white light, not at steady state.

	δ(^{195}Pt)/ppm in $CDCl_3$[b]	
Complex[a]	*cis* isomer	*trans* isomer
[Pt(L^1-*S,O*)$_2$]	−2720	−1981
[Pt(L^2-*S,O*)$_2$]	−2733	−1991
[Pt(L^3-*S,O*)$_2$]	−2721	−1978
[Pt(L^6-*S,O*)$_2$]	−2707	−1975

[a]Concentration ~50 mg mL^{-1}.
[b]δ(^{195}Pt) ±2 ppm relative to external reference of $[PtCl_6]^{2-}$ at δ^{195}Pt = 0 ppm (+4522 ppm relative to Ξ at 21.496 Hz]).

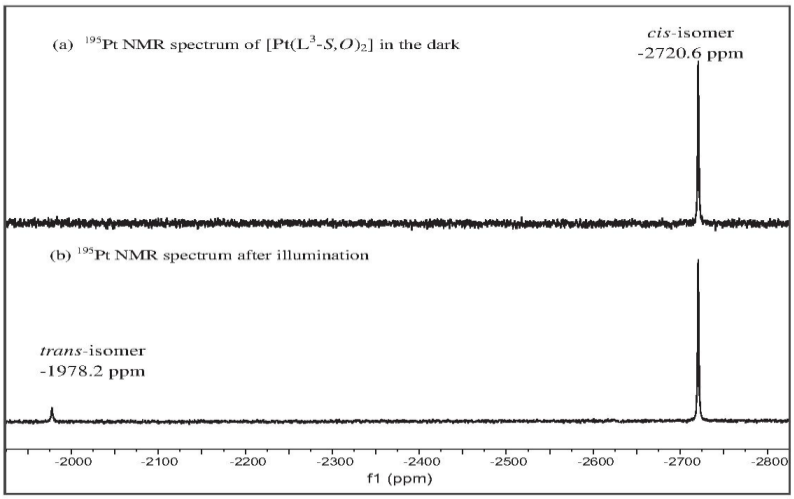

Figure 3. (a) ^{195}Pt{^{1}H} NMR spectrum of *cis*-[Pt(L^3-*S,O*)$_2$] in $CDCl_3$ in dark; (b) after irradiation with intense white light for 30 min show both the *cis* and *trans*-isomers in solution at 298 K.

trans geometric isomers ranging from ~250 to ~500 ppm, respectively, have been reported [26, 27]. Given the lack of reliable ^{195}Pt shielding trends particularly for [PtS_2O_2]-type complexes similar to the *cis/trans*-[Pt(L$''$-*S,O*)$_2$] (n = 1–3,6) complexes studied here, any generalizations on the origin of the observed ^{195}Pt NMR shielding trends of these compounds must remain speculative until insights from more detailed computational studies currently in progress are available.

In view of the relatively long spectral acquisition times for ^{195}Pt{^{1}H} NMR spectra (*ca* 15–20 min) using typical complex concentrations of *ca* 50 mg mL^{-1} in $CDCl_3$, it is not sensible to estimate a *trans : cis* ratio from relative ^{195}Pt NMR peak intensities, since during acquisition, the intensities of the ^{195}Pt{^{1}H} peaks may change as a result of slow reversion of the *trans* → *cis* complexes (in the dark). While the above ^{1}H and ^{195}Pt{^{1}H} NMR results are useful in elucidating the nature of the light-induced *cis* → *trans* isomerization of the Pt complexes, the disadvantage of using ^{195}Pt NMR for these studies is the requirement for fairly concentrated solutions. This limitation, together with the potential photochemical decomposition of *cis*-[Pt(L$''$-*S,O*)$_2$] alluded to above on prolonged irradiation with light, complicated further study of these complexes using NMR spectroscopy. For this reason we will focus only on the *cis*-[Pd(L$''$-*S,O*)$_2$] complexes for the remainder of this study.

Preliminary experiments show that the *cis*-[Pd(L$''$-*S,O*)$_2$] complexes are more kinetically labile requiring shorter light irradiation times as well as being more soluble in solvents other than chloroform, such as acetonitrile. In order to probe the relative rates of isomerization in differing solvents, we carried out a preliminary *in situ* laser-induced isomerization of *cis*-[Pd(L^2-*S,O*)$_2$] in $CDCl_3$ using a blue–violet laser (λ = 405 nm) guided directly into an NMR tube using an optical fiber, while monitoring the ^{1}H NMR signals as a function of

irradiation time (figure 4). This experiment clearly confirms a facile photo-isomerization of *cis*-[Pd(L^2-*S,O*)$_2$] ⟶ *trans*-[Pd(L^2-*S,O*)$_2$] induced by monochromatic 405 nm laser light; when the laser is switched off a slow reversion of the *trans*-[Pd(L^2-*S,O*)$_2$] complex back to its *cis* isomer commences as illustrated in figure 4(a). The relatively rapid *cis* ⟶ *trans* isomerism in the fairly concentrated 20–25 mg mL^{-1} solutions of *cis*-[Pd(L^2-*S,O*)$_2$] in $CDCl_3$ which reach steady state in approximately 20 min, with low power (~100 mW) laser light is noteworthy, in contrast to the very slow reversion of the *trans*-[Pd(L^2-*S,O*)$_2$] complex to the *cis* commencing with the laser "off" in figure 4(a). By contrast in acdetonitrile-d_6 (not shown), the overall relative rate of *cis*-[Pd(L^2-*S,O*)$_2$] ⟶ *trans*-[Pd(L^2-*S,O*)$_2$] is significantly more rapid.

To illustrate the importance of the solvent for the *cis* ⇆ *trans* isomerization of *cis*-[Pd(L^2-*S,O*)$_2$], we estimated qualitatively the relative rates of the reversion *trans* ⟶ *cis* reaction in the absence of light at 298 K by ^{1}H NMR, immediately after a laser light-induced steady-state *trans* : *cis* ratio had been reached in chloroform-d, benzene-d_6, and acetonitrile-d_6 [figure 4(b)]. It is clear that in both $CDCl_3$ and C_6D_6, the "dark" *trans* ⟶ *cis* (presumably

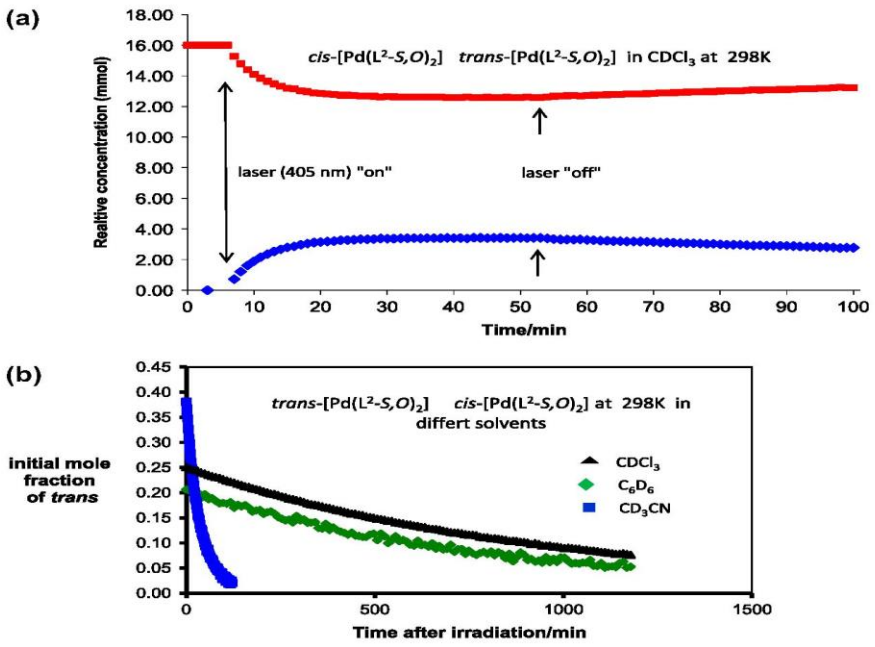

Figure 4. (a) *In situ* laser irradiation with ^{1}H NMR monitoring of the isomerism *cis*-[Pd(L^2-*S,O*)$_2$] ⟶ *trans* in $CDCl_3$ at 298 K as a function of time: (■) indicates the relative intensity of the $\delta(^1H)$ ~7.29 ppm doublet corresponding to the $H^{3/5}$ of *cis*-[Pd(L^2-*S,O*)$_2$], while (◆) represents the growth of the corresponding resonance at $\delta(^1H)$ ~7.13 ppm of the *trans* complex. The *trans* complex only disappears entirely from the spectrum after *ca* 17 h in the dark. (b) Reversion of the *trans*-[Pd(L^2-*S,O*)$_2$] ⟶ *cis* in the dark as in $CDCl_3$. C_6D_6 and CD_3CN at 298 K, after reaching steady state on laser irradiation.

thermal) reaction is extremely slow; it takes more than 1000 min (*ca* 17 h) for the *trans* to completely disappear from solution, with concomitant growth of ^{1}H NMR peaks of the *cis* compound back to their original intensity. The thermal nature of the reverse reaction is supported by higher rates of disappearance of the *trans* complex in chloroform at 323 K (50 °C) in the dark; the last trace of *trans* isomer vanishes from the ^{1}H NMR spectrum in *ca* 500 min. By contrast, in acetonitrile-d_6, the relative rate of disappearance of ^{1}H NMR peaks of the *trans*-[Pd(L^2-*S*,*O*)$_2$] complex is much higher than in chloroform or benzene, with all traces of the *trans* isomer vanishing from the ^{1}H NMR spectrum after *ca* 180 min. These experiments indicate that the solvent plays a significant role at least for the *trans* → *cis* process in the absence of light. This may be the result of differences in the relative solvent polarity and/or differences in solvent donor properties. The trends in figure 4(b) also indirectly confirm that the extent of *cis* → *trans* isomerization under the influence of light similarly depends on the nature of the solvent, as indicated by the initial mole fraction of the *trans* isomer in acetonitrile being almost double that in chloroform/benzene after laser irradiation for *ca* 30 min to steady state, at the start of the ^{1}H NMR monitoring of the reversion reaction at 298 K. The role of acetonitrile is reasonable in the light of studies by Kukushkin *et al.* who have shown that nitriles, such as CH_3CN used as solvent in this work, are well known to coordinate with Pt(II) complexes resulting in stable, isolable *cis*/*trans*-[MX_2(R-CN)$_2$] (M = Pt(II) and X = Cl^-) complexes [28]. Thus in the case of photo-induced isomerization in question here, it is likely that CH_3CN is in not an innocent solvent involved in the overall photo-induced *cis* → *trans* isomerization, as well as in the reverse *trans* → *cis* "dark" reaction of [M(L''-*S*,*O*)$_2$]. Such postulated effects are supported by a preliminary theoretical DFT study of the possible mechanism of the interesting *cis* ⇆ *trans* process, suggesting that on irradiation, the S,O-chelate undergoes ring opening, which would certainly be stabilized in the presence of coordinating acetonitrile [18]. It should, nevertheless, be emphasized that any conclusions concerning relative rates of *cis/trans* isomerization should only be viewed as qualitative at this stage, since it has not been possible to estimate the laser light intensity accurately nor has any reliable measurement of the quantum yields of this interesting photo-induced isomerization process been possible to date.

3.3. *Monitoring of the light-induced isomerization of cis-[Pd(L''-S,O)$_2$] complexes by rp-HPLC*

To circumvent the limitations of ^{1}H NMR spectroscopy for the study of the photo-induced isomerization, we used *rp*-HPLC to examine the isomerization of several of the *cis*-[Pd(L''-*S*,*O*)$_2$] complexes in much more dilute acetonitrile solutions, since this separation methodology has been shown to be useful for easy separation of uncharged *cis*-[Pt/Pd(L''-*S*,*O*)$_2$] complexes [10, 19]. However, the very much lower rates of isomerization of the corresponding platinum complexes found by means of ^{1}H NMR above necessitating prolonged irradiation times, which result in apparent photo-decompostion products as indicated above, is also evident for the *cis*-[Pt(L^3-*S*,*O*)$_2$] complexes by *rp*-HPLC (figure S2b), so that only palladium compounds will be discussed further.

A representative mixture of *cis*-[Pd(L^1-*S*,*O*)$_2$], *cis*-[Pd(L^3-*S*,*O*)$_2$], *cis*-[Pd(L^4-*S*,*O*)$_2$], and *cis*-[Pd(L^5-*S*,*O*)$_2$] complexes freshly dissolved in acetonitrile in typical concentrations between 100 and 200 μg mL^{-1} show these compounds to be readily separable by *rp*-HPLC using isocratic elution with a buffered aqueous acetonitrile mobile phase (typically 85 : 15

v/v% acetonitrile:0.1 M acetate buffer pH 6) at room temperature, illustrated in figure 5(a). The influence of ligand structure on the retention behavior of these complexes is also clearly apparent, with retention times differing significantly for various ligand structures in these complexes. Although this retention behavior is not the focus of this study, it is noteworthy that the retention time of *cis*-[Pd(L^1-*S*,*O*)$_2$] from the unsubstituted *N*,*N*-diethyl-*N*′-benzoylthiourea is much shorter (t_R = 23.2 min) than, for example, the corresponding 4-chlorobenzoylthiourea *cis*-[Pd(L^4-*S*,*O*)$_2$] complex (*ca* t_R = 62.2 min), while being similar

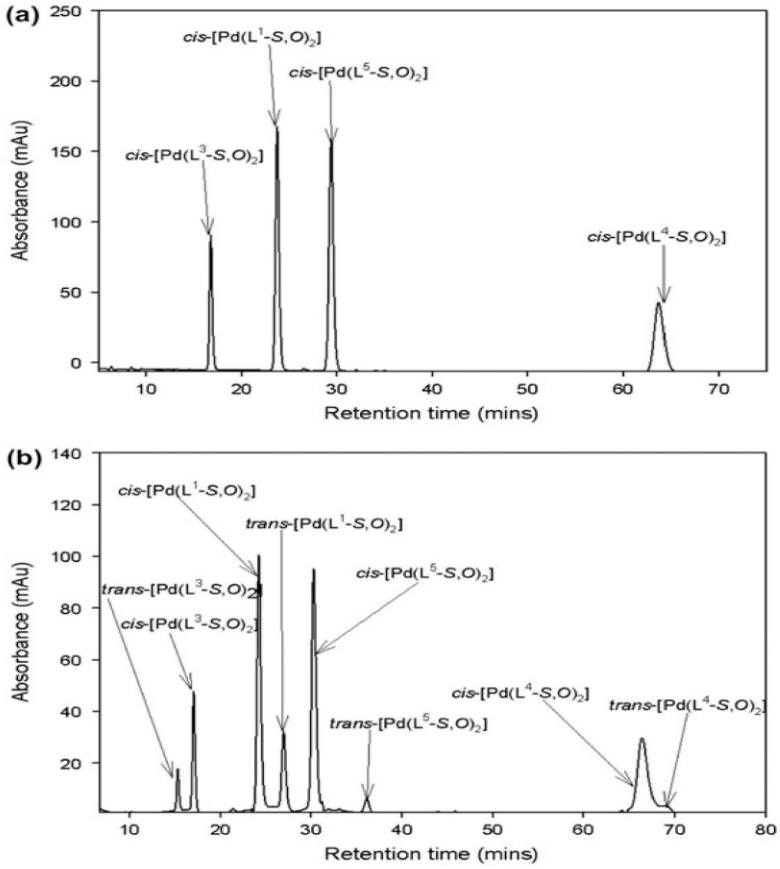

Figure 5. (a) Chromatogram representing the RP-HPLC separation of acetonitrile solution of a mixture of *cis*-[Pd(L^1-*S*,*O*)$_2$], *cis*-[Pd(L^3-*S*,*O*)$_2$], *cis*-[Pd(L^4-*S*,*O*)$_2$], and *cis*-[Pd(L^5-*S*,*O*)$_2$] in the dark; (b) Chromatogram of *cis* and *trans* isomers of [Pd(L^1-*S*,*O*)$_2$], [Pd(L^3-*S*,*O*)$_2$], [Pd(L^4-*S*,*O*)$_2$], and [Pd(L^5-*S*,*O*)$_2$] in acetonitrile, after irradiation with Hg UV light; conditions: GEMINI C_{18} 5 μm, 150 × 4.6 mm column, mobile phase 85 : 15 (% v/v) acetonitrile:0.1 M acetate buffer (pH 6) flow rate 1 mL min^{-1}, injection volume 20 μL, 262 nm detection.

to that of the 4-methoxybenzolyl complex *cis*-[Pd(L^2-*S*,*O*)$_2$] (ca t_R = 25.5 min), but longer than the 3,4,5-trimethoxybenzoylthiourea complex *cis*-[Pd(L^3-*S*,*O*)$_2$] (16.3 min). Under similar conditions, the corresponding *N*-piperidylbenzoylthiourea complex *cis*-[Pd(L^5-*S*,*O*)$_2$] shows a longer retention time (28.5 min) than its *N*,*N*-diethyl-*N*′-benzoylthiourea analog, *cis*-[Pd(L^1-*S*,*O*)$_2$]. These trends suggest that the *rp*-HPLC retention times of the series of complexes are sensitive indicators of the relative polarity of the individual compounds, and consequently their degree of partition between the less polar stationary phase and the more polar mobile phase. Such arguments qualitatively account for the long retention time of the more hydrophobic 4-chlorobenzoylthiourea *cis*-[Pd(L^4-*S*,*O*)$_2$] complex compared with the presumably more hydrophillic 3,4,5-trimethoxybenzoylthiourea *cis*-[Pd(L^3-*S*,*O*)$_2$] complex. Evindently, the use of *rp*-HPLC not only confirms the isomeric purity of the above (*cis*) complexes in dilute solutions not previously exposed to light, but confirms this to be an excellent separation technique for the study of photo-induced isomerization of *cis*-[Pd(L''-*S*,*O*)$_2$] complexes, at two orders of magnitude lower complex concentrations.

The *rp*-HPLC chromatogram obtained after injection of a 20 μL aliquot of a mixture of *cis*-[Pd(L^1-*S*,*O*)$_2$], *cis*-[Pd(L^3-*S*,*O*)$_2$], *cis*-[Pd(L^4-S,O)$_2$], and *cis*-[Pd(L^5-*S*,*O*)$_2$] in acetonitrile irradiated using the pre-column Hg UV lamp photo-reactor (figure S1) clearly shows that good separation between the *cis* and photo-induced *trans* isomers is achieved in most cases. With the exception of the *cis*-[Pd(L^3-*S*,*O*)$_2$] complex, the *trans* isomer of the other three complexes tend to have longer retention times compared with their *cis* analogs under identical conditions, consistent with the expected low relative dipole moment of the symmetrical *trans* isomers. The above chromatographic assignments were confirmed by comparison of retention times obtained from single-component sample aliquots containing only one of the *cis*-[Pd(L''-*S*,*O*)$_2$] (n = 1–5) complexes with and without sample irradiation. The retention times of individual *cis/trans* pairs so generated gave consistent retention times, and from the relative chromatographic peak areas, the *trans : cis* ratios could readily be measured at 262 nm photometrically for each individual complex. The validity of using chromatographic peak areas as a measure of the *trans : cis* ratios of the separated *cis/trans* isomer pairs was confirmed by the UV/visible light absorption profiles determined for all individual *cis/trans* complexes recorded by means of diode-array detector. Virtually identical absorption profiles and molar absorptivities at 262 nm are obtained for all *cis/trans* complex pairs, which allow for the photometric determination of the chromatographic area ratio directly proportional to the *trans : cis* ratio within minimal experimental error, without a need to perform any calibration (see figure S2). In this way, steady-state *trans : cis* ratios (K_e) for each of the *cis*-[Pd(L''-*S*,*O*)$_2$] (n = 1–5) complexes can be estimated by variation of the effective flow rate and the Teflon coil length in the photo-reactor as described in the experimental section; thus, the length of time for which each particular complex is exposed to the Hg UV lamp irradiation can be varied until ultimately a steady-state *trans : cis* ratio K_e may be determined. While this methodology gives reproducible K_e values, unfortunately several disadvantages using the Hg UV lamp pre-column photo-reactor are apparent. One is the degree of photochemical decomposition of complexes which occurs under prolonged UV light irradiation times using the Hg lamp, particularly at relatively low flow-rates necessary for the optimum analytical *rp*-HPLC separation of products. Moreover at the low flow rates necessary for optimum analytical separations, a previously irradiated sample spends a substantial time in the "dark", while being transported to the analyitcal column. This could result in the *trans/cis* ratio measured in this way and may not be an accurate reflection of a "true" steady-state *trans/cis* ratio, since the reversion *trans* → *cis* commences immediately in the dark, while being transported to the analytical column.

For this reason, we explored an alternative "off-line" photo-induced isomerization methodology using a manual irradiation of samples to steady state with 100 mW blue–violet laser light (405 nm), followed by immediate injection of a laser light-irradiated aliquot into the analytical *rp*-HPLC column. This procedure gave good, reproducible results, showing also that treatment with 405 nm laser light apparently results in more rapid *cis* → *trans* conversion for these [Pd(L^n-*S*,*O*)$_2$] (n = 1–5) complexes in acetonitrile, and generally results in much "cleaner" chromatograms free from potential photochemical decomposition. In this way, steady-state K_e values could be measured in an overall shorter time. The conditional experimental K_e values obtained using blue–violet laser light at room temperature are listed in table 2 for selected *cis*-[Pd(L^n-*S*,*O*)$_2$] (n = 1–5) complexes.

The data are interesting, showing differences in the relative K_e values measured from chromatographic peak areas for the selected [Pd(L^n-*S*,*O*)$_2$] complexes in acetonitrile after irradiation by blue–violet laser light. Comparison of K_e values of these *cis/trans* pairs of [Pd(L^n-*S*,*O*)$_2$] complexes indicates some influence of ligand structure on the apparent steady-state K_e values as obtained by this methodology. Thus, the *cis*-[Pd(L^1-*S*,*O*)$_2$] and *cis*-[Pd(L^2-*S*,*O*)$_2$] derived from the unsubstituted benzoyl and 4-methoxy-benzoyl ligands, respectively, show virtually identical relative K_e values at ~1.5, indicating that the *para* methoxy-substituent in *cis*-[Pd(L^2-*S*,*O*)$_2$] has little effect on the effective steady-state *trans/cis* ratio under these conditions. By contrast, significantly lower K_e values of ~0.33 and ~0.13 for the *cis*-[Pd(L^3-*S*,*O*)$_2$] and *cis*-[Pd(L^5-*S*,*O*)$_2$], are obtained under identical conditions respectively. These K_e values should not be seen as "absolute" thermodynamic or equilibrium values since they are conditional on the experimental methodology used, given the lack of estimates of the quantum yield for the photo-induced process at 405 nm which may differ for different complexes. The monochromatic laser light at 405 nm appears to efficiently and rapidly induce isomerization to steady state as is apparent from the data in table 2, showing fairly short times of between 3 and 4 min to attain the steady-state K_e value in dilute acetonitrile solutions at room temperature. While the polychromatic UV/visible spectrum from a Hg lamp as well as those from conventional tungsten or LED white light sources also result in such isomerism, this appears to take place at differing relative rates and to differing extents, requiring generally longer exposure times. Since it is known that the reverse *trans* → *cis* reaction takes place in the absence of light at differing rates for the *cis*-[Pd(L^3-*S*,*O*)$_2$] complex as shown from *in situ* ^{1}H NMR data in significantly more concentrated solutions [figure 4(b)], quantitative comparisons of K_e cannot reasonably be made from the current data. The K_e values presumably reflect equal relative rates of the forward photo-induced *cis* → *trans* process relative to the thermal reverse *trans* → *cis* reversion rate under particular conditions. The apparent steady state probably depends also on

Table 2. Approximate relative times to steady state and the K_e value for *cis* → *trans* photo-induced isomerization of [Pd(L^1-*S*,*O*)$_2$], [Pd(L^2-*S*,*O*)$_2$], [Pd(L^3-*S*,*O*)$_2$], [Pd(L^5-*S*,*O*)$_2$], and [Pt(L^3-*S*,*O*)$_2$] in acetonitrile as monitored by PR-HPLC after irradiation of injected aliquots with a blue–violet laser (100 mW, 450 nm) at room temperature. (chromatographic conditions in figure 5).

Complex	Retention time (min)		Time to steady state (min)	K_e ~[*trans*]/[*cis*]
	cis	*trans*		
[Pd(L^1-*S*,*O*)$_2$]	21.03	23.15	4	1.46
[Pd(L^2-*S*,*O*)$_2$]	25.97	24.73	3	1.52
[Pd(L^3-*S*,*O*)$_2$]	15.58	14.26	3	0.33
[Pd(L^5-*S*,*O*)$_2$]	25.93	30.51	3	0.13

the nature of the palladium complex and the experimental conditions after irradiation by whatever means from a particular light source at room temperature. Preliminary results show that after laser light irradiation of dilute solutions of the *cis*-[Pd(L^3-*S*,*O*)$_2$] complex in acetonitrile, the *trans* isomer rapidly reverts completely back to the *cis* after only *ca* 3 min in the absence of light, while the corresponding *trans*-[Pd(L^1-*S*,*O*)$_2$] and *trans*-[Pd(L^2-*S*,*O*)$_2$] complexes persist in solution for approximately 420 min in solution, before the last traces of *trans* isomer vanishes from solution after irradiation is discontinued (figure S5). Therefore, in view of the potential complexity of this interesting photochemical/thermal *cis* ⇆ *trans* isomerism, a more detailed mechanistic and thermodynamic interpretation based on current data is beyond the scope of this paper.

In summary, all the experimental findings described point to the interesting photo-induced *cis* → *trans* isomerization in *cis*-[M(L^n-*S*,*O*)$_2$] (M = Pd(II) and Pt(II)) complexes of *N*,*N*-dialkyl-*N*′-aroylthioureas. This process is the key factor in the formation of the *trans*-[M(L^n-*S*,*O*)$_2$] complexes, at least of complexes with the d^8 Pt(II) and Pd(II) metal ions, which to our knowledge have not been obtainable by any conventional synthetic means.

Finally, to confirm the above conclusions in particular with the practical objective of reliably preparing and isolating *trans*-[Pd(L^n-*S*,*O*)$_2$] in the solid state, we devised a simple procedure with which it is possible to reliably isolate *trans* complexes of palladium(II) under conditions of photo-isomerization. Thus, the *trans*-[Pd(L^1-*S*,*O*)$_2$] complexes could readily be isolated by means of a vapor diffusion-induced crystallization from solutions of authentic *cis*-[Pd(L^1-*S*,*O*)$_2$] complexes in acetonitrile under continuous irradiation with a low-heat LED white light source at room temperature. Irradiation of an acetonitrile solution of *cis*-bis(*N*,*N*-diethyl-*N*′-benzoylthioureato)-palladium(II) at room temperature between 30 and 60 min with simultaneous slow vapor diffusion of diethylether in a closed specifically designed glass apparatus results in the crystallization of a good crop of pure yellow needles of the sparingly soluble *trans*-bis(*N*,*N*-diethyl-*N*′-benzoylthioureato)palladium(II). The crystal and molecular structure of which were established by single-crystal X-ray diffraction shown in figure 6. To the best of our knowledge, this is a first example of a *trans*-[Pd(L^1-*S*,*O*)$_2$] complex prepared by *deliberate experimental* design involving irradiation. It is of interest to note that the crystals of *trans*-[Pd(L^1-*S*,*O*)$_2$] have a significantly higher melting point (194–196 °C) compared with the *cis* isomer (159–163 °C). The molecular structure of the corresponding *cis*-bis(*N*,*N*-diethyl-*N*′-benzoylthioureato)palladium(II) previously prepared by conventional means has been characterized by X-ray diffraction [29, 30] and is as expected, isostructural with the analogous *cis*-bis(*N*,*N*-diethyl-*N*′-benzoylthioureato) platinum(II) [31].

The square planar *trans*-[Pd(L^1-*S*,*O*)$_2$] complex crystallizes in a monoclinic $P2_1/n$ space group, with relevant crystallographic details given in table S3 in supplementary data. Inspection of the molecular structure of *trans*-[Pd(L^1-*S*,*O*)$_2$] shows that in the six-membered Pd1–S1–C8–N1–C7–O1 chelate ring, the Pd–S (2.2830 Å) and the Pd–O (1.9920 Å) bond lengths are significantly longer and shorter than in the previously *cis*-[Pd(L-*S*,*O*)$_2$] complex at 2.2310 and 2.0170 Å, respectively. This is consistent with the higher *trans* influence expected for the *S*-donor resulting in somewhat longer Pd–S and concomitant shorter bond Pd–O distances in the *trans* isomer. Moreover, the *trans* structure shows virtually ideal square planar coordination to Pd as indicated by the S(1)–Pd(1)–S(1a) and O(1)–Pd(1)–O(1a) bond angles of 180°, whereas the bite angle S(1)–Pd(1)–O(2) of 178.34(4)° in the *cis* isomers deviates somewhat from the ideal linearity, as has been noted in some of the many analogous *cis*-[M(L^n-*S*,*O*)$_2$] (M = Pt and Pd) complexes [8–10, 14, 31] in the literature.

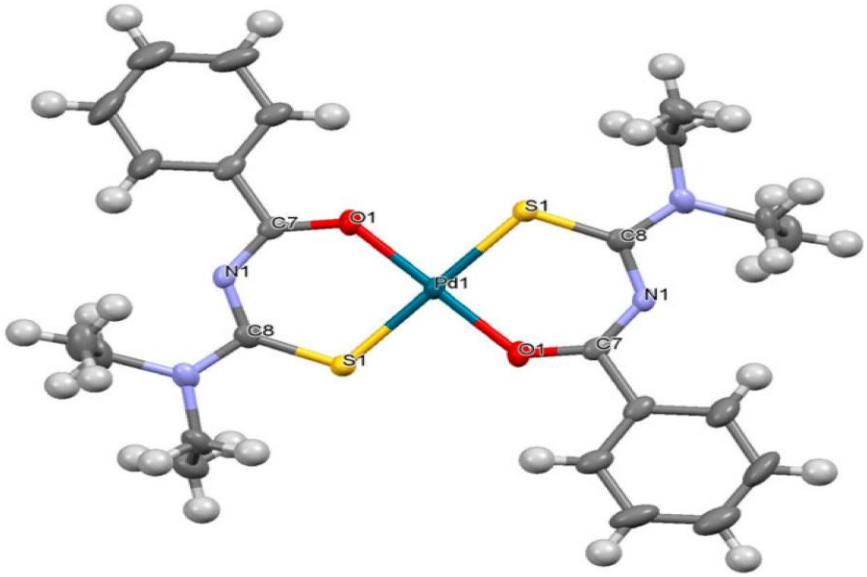

Figure 6. Molecular structure of the first example of a *trans*-bis(*N,N*-diethyl-*N′*-(benzoyl-thioureato)palladium(II), *trans*-[Pd(L^1-*S,O*)$_2$] isolated by irradiation of *cis*-[Pd(L^1-*S,O*)$_2$] in acetonitrile with while light and vapor diffusion crystallization; selected bond lengths (Å) and angles (°):Pd(1)–S(1) 2.2830(11), Pd(1)–O(1) 1.992(2), Pd(1)–S(1_a) 2.2830(11), Pd(1)–O(1_a) 1.992(2), S(1)–C(8) 1.713(4), O(1)–C(7) 1.286(5), N(1)–C(7) 1.321(5), N(1)–C(8) 1.344 (5); S(1)–Pd(1)–O(1) 94.23(7), S(1)–Pd(1)–(S1_a) 180.00, S(1)–Pd(1)–O(1_a) 85.77(7), S(1_a)–Pd(1)–O(1) 85.77 (7), O(1)–Pd(1)–O(1_a) 180.00, S(1_a)–Pd(1)–O(1_a) 94.23(14), Pd(1)–S(1)–C(8) 107.20(2), Pd(1)–O(1)–C(7) 128.8(2), C(7)–N(1)–C(8) 126.9(3).

4. Conclusion

The uncharged *cis*-[M(L-*S,O*)$_2$] complexes prepared by conventional synthetic means from *N,N*-dialkyl-*N′*-benzoylthiourea (LH) and the d^8 metals Pt(II) and Pd(II), which are usually the sole reaction product, undergo a facile light-induced *cis* → *trans* isomerization in organic solvents such as chloroform and particularly acetonitrile. This deceptively simple photo-induced *cis* → *trans* isomerization of the series of *cis*-[M(L-*S,O*)$_2$] ($M = Pt^{II}$, Pd^{II}) complexes results in significant quantities of the corresponding *trans* isomer appearing in solution at room temperature on irradiation with various sources of intense polychromatic or monochromatic light with $\lambda < 500$ nm. The rate and extent of the *cis* → *trans* conversion appears to depend on several factors, such as the ligand structure, the solvent the *cis* isomer is dissolved in, the d^8 metal ion (Pt or Pd), the temperature, and the light source. A simple 100 mW blue–violet laser emitting at 405 nm, efficiently results in substantial amounts of the *trans* isomer appearing in solutions. These geometrical isomers are apparently in a photo-thermal equilibrium between the thermodynamically favored *cis* isomer and its light-induced *trans* counterpart. In the absence of light, the *trans* isomer reverts back to the *cis* complex in a thermal process. This *cis* → *trans* process is the key to preparing and

isolating examples of the rare *trans* complexes. This is confirmed by the first deliberately prepared example of *trans*-[Pd(L^1-*S*,*O*)$_2$] characterized by single-crystal X-ray diffraction, after photo-induced isomerization from its corresponding *cis* complex.in acetonitrile solution and crystallization by vapor diffusion.

Supplementary material

Crystallographic data for *cis*-[Pd(L^2-*S*,*O*)$_2$], *cis*-[Pd(L^3-*S*,*O*)$_2$] and *trans*-[Pd(L^1-*S*,*O*)$_2$] have been deposited with the Cambridge Crystallographic Data Center, CCDC Numbers 1022563, 1005249 and 1022562, respectively. Copies of this information may be obtained free of charge from the Director, CCDC, 12 Union Road, Cambridge, CB2 1EZ, UK (E-mail: deposit@ccdc.cam.ca.uk or http://www.ccdc.cam.ac.uk).

Funding

Financial and material support from the University of Stellenbosch, Angloplatinum Ltd, and the National Research Foundation [grant number 76678] is gratefully acknowledged. We thank Mr. James Odendal for assistance in processing of the disordered crystal and molecular structure of the *cis*-[Pd(L^3-*S*,*O*)$_2$] complex, CCDC Number 1005249.

References

[1] I.B. Douglass, F.B. Dains. *J. Am. Chem. Soc.*, **56**, 719 (1934).
[2] L. Beyer, E. Hoyer, H. Hartman, J. Liebscher. *Z. Chem.*, **21**, 81 (1981).
[3] P. Muhl, K. Gloe, F. Dietze, E. Hoyer, L. Beyer. *Z. Chem.*, **26**, 81 (1986).
[4] K.-H. Konig, M. Schuster, B. Steinbrech, G. Schneeweis, R. Schlodder. *Fresenius Z. Anal. Chem.*, **321**, 457 (1985).
[5] K.-H. Konig, M. Schuster. *Fresenius Z. Anal. Chem.*, **342**, 791 (1992).
[6] M. Schuster, M. Schwarzer. *Anal. Chim. Acta*, **328**, 1 (1996).
[7] M. Schuster, M. Sandor. *Fresenius Z. Anal. Chem.*, **356**, 326 (1996).
[8] K.R. Koch. *Coord. Chem. Rev.*, 216-217, 473 (2001).
[9] A. Saeed, U. Flörke, M.F. Erben. *J. Sulphur Chem.*, **35**, 318 (2014).
[10] A.N. Mautjana, J.D. Miller, A. Gie, S.A. Bourne, K.R. Koch. *J. Chem. Soc., Dalton Trans.*, 1952 (2003).
[11] K.R. Koch, S.A. Bourne, A. Coetzee, J. Miller. *J. Chem. Soc., Dalton Trans.*, 3157 (1999).
[12] (a) A.N. Westra, S.A. Bourne, K.R. Koch. *Dalton Trans.*, 2916 (2005); (b) A.N. Westra, S.A. Bourne, C. Esterhuysen, K.R. Koch. *Dalton Trans.*, 2162 (2005).
[13] F.H. Allen. *Acta Cryst.*, **B85** (2002), 380; CSC (Version 5.25) updates (July 2004).
[14] K.R. Koch, J. Du Toit, M.R. Caira, C. Sacht. *J. Chem. Soc., Dalton Trans.*, 785 (1994).
[15] W. Hernández, E. Spodine, A. Vega, R. Richter, J. Griebel, R. Kirmse, U. Schröder, L. Beyer. *Z. Anorg. Allg. Chem.*, **630**, 1381 (2004).
[16] H. Arslan, U. Flörke, N. Külcü, M.F. Emen. *J. Coord. Chem.*, **59**, 223 (2006).
[17] J.E. Huheey. In *Inorganic Chemistry, Principles of Structure and Reactivity*, 2nd Edn, pp. 276–288, Harper & Row, New York (1978).
[18] M. Burger. Condensed phase properties of platinum group metal complexes from computational simulations. PhD thesis, University of Stellenbosch (2004).
[19] D. Hanekom, J.M. McKenzie, N.M. Derix, K.R. Koch. *Chem. Commun.*, 767 (2005).
[20] F. Scandola, O. Traverso, V. Balzani, G.L. Zucchini, V. Carassiti. *Inorg. Chim. Acta*, **1**, 76 (1967).
[21] V. Balzani, V. Carassiti. *J. Phys. Chem.*, **72**, 383 (1968).
[22] Bruker Analytical X-ray Systems, *SAINT, Software for CCD Detector System (Version 6.45)*, Bruker AXS Inc., Madison, WI, USA (2003).
[23] (a) Bruker Analytical X-ray Systems, *SADABS, Software for CCD Detector System (Version 2.05)*, Bruker AXS Inc., Madison, WI, USA (2002); (b) R.H. Blessing. *Acta Crystallogr., Sect. A: Found. Crystallogr.*, **51**, 33 (1995).

[24] G.M. Sheldrick. *SHELXL 97, Programs for the Solution and Refinement of Crystal Structures*, University of Göttingen, Göttingen (1997).
[25] L.J. Barbour. *J. Supramol. Chem.*, **1**, 189 (2003).
[26] P.S. Pregosin. *Coord. Chem. Rev.*, **44**, 247 (1982).
[27] J.R.L. Priqueler, I.S. Butler, F.D. Rochon. *Appl. Spectrosc. Rev.*, **41**, 185 (2006).
[28] (a) P. Svensson, K. Lövqvist, V. Yu Kukushkin. *Á. Oskarsson. Acta Chem. Scand.*, **49**, 72 (1975); (b) K.V. Luzyanin, V. Yu Kukushkin, A.D. Ryabov, M. Haukka, A.J.L. Pombeiro. *Inorg. Chem.*, **44**, 2944 (2005).
[29] M. Domínguez, E. Anticó, L. Beyer, A. Aguirre, S. García-Granda, V. Salvadó. *Polyhedron*, **21**, 1429 (2002).
[30] N. Selvakumaran, S.W. Ng, E.R.T. Tiekink, R. Karvembu. *Inorg. Chim. Acta*, **376**, 278 (2011).
[31] C. Sacht, M.S. Datt, S. Otto, A. Roodt. *J. Chem. Soc., Dalton Trans.*, 727 (2000).

Appendix C: CIFCHECK reports

checkCIF/PLATON report

Structure factors have been supplied for datablock(s) I

THIS REPORT IS FOR GUIDANCE ONLY. IF USED AS PART OF A REVIEW PROCEDURE FOR PUBLICATION, IT SHOULD NOT REPLACE THE EXPERTISE OF AN EXPERIENCED CRYSTALLOGRAPHIC REFEREE.

No syntax errors found. CIF dictionary Interpreting this report

Datablock: I trans-bis(N,N-diethyl-N'-benzoylthioureato)-palladium(II)

Bond precision: C-C = 0.0059 A Wavelength=0.71073

Cell: a=12.302(3) b=8.4560(18) c=13.092(3)
alpha=90 beta=110.198(3) gamma=90
Temperature: 100 K

	Calculated	Reported
Volume	1278.2(5)	1278.2(5)
Space group	P 21/n	P 21/n
Hall group	-P 2yn	-P 2yn
Moiety formula	C24 H30 N4 O2 Pd S2	C24 H30 N4 O2 Pd S2
Sum formula	C24 H30 N4 O2 Pd S2	C24 H30 N4 O2 Pd S2
Mr	577.04	577.04
Dx,g cm-3	1.499	1.499
Z	2	2
Mu (mm-1)	0.917	0.917
F000	592.0	592.0
F000'	590.67	
h,k,lmax	16,11,17	15,11,17
Nref	3225	2933
Tmin,Tmax	0.867,0.912	0.817,0.916
Tmin'	0.810	

Correction method= MULTI-SCAN

Data completeness= 0.909 Theta(max)= 28.460

R(reflections)= 0.0408(2240) wR2(reflections)= 0.0981(2933)

S = 1.058 Npar= 153

The following ALERTS were generated. Each ALERT has the format
test-name_ALERT_alert-type_alert-level.
Click on the hyperlinks for more details of the test.

checkCIF/PLATON report

Structure factors have been supplied for datablock(s) I

THIS REPORT IS FOR GUIDANCE ONLY. IF USED AS PART OF A REVIEW PROCEDURE FOR PUBLICATION, IT SHOULD NOT REPLACE THE EXPERTISE OF AN EXPERIENCED CRYSTALLOGRAPHIC REFEREE.

No syntax errors found. CIF dictionary Interpreting this report

Datablock: I cis-bis(N,N-diethyl-N'-4-methoxy-benzoylthioureato)-palladium(II)

Bond precision: C-C = 0.0021 A Wavelength=0.71073

Cell: a=10.8538(4) b=9.7700(4) c=27.0136(11)
alpha=90 beta=98.398(1) gamma=90
Temperature: 100 K

	Calculated	Reported
Volume	2833.85(19)	2833.85(19)
Space group	P 21/c	P 21/c
Hall group	-P 2ybc	-P 2ybc
Moiety formula	C26 H34 N4 O4 Pd S2	C26 H34 N4 O4 Pd S2
Sum formula	C26 H34 N4 O4 Pd S2	C26 H34 N4 O4 Pd S2
Mr	637.09	637.09
Dx,g cm-3	1.493	1.493
Z	4	4
Mu (mm-1)	0.840	0.840
F000	1312.0	1312.0
F000'	1309.44	
h,k,lmax	14,12,35	14,12,35
Nref	6967	6501
Tmin,Tmax	0.809,0.845	0.642,0.851
Tmin'	0.614	

Correction method= MULTI-SCAN

Data completeness= 0.933 Theta(max)= 28.180

R(reflections)= 0.0210(5976) wR2(reflections)= 0.0500(6501)

S = 1.026 Npar= 340

The following ALERTS were generated. Each ALERT has the format
test-name_ALERT_alert-type_alert-level.
Click on the hyperlinks for more details of the test.

trans-S,N-bis(N,N-diethyl-N'-napthoylthioureato)-palladium(II)

checkCIF/PLATON report

You have not supplied any structure factors. As a result the full set of tests cannot be run.

THIS REPORT IS FOR GUIDANCE ONLY. IF USED AS PART OF A REVIEW PROCEDURE FOR PUBLICATION, IT SHOULD NOT REPLACE THE EXPERTISE OF AN EXPERIENCED CRYSTALLOGRAPHIC REFEREE.

No syntax errors found. CIF dictionary Interpreting this report

Datablock: c__frames_week52_guest_hn_bdd~3_work_solve1

Bond precision: C-C = 0.0041 A Wavelength=0.71073

Cell: a=12.471(3) b=7.397(2) c=15.924(5)
alpha=90 beta=92.975(4) gamma=90
Temperature: 296 K

	Calculated	Reported
Volume	1467.0(7)	1467.1(7)
Space group	P 21/n	P21/n
Hall group	-P 2yn	?
Moiety formula	C32 H34 N4 O2 Pd S2	?
Sum formula	C32 H34 N4 O2 Pd S2	C32 H34 C10 N4 O2 Pd S2
Mr	677.15	677.15
Dx,g cm-3	1.533	1.533
Z	2	2
Mu (mm-1)	0.812	0.812
F000	696.0	696.0
F000'	694.71	
h,k,lmax	16,9,21	15,9,21
Nref	3636	3387
Tmin,Tmax	0.856,0.922	0.835,0.921
Tmin'	0.830	

Correction method= # Reported T Limits: Tmin=0.835 Tmax=0.921
AbsCorr = MULTI-SCAN

Data completeness= 0.932 Theta(max)= 28.260

R(reflections)= 0.0382(2744) wR2(reflections)= 0.0816(3387)

S = 1.030 Npar= 189

The following ALERTS were generated. Each ALERT has the format
test-name_ALERT_alert-type_alert-level.
Click on the hyperlinks for more details of the test.

checkCIF/PLATON report

You have not supplied any structure factors. As a result the full set of tests cannot be run.

THIS REPORT IS FOR GUIDANCE ONLY. IF USED AS PART OF A REVIEW PROCEDURE FOR PUBLICATION, IT SHOULD NOT REPLACE THE EXPERTISE OF AN EXPERIENCED CRYSTALLOGRAPHIC REFEREE.

No syntax errors found. CIF dictionary Interpreting this report

Datablock: I trans-bis(N,N-diethyl-N'-4-methyl-benzoylthioureato)palladium(II)

Bond precision: C-C = 0.0097 A Wavelength=0.71073

Cell: a=10.712(11) b=10.683(11) c=11.996(12)
alpha=90 beta=99.463(13) gamma=90
Temperature: 100 K

	Calculated	Reported
Volume	1354(2)	1354(2)
Space group	P 21/n	P21/n
Hall group	-P 2yn	-P2yn
Moiety formula	C26 H34 N4 O2 Pd S2	C26 H34 N4 O2 Pd S2
Sum formula	C26 H34 N4 O2 Pd S2	C26 H34 N4 O2 Pd S2
Mr	605.09	605.10
Dx,g cm-3	1.484	1.484
Z	2	2
Mu (mm-1)	0.870	0.864
F000	624.0	552.0
F000'	622.68	
h,k,lmax	14,14,15	14,13,15
Nref	3347	3121
Tmin,Tmax	0.780,0.902	0.642,0.909
Tmin'	0.601	

Correction method= # Reported T Limits: Tmin=0.642 Tmax=0.909
AbsCorr = MULTI-SCAN

Data completeness= 0.932 Theta(max)= 28.230

R(reflections)= 0.0526(2044) wR2(reflections)= 0.2102(3121)

S = 0.752 Npar= 164

The following ALERTS were generated. Each ALERT has the format
test-name_ALERT_alert-type_alert-level.
Click on the hyperlinks for more details of the test.

checkCIF/PLATON report

You have not supplied any structure factors. As a result the full set of tests cannot be run.

THIS REPORT IS FOR GUIDANCE ONLY. IF USED AS PART OF A REVIEW PROCEDURE FOR PUBLICATION, IT SHOULD NOT REPLACE THE EXPERTISE OF AN EXPERIENCED CRYSTALLOGRAPHIC REFEREE.

No syntax errors found. CIF dictionary Interpreting this report

Datablock: I cis-bis(N-methyl-N-ethyl, N'-benzoylthioureato)platinum(II)

Bond precision: C-C = 0.0055 A Wavelength=0.71073

Cell: a=12.7293(14) b=11.7920(12) c=15.2466(16)
alpha=90 beta=93.259(1) gamma=90
Temperature: 100 K

	Calculated	Reported
Volume	2284.9(4)	2284.9(4)
Space group	P 21/c	P21/c
Hall group	-P 2ybc	-P 2ybc
Moiety formula	C22 H26 N4 O2 Pt S2	C22 H26 N4 O2 Pt S2
Sum formula	C22 H26 N4 O2 Pt S2	C22 H26 N4 O2 Pt S2
Mr	637.67	637.68
Dx,g cm-3	1.854	1.854
Z	4	4
Mu (mm-1)	6.351	6.351
F000	1248.0	1248.0
F000'	1242.80	
h,k,lmax	16,15,20	16,15,20
Nref	5641	5253
Tmin,Tmax	0.175,0.467	0.642,0.909
Tmin'	0.022	

Correction method= # Reported T Limits: Tmin=0.642 Tmax=0.909
AbsCorr = MULTI-SCAN

Data completeness= 0.931 Theta(max)= 28.230

R(reflections)= 0.0265(4965) wR2(reflections)= 0.0589(5253)

S = 1.090 Npar= 285

The following ALERTS were generated. Each ALERT has the format
test-name_ALERT_alert-type_alert-level.
Click on the hyperlinks for more details of the test.

checkCIF/PLATON report

You have not supplied any structure factors. As a result the full set of tests cannot be run.

THIS REPORT IS FOR GUIDANCE ONLY. IF USED AS PART OF A REVIEW PROCEDURE FOR PUBLICATION, IT SHOULD NOT REPLACE THE EXPERTISE OF AN EXPERIENCED CRYSTALLOGRAPHIC REFEREE.

No syntax errors found. CIF dictionary Interpreting this report

Datablock: I

Bond precision: C-C = 0.0060 A Wavelength=0.71073

Cell: a=10.1143(12) b=12.3425(14) c=14.5671(17)
alpha=74.513(2) beta=86.974(2) gamma=77.703(2)
Temperature: 173 K

	Calculated	Reported
Volume	1712.2(3)	1712.2(3)
Space group	P -1	P-1
Hall group	-P 1	-P 1
Moiety formula	C32 H46 N4 O4 Pt S2	C32 H46 N4 O4 Pt S2
Sum formula	C32 H46 N4 O4 Pt S2	C32 H46 N4 O4 Pt S2
Mr	809.93	809.94
Dx,g cm-3	1.571	1.571
Z	2	2
Mu (mm-1)	4.260	4.260
F000	816.0	816.0
F000'	813.43	
h,k,lmax	13,16,19	13,16,19
Nref	8913	8042
Tmin,Tmax	0.305,0.600	0.305,0.600
Tmin'	0.078	

Correction method= # Reported T Limits: Tmin=0.305 Tmax=0.600
AbsCorr = MULTI-SCAN

Data completeness= 0.902 Theta(max)= 28.760

R(reflections)= 0.0353(7150) wR2(reflections)= 0.0749(8042)

S = 0.957 Npar= 401

The following ALERTS were generated. Each ALERT has the format
test-name_ALERT_alert-type_alert-level.
Click on the hyperlinks for more details of the test.

checkCIF/PLATON report

You have not supplied any structure factors. As a result the full set of tests cannot be run.

THIS REPORT IS FOR GUIDANCE ONLY. IF USED AS PART OF A REVIEW PROCEDURE FOR PUBLICATION, IT SHOULD NOT REPLACE THE EXPERTISE OF AN EXPERIENCED CRYSTALLOGRAPHIC REFEREE.

No syntax errors found. CIF dictionary Interpreting this report

Datablock: I cis-bis(N-methyl,N-ethyl-N'-benzoylthioureato)palladium(II)

Bond precision: C-C = 0.0056 A Wavelength=0.71073

Cell: a=12.684(5) b=11.806(5) c=15.285(6)
alpha=90 beta=93.008(6) gamma=90
Temperature: 173 K

	Calculated	Reported
Volume	2285.7(16)	2285.7(16)
Space group	P 21/c	P21/c
Hall group	-P 2ybc	-P 2ybc
Moiety formula	C22 H26 N4 O2 Pd S2	C22 H26 N4 O2 Pd S2
Sum formula	C22 H26 N4 O2 Pd S2	C22 H26 N4 O2 Pd S2
Mr	548.99	548.99
Dx,g cm-3	1.595	1.595
Z	4	4
Mu (mm-1)	1.021	1.020
F000	1120.0	1120.0
F000'	1117.32	
h,k,lmax	16,15,20	16,15,19
Nref	5688	5308
Tmin,Tmax	0.745,0.885	0.642,0.909
Tmin'	0.548	

Correction method= # Reported T Limits: Tmin=0.642 Tmax=0.909
AbsCorr = MULTI-SCAN

Data completeness= 0.933 Theta(max)= 28.300

R(reflections)= 0.0432(4229) wR2(reflections)= 0.0973(5308)

S = 1.042 Npar= 285

The following ALERTS were generated. Each ALERT has the format
test-name_ALERT_alert-type_alert-level.
Click on the hyperlinks for more details of the test.

checkCIF/PLATON report

You have not supplied any structure factors. As a result the full set of tests cannot be run.

THIS REPORT IS FOR GUIDANCE ONLY. IF USED AS PART OF A REVIEW PROCEDURE FOR PUBLICATION, IT SHOULD NOT REPLACE THE EXPERTISE OF AN EXPERIENCED CRYSTALLOGRAPHIC REFEREE.

No syntax errors found. CIF dictionary Interpreting this report

Datablock: C_

Bond precision: C-C = 0.0041 A Wavelength=0.71073

Cell: a=5.680(2) b=21.231(9) c=8.498(4)
alpha=90 beta=93.332(5) gamma=90
Temperature: 100 K

	Calculated	Reported
Volume	1023.1(7)	1023.2(7)
Space group	P 21/n	P 21/n
Hall group	-P 2yn	-P 2yn
Moiety formula	C20 H22 N4 O2 Pd S2	C20 H22 N4 O2 Pd S2
Sum formula	C20 H22 N4 O2 Pd S2	C20 H22 N4 O2 Pd S2
Mr	520.94	520.94
Dx,g cm-3	1.691	1.691
Z	2	2
Mu (mm-1)	1.136	1.136
F000	528.0	528.0
F000'	526.65	
h,k,lmax	7,28,11	7,27,10
Nref	2578	2183
Tmin,Tmax	0.861,0.893	0.701,0.899
Tmin'	0.680	

Correction method= # Reported T Limits: Tmin=0.701 Tmax=0.899
AbsCorr = MULTI-SCAN

Data completeness= 0.847 Theta(max)= 28.380

R(reflections)= 0.0317(1875) wR2(reflections)= 0.0682(2183)

S = 1.037 Npar= 135

The following ALERTS were generated. Each ALERT has the format
test-name_ALERT_alert-type_alert-level.
Click on the hyperlinks for more details of the test.

checkCIF/PLATON report

You have not supplied any structure factors. As a result the full set of tests cannot be run.

THIS REPORT IS FOR GUIDANCE ONLY. IF USED AS PART OF A REVIEW PROCEDURE FOR PUBLICATION, IT SHOULD NOT REPLACE THE EXPERTISE OF AN EXPERIENCED CRYSTALLOGRAPHIC REFEREE.

No syntax errors found. CIF dictionary Interpreting this report

Datablock: I

Bond precision: C-C = 0.0020 A Wavelength=0.71073

Cell: a=7.7885(4) b=13.6967(7) c=13.8810(7)
alpha=112.377(1) beta=96.161(1) gamma=91.759(1)
Temperature: 173 K

	Calculated	Reported
Volume	1357.24(12)	1357.24(12)
Space group	P -1	P-1
Hall group	-P 1	-P 1
Moiety formula	C26 H34 N4 O2 Pd S2	C26 H34 N4 O2 Pd S2
Sum formula	C26 H34 N4 O2 Pd S2	C26 H34 N4 O2 Pd S2
Mr	605.09	605.09
Dx,g cm-3	1.481	1.481
Z	2	2
Mu (mm-1)	0.868	0.868
F000	624.0	624.0
F000'	622.68	
h,k,lmax	10,17,17	10,17,17
Nref	6182	6062
Tmin,Tmax	0.779,0.901	0.779,0.901
Tmin'	0.599	

Correction method= # Reported T Limits: Tmin=0.779 Tmax=0.901
AbsCorr = MULTI-SCAN

Data completeness= 0.981 Theta(max)= 27.410

R(reflections)= 0.0175(5871) wR2(reflections)= 0.0439(6062)

S = 1.088 Npar= 323

The following ALERTS were generated. Each ALERT has the format
test-name_ALERT_alert-type_alert-level.
Click on the hyperlinks for more details of the test.

checkCIF/PLATON report

You have not supplied any structure factors. As a result the full set of tests cannot be run.

THIS REPORT IS FOR GUIDANCE ONLY. IF USED AS PART OF A REVIEW PROCEDURE FOR PUBLICATION, IT SHOULD NOT REPLACE THE EXPERTISE OF AN EXPERIENCED CRYSTALLOGRAPHIC REFEREE.

No syntax errors found. CIF dictionary Interpreting this report

Datablock: F__X-ray_cis-S,OPdDiMetBzTu_Solve2.CIF

Bond precision: C-C = 0.0047 A Wavelength=0.71073

Cell: a=11.5686(17) b=11.8051(18) c=15.199(2)
alpha=90 beta=94.540(2) gamma=90
Temperature: 100 K

	Calculated	Reported
Volume	2069.2(5)	2069.1(5)
Space group	P 21/c	P21/c
Hall group	-P 2ybc	?
Moiety formula	C20 H22 N4 O2 Pd S2	?
Sum formula	C20 H22 N4 O2 Pd S2	C20 H22 N4 O2 Pd S2
Mr	520.94	520.94
Dx,g cm-3	1.672	1.672
Z	4	4
Mu (mm-1)	1.123	1.123
F000	1056.0	1056.0
F000'	1053.30	
h,k,lmax	15,15,20	14,15,20
Nref	5084	4779
Tmin,Tmax	0.774,0.855	0.624,0.859
Tmin'	0.597	

Correction method= # Reported T Limits: Tmin=0.624 Tmax=0.859
AbsCorr = MULTI-SCAN

Data completeness= 0.940 Theta(max)= 28.190

R(reflections)= 0.0417(4405) wR2(reflections)= 0.1064(4779)

S = 1.006 Npar= 267

The following ALERTS were generated. Each ALERT has the format
test-name_ALERT_alert-type_alert-level.
Click on the hyperlinks for more details of the test.

checkCIF/PLATON report

You have not supplied any structure factors. As a result the full set of tests cannot be run.

THIS REPORT IS FOR GUIDANCE ONLY. IF USED AS PART OF A REVIEW PROCEDURE FOR PUBLICATION, IT SHOULD NOT REPLACE THE EXPERTISE OF AN EXPERIENCED CRYSTALLOGRAPHIC REFEREE.

No syntax errors found. CIF dictionary Interpreting this report

Datablock: solve1

cis-S,O-bis(N,N-diethyl-N'-naphthoylthioureato)-palladium(II)

Bond precision: C-C = 0.0051 A Wavelength=0.71073

Cell: a=43.067(8) b=9.3233(18) c=15.204(3)
alpha=90 beta=90 gamma=90
Temperature: 100 K

	Calculated	Reported
Volume	6105(2)	6105(2)
Space group	P b c n	P b c n
Hall group	-P 2n 2ab	-P 2n 2ab
Moiety formula	C32 H34 N4 O2 Pd S2	C32 H34 N4 O2 Pd S2
Sum formula	C32 H34 N4 O2 Pd S2	C128 H136 N16 O8 Pd4 S8
Mr	677.15	2708.61
Dx,g cm-3	1.474	1.474
Z	8	2
Mu (mm-1)	0.781	0.781
F000	2784.0	2784.0
F000'	2778.84	
h,k,lmax	57,12,20	57,11,19
Nref	7600	7077
Tmin,Tmax	0.821,0.883	0.788,0.885
Tmin'	0.779	

Correction method= # Reported T Limits: Tmin=0.788 Tmax=0.885
AbsCorr = MULTI-SCAN

Data completeness= 0.931 Theta(max)= 28.290

R(reflections)= 0.0490(4936) wR2(reflections)= 0.1043(7077)

S = 1.040 Npar= 374

The following ALERTS were generated. Each ALERT has the format
test-name_ALERT_alert-type_alert-level.
Click on the hyperlinks for more details of the test.

checkCIF/PLATON report

You have not supplied any structure factors. As a result the full set of tests cannot be run.

THIS REPORT IS FOR GUIDANCE ONLY. IF USED AS PART OF A REVIEW PROCEDURE FOR PUBLICATION, IT SHOULD NOT REPLACE THE EXPERTISE OF AN EXPERIENCED CRYSTALLOGRAPHIC REFEREE.

No syntax errors found. CIF dictionary Interpreting this report

Datablock: C_ trans-S,O-bis(N,N-diethyl-N'-napthoylthioureato)palladium(II)

Bond precision: C-C = 0.0026 A Wavelength=0.71073

Cell: a=11.6405(15) b=8.4440(11) c=14.7953(19)
alpha=90 beta=96.132(2) gamma=90
Temperature: 100 K

	Calculated	Reported
Volume	1445.9(3)	1445.9(3)
Space group	P 21/c	P 21/c
Hall group	-P 2ybc	-P 2ybc
Moiety formula	C32 H34 N4 O2 Pd S2	C32 H34 N4 O2 Pd S2
Sum formula	C32 H34 N4 O2 Pd S2	C32 H34 N4 O2 Pd S2
Mr	677.15	677.15
Dx,g cm-3	1.555	1.555
Z	2	2
Mu (mm-1)	0.824	0.824
F000	696.0	696.0
F000'	694.71	
h,k,lmax	15,11,19	14,11,19
Nref	3562	3344
Tmin,Tmax	0.789,0.906	0.642,0.909
Tmin'	0.615	

Correction method= # Reported T Limits: Tmin=0.642 Tmax=0.909
AbsCorr = MULTI-SCAN

Data completeness= 0.939 Theta(max)= 28.200

R(reflections)= 0.0235(2857) wR2(reflections)= 0.0629(3344)

S = 1.071 Npar= 230

The following ALERTS were generated. Each ALERT has the format
test-name_ALERT_alert-type_alert-level.
Click on the hyperlinks for more details of the test.